REMARKS

Reconsideration of the Office Action mailed July 17, 2002, (hereinafter "instant Office Action"), entry of the foregoing amendments, withdrawal of the objection and withdrawal of the rejection of claims 1-13, 15-25 and 27-29, are respectfully requested.

The instant Office Action lists claims 1-29 as pending, claims 14 and 26 as withdrawn from consideration and claims 1-13, 15-25 and 27-29 as rejected.

Attached hereto as Appendix A is a marked-up version of the changes made to the claims by the current amendments. Appendix A is captioned **"Version with markings to show changes made"**.

In the instant Office Action, the Examiner acknowledges that applicants have elected group I in response to the restriction requirement. The Examiner further states that claims 14 and 26 are withdrawn from further consideration as being drawn to non-elected inventions. The Examiner has made the restriction requirement final. Applicants have cancelled claims 14 and 26 without waiver or prejudice in response to the restriction requirement.

In the instant Office Action, the Examiner notes that the instant application does not contain an abstract of the disclosure as required by 37 CFR 1.72(b). The abstract for the instant application is attached hereto as Appendix B.

In the instant Office Action, Claims 12 and 19 are rejected under 35 U.S.C. §112, first paragraph, because the Examiner alleges that the specification, while being enabling for treating vascular hyperpermeability and therefore, edema, diapedesis and vascular hypotension, does not reasonably provide enablement for treating all other disorders listed in Claims 12, 16, and 19 such as brain tumors, liver cirrhosis, etc. The Examiner further alleges that there is no guidance or direction in the specification as well as no examples provided to show how the instant compound will have utility in treating all other disorders besides edema, diapedesis and vascular hypotension and that it would require undue experimentation to demonstrate the effectiveness of the instant compound in treating other disorders. Applicants respectfully traverse this rejection.

The Examiner alleges that there is no teaching in the specification or prior art that specific inhibitors of catalytic responses of KDR/VEGFR-2 without affecting activity of Flt-1/VEGFR-1

will treat all other diseases such as brain tumors, liver cirrhosis, etc. As described on page 1, lines 16-25 of the instant specification, VEGF is known to be an important mediator in one or more of the mechanisms that underlie edema and the formation of the edematous state in an individual. VEGF causes an increase in permeability in vascular beds. VEGF is expressed by inflammatory T-cells, macrophages, neutrophils and eosinophils at sites of inflammation.

It is well known that overproduction of VEGF results in vascular hyperpermeability, which can be accompanied by edema, diapedesis, aberrant trans-endothelial exchange and matrix deposition among other physiological events. These states are present in or contribute toward the onset of a wide variety of diseases, as discussed above. The common thread linking the list of diseases in claims 12 and 19 which can be treated with the compounds of the instant invention is the presence of excessive amounts of VEGF which result in symptoms commonly associated with each of these indications. Applicants teach that inhibition of the formation these conditions via inhibition of VEGF can hinder the progression of these diseases.

The Examiner acknowledges that the instant compound selectively inhibits KDR and more specifically catalytic responses of KDR/VEGFR-2 without affecting activity of Flt-1/VEGFR-1 and therefore, will have utility in treating vascular hyperpermeability and therefore, edema, diapedesis and vascular hypotension. Applicants point out that VEGF is well documented as the most potent inducer of vascular hyperpermeability resulting in the leakage of fluids and extravasation of plasma proteins & fluids into tissues leading to interstitial fluid which is observed as swelling or edema. The term used to describe the condition depends on where the extravasated fluid accumulates. If the vascular leakage occurs into the peritoneal cavity the result is ascites. If vascular leakage occurs into the "sac" surrounding the heart or lungs the result is pericardial or pleural effusions. If it occurs through the body surface it is an exudate. Accordingly, ascites, effusions and exudates are enabled since their principle difference with edema is the region within which the fluid accumulates.

Applicants respectfully direct the Examiner's attention to page 11, line 34 through page 12, line 6 of the instant specification wherein Applicants state

> Vascular hyperpermability, associated edema, altered transendothelial exchange and macromolecular extravasation, which is often accompanied by diapedesis, can result in excessive matrix deposition, aberrant stromal

proliferation, fibrosis etc. Hence, VEGF-mediated hyperpermeability can significantly contribute to disorders with these etiologic features.

Applicants list from page 12, line 3 to page 17, line 17 examples of disorders exhibiting increased levels of VEGF wherein inhibition of KDR/VEGFR-2 and the corresponding minimization of the accompanying edematous state by the instant compound would inhibit the formation of such disease states. For instance, increases in VEGF and microvascular hyperpermeability are associated with psoriasis. Circulating serum VEGF levels are dramatically increased in victims of polytrauma and burns (Grad et al. 1998. *Clin. Chem. Lab. Med.*, 36(6): 379-383, attached hereto for the Examiner's convenience as Exhibit 1). Edema formation is associated with sunburns, erythedema, persistent acrodema and bullous diseases. Inflammatory and neoplastic disorders are commonly characterized by enhanced microvascular permeability. VEGF has been implicated in macular or other ocular edema, ocular ischemia and vascular edema. Increased intraocular pressures caused by VEGF overproduction and edema can result in glaucoma. Also, vascular hyperpermeability is often associated with conjunctivitis. The production of VEGF can disrupt exchange across pulmonary endothelia and thereby cause pulmonary edema. Increases in VEGF production have been associated with ovarian hyperstimulation syndrome (Levin et al. 1998. *J. of Clinical Investigation*, 102(11):1978-1985, attached as Exhibit 2) and polycystic ovarian syndrome. VEGF is believed to account for the pathogenomonic histopathology and clinical features of glioblastoma tumors (Goldman et al. 1997. *Neurosurgery*, 40(6): 1269-1277, attached hereto as Exhibit 3) and increased cerebral edema (Xu et al., 1998. *J. Appl. Physiol.*, 85: 53-57, attached hereto as Exhibit 4). VEGF overproduction is observed in patients with lung, (Yano et al., 2000. *Clin. Cancer Research*, 6: 957-965 attached hereto as Exhibit 5), breast or colon (Ellis et al, 1998 *J. of Biological Chemistry*, 273(2): 1052-1057, attached hereto as Exhibit 6) carcinomas, lymphomas and leukemias. Elevated levels of VEGF and the resulting vascular hyperpermeability are found in renal disorders such as microalbuminuria, proteinuria, oliguria, electrolyte imbalance and nephrotic syndrome. Protein extravasation and diapedesis that commonly accompanies edema and leads to excessive matrix deposition and stromal proliferation contribute to the progression of disorders such as hyperviscosity syndrome, liver cirrhosis (Rosmorduc et al., 1998. *American J. of Pathology*, 155(4): 1065-1073, attached as Exhibit 7), fibroses, keloid and formation of

undesired scar tissue. VEGF has also been implicated in inflammatory diseases such as asthma and chronic bronchitis (McDonald, D.M., *Am. J. Respir. Crit. Care Med.*, 2001. 164: S39-S45, attached hereto as Exhibit 8), malignant ascites formation (Yoshiji et al., 2001. *Hepatology*, 33(4): 841-947, attached hereto as Exhibit 9), and ovarian cancer (Mesiano et al.,1998. *Am. J. of Pathology*, 153:1249-1256, attached hereto as Exhibit 10). Contrary to the Examiner's allegation that the specification is not enabled when considering the state of the prior art, the state of the prior art clearly shows that VEGF is implicated in a large number of different diseases.

With respect to the Examiner's allegation that undue experimentation is required to use the instant invention, the determination of what constitutes undue experimentation in a given case requires the application of a standard of reasonableness, having due regard for the nature of the invention and the state of the art: Ansul Co. v. Uniroyal, Inc., 4 F.2d 872 (2d Cir. 1971). The test is not merely quantitative, since a considerable amount of experimentation is permissible, if it is merely routine, or if the specification in question provides a reasonable amount of guidance with respect to the direction in which the experimentation should proceed to enable the determination of how to practice a desired embodiment of the invention claimed. The factors to be considered have been summarized as the quantity of experimentation necessary, the amount of direction or guidance presented, the presence or absence of working examples, the nature of the invention, the state of the prior art, the relative skill of those in that art, the predictability or unpredictability of the art and the breadth of the claims. In re Rainer, 52 CCPA 1593, 347 F.2d 574, 146 USPQ 218 (1965); In re Colonianni, 561 F.2d 220, 224, 195 USPQ 150, 153 (CCPA 1977).

In the instant specification the assays used to determine the level of activity and effect of the different compounds of the invention are described on pages 25-36 of the instant application. The protocols used in the assays are either well known to those skilled in the art, detailed in the instant specification or, in some cases, a published reference is cited (see page 32, line 10 of the published PCT application). The amount of experimentation required to utilize the instant invention is routine in the field of medicinal chemistry, and, thus, is not undue.

With respect to the Examiner's allegation that the specification is not enabling based on the presence or absence of working examples provided in the instant specification, Applicants

direct the Examiner's attention to the table on page 34 of the corresponding published PCT application, WO00/27414, which lists results demonstrating the inhibitory activity of the compounds of the instant invention for KDR tyrosine kinase activity. Applicants respectfully point out that there is no requirement as to how many working examples must be provided in a patent application. Further, the Court of Customs and Patent Appeals had stated earlier in In re Cavallito and Gray, 282 F. 2d 363, 127 USPQ 206 (CCPA 1960), in deciding the issue of sufficiency of disclosure of the appellant's specification, that "....it is the nature of the disclosure rather than the number of examples given which determines the sufficiency of the disclosure...." In re Cavallito and Gray, supra 127 USPQ 208.

With respect to the Examiner's allegation that the instant specification is not enabling based on the amount of direction or guidance provided, Applicants submit that they have provided the structure of a representative compound used to inhibit VEGF activity and detailed the assays used to measure the inhibitory effects of said compound. Pharmaceutical formulations, routes of administrations, composition/formulation and effective dosage have been described on pages 19-25 of the corresponding published PCT application, WO00/27414. Applicants have clearly enabled others to use the instant invention.

Based on the foregoing, the rejection of claims 12 and 19 under 35 U.S.C.§112, first paragraph is obviated and should be withdrawn.

In the instant Office Action, claims 1-13, 15-25 and 27-29 are rejected under 35 U.S.C. §112, second paragraph as allegedly being indefinite for failing to point out and distinctly claim the subject matter which Applicants regard as the invention. Claims 2-13 and 15 depend upon claim 1 and claims 17-25 and 27-29 depend upon claim 16. The Examiner has pointed out that amending claims 1 and 16 to include the term "therapeutically effective amount of a" before the word "compound" will overcome the rejections of claims 2-10, 12-13, 15, 17-25 and 27-29. Applicants have amended claims 1 and 16 to include the phrase suggested by the Examiner.

In the instant Office Action, claims 1-13, 15-25 and 27-29 are objected to as being directed to an Improper Markush Group since antibodies, peptides, ribozymes and antisense polynucleotides are not part of the invention presently under prosecution as a result of the restriction requirement. Applicants have amended claims 11 and 18 by deleting references to peptides and antibodies as suggested by the Examiner to overcome this objection. Therefore, the

objection to claims 1-13, 15-25 and 27-29 as being directed to an Improper Markush Group should be withdrawn.

Claims 11 and 18 are rejected as allegedly being directed to using peptides and antibodies as compounds and that peptides and antibodies are not compounds. Applicants respectfully point out that anything can be a compound and that on page 10, line 10 and line 27 compounds having the requisite KDR tyrosine kinase inhibition property are defined as antibodies, peptides and organic molecules. Nonwithstanding the foregoing, Claims 11 and 18 have been amended in response to the foregoing Improper Markush Group objection to remove references to peptides and antibodies. Therefore, the rejection to claims 1-13, 15-25 and 27-29 under 35 U.S.C.§112, second paragraph is obviated and should be withdrawn.

Applicants gratefully acknowledge the Examiner's indication of allowable subject matter that the instant method of inhibiting vascular hyperpermeability by administering the instant pyrazole compound is allowable over the prior art since it is neither disclosed nor obvious over the prior art (Habeck, U.S. Patent No. 3,932,430), because the prior art discloses substituted naphtho pyrazoles as anti-fertility and antihypertensive agents but there is no teaching or suggestion for using these compounds to treat vascular hyperpermeability.

Based upon the foregoing, Applicants believe that claims 1-13, 15-25 and 27-29 are in condition for allowance. Prompt and favorable action is earnestly solicited.

If the Examiner believes that a telephone conference would advance the condition of the instant application for allowance, Applicants invite the Examiner to call Applicants' agent at the number noted below.

Respectfully submitted,

Date: November 18, 2002

Gayle O'Brien

Gayle B. O'Brien
Agent for Applicants
Reg. No. 48,812

Abbott Bioresearch Center, Inc.
100 Research Drive
Worcester, MA 01605

(508) 688-8053

APPENDIX A

VERSION WITH MARKINGS TO SHOW CHANGES MADE

1. (Amended) A method of inhibiting vascular hyperpermeability in an individual comprising the step of administering to said individual a therapeutically effective amount of a compound that inhibits the cellular signaling function of KDR.

11. (Amended) The method of Claim 10 wherein said compound is [selected from the group consisting of peptides, antibodies and] an organic molecule[s,] wherein said compound binds to said KDR tyrosine kinase.

16. (Amended) A method of inhibiting a physiological process or state in an individual, said physiological process or state selected from the group consisting of edema formation, diapedesis, extravasation, effusion, exudation, ascites formation, matrix deposition and vascular hypotension, wherein said inhibiting comprises the administration of a therapeutically effective amount of a compound that inhibits the cellular signaling function of KDR.

18. (Amended) The method of Claim 17 wherein said compound is [selected from the group consisting of peptides, antibodies and] an organic molecule[s] wherein said compound binds to said KDR tyrosine kinase.

APPENDIX B

ABSTRACT

Vascular hyperpermeability in individuals is a prelude to a number of physiological events that are often deleterious. Among these events is the formation of edema, diapedesis, aberrant trans-endothelial exchange, extravasation exudation and effusion, matrix deposition (often with abnormal stromal proliferation) and vascular hypotension. Vascular hyperpermeability and the subsequent events can be inhibited by the administration of a compound that inhibits the enzyme activity of the VEGF tyrosine kinase receptor known as KDR tyrosine kinase. Preferred administered compounds selectively inhibit the function of KDR tyrosine kinase but do not block the activity of Flt-1 tyrosine kinase which is another VEGF tyrosine kinase receptor.

Exhibit 1

Clin Chem Lab Med 1998; 36(6):379–383 © 1998 by Walter de Gruyter · Berlin · New York

Strongly Enhanced Serum Levels of Vascular Endothelial Growth Factor (VEGF) after Polytrauma and Burn

Sibylle Grad[1], Wolfgang Ertel[2], Marius Keel[2], Manfred Infanger[3], Dieter J. Vonderschmitt[1] and Friedrich E. Maly[1]

[1] Institut für Klinische Chemie, Universitätsspital, Zürich, Switzerland
[2] Klinik für Unfallchirurgie, Department Chirurgie, Universitätsspital, Zürich, Switzerland
[3] Klinik für Wiederherstellungschirurgie, Department Chirurgie, Universitätsspital, Zürich, Switzerland

Angiogenesis is a key component of the repair mechanisms triggered by tissue injury. Vascular endothelial growth factor (VEGF) is an important mediator of angiogenesis, as it acts directly and specifically on endothelial cells. VEGF produced locally in regenerating tissue may spill over into the systemic circulation, and measuring levels of circulating VEGF may allow monitoring of angiogenesis. To determine whether circulating VEGF is increased after severe injury, we measured concentrations of VEGF in serial serum samples of 23 mechanical burn patients, 55 patients with multiple trauma and 56 healthy normal controls, using a newly established ELISA assay. In burn patients, serum VEGF was increased on day 1 (369.4 ± 88.0 pg/ml) and on day 3 (452.0 ± 65.3 pg/ml), reached highest levels on day 14 (1809.5 ± 239.7 pg/ml) and was still elevated on day 21 post-burn (1339.8 ± 208.7 pg/ml) (mean ± SEM, p<0.01), when compared with healthy controls (82.2 ± 10.8 pg/ml (mean ± SEM)). Likewise, in trauma patients, serum VEGF showed a trend towards elevated values on the day of admission (186.9 ± 43.9 pg/ml) and on day 3 after injury (193.2 ± 62.1 pg/ml). Thereafter, serum VEGF increased further (day 7, 507.0 ± 114.7 pg/ml), peaked on day 14 (742.4 ± 151.8 pg/ml) and was still elevated on day 21 after injury (693.1 ± 218.6 pg/ml (mean ± SEM, p<0.01)). No significant correlation was observed between peak serum VEGF and initial severity of mechanical (Injury Severity Score) or burn injury (percentage of body surface burned). However, in both burn and trauma patients, the subgroup of patients with uncomplicated healing showed significantly higher increases of serum VEGF than the subgroup who developed severe complications during the post-traumatic course, such as sepsis, adult respiratory distress syndrome or multiple organ failure (p<0.05). Thus, markedly enhanced levels of serum VEGF are present one to three weeks after trauma or burn injury. Further, occurrence of severe complications during the post-traumatic period is associated with lesser increases of serum VEGF.

Key words: Multiple trauma; Burn injury; Complications; Angiogenesis factor; Vascular endothelial growth factor (VEGF).

Introduction

Tissue injury by trauma or burn injury activates repair mechanisms, including inflammation, cell migration and proliferation, synthesis and remodeling of extracellular matrix, and angiogenesis (1,2). Angiogenesis in particular is regulated by a number of peptide growth factors (3 – 5), among which vascular endothelial growth factor (VEGF), a secretory disulphide-linked dimeric glycoprotein with structural homology to platelet-derived growth factor (6 – 8), is special in that it interacts directly with endothelial cells. VEGF is a potent mitogen for endothelial cells *in vitro* and *in vivo* and exerts its action by way of two class III receptor tyrosine kinases, flt-1 and KDR (9).

Animal and *in vitro* studies suggest that VEGF plays an important role in wound healing and tissue repair: markedly up-regulated VEGF expression has been found in the activated keratinocytes involved in wound healing (10). Different cytokines that are present at the wound site during the healing process have been shown to induce VEGF expression, and wound healing defects of diabetic db/db mice are associated with impaired VEGF-expression (11,12). Further, insulin-like growth factor-I-induced VEGF in osteoblasts may be essential for remodeling of bone in a healing fracture (13).

Given the importance of angiogenesis in the healing of wounds, a means to monitor angiogenesis non-invasively would be desirable to follow the healing process in injured patients. VEGF has so far been regarded as a locally acting autocrine factor, but several recent studies have documented that it is also detectable in serum, most likely due to a spill-over from its site of production. Therefore, we investigated the levels and kinetics of VEGF in the circulation of otherwise healthy burn and trauma patients. A sandwich-type ELISA based on a capture monoclonal antibody to VEGF and a polyclonal antibody to VEGF was set up and used for these studies.

Materials and Methods

Serum samples

Serum samples were obtained from healthy individuals and patients after informed consent. Fifty-five patients with mechanical trauma (36 males, 19 females, age 40.0 ± 1.9 years (means ± SEM, range 21-75 years) were entered into this study. Injury Severity Score (ISS) ranged from 10 to 75 points (31.4 ± 2.1 points). Blood was collected on admission and on days 3, 7, 14, and 21 after injury. In addition, 23 burn patients (18 males, 5 females, age 42.7 ± 3.1 years, range 18-72 years) were studied. Burn surface area ranged from 10.5 to 71.5 %

(46.7 ± 4.6 %). Blood was collected on days 1, 3, 7, 14, and 21 post-burn. Both patient groups were categorized into two subgroups depending on the post traumatic course. In subgroup (a), all patients were included who developed any type of severe complication, i.e. sepsis, adult respiratory distress syndrome (ARDS), or multiple organ dysfunction syndrome (MODS) during the observation period of 21 days. Subgroup (b) consisted of patients without these complications. Twenty-five of 55 trauma patients and 10 of 23 burn patients were assigned to group (a), 30 trauma and 13 burn patients to group (b). Fifty-six healthy volunteers (30 males, 26 females, age 36.6 ± 1.7 years, range 19 61 years) provided blood for use as controls. After collection, blood samples were allowed to clot and were separated by centrifugation 2800 *g* at 4 °C. Serum aliquots were stored at –70 °C until used for assay.

Cell lines

Human hepatoma cell lines HepG2 and Hep3B were obtained from American Type Culture Collection (ATCC) (Manassas, VA, USA) and were cultured in Dulbecco's Modified Eagle Medium (DMEM), supplemented with 4.5 g/l glucose and 10% foetal calf serum. To induce VEGF synthesis, they were cultured for 18 hours in an atmosphere of 1% O_2. Supernatants were harvested, centrifuged, aliquotted and stored at –70 °C until use.

VEGF measurement using ELISA

Reagents and antibodies

Recombinant human VEGF (rhVEGF) was purchased from Cytimmune Sciences Inc. (College Park, MD, USA). The mouse monoclonal antibody to human VEGF was from R&D Systems (Minneapolis, MN, USA), the rabbit polyclonal antibody to human VEGF from Pepro Tech Inc. (Rocky Hill, NJ, USA), and horseradish peroxidase-labeled goat anti rabbit immunoglobulins (G+L) from Biosource International (Camarillo, CA, USA). Tetramethylbenzidine (TMB) peroxidase EIA substrate system was obtained from Bio-Rad Laboratories (Hercules, CA, USA). Assay buffer contained phosphate-buffered saline pH 7.4, with 0.05% Tween 20 and 0.5% bovine serum albumin, and the washing solution contained phosphate-buffered saline with 0.05% Tween 20.

Assay procedure

Wells of 96-well microtitre plates (Costar Corporation, Cambridge, MA, USA) were coated with 50 ml of a 2.5 mg/ml solution of mouse monoclonal anti rhVEGF antibody in 50 mmol/l carbonate buffer, pH 9.4. The plates were sealed and incubated at room temperature for two hours. After washing three times, wells were blocked by incubation with 250 µl of assay buffer at 4 °C overnight. Following three washes, standard and samples were added in duplicates at 100 µl/well. A standard titration curve was obtained from a serial dilution of rhVEGF in foetal calf serum, concentrations ranging from 15.6 pg/ml to 1000 pg/ml. Samples containing more than 1000 pg/ml of VEGF were diluted 1:5 in foetal calf serum. The plates were sealed and incubated at room temperature for two hours. After washing four times, 50 µl of a 4 µg/ml solution of rabbit polyclonal anti-rhVEGF antibody in assay buffer was added to each well. Plates were sealed, incubated at room temperature for one hour and washed again four times. A 1:5000 dilution of horseradish peroxidase-labeled goat anti-rabbit immunoglobulins in assay buffer was dispensed at 50 µl/well, the plates were sealed and incubated at room temperature for one hour. Following six further washes, 100 µl of TMB peroxidase EIA substrate was added to each well. After 10 min incubation at room temperature, the enzyme reaction was stopped by adding 100 µl of 0.18 mol/l sulphuric acid per well. Absorbance values were read at 450 nm (reference at 620 nm) on an ELISA plate reader (Anthos Labtec Instruments, Salzburg, Austria). Four-parameter logistic curve-fitting was used to calculate the results.

Statistical analysis

For comparisons between groups the Mann-Whitney U test was used. $p<0.05$ was chosen as the level of significance. Unless otherwise stated mean values ± SEM are given throughout.

Results

Performance characteristics of the VEGF-ELISA

A typical standard curve of the ELISA for recombinant human VEGF is shown in Figure 1. With rhVEGF standards ranging from 15.6 pg/ml to 1000 pg/ml, the detection limit, defined as the concentration corresponding to the mean OD at 0 pg/ml of rhVEGF plus 2 SD was estimated from 20 determinations to be 10.0 pg/ml. For assessment of imprecision, reproducibility and linearity, we used VEGF-containing culture supernatants of the human hepatoma cell lines HepG2 and Hep3B that had been stimulated by exposure to hypoxia (1% O_2). Intra-assay coefficients of variation (CV) were calculated on the VEGF concentrations of four different samples, these having been measured 20 times during the same experiment. Inter-assay CVs were calculated from the VEGF values of three different samples measured 12 times in 12 different assays. Intra- and inter-assay CVs were thus determined as 3.4% to 6.4% and 7.3% to 15.5%, respectively. To assess linearity, culture supernatants of Hep3B cells were diluted 1:10, 1:20, and 1:40. Ranges of the expected values were between 89.6% and 105.3%, 94.7% and 115.2%, and 90.5% and 124.7%, respectively. Recovery was assessed by the addition of 50 pg/ml and 250 pg/ml of rhVEGF to six serum samples. The recovery rates were between 88.0% and 119.1% and between 85.9% and 111.5%, respectively.

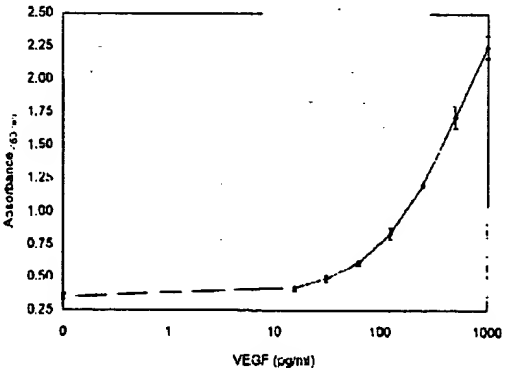

Fig. 1 Standard curve of recombinant human VEGF in foetal calf serum using a sandwich ELISA. Each point represents mean ± SD of n=6 measurements.

VEGF serum levels in healthy individuals, burn and polytrauma patients

In healthy controls, serum VEGF varied from undetectable to 338.6 pg/ml (82.2 ± 10.8 pg/ml, n=56). In burn patients, VEGF concentration was significantly elevated on day 1 (369.4 ± 88.0 pg/ml) and on day 3 (452.0 ± 65.3 pg/ml) post-burn compared with the control group. Serum VEGF further increased on day 7 (1125.5 ± 156.9 pg/ml), reached its highest level on day 14 (1809.5 ± 239.7 pg/ml) and was still elevated on day 21 post-burn (1339.8 ± 208.7 pg/ml) (n=23, p<0.01) (Fig. 2).

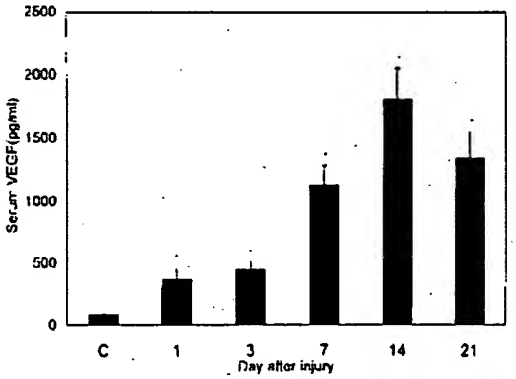

Fig. 2 Concentration of VEGF (pg/ml) in serum of 23 burn patients on days 1, 3, 7, 14, and 21 post-burn in comparison with 56 healthy controls. Values represent mean ± SEM. *p<0.001 compared to controls (C).

There was no significant correlation between peak serum VEGF levels and extent of burn injury (% burned body surface, data not shown). When burn patients were divided into patients with complications, i.e. sepsis, ARDS or MODS during the post-traumatic course (subgroup a) and compared with patients that experienced no such complications (subgroup b), generally lower circulating VEGF was detected in the group with complications (Fig. 3). Statistically significant differences in serum VEGF between subgroups (a) and (b) of

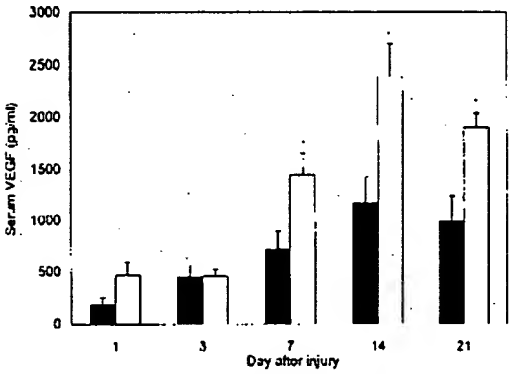

Fig. 3 Concentration of VEGF (pg/ml) in serum of burn patients on days 1, 3, 7, 14, and 21 post burn. Group (a) of 10 patients with complications (■) in comparison with group (b) of 13 patients without complications (□). Values represent mean ± SEM. *p<0.05 group (a) vs. group (b).

burn patients were found on day 7 (712.2 ± 175.8 pg/ml, group (a), 1443.4 ± 206.5 pg/ml, group (b)), on day 14 (1174.1 ± 247.1 pg/ml, group (a), 2387.2 ± 315.1 pg/ml, group (b)), and on day 21 (983.6 ± 252.9 pg/ml, group (a), 1901.5 ± 138.7 pg/ml, group (b)) (p<0.05, group (a) n=10, group (b) n=13).

In trauma patients, serum VEGF concentrations were 186.9 ± 43.9 pg/ml on the day of admission and 193.2 ± 62.1 pg/ml on day 3 after injury (both not statistically different from the control group). However, in these patients serum VEGF concentrations rose markedly during further post-traumatic course of these patients: On day 7, VEGF levels were significantly increased (507.0 ± 114.7 pg/ml) compared to the control group and also compared to the levels on day of admission. The highest VEGF concentrations were reached on day 14 (742.4 ± 151.8 pg/ml), and they were still elevated on day 21 after injury (693.1 ± 218.6 pg/ml) (n=55, p<0.01) (Fig. 4).

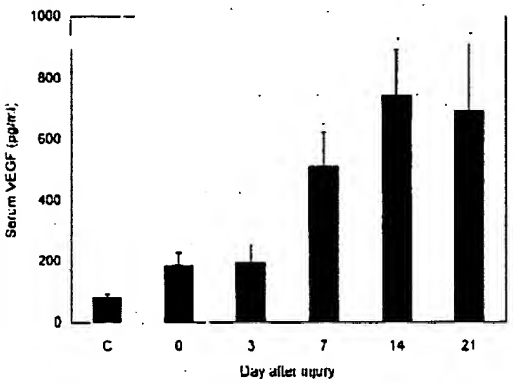

Fig. 4 Concentration of VEGF (pg/ml) in serum of 55 patients with mechanical trauma on the day of admission (day 0) and on days 3, 7, 14, and 21 after injury in comparison with 56 healthy controls (C). Values represent mean ± SEM. *p<0.001 trauma compared to control.

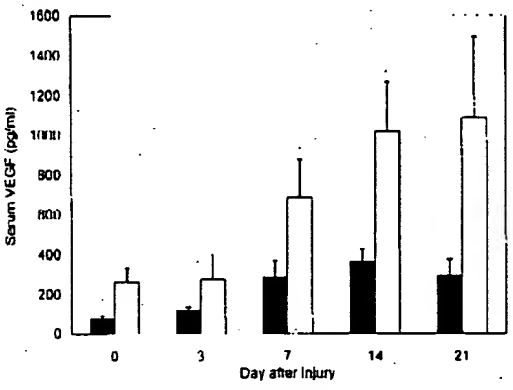

Fig. 5 Concentration of VEGF (pg/ml) in serum of patients with mechanical trauma on the day of admission (day 0) and on days 3, 7, 14, and 21 after injury. Group (a), 25 patients with complications (■) in comparison with group (b), 30 patients without complications (□). Values represent mean ± SEM. *p<0.05 group (a) vs. group (b).

Again, no correlation was observed between peak serum VEGF levels and severity of injury, assessed us-

ing the ISS (data not shown). When trauma patients were divided into patients with complications, such as sepsis, ARDS or MODS during the post-traumatic course (subgroup a) and compared with patients with no such complications (subgroup b), generally lower circulating VEGF was again detected in the group with complications (Fig. 5). Differences between subgroups (a) and (b) of trauma patients were statistically significant on days 7 and 14 after injury ($p<0.05$): on day 7, 286.7 ± 84.0 pg/ml VEGF in group (a), vs. 689.0 ± 191.4 pg/ml in group (b), and on day 14, 365.1 ± 64.6 pg/ml in group (a), vs. 1021.9 ± 405.6 pg/ml in group (b) (group (a) n=25, group (b) n=30).

Discussion

In this study, we demonstrate the presence of elevated levels of VEGF in sera from patients recovering from mechanical trauma or burn injury, compared with a control group of 56 healthy subjects. In these individuals, our ELISA yielded a mean serum VEGF concentration of 82.2 pg/ml, consistent with previous reports of other authors (14-16).

Peak VEGF serum concentrations did not correlate with either injury severity as quantified by ISS in case of multiple trauma patients, or the percentage of body surface burned in case of burn patients. Hence, the extent of the initial injury appears quantitatively unrelated to the serum VEGF response. Rather, the serum VEGF response exhibits the character of a general reaction of the body to burn or physical trauma, similar to neuroendocrine stress responses such as orientation response and catecholamine release (17), albeit with a significantly prolonged timescale.

Mechanical trauma and burn injury cause tissue damage. Since the ensuing processes of wound healing and tissue repair necessitate neovascularization (1,2) and as VEGF is an important mediator of angiogenesis, we had expected to find elevated serum VEGF in patients with severe trauma or burn injury. However, the intensity of the response was unexpected. Both we and other authors have earlier documented higher than normal concentrations of serum VEGF in cancer patients (14,16), inflammatory bowel disease (18) and particularly high values in the POEM-syndrome, a rare form of plasma-cell dyscrasia with polyneuropathy, organomegaly, endocrinopathy, M proteinaemia and skin changes (15). The present study expands the spectrum of disease states in which increased angiogenesis and increased serum levels of VEGF occur. The peak concentrations of VEGF found in polytrauma and burn patients are in the ng/ml-range and extend into the range of the VEGF concentrations described in patients suffering from the POEM syndrome. The time course of the serum VEGF response turned out to be unusual. Whereas basic fibroblast growth factor (bFGF), another important angiogenesis factor, appears early in the burn or post-surgical wound (19,20), serum VEGF levels were highest in the late phase of the response to injury, i.e. during the second and third week of the wound healing process. Interestingly, in experimental models of matrix-induced endochondral ossification, vascular invasion is an essential step in osteogenesis, and usually occurs on about day 9 and may be dependent on neovascular growth factors like VEGF (21). In addition, blood flow at fracture sites has been shown to reach a peak level at approximately 14 days after fracture (22). Also, others have demonstrated in an animal model after tibial osteotomy a serum activity designated endothelial cell stimulating angiogenesis factor (ESAF) with a prolonged time course similar to the serum VEGF response we describe here (23). The possible relationship between this low molecular weight factor and VEGF remains to be investigated. Further, the cellular source(s) of VEGF in trauma and burn patients remain to be identified, though a "spill-over" of VEGF from sites of angiogenesis into the general circulation would seem a probable explanation. In view of the fact that many cell types of different tissue origin, such as keratinocytes, osteoblasts, lymphocytes, neutrophils or cardiac muscle cells, are able to generate VEGF *in vivo* or *in vitro*, it is likely that several tissues and cell types participate in the VEGF response to trauma or burns.

Surprisingly, a stronger increase in serum VEGF was observed in patients with unimpaired healing, whereas the VEGF increase was reduced or delayed in the sub groups of burn and trauma patients in whom serious complications – sepsis, adult respiratory distress syndrome (ARDS), or multiple organ dysfunction syndrome (MODS) – developed. A dampened serum VEGF response may reflect a state of compromised angiogenesis that predisposes to complications, or could merely be a consequence of a developing complication. Further studies are needed to address the cause-and-effect relationship between the serum VEGF response and the occurrence of serious complications after multiple trauma or burn injury.

References

1. Clark RAF. Basics of cutaneous wound repair. J Dermatol Surg Oncol 1993; 19:693–706.
2. Klrsner RS, Eaglstein WH. The wound healing process. Dermatol Clin 1993; 11:629–40.
3. Bennett NT, Schultz GS. Growth factors and wound healing: Part II. Role in normal and chronic wound healing. Am J Surg 1993; 166:74–81.
4. Martin P, Hopkinson-Woolley J, McCluskey J. Growth factors and cutaneous wound repair. Prog Growth Factor Res 1992; 4:25–44.
5. Kiritsy CP, Lynch AB, Lynch SE. Role of growth factors in cutaneous wound healing: a review. Crit Rev Oral Biol Med 1993; 4:729–60.
6. Ferrara N, Houck K, Jakeman L, Leung DW. Molecular and biological properties of the vascular endothelial growth factor family of proteins. Endocr Rev 1992; 13:18–32.
7. Kim KJ, Li B, Houck K, Winer J, Ferrara N. The vascular endothelial growth factor proteins: identification of biologically relevant regions by neutralizing monoclonal antibodies. Growth Factors 1992; 7:53–64.
8. Houck KA, Leung DW, Rowland AM, Winer J, Ferrara N. Dual regulation of vascular endothelial growth factor bio-

availability by genetic and proteolytic mechanisms. J Biol Chem 1992; 267:26031–7.
9. Dvorak HF, Brown LF, Detmar M, Dvorak AM. Vascular permeability factor/vascular endothelial growth factor, microvascular hyperpermeability, and angiogenesis. Am J Pathol 1995; 146:1029–39.
10. Brown LF, Yeo KT, Berse B, Yeo TK, Senger DR, Dvorak HF, *et al.* Expression of vascular permeability factor (vascular endothelial growth factor) by epidermal keratinocytes during wound healing. J Exp Med 1992; 176:1375–9.
11. Detmar M, Yeo KT, Nagy JA, Van de Water L, Brown LF, Berse B, *et al.* Keratinocyte-derived vascular permeability factor (vascular endothelial growth factor) is a potent mitogen for dermal microvascular endothelial cells. J Invest Dermatol 1995; 105:44–50.
12. Frank S, Hübner G, Breier G, Longaker MT, Greenhalgh DG, Werner S. Regulation of vascular endothelial growth factor expression in cultured keratinocytes. Implications for normal and impaired wound healing. J Biol Chem 1995; 270:12607–13.
13. Goad DL, Rubin J, Wang H, Tashjian AH, Patterson C. Enhanced expression of vascular endothelial growth factor in human SaOS-2 osteoblast-like cells and murine osteoblasts induced by insulin-like growth factor 1. Endocrinology 1996; 137:2262–8.
14. Yamamoto Y, Toi M, Kondo S, Matsumoto T, Suzuki H, Kitamura M, *et al.* Concentrations of vascular endothelial growth factor in the sera of normal controls and cancer patients. Clin Cancer Res 1996; 2:821–6.
15. Watanabe O, Arimura K, Kitajima I, Osame M, Maruyama I. Greatly raised vascular endothelial growth factor (VEGF) in POEMS syndrome. Lancet 1996; 347:702.
16. Takano S, Yoshii Y, Kondo S, Suzuki H, Maruno T, Shirai S, Nose T. Concentration of vascular endothelial growth factor in the serum and tumor tissue of brain tumor patients. Cancer Res 1996; 56:2185–90.
17. Kopin IJ. Definitions of stress and sympathetic neuronal responses. Ann NY Acad Sci 1995; 771: 19–30.
18. Schürer-Maly CC, Fried M, Maly FF, Rinak J, Frenzer A. Vascular endothelial growth factor in serum of patients with inflammatory bowel disease. Scand J Gastroenterol 1997; 32:959–60.
19. Gibran NS, Isik FF, Heimbach DM, Gordon D. Basic fibroblast growth factor in the early human burn wound. J Surg Res 1996; 56:226–34.
20. Nissen NN, Polverini PJ, Gamelli RL, Di Pietro LA. Basic fibroblast growth factor mediates angiogenic activity in early surgical wounds. Surgery 1996; 119:457–65.
21. Weiss RE, Reddi AH. Appearance of fibronectin during the differentiation of cartilage, bone, and bone marrow. J Cell Biol 1981; 88:630–6.
22. Paradis GR, Kelly PJ. Blood flow and mineral deposition in canine tibial fractures. J Bone Joint Surg Am 1975; 57:220–6.
23. Wallace AL, Makki R, Weiss JB, Hughes SPF. Measurement of serum angiogenic factor in devascularized experimental tibial fractures. J Orthop Trauma 1995; 9:324–32.

Received 5 January 1998; accepted 26 March 1998

Corresponding author: PD Dr. med. Friedrich E. Maly, Institut für Klinische Chemie, Universitätsspital, Rämistrasse 100, CH-8091 Zürich, Switzerland
Tel.: +41-1-2552146; Fax: +41-1-2554590

Role of Vascular Endothelial Cell Growth Factor in Ovarian Hyperstimulation Syndrome

Ellis R. Levin,*‡ Gregory F. Rosen,§ Denise L. Cassidenti,§ Bill Yee,§ David Meldrum,§ Arthur Wisot,§ and Ali Pedram*‡
*Department of Medicine, the Long Beach Veterans Hospital, Long Beach, California 90822, and ‡University of California, Irvine, Irvine, California 92717, and the §Long Beach Memorial Medical Center and Centers for Advanced Reproductive Care, Long Beach, California 90806 and Redondo Beach, California 90277.

Abstract

Controlled ovarian hyperstimulation with gonadotropins is followed by Ovarian Hyperstimulation Syndrome (OHSS) in some women. An unidentified capillary permeability factor from the ovary has been implicated, and vascular endothelial cell growth/permeability factor (VEGF) is a candidate protein. Follicular fluids (FF) from 80 women who received hormonal induction for infertility were studied. FFs were grouped according to oocyte production, from group I (0–7 oocytes) through group IV (23–31 oocytes). Group IV was comprised of four women with the most severe symptoms of OHSS. Endothelial cell (EC) permeability induced by the individual FF was highly correlated to oocytes produced (r^2 = 0.73, $P < 0.001$). Group IV FF stimulated a 63±4% greater permeability than FF from group I patients ($P < 0.01$), reversed 98% by anti-VEGF antibody. Group IV fluids contained the VEGF165 isoform and significantly greater concentrations of VEGF as compared with group I (1,105±87 pg/ml vs. 353±28 pg/ml, $P < 0.05$). Significant cytoskeletal rearrangement of F-actin into stress fibers and a destruction of ZO-1 tight junction protein alignment was caused by group IV FF, mediated in part by nitric oxide. These mechanisms, which lead to increased EC permeability, were reversed by the VEGF antibody. Our results indicate that VEGF is the FF factor responsible for increased vascular permeability, thereby contributing to the pathogenesis of OHSS. (*J. Clin. Invest.* 1998. 102:1978 1985.) Key words: estrogen • vascular permeability • infertility • controlled ovarian hyperstimulation

Introduction

The Ovarian Hyperstimulation Syndrome (OHSS)[1] is the collection of clinical findings that occur as the most serious complication resulting from the use of gonadotropins for ovulation induction (1). Although the mechanisms that lead to the development of the syndrome are not clearly understood, two major syndrome components are ovarian enlargement and increased vascular permeability. Increased vascular permeability leads to extravasation of protein rich fluid out of the intravascular space, and this can account for virtually all the manifestations of the syndrome. The signs include the accumulation of peritoneal (and rarely pleural or pericardial) fluid, edema, and hypovolemia, leading to anuria or hypotension in the most severe form (1–3). It has been postulated that a vasoactive substance is released from the ovary in response to hormonal stimulation and causes increased vascular permeability (2–4). Ovarian follicular fluid (FF) obtained from patients at risk for developing OHSS significantly augments in vitro permeability of endothelial cells (ECs) (5).

The substance responsible for inducing the manifestations of this syndrome has not been conclusively identified. One candidate as the responsible factor is vascular endothelial cell growth factor (VEGF). This glycoprotein was originally isolated as a vascular permeability factor (6) because it potently stimulates fluid transgression through EC tight junctions (7, 8). VEGF also is a mitogen for ECs (9), contributing to neovascularization in the ischemic diabetic retina (10) or tumor metastasis (11, 12). VEGF is secreted by a variety of cells and binds to several transmembrane receptors expressed on ECs, most importantly *Flt* and *KDR* (or VEGFR-1 and -2) (13, 14). This growth/permeability factor is produced by normal and neoplastic human ovaries (15), including ovarian granulosa cells from women undergoing stimulation for in vitro fertilization (16).

In this study, we sought to identify VEGF as the factor contained in the FF from women undergoing hormonally induced oocyte production that induces EC permeability. We also characterized the cytoskeletal changes induced by the FF to provide a mechanistic basis for the increased EC permeability, which leads to the clinical manifestations of this syndrome.

Methods

Subjects. 80 female patients between the ages of 29 and 41 were studied; they were not receiving hormonal medications other than as prescribed by us for ovulatory induction. All gave informed consent to procurement and experimental use of their FF, as per the protocol approved by the Institutional Review Board of the Long Beach Memorial Medical Center. Using an unused aspiration cannula, each FF was obtained while a patient underwent transvaginal aspiration of follicles for in vitro fertilization. FF was obtained after hormone administration to stimulate oocyte production; the protocol included luteal phase administration of leuprolide acetate, 1 mg/day, followed

Address correspondence to Ellis R. Levin, M.D., Long Beach Veterans Hospital, Medical Service (111 I), 5901 E 7th St., Long Beach, CA 90822. Phone: 562-494-2611 x5748; FAX: 562-494-5615; E-mail: elevin@pop.long-beach.va.gov

Received for publication 5 August 1998 and accepted in revised form 7 October 1998.

1. *Abbreviations used in this paper:* BAEC, bovine aortic endothelial cell; bFGF, basic fibroblast growth factor; dpm, disintegrations per minute; EC, endothelial cell; ET-1, human endothelin-1; FF, follicular fluid; GC, granulosa cells; hCG, human chorionic gonadotropin; hFSH, human follicle-stimulating hormone; L-NMMA, monomethyl L-arginine; NO, nitric oxide; OHSS, Ovarian Hyperstimulation Syndrome; VEGF, vascular endothelial cell growth factor.

by daily administration of 150–450 IU of human follicle–stimulating hormone (hFSH), based upon the women's age and past response history when applicable. Human chorionic gonadotropin (hCG), 10,000 IU, was administered 34–36 h before aspiration, and ovulation induction was monitored with vaginal ultrasound. The obtained fluid was not bloody, was not diluted, and was briefly centrifuged at low speed to remove debris or cells before freezing at −70°C for subsequent assays within 1–2 mo. Fluids were subsequently grouped according to the number of oocytes retrieved: (group I, 0–7 oocytes; group II, 8–14; group III, 15–22; and group IV, 23–31). Patients underwent routine monitoring for signs of the development of OHSS.

Patients in groups I and II were asymptomatic for OHSS; in contrast, two patients in group III complained of significant "bloating and edema of their extremities," but this was not clinically apparent. Two additional patients in group III were noted on physical examination to have mild edema of their lower extremities but no evidence of ascites; their FFs induced the highest permeabilities in their group (see below). The edema responded to discontinuation of further hormonal induction and dietary salt restriction. The four patients that comprised group IV were the most symptomatic, developing moderately severe lower extremity edema in all and significant ascites in two patients. These patients were treated with discontinuation of hormonal induction and diuretics. All symptoms and signs resolved within 4 d.

FF processing. Purification of FF for use in Western immunoblot and RIA was accomplished by affi-gel blue column, then desalting column elution, followed by dialysis against 20 mM PBS for 12 h. The resulting samples were concentrated fivefold by lyophilization, then reconstituted in water (immunoblot) or RIA buffer. Samples for immunoblot were pooled from four random patients in each group, except group IV (all samples used).

EC permeability assay. Bovine aortic ECs were isolated as previously described (17). BAEC formed a monolayer that displayed the typical EC cobblestone appearance and contact inhibition and uniformly tested positive for factor VIII–related antigen. Primary cultures of bovine aortic endothelial cells (BAEC), cultured in DMEM with 10% FBS, were seeded onto 0.45-μM CM filters (Millipore, Bedford, MA) coated with rat tail collagen and contained within plastic inserts; the inserts were placed into 24-well plates and grown to confluence over ~ 5 d. 2 d after confluence, chambers were created by placing medium inside the inner insert and the outer wells, with the endothelial cell monolayer on the insert filter (18). The cells were washed and then subjected to FF incubation at 37°C in a CO_2 incubator for 24 h. FF was added to both aspects of the chamber, in unequal volumes, as explained below. After 24 h, all medium was aspirated and discarded. To the apical surface (insert containing the cells on filter) was then added an experimental sample, containing 395 μl of FF, 4 μl of 100 mM mannitol, and 1 μl of H^3-mannitol (1 × 10^6 cpm). To the basolateral surface of the chamber (outer well), 600 μl of FF was added. These specific volumes equalized fluid heights in the two chambers, so that only diffusive forces would be involved in permeability of the BAEC. Similar equalization occurred during the 24 h preceding the incubation period. After 2 h at 37°C in the incubator, flux rate was determined over 24 h by measuring the amount of H^3-mannitol permeating to the basolateral compartment. This was determined by counting disintegrations per minute (dpm) in the aspirated well fluid by using a β-counter. In some studies, we coadded antibodies that bind to either human endothelin-1 (ET-1; Peninsula Labs, Belmont, CA), VEGF, or basic fibroblast growth factor (bFGF; Santa Cruz Biotechnology, Santa Cruz, CA). In other experiments, exogenous VEGF (Upstate Biotechnology, Lake Placid, NY) was added to EC cultures or the nitric oxide (NO) synthase inhibitor, monomethyl L-arginine (10 μM L-NMMA; CalBiochem, San Diego, CA) 30 min before the addition of FF. DMEM culture media alone (no serum or added peptides) was used for control permeability assessments.

Radioimmunoassay. VEGF immunoreactivity was measured by a double antibody, nonequilibrium assay carried out over 48 h. VEGF was radiolabeled to a specific activity of ~ 1,000 Ci/mmol by the iodogen method (19, 20). There was no cross-reactivity of the first antibody used in the assay with other peptides, including ET-1, atrial natriuretic peptide, angiotensin II, or bFGF. The sensitivity of the assay was 10 pg per tube and the intra- and interassay coefficients of variation were < 10%. Extraction efficiency of the VEGF in FF was 79.6–86% across all samples, and the values were accordingly corrected.

Western immunoblot. Follicular fluid (5 ml) from each of four randomly selected patients in each of the groups (except IV) were processed, individually reconstituted, and aliquots from each sample (20 μl) were pooled after reconstitution. Samples were processed as described above. Before separation by gel electrophoresis, the samples were not adjusted for protein because the permeability determinations on these same samples were also not adjusted for protein content, maintaining consistency.

Immunoprecipitation was performed on 100 μl of pooled, reconstituted samples from each group (20), by using a polyclonal VEGF antibody directed against the first 22 amino acids of N-terminal bovine VEGF. Immunoprecipitates were dissolved in SDS sample buffer, boiled, separated, and then transferred to nitrocellulose. VEGF protein was detected using the ECL Western blot kit (Amersham Life Sciences, Arlington Heights, IL), the first antibody at 1:500 dilution. Protein molecular weight markers and synthetic VEGF were run in parallel, bands were quantitated by laser densitometry, and the samples were used for a second, confirmatory immunoblot.

Cytoskeleton integrity. ECs were cultured to confluence on glass coverslips, then incubated with exogenous VEGF (1 ng/ml) or FF from group I or group IV patients for 24 h, in the presence or absence of VEGF antibody. The cells were fixed with 3.75% formalin, washed, then followed by cold acetone fixation and permeabilization, and then stained with biotin-XX phalloidin (Molecular Probes, Eugene, OR); this demonstrated actin fibers, which are crucial to maintaining EC tight junctions (impermeability). In additional experiments, cells were pretreated with L-NMMA for 30 min before the addition of group IV FF.

ZO-1 protein was assessed by immunocytochemistry. ECs were grown to postconfluence, then fixed, permeabilized, and then stained with anti–ZO-1 antibody (Zymed Corp., San Francisco, CA). Secondary antibody conjugated to biotin was incubated, followed by the addition of FITC–strepavidin for purposes of fluorescent microscopic visualization of ZO-1.

Statistical analysis. Individual or pooled patient data from the permeability assays were compared by ANOVA plus Scheffe's test, using the StatView statistical program ($P < 0.05$ as significant). The same program was used to calculate correlation coefficients by linear regression analysis for oocyte production and EC permeability. VEGF concentrations were similarly analyzed and are expressed as the mean±SEM. Western immunoblots were compared by laser densitometry.

Results

Effects of follicular fluid on endothelial cell permeability. We first characterized our in vitro assay by its response to exogenously added VEGF. Incubation of the BAEC with VEGF, 1 ng/ml, significantly stimulated transgression of labeled mannitol across the endothelial cell barrier by 4 h, and the maximum increase of 62% was seen at 24 h, compared with the basal permeability (0 h), (basal permeability 6,206±63 cpm, 24-h permeability 10,073±81 cpm, $n = 6$ per condition, $P < 0.05$) (Table I). Permeability of the EC in the absence of VEGF increased by ~ 7% over the 24 h, and so the corrected increase in specific permeability at this time, induced by exogenous VEGF, was 55%. Increased permeability stimulated by VEGF at 24 h was 97% prevented by coincubation with a monoclonal

Table I. Effects of Exogenous VEGF on Endothelial Cell Permeability In Vitro

	Permeability (dpm)	
	VEGF 1 ng/ml	DMEM (no VEGF)
Time of cell incubation (h)		
0	6206±63	6096±48
2	7133±131	6138±70
4	7795±31*	6321±86
8	8934±91*	6484±65
24	10073±81*	6566±48
VEGF concentration (ng/ml)		
No peptide	6114±17	
0.1	6191±36	
0.5	7189±153	
1	10483±160*	
2	11314±186*	

Data represent the combined results from two experiments, each done in triplicate (n = 6 observations per condition) and are the mean±SEM. *$P < 0.05$ by ANOVA plus Scheffe's F-test for condition vs. 0 h or vs. no VEGF peptide added to the cells. Hour 0 indicates the basal permeability of the endothelial cells before the addition of VEGF. Bottom data set represents the permeabilities induced by exogenous VEGF at 24 h.

antibody to this growth factor, diluted to 1:100 (data not shown). In dose-related fashion, VEGF caused a significant increase in endothelial cell permeability. Increased permeability was first observed at a concentration of 0.5 ng/ml at 24 h, but a substantial increase of 71% was seen at 1 ng/ml of VEGF (Table I).

We then examined the permeabilities induced by the FF. The induced permeabilities positively correlated with the number of oocytes produced by the individual patients (Fig. 1 *A*) (correlation coefficient, $r^2 = 0.71$, $P < 0.001$). 15 of the individual patients overlapped and hence are not represented as discrete circles on the figure. Comparable correlation was seen when the patients were represented as group mean oocyte production (Fig. 1 *B*) ($r^2 = 0.73$, $P < 0.001$). The values for each group are shown in Table II. Women who produced 15–22 oocytes had a mean permeability of 7,954 cpm, which was significantly increased from group I by 30±3%, while group IV fluids (23–31 oocytes) induced a 63±4% increase in permeability ($P < 0.01$). The significantly increased permeability induced by the FF from the group IV patients correlated to their development of edema or ascites. Follicular fluids from women producing 8–14 oocytes (group II) produced a permeability modestly greater (14%) than group I fluids (0–7 oocytes), and women in both groups were asymptomatic.

Identification of VEGF as the permeability factor. We then sought to determine the identity of the permeability factor in the FF, theorizing that VEGF was the best candidate based upon existing studies. We coincubated the endothelial cells with pooled FF from group III or IV patients and an antibody that binds human VEGF. The VEGF antibody reversed the mean FF-stimulated permeabilities (above those of group I) by 95 and 98%, respectively (Table II) ($P < 0.05$ compared with group III or IV FF alone). In contrast, antibody to human ET-1 or bFGF caused an insignificant reversal. These specificity controls were used because ET-1 and bFGF have been identified to stimulate increased vascular permeability in some situations. Similarly, nonspecific human IgG antibody did not affect the group IV–induced permeability (data not shown).

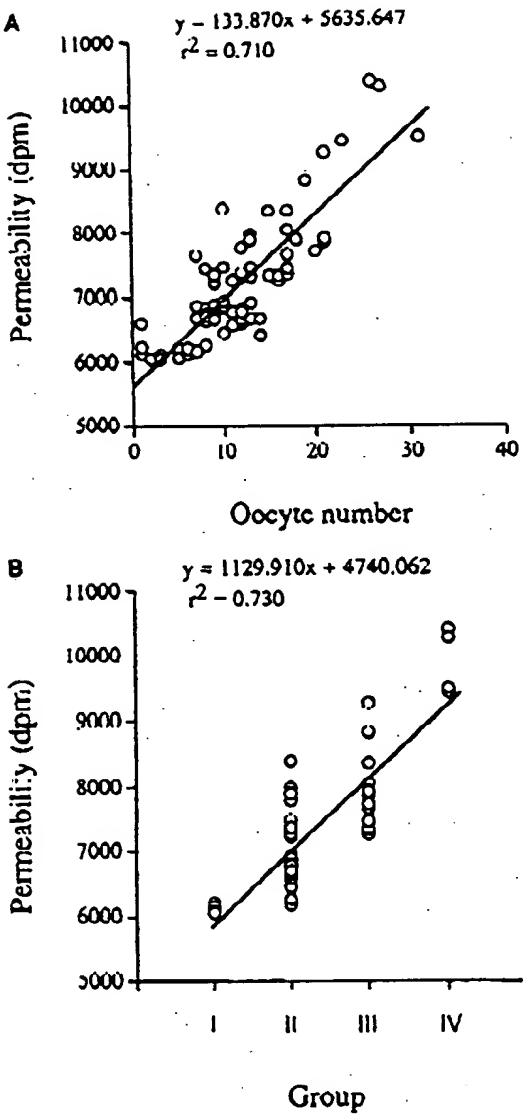

Figure 1 (*A*) Correlation of number of oocytes retrieved from women after hormonal stimulation of the ovary with in vitro endothelial cell permeability stimulated by their individual ovarian FF. Each circle represents the permeability to mannitol that transgresses an endothelial cell monolayer in culture at 24 h, as described in Methods, as a function of the number of oocytes produced. FF samples from 80 women were studied, but only 65 discrete circles are shown because of overlapping values. (*B*) Group correlations for oocyte production and FF-induced permeability. Some patient values overlap and hence are not shown as discrete circles.

The ability of VEGF to enact increased cell growth or other actions is felt to be mediated at least in part by the generation of NO (21). To determine a possible role for NO in the action of FF, L-NMMA was added before FF or exogenous VEGF addition. The increased permeability stimulated by

Table II. Stimulation of In Vitro Endothelial Cell Permeability by Follicular Fluids and Reversed by VEGF Antibody

Group	n	Oocyte number	Permeability (cpm) FF	FF+VEGFab	FF+ET-1ab	FF+bFGFab
C	—	—	6008±28	—	—	—
I	11	0–7	6130±18	—	—	—
II	50	8–14	6963±68*	—	—	—
III	15	15–22	7954±156*	6436±51†	7903±103*	—
IV	4	23–31	10014±294*	6252±45†	9846±68*	9731±77*

Permeability data for each group are the mean±SEM. The permeability induced by the FF from individual patients reflected duplicate in vitro determinations for each patient's sample assessed at 24 h. *n* is the number of individual patients within each group. *$P < 0.05$ vs. permeability induced by group I FF. †$P < 0.05$ for FF vs. FF plus VEGF antibody. C, control media (no FF); FF, follicular fluid; ab, antibody; ET-1, endothelin-1; bFGF, basic fibroblast growth factor.

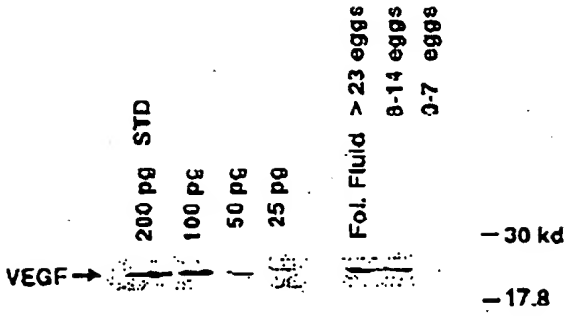

Figure 2. Immunoblot of VEGF contained within the FF of women undergoing ovarian stimulation by hormonal administration. Lanes are exogenous VEGF (200, 100, 50, and 25 pg) and pooled FF from groups IV (> 23 oocytes), II, and I, respectively. Molecular weight markers run in parallel during gel separation are shown on the right side of the figure.

group IV FF was reversed 52% by inhibition of NO synthase (Table III). Similarly, exogenous VEGF-stimulated permeability was reversed 47% by this inhibitor of NO production.

Detection and quantitation of VEGF in FF. We determined both qualitatively and quantitatively the VEGF contained in the FFs. Known amounts of exogenous human VEGF165 were separated on gel in parallel with the patient samples; all samples were membrane transferred and immunoblotted with the growth factor antibody. Exogenous VEGF produced an expected single discrete band, in dose-related fashion, which was ~23 kD in size as a monomer (Fig. 2). This corresponds to the gel migration of endogenous VEGF165 detected in vascular smooth muscle cells (22). A single, same-sized band was detected in the FF samples, indicating that the 165-amino acid isoform of VEGF predominates in the ovary. In groups I or II, little VEGF was detected. In contrast, the samples from the women producing > 23 oocytes (group IV) had clearly detectable VEGF protein, and the VEGF band density correlated with the degree of ovarian stimulation (oocyte number). The density of the VEGF band from group IV samples was roughly comparable with that produced by 100 pg of exogenous VEGF.

To precisely determine the concentration of VEGF in the FFs, we developed an RIA for the growth/permeability factor.

Table III. Reversal of Endothelial Cell Permeability by NO Synthase Inhibition

Group	Permeability (dpm) (% of control) L-NMMA	D-NMMA
Control	100	101±3
FF Group IV	161±3*	128±6†
VEGF 1 ng/ml	164±4*	134±2†

Data are the mean±SEM permeability for each treatment (six replications per condition) carried out for 24 h and are derived from three experiments. FF or VEGF data are compared with permeability from control EC in DMEM in the absence of any FF added to the chambers. *$P <$ 0.05 for permeability induced by FF or VEGF vs. permeability of control EC. †$P < 0.05$ for FF or VEGF vs. FF or VEGF + L-NMMA, 10 μM.

As seen in Fig. 3, VEGF concentrations from the four groups progressively increased. Group I patients had a mean VEGF value of 353±28 pg/ml, increased to a mean of 511±46 pg/ml in group II ($P < 0.05$). Group III patients had a mean VEGF concentration of 805±62 pg/ml, and group IV patients had threefold the VEGF level of group I, at 1105±87 pg/ml. The values obtained by RIA correlated well with oocyte produc-

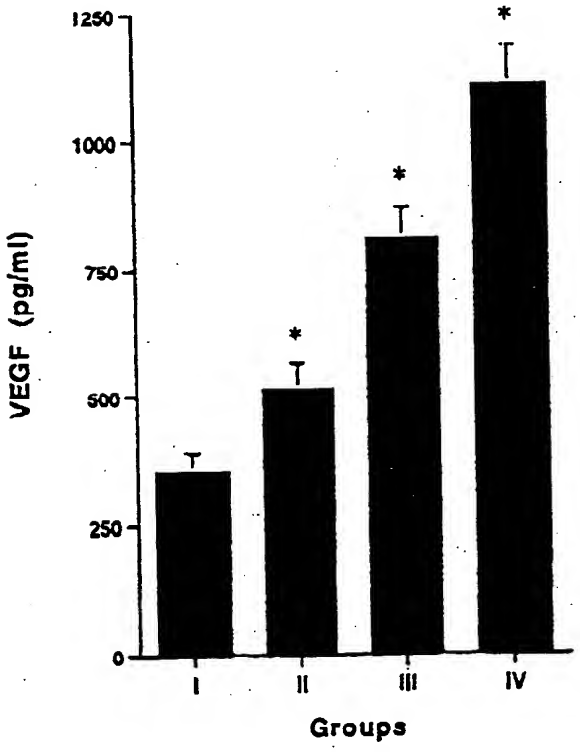

Figure 3. VEGF concentration in the follicular fluids of patients in groups I–IV. Each bar is the mean±SEM of the samples in the group. Asterisks indicate $P < 0.05$ by ANOVA plus Scheffe's F-test vs. group I.

tion and generally paralleled the results from Western immunoblot, which is not quantitative.

Cytoskeletal rearrangement induced by group IV FF. We then assessed the mechanism that leads to increased EC permeability. ECs form tight junction associations, regulating the bidirectional passage of ions, nutrients, and fluids through the endothelial lining (23). This limits the transgression of fluid and protein out of the intravascular space to the peripheral tissues. One important regulatory mechanism for the integrity of tight junction maintenance is distribution of actin to a cortical (peripheral) pattern, precluding stress fiber formation. This situation is demonstrated by EC cultured on glass coverslips in DME and stained to show F-actin (Fig. 4 *a*, *A*). A similar pattern of peripheral actin fiber localization in the cell is seen when ECs are incubated with FFs from group I patients (Fig. 4 *a*, *B*). In contrast, incubation of the cells with either group IV FF (*C*) or exogenous VEGF (*D*) caused a marked redistribution of actin fibers to transversely span the entire cell, with resulting stress fiber formation. Actin redistribution induced by either exogenous VEGF or group IV FF was substantially reversed by coincubation with VEGF antibody (*E* and *F*, respectively). This indicated that the VEGF content of the group IV FF was responsible for this architectural change within the EC, leading to increased vascular permeability.

Since we found that NO contributed to the increased permeability stimulated by group IV FF or exogenous VEGF, we assessed its contribution to the redistribution of actin. We found that L-NMMA significantly reversed the effect of the group IV FF to stimulate stress fiber formation (Fig. 4 *b*). These results provide a mechanism to understand the contribution by NO to the permeability enhancing action of the group IV FF.

We also examined the integrity of ZO-1 tight junction protein alignment at the borders of the apposed EC (Fig. 5). The distribution of ZO-1 at the borders is known to be discontinuous around the normal EC (24), as seen in *A*. Group I FF had no effect on this pattern (*B*). Group IV FF or exogenous VEGF each induced significant clumping and disruption of the ZO-1 tight junction protein (*C* and *D*), often leaving large gaps in ZO-1 expression (*arrowheads*). The disruption highly correlates with increased cell permeability (25). Coincubation of the cells with VEGF ab again substantially reversed the effects of either FF (*E*) or exogenous VEGF (*F*). This indicates an additional mechanism by which the VEGF in FF disrupts the integrity of EC tight junctions, leading to increased permeability.

Discussion

The symptoms that comprise the Ovarian Hyperstimulation Syndrome are felt to mainly result from the leakage of fluid from capillaries stimulated by an ovary-derived permeability factor. It is proposed that production of this factor is aug-

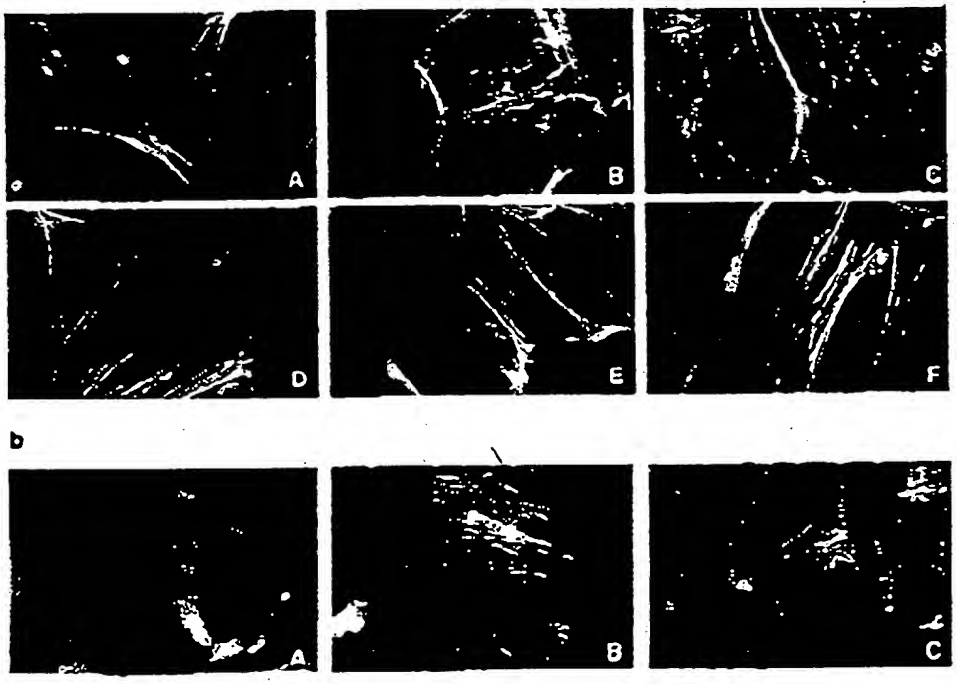

Figure 4 (*a*) F-actin distribution in cultured EC and the effects of FF or exogenous VEGF, 1 ng/ml. The white transverse lines represent phalloidin staining of the actin microfilaments. *A* is EC cultured in media alone; *B* is EC in the presence of group I FF; *C* is group IV (high oocytes) FF; *D* is exogenous VEGF, 1 ng; *E* is exogenous VEGF plus VEGF antibody; *F* is group IV FF plus VEGF antibody. A cortical (peripheral) distribution is seen in the control or low oocytes FF, but a transverse (stress fibers) distribution occurs in response to high oocyte FF or exogenous VEGF. Effects of FF or VEGF are substantially prevented by VEGF antibody. This study is representative of three separate studies. (*b*) Effect of L-NMMA on F-actin distribution induced by group IV FF. *A* is EC cultured in media alone; *B* is group IV FF-incubated EC; *C* is group IV FF plus L-NMMA, 10 μM. This study was repeated twice.

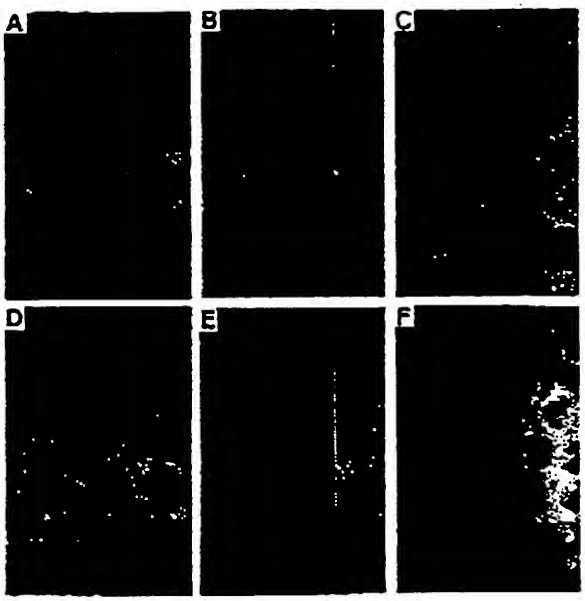

Figure 5. Distribution of the tight junction protein ZO-1 around apposed endothelial cells in response to FF or exogenous VEGF. Basal, discontinuous distribution of ZO-1 in EC is shown in *A*. *B* is EC in the presence of group I FF; *C* is group IV (high oocytes) FF; *D* is exogenous VEGF, 1 ng/ml; *E* is exogenous VEGF plus VEGF antibody; *F* is group IV FF plus VEGF antibody. Arrowheads denote areas of typical ZO-1 disruption (*C* and *D*). This representative study was repeated twice.

mented by gonadotropic hormones administered as part of the fertility procedure (2–4); the factor is then secreted or is leaked from the massively enlarged ovaries. The resulting vascular permeability leads mainly to peritoneal fluid collection, edema, and occasionally hypovolemia. Loss of intravascular volume is largely responsible for the morbidity and occasional mortality associated with OHSS (3).

The development of this syndrome correlates well with the ovarian response to gonadotropic hormones. This response includes large numbers of stimulated follicles and increased serum estradiol (E2) levels, parameters that define patients at increased risk for developing this disorder (26, 27). Previous studies have correlated vasoactive substance levels in the vasculature of ovary with the temporal development of OHSS. As a result, various intra- and extra-ovarian substances have been postulated to contribute to OHSS, including prostaglandins, histamine, serotonin, prolactin, angiotensin, and interleukin-2 (28–33). Our results here implicate VEGF as the ovarian factor produced during hormonal induction which directly leads to increased vascular permeability. VEGF is therefore likely to cause the manifestations of OHSS.

The actions of VEGF to enhance vascular permeability (6) may result in part from the effects of other vasoactive substances (34). Several actions of exogenous VEGF in vitro are partially dependent on the generation of NO from the target cell/organ, such as EC (34, 35). Our results indicate that the ability of the group IV FF to induce increased EC permeability is significantly, though not totally, dependent upon the generation of NO. We found similar dependance on NO for the permeability response to exogenous VEGF, supporting the findings of Murohara et al. (21). NO can induce increased vascular permeability through the activation of protein kinase G (36). NO can associate with and disrupt cytoskeletal protein complexing (37, 38) and can deplete ATP, leading to dilation of EC tight junctions (37) and the rearrangement of the actin cytoskeleton (39). The significant alterations of the cytoskeletal proteins of EC demonstrated in this study result in part from NO action.

The formation of the EC TJ modulates transendothelial solute exchange, and several proteins have been implicated in the dynamic formation of junctions. The association of TJ proteins (including ZO-1, ZO-2, and occludin) with both the actin cytoskeleton (40) and cadherin–catenin complex (41) are felt to play important roles (42). Disrupting EC tight junction protein complex formation results from the disorganization of the actin cytoskeleton (43, 44) and would lead to the endothelial fenestrations induced by VEGF (45). We believe this sequence of events underlies OHSS since we found that F-actin redistribution, formation of stress fibers, and ZO-1 protein destruction in response to group IV FF were each reversed by VEGF antibody. Recent in vitro studies showed that cadherin and occludin become disorganized at endothelial cell junctions in response to exogenous VEGF (46). Normally, complexing of ZO-1 proteins with occludin mediates occludin's localization to the tight junction and association with the cytoskeleton (25). VEGF-induced disruption of ZO-1 would 1) prevent this localization, and 2) markedly lower the electrical resistance of EC, resistance typifying an ionic barrier function (47).

Regarding the source of the permeability factor, VEGF transcripts and the protein isoforms VEGF121 and especially VEGF165 have been found in human ovarian tissue (15). Luteinized human ovarian granulosa cells, isolated from women undergoing hormonal stimulation for in vitro fertilization, express high concentrations of VEGF mRNA (16). In cultured bovine ovarian granulosa cells (GC), either LH or E2 can stimulate VEGF mRNA expression, but the effects of LH are more rapid (48). Cultured human GC respond to hCG with increased VEGF mRNA production (49); this leads us to speculate that in our patients there is a sequential action of the administered hormones (FSH, human menopausal gonadotropins, and hCG) to first directly stimulate VEGF production. This is followed by increased estrogen production that independently augments VEGF. High intraovarian levels of E2 are probably necessary for VEGF production and the clinical syndrome (50). Presumably, VEGF produced in the ovary acts locally, spills into the peritoneal cavity, and is also secreted into the blood. It has been shown that some women who develop OHSS have elevated levels of VEGF in their blood (51, 52), although the source of the VEGF is not clear, since vascular smooth muscle cells potently produce this growth factor. We found that ovarian FF contained the VEGF165 isoform by immunoblot. Since this same antibody blocked the ability of the FF to stimulate endothelial cell permeability, we propose that ovarian VEGF165 contributes to the clinical symptomatology.

Since increased vascular permeability also occurs at ovulation (53, 54), OHSS could be viewed as an exaggeration of the events that occur during the menstrual cycle. When this growth/permeability factor is produced in excess by the supraphysiologic hormonal induction of ovulation, it can lead to the clinical syndrome of OHSS. Recently, Kobayashi et al. (55) measured low levels of VEGF in the ascites from three women with OHSS, concentrations that did not produce increased

capillary permeability. This led them to conclude that VEGF may not be involved in the pathogenesis of this syndrome. In contrast, several studies have measured much higher concentrations of VEGF in th peritoneal fluid and/or serum of women who developed OHSS after fertility induction (50, 52, 56). In a previous study, peritoneal fluid from three women with OHSS induced increased capillary permeability, which was prevented by the VEGF antibody (57). There was no determination of the source of VEGF or mechanism of VEGF action. Our patients in group IV developed significant signs of OHSS, including edema and ascites, requiring bed rest and diuresis. Their FFs induced the greatest EC permeabilities, which were 98% reversed by the VEGF antibody. VEGF concentrations in the FF from the four group IV patients were more than three times those of group I patients, who were asymptomatic. Group IV individuals also produced the largest numbers of oocytes, and their FF caused EC cytoskeletal rearrangement, F-actin redistribution, and degradation of ZO-1 protein at the tight junction.

The collective data therefore supports an important role for VEGF in this syndrome. The increase in permeability stimulated by the FF from our patients was not linearly related to the absolute VEGF concentrations. This suggests that there is a threshold concentration of VEGF, which is necessary to induce EC permeability. It is difficult to definitively identify VEGF as the causative factor in vivo, because there is no VEGF receptor antagonist currently available. A naturally occurring truncated form of the VEGF receptor, *flt*, is an antagonist of some actions of VEGF (58), but its therapeutic use is unknown. We have recently demonstrated that stimulation of VEGF synthesis in cultured vascular smooth muscle cells is substantially inhibited by members of the natriuretic peptide family (59). Administration of these peptides might limit production of this growth factor in OHSS, potentially serving as a therapeutic approach in predisposed individuals.

In summary, FF from women undergoing hormonal ovarian stimulation significantly increased endothelial cell permeability, which correlated with the magnitude of oocyte production (an important index of the degree of stimulation). We have demonstrated that the FF factor responsible for increased EC permeability is VEGF and therefore is the likely factor leading to the important manifestations of OHSS. Rearrangement of the actin cytoskeleton and disruption of ZO-1 protein is a likely primary mechanism by which VEGF in the FF disrupts the EC tight junctions and increases permeability. Receptor antagonists or inhibitors of VEGF synthesis should prove useful in preventing the development of this disorder.

Acknowledgments

We would like to thank Dr. Rick Kendall (Merck Inc.) for providing VEGF protein and helpful discussions. This work was supported by grants from the Research Service of the Veteran's Administration, and the National Institutes of Health (NS-30521) to E.R. Levin.

References

1. Editorial. 1991. Ovarian hyper stimulation syndrome. *Lancet.* 337:1111–1112.

2. Polishuk, W.Z., and J.G. Schenker. 1969. Ovarian hyperstimulation syndrome. *Fertil. Steril.* 20:443–450.

3. Schenker, J., and D. Weinstein. 1978. Ovarian hyperstimulation syndrome: a current survey. *Fertil. Steril.* 30:225–267.

4. Haning, R., Jr., E. Strawn, and W. Nolten.1985. Pathophysiology of the ovarian hyperstimulation syndrome. *Obstet. Gynecol.* 166:220–224.

5. Goldsman, M., A. Pedram, C. Dominguez, L. Ciuffardi, E. Levin, and R.H. Asch. 1995. Increased capillary permeability induced by human follicular fluid: a hypothesis for an ovarian origin of the hyperstimulation syndrome. *Fertil. Steril.* 63:268–272.

6. Senger, D.R., S.J. Galli, A.M. Dvorak, C.A. Peruzzi, V.S. Harvey, and H.F. Dvorak. 1983. Tumor cells secrete a vascular permeability factor that promotes accumulation of ascites fluid. *Science.* 219:983–985.

7. Milton, S.G., and K.P. Knutson. 1990. Comparison of the function of the tight junctions of the endothelial cells and epithelial cells in regulating the movement of electrolytes and macromolecules across the cell monolayer. *J. Cell. Physiol.* 144:498–504.

8. Larson, D.M. 1988. Intercellular junctions and junctional transfer in the blood vessel wall. *In* Endothelial Cells. Vol III. U.S. Ryan, editor. CRC Press, Boca Raton, FL. 75–84.

9. Keck, P.J., S.D. Hauser, G. Krivi, K. Sanzo, T. Warren, J. Feder, and D.T. Connolly. 1989. Vascular permeability factor, an endothelial cell mitogen related to PDGF. *Science.* 246:1309–1312.

10. Aiello, L.P., R.L. Avery, P.G. Arrigg, B.A. Keyt, H.D. Jampel, S.T. Shah, L.R. Pasquale, H. Thieme, M.A. Iwamoto, J.E. Park, et al. 1994. Vascular endothelial cell growth factor in ocular fluid of patients with diabetic retinopathy and other retinal disorders. *N. Engl. J. Med.* 331:1480–1487.

11. Kim, K.J., B. Li, J. Winer, M. Armanini, N. Gillett, H.S. Phillips, and N. Ferrara. 1993. Inhibition of vascular endothelial cell growth factor-induced angiogenesis suppresses tumor growth in vivo. *Nature.* 362:841–844.

12. Millauer, B., L.K. Shawver, K.H. Plate, W. Risau, and A. Ullrich. 1994. Glioblastoma growth inhibited in vivo by a dominant negative Flk-1 mutant. *Nature.* 367:576–579.

13. Terman, B.I., M. Dougher-Vermazen, M.E. Carrion, D. Dimitrov, D.C. Armellino, D. Gospodarowicz, and P. Böhlen. 1992. Identification of the KDR tyrosine kinase as a receptor for vascular endothelial cell growth factor. *Biochem. Biophys. Res. Commun.* 187:1579–1586.

14. deVries, C., J.A. Escobedo, H. Ueno, K. Houck, N. Ferrarra, and L.T. Williams. 1992. The fms-like tyrosine kinase, a receptor for vascular endothelial cell growth factor. *Science.* 255:989–991.

15. Olson, T.A., D. Mohanraj, L.F. Carson, and S. Ramakrishnan. 1994. Vascular permeability factor gene expression in normal and neoplastic human ovaries. *Cancer Res.* 54:276–280.

16. Yan, Z., H.A. Weich, W. Bernart, M. Breckwoldt, and J. Neulen. 1993. Vascular endothelial cell growth factor (VEGF) messenger ribonucleic acid (mRNA) expression in luteinized human granulosa cells in vitro. *J. Clin. Endocrinol. Metab.* 77:1723–1725.

17. Prins, B., R.M. Hu, B. Nazario, A. Pedram, H.J.L. Frank, M. Weber, and E.R. Levin. 1994. Prostaglandin E_2 and prostacyclin inhibit the production and secretion of endothelin from cultured endothelial cells. *J. Biol. Chem.* 269: 11938–11944.

18. Ma, T.Y., D. Hollander, D. Bhalla, H. Nguyen, and P. Krugliak. 1992. IEC-18 a nontransfromed small intestinal cell line for studying epithelial permeability. *J. Lab. Clin. Med.* 120:329–341.

19. Levin, E.R. 1988. Atrial natriuretic factor is detectable in human cerebrospinal fluid. *J. Clin. Endocrinol. Metab.* 66:1080–1083.

20. Hu, R.M., E.R. Levin, A. Pedram, and H.J.L. Frank. 1992. Atrial natriuretic peptide inhibits the translation and secretion of endothelin from cultured bovine aortic endothelial cells: mediation through C receptors. *J. Biol. Chem.* 267:17384–17389.

21. Murohara, T., J.R. Horowitz, M. Silver, Y. Tsurumi, D. Chen, A. Sullivan, and J.M. Isner. 1998. Vascular endothelial growth factor/vascular permeability factor enhances vascular permeability via nitric oxide and prostacyclin. *Circulation.* 97:99–107.

22. Ferrara, N., J. Winer, and T. Burton. 1991. Aortic smooth muscle cells express and secrete vascular endothelial cell growth factor. *Growth Factors.* 5: 141–148.

23. Schneeberger, E.E., and R.D. Lynch. 1992. Structure, function, and regulation of cellular tight junctions. *Am. J. Physiol.* 262:L647–L661.

24. Barry, P.A., W.M. Petroll, P.M. Andrews, H.D. Cavanagh, and J.V. Jester. 1995. The spatial organization of corneal endothelial cytoskeletal proteins and their relationship to the apical junctional complex. *Invest. Ophthalmol. Vis. Sci.* 36:1115–1124.

25. Furuse, M., M. Itoh, T. Hirase, A. Nagafuchi, S. Yonemura, and S. Tsukita. 1994. Direct association of occludin with ZO-1 and its possible involvement in the localization of occludin at tight junctions. *J. Cell Biol.* 127:1617–1626.

26. Haning, R.V., Jr., C.W. Austin, I.H. Carlson, D.L. Kuzma, S.S. Shapiro, and W.J. Zweibel. 1983. Plasma estradiol is superior to ultrasound and urinary estriol glucuronide as a predictor of ovarian hyperstimulation during induction of ovulation with menotropins. *Fertil. Steril.* 40:31–36.

27. Asch, R.H., H.P. Li, J.P. Balmaceda, L.N. Weckstein, and S.C. Stone. 1991. Severe ovarian hyperstimulation syndrome in assisted reproductive technology: definition of high risk groups. *Hum. Reprod.* 6:1395–1399.

28. Schenker, J., and W. Polishuk. 1976. The role of prostaglandins in the

hyperstimulation syndrome. *Eur. J. Obstet. Gynecol. Reprod. Biol.* 6:47–52.

29. Pride, S., B. Yuen, and Y. Moon. 1984. Clinical, endocrinologic and intraovarian prostaglandin responses to H1 receptor blockade in the ovarian hyperstimulation syndrome: studies in the rabbit model. *Am. J. Obstet. Gynecol.* 148:670–674.

30. Zaidse, L., M. Friedman, E. Lindenbaum, R. Askenazi, B. Peretz, and E. Paldi. 1983. Serotonin and the ovarian hyperstimulation syndrome. *Eur. J. Obstet. Gynecol. Reprod. Biol.* 15:55–60.

31. Leung, P., B. Yuen, and Y. Moon. 1983. Effect of prolactin in an experimental model of the ovarian hyperstimulation syndrome. *Am. J. Obstet. Gynecol.* 145:847–850.

32. Navot, D., L.J. Margalioth, N. Laufer, A. Drzejinski, A. Biderfeld, and J.G. Schenker. 1987. Direct correlation between plasma renin activity and severity of the ovarian hyperstimulation syndrome. *Fertil. Steril.* 48:57–61.

33. Orvieto, R., I. Volfovitch, P. Fishman, and Z. Ben-Rafael. 1995. Interleukin-2 and ovarian hyperstimulation syndrome: a pilot study. *Hum. Reprod.* 10:24–27.

34. Wu, H.M., H. Qiaobing, Y. Yuan, and H.J. Granger. 1996. VEGF induces NO-dependent hyperpermeability in coronary venules. *Am. J. Physiol.* 271:H2735–H2739.

35. Zicha, M., L. Morbidelli, R. Choudhuri, H.T. Zhang, S. Donnini, H.J. Granger, and R. Bicknell. 1997. Nitric oxide synthase lies downstream of vascular endothelial cell growth factor–induced but not fibroblast growth factor–induced angiogenesis. *J. Clin. Invest.* 11:2625–2634.

36. Venema, V.J., M.B. Marrero, and R.C. Venema. 1996. Bradykinin-stimulated protein tyrosine kinase phosphorylation promotes endothelial nitric oxide synthase translocation to the nucleus. *Biochem. Biophys. Res. Commun.* 226:703–710.

37. Clancy, R.M., J. Rediske, X. Tang, N. Nijher, S. Frenkel, M. Philips, and S.B. Abramson. 1997. Outside-in signaling in the chondrocyte. Nitric oxide disrupts fibronectin-induced assembly of a subplasmalemmal actin/rho A/focal adhesion kinase signaling complex. *J. Clin. Invest.* 100:1789–1796.

38. Salzman, A.L., M.J. Menconi, N. Unno, R.M. Bezzell, D.M. Casey, P.K. Gonzalez, and M.P. Fink. 1995. Nitric oxide dilates tight junctions and depletes ATP in cultured Caco-2BBe intestinal epithelial monolayers. *Am. J. Physiol.* 268:G361–G373.

39. Bacallao, R., A. Garfinkel, S. Monke, G. Zampighi, and L.J. Mandel. 1994. ATP depletion: a novel method to study junctional properties in epithelial tissues. I. Rearrangement of the actin cytoskeleton. *J. Cell Sci.* 107:3301–3313.

40. Gumbiner, B.M. 1996. Cell adhesion: the molecular basis of tissue architecture and morphogenesis. *Cell.* 84:345–357.

41. Haselton, F.R., and R.L. Heimark. 1997. Role of cadherins 5 and 13 in the aortic endothelial barrier. *J. Cell. Physiol.* 171:243–251.

42. Tsukamoto, T., and S.K. Nigam. 1997. Tight junction proteins form large complexes and associate with the cytoskeleton in an ATP depletion model for reversible junction assembly. *J. Biol. Chem.* 272:16133–16139.

43. Bacallao, R., A. Garfinkel, S. Monke, G. Zampighi, and L.J. Mandel. 1994. ATP depletion: a novel method to study junctional properties in epithelial tissues. I. Rearrangement of the actin cytoskeleton. *J. Cell Sci.* 107:3301–3313.

44. Kwon, O., W.J. Nelson, R. Sibley, P. Huie, J.D. Scandling, D. Dafoe, F. Alfrey, and R.D. Myers. 1998. Backleak, tight junctions, and cell-cell adhesion in postischemic injury to the renal allograft. *J. Clin. Invest.* 101:2054–2064.

45. Roberts, W.G., and G.E. Palade. 1995. Increased microvascular permeability and endothelial fenestration induced by vascular endothelial growth factor. *J. Cell Sci.* 108:2369–2379.

46. Kevil, C.G., D.K. Payne, E. Mire, and J.S. Alexander. 1998. Vascular permeability factor/vascular endothelial cell growth factor–mediated permeability occurs through disorganization of endothelial junctional proteins. *J. Biol. Chem.* 273:15099–15103.

47. Blum, M.S., F. Toninelli, J.M. Anderson, M.S. Balda, J. Zhou, L. O'Donnell, R. Pardi, and J.R. Bender. 1997. Cytoskeletal rearrangement mediates human microvascular endothelial tight junction modulation by cytokines. *Am. J. Physiol.* 273:H286–H294.

48. Garmoo, C., S. Saule, and D. Gospodarowicz. 1993. Transcriptional regulation of vascular endothelial cell growth factor gene expression in ovarian bovine granulosa cells. *Growth Factors.* 8:109–117.

49. Neulen, J., Y. Yan, S. Raczek, K. Weindel, C. Keck, H.A. Weich, D. Marmé, and M. Breckwoldt. 1995. Human chorionic gonadotropin-dependent expression of vascular endothelial growth factor/vascular permeability factor in human granulosa cells: importance in ovarian hyperstimulation syndrome. *J. Clin. Endocrinol. Metab.* 80:1967–1971.

50. Krasnow, J.S., S.L. Berga, D.S. Guzick, A.J. Zeleznik, and K.T. Yeo. 1996. Vascular permeability factor and vascular endothelial growth factor in ovarian hyperstimulation syndrome: a preliminary report. *Fertil. Steril.* 65:552–555.

51. Pride, S.M., C. James, and B. Yuen. 1990. The ovarian hyperstimulation syndrome. *Semin. Reprod. Med.* 8:241–249.

52. Abramov, Y., V. Barak, B. Nisman, and J.G. Schenker. 1997. Vascular endothelial cell growth factor plasma levels correlate to the clinical picture in severe ovarian hyperstimulation syndrome. *Fertil. Steril.* 67:261–265.

53. Bassett, D.L. 1943. The changes in the vascular pattern of the ovary of the albino rat during estrus cycle. *Am. J. Anat.* 73:251–291.

54. Carcuder, J.L., and W.J. Murdoch. 1988. Morphological studies of the microcirculatory system of periovulatory ovine follicles. *Biol. Reprod.* 39:989–997.

55. Kobayashi, H., Y. Okada, T. Asahina, J. Gotoh, and T. Terao. 1998. The kallikrein-kinin system, but not vascular endothelial cell growth factor, plays a role in the increased vascular permeability associated with ovarian hyperstimulation syndrome. *J. Mol. Endocrinol.* 20:363–374.

56. Lee, A., L.K. Christenson, R.L. Stouffer, K.A. Burry, and P.E. Patton. 1997. Vascular endothelial cell growth factor levels in serum and follicular fluid of patients undergoing in vitro fertilization. *Fertil. Steril.* 68:305–311.

57. McClure, N., D.L. Healy, and P.A.W. Rogers. 1994. Vascular endothelial cell growth factor as permeability agent in ovarian hyperstimulation syndrome. *Lancet.* 344:235–236.

58. Kendall, R.L., and K.A. Thomas. 1993. Inhibition of vascular endothelial cell growth factor activity by an endogenously encoded soluble receptor. *Proc. Natl. Acad. Sci. USA.* 90:10705–10709.

59. Pedram, A., M. Razandi, R.M. Hu, and E.R. Levin. 1997. Vasoactive peptides modulate vascular endothelial cell growth factor production and endothelial cell proliferation and invasion. *J. Biol. Chem.* 272:17097–17103.

Brain edema in meningiomas is associated with increased vascular endothelial growth factor expression.

Goldman CK; Bharara S; Palmer CA; Vitek J; Tsai JC; Weiss HL; Gillespie GY

Brain Tumor Research Laboratories, University of Alabama School of Medicine, Birmingham, USA.

Neurosurgery (UNITED STATES) Jun 1997, 40 (6) p1269-77, ISSN 0148-396X Journal Code: NZL

Contract/Grant No.: NS31096, NS, NINDS; CA13148, CA, NCI

Languages: ENGLISH

Document type: JOURNAL ARTICLE

JOURNAL ANNOUNCEMENT: 9710

Subfile: INDEX MEDICUS

OBJECTIVE: Vascular permeability factor/vascular endothelial growth factor (VPF/VEGF), an endothelial cell-specific cytokine, induces proliferation of endothelial cells and increases vascular permeability dramatically. All gliomas secrete significant amounts of VEGF, whereas meningiomas are variable in expression. Thus, we sought to determine whether the extent of VPF/VEGF expression in meningiomas correlated with differences in brain edema associated with these tumors. METHODS: Meningioma tissue samples from 37 patients (15 men, average age 65 +/- 13 yr; 22 women, average age 60 +/- 10 yr) who underwent surgery at or were referred to the University of Alabama Hospital were examined retrospectively for the extent of expression of immunoreactive VPF/VEGF. Additionally, peritumoral edema was assessed on a blinded basis radiographically from preoperative magnetic resonance imaging scans. Selected specimens were examined by in situ hybridization to document the source of VPF/VEGF. RESULTS: The predominant meningioma subclassifications were transitional (57%) or meningothelial (27%) subtypes. VPF/VEGF immunoreactivity ranged from 0 to 3.5, with a median value of 2 on a subjective 5-point scale; magnetic resonance imaging-assessed edema ranged in extent from 0 to 4 (subjective 5-point scale), with a median value of 2.5. The correlation of determination (R2) of magnetic resonance imaging-assessed tumor edema rating and VPF/VEGF staining intensity rating was 0.6087 ($r = 0.78$; $P = 0.0001$). In situ hybridization localized VPF/VEGF messenger ribonucleic acid in meningioma cells and not in normal parenchymal brain cells. CONCLUSION: These data suggest that meningioma-associated edema may be a result of the capacity of meningioma cells to produce VPF/VEGF locally, leading to increased tumor neovascularization and enhanced vascular permeability.

Rat brain VEGF expression in alveolar hypoxia: possible role in high-altitude cerebral edema

FENGPING XU AND JOHN W. SEVERINGHAUS
Department of Anesthesia, University of California Medical School, San Francisco, California 94143-0542

Xu, Fengping, and John W. Severinghaus. Rat brain VEGF expression in alveolar hypoxia: possible role in high-altitude cerebral edema. *J. Appl. Physiol.* 85(1): 53–57, 1998.—The mechanism by which hypoxia causes high-altitude cerebral edema (HACE) is unknown. Tissue hypoxia triggers angiogenesis, initially by expressing vascular endothelial growth factor (VEGF), which has been shown to increase extracerebral capillary permeability. This study investigated brain VEGF expression in 32 rats exposed to progressively severe normobaric hypoxia (9–6% O_2) for 0 (control), 3, 6, or 12 h or 1, 2, 3, or 6 days. O_2 concentration was adjusted intermittently to the limit of tolerance by activity and intake, but no attempt was made to detect HACE. Northern blot analysis demonstrated that two molecular bands of transcribed VEGF mRNA (~3.9 and 4.7 kb) were upregulated in cortex and cerebellum after as little as 3 h of hypoxia, with a threefold increase peaking at 12–24 h. Western blot revealed that VEGF protein was increased after 12 h of hypoxia, reaching a maximum in ~2 days. The expression of *flt-1* mRNA was enhanced after 3 days of hypoxia. We conclude that VEGF production in hypoxia is consistent with the hypothesis that angiogenesis may be involved in HACE.

angiogenesis; cytokines; brain capillary leak; acute mountain sickness

HIGH-ALTITUDE CEREBRAL EDEMA (HACE) is one form of severe acute mountain sickness. The pathophysiological link between hypoxia and HACE is poorly understood. Pathological findings include retinal and presumably other cerebral petechial hemorrhages, cerebral thrombosis, and brain edema (21). The possibility that hypoxia might initiate angiogenesis in brain and underlie HACE was supported by the finding of increased capillary density in hypoxic rat brain (9, 14, 15) and by the observation that dexamethasone, widely used to prevent and treat HACE, is an effective blocker of angiogenesis (21).

Tissue hypoxia is thought to upregulate a series of local factors that contribute to angiogenesis, the growth of new capillary vessels. A complex cascade of cellular responses, triggered by local hypoxia, increased lactate, and/or low redox state, results in capillary basement membrane dissolution and rupture, as well as plasma and red blood cell extravasation. Endothelial cell budding and growth toward the hypoxic region normally follow. In recent years, many putative angiogenic factors have been identified, including vascular endothelial growth factor (VEGF), epidermal growth factor, transforming growth factors-α and -β, tumor angiogenesis factor, angiogenin, tumor necrosis factor-α, acidic and basic fibroblast growth factors, platelet-derived endothelial cell growth factor, and interleukin-8. Among these, VEGF is thought to be the most potent and specific in the basement membrane destruction and leakage. VEGF has been described as a specific in vitro endothelial cell mitogen and as an angiogenic inducer in several in vivo models (1). It is also known as a vascular permeability factor by virtue of its permeability-enhancing effects that, on a molar basis, enhanced the permeability of normal venules and small veins with a potency some 50,000 times that of histamine (20). VEGF has been shown to be upregulated by hypoxia both in vitro and in vivo (17, 24). It has not previously been sought during systemic hypoxia in brain where the blood-brain barrier might exclude such protein cytokines.

Angiogenesis in the brain normally occurs only during growth (19). Endothelial cell proliferation is low in the adult brain. Angiogenesis can occur in brain under pathological conditions such as infarction and tumor growth. VEGF has been detected in brain tumor tissue and was reported to be expressed in rat cerebellum and mouse choroid plexus (3, 16) and after surgical trauma (tumor removal) (21). Cerebral venous thrombosis, a complication of HACE, is consistent with the ability of VEGF to increase von Willebrand factor release (4) and thromboplastin activity (7).

We report here the expression of both VEGF mRNA and VEGF protein in rat brain as a function of time of inhalational hypoxic exposure, and we suggest that this may contribute to HACE.

MATERIALS AND METHODS

Animal experiments. All studies had prior approval of the committee on Animal Research, University of California, San Francisco. Adult Sprague-Dawley rats (Hilltop Strain, Banpin & Kingman) of either sex (weight 280–300 g) were housed in an aquarium with a plastic cover, kept in normal circadian rhythms (dark at night), and were supplied with food and water. A continuous fresh gas flow was supplied to the chamber, keeping the CO_2 concentration below 1%. Ambient O_2 concentration was reduced to ~9% initially, and it was reduced progressively over the next hours, in response to activity, to as low as 6%. Generally, the O_2 concentration was lowered ~1% every 3 h during the first day until the animals showed little activity and a decreased intake of food and water. Eight rats were housed in the same chamber for each group to ensure equal hypoxic exposures for all animals. The rats were harvested one at a time after eight hypoxic exposures of 0 (control), 3, 6, or 12 h or 1, 2, 3, or 6 days. The procedure was repeated for a total of four runs, each with eight rats. General appearance, activity, response to stimuli, and intake and excretion were recorded daily. O_2 and CO_2 concentrations were continuously monitored over the 6-day period with use of a PDP 11/44 computer and Perkin Elmer 1100 mass spectrometer. The rats were anesthetized with halothane and then decapitated. Brains were quickly re-

moved, frozen with liquid nitrogen, and stored at −80°C. Brain edema was not quantified.

Biochemical and biological reagents. Recombinant human $VEGF_{165}$ ($rhVEGF_{165}$) (R & D Systems, Minneapolis, MN) was diluted with PBS/BSA (0.3%) to 1 μg/5 ml, aliquoted, and stored at −80°C. VEGF cDNA (393 bp cloned into pGEM3 plasmid) was a gift from Dr. Larry Brown (Beth Israel Hospital, Boston, MA). *Flt-1* cDNA (458 bp in pGEM3Z) was a gift from Dr. Rubin M. Tuder (Department of Pathology, University of Colorado Health Sciences Center). Mouse β-actin (Ambion, Austin, TX) is a linearized pTRPLEscript plasmid containing a 250-bp mouse β-actin gene fragment. 28S ribosome (Ambion) is a linearized pTRPLEscript plasmid containing a 115-bp cDNA fragment of the human 28S rRNA gene. Polyclonal rabbit antibody against rhVEGF was purchased from Santa Cruz Biotechnology. Anti-rabbit IgG conjugated with horseradish peroxidase was obtained from Vector Laboratories (Burlingame, CA). The 0.24- to 9.5-kb RNA ladder used in Northern blot analysis was obtained from GIBCO-BRL Life Technologies. The rainbow-colored protein molecular-weight marker used in Western blot analysis was purchased from Amersham Life Science.

Northern blot hybridization. Total RNA was isolated from 100-mg pieces from cerebral cortex of rat brain by using a single-step method. Tissue was homogenized in 1 ml of RNA STAT-60 (TEL-TEST"B", Friendswood, TX) by using polytron homogenizer. The total RNA was extracted with chloroform and precipitated with isopropanol followed by a wash with 70% ethanol. The RNA pellet was dissolved in Tris-EDTA buffer (pH 7.5), and the optical density was determined by Shimadzu Recording Spectrophotometer UV-1601. Ten micrograms of total RNA were denatured at 65°C in formamide- and bromide-containing loading buffer and were subsequently electrophoresed on a 1% agarose gel containing 2.2 M formaldehyde in 1× MOPS-EDTA-NaOAc buffer. RNA was transferred to nylon membranes (Hybond N, Amersham International PLC, Aylesbury, Bucks, UK) in 20× NaCl-NaH_2PO_4-EDTA buffer. Blots were cross-linked by ultraviolet irradiation (UV Statalinker, Stratagene), prehybridized in a seal-a-meal bag at 50°C for 1 h in prehybridization solution (1 M NaCl, 1% SDS), and then hybridized at 65°C overnight in hybridization solution (1 M NaCl, 1% dextran sulfate, and 100 μg/ml denatured salmon sperm DNA). The cDNA probes used for hybridization were labeled with [^{32}P]dCTP (New England Nuclear, Boston, MA) to a specific activity of $1–2\times10^9$ counts · min^{-1} · μg DNA^{-1} by using the random dexamer labeling method (Redprime DNA Labeling System, Amersham). Denatured labeled DNA probe was added to the hybridization solution to a final concentration of 1×10^6 counts · min^{-1} · ml^{-1}. After overnight hybridization, the blots were washed twice in 2× NaCl-NaH_2PO_4-EDTA buffer with 0.1% SDS at room temperature for 5 min each, and then at 65°C for 5–30 min, and were exposed overnight to X-ray film with intensifying screens at −80°C. Blots probed for VEGF mRNA were stripped by boiling in 0.1% SDS for 5 min, and the blot was left in the solution until the solution returned to room temperature. All the blots were reprobed for β-actin and 28S antisense RNA probe in a similar manner to permit loading and blotting differences between lanes to be compensated. β-Actin and 28S RNA probes were prepared by T7 RNA polymerase and labeled with [^{32}P]UTP (>2,000 Ci/mmol; New England Nuclear, Boston, MA) with the use of MAXIscript in vitro transcription kits (Ambion). The intensity of the signals was quantified by a scanning densitometer.

Western blot analysis. Samples (100 mg) of rat brain cortex from the same brains used for Northern blot analysis were homogenized thoroughly in 1 ml of lysis buffer (0.01 M Tris · HCl, pH 7.6, 0.1 M NaCl, 0.1 mM dithiothreitol, 0.001 M EDTA, 0.1% NaN_3, 1 μg/μl leupeptin, 100 μg/ml phenylmethylsulfonyl fluoride, 1 μg/μl aprotinin, 1% NP-40). The extracts were centrifuged in a microfuge at 12,000 *g* for 5 min to remove particles. Total protein was determined by using bicinchoninic acid protein assay reagent (Pierce, Rochford, IL). Forty micrograms of total protein dissolved in sampler buffer containing 2-mercaptoethanol were loaded into each individual lane. Twenty micrograms of 1 μg/ml rhVEGF were used as a positive control. The proteins were then separated by 10% SDS-PAGE at 4°C at 15 mA for 30 min followed by 20 mA for 2–3 h until the blue dye reached the bottom of the gel. The proteins were then transferred onto Hybond enhanced chemiluminescence (ECL) nitrocellulose membrane (Amersham) with constant current of 200 mA at 4°C for at least 4 h. After transfer, the nitrocellulose blot was blocked overnight with 10% solution of dry milk to prevent nonspecific staining. It was then incubated for 1 h at room temperature with polyclonal antibody against rhVEGF, at a 1:500 dilution, in 10% dry milk in Tris-buffered saline/0.1% Tween, with gentle agitation. Subsequently, the filter was rinsed several times and incubated for 1 h at room temperature with anti-rabbit IgG horseradish peroxidase conjugate at a dilution of 1:20,000 in 1% solution of dry milk. Immunoreactive proteins were detected with use of the ECL Western Blotting Detection System (Amersham). The membrane was exposed to Hyper film ECL (Amersham) at room temperature for 5 min to 2 h.

Statistics. Results are expressed as a ratio of relative intensity of VEGF to β-actin at the corresponding time point. Mean values for total VEGF/β-actin, upper bands of VEGF/β-actin, as well as lower bands of VEGF/β-actin were compared by unpaired Student's *t*-test statistical analysis. Results were considered as statistically significant at $P < 0.05$.

RESULTS

Expression of VEGF mRNA in response to hypoxia in vivo. Figure 1 shows autoradiographs of Northern blots of total RNA from rat brain cortex for one run, with samples after each of the eight test periods. The *top* panel shows the hybridization signal for VEGF, the *middle* panel shows the signal for mouse β-actin, and the *bottom* panel shows the signal for the 28S ribosome. RNA from rat brain exhibited two hybridization signal bands for VEGF at ~3.9 and 4.7 kb. Hybridization patterns with RNA for β-actin were used as an index of the amount of total RNA applied to each lane. 28S ribosome was also used to correct for loading variation of total RNA on each lane. To normalize the data between individual blots, the relative intensities for the hybridization signal (intensity of VEGF mRNA signal divided by intensity of respective β-actin or 28S) are presented in Fig. 2. There are significant ($P < 0.05$) differences in the relative intensities of both 3.9 and 4.7 kb, as well as the total VEGF mRNA signal between the normal and hypoxic rat brains. No differences were observed between the relative intensities when β-actin was used as reference and those when 28S was used as reference.

After the rats were exposed to hypoxia for as little as 3 h, their VEGF mRNA levels were remarkably increased, reaching a maximum at ~12 h. Brain VEGF mRNA increased about threefold within the first 24 h. Scanning densitometric analysis showed that the maxi-

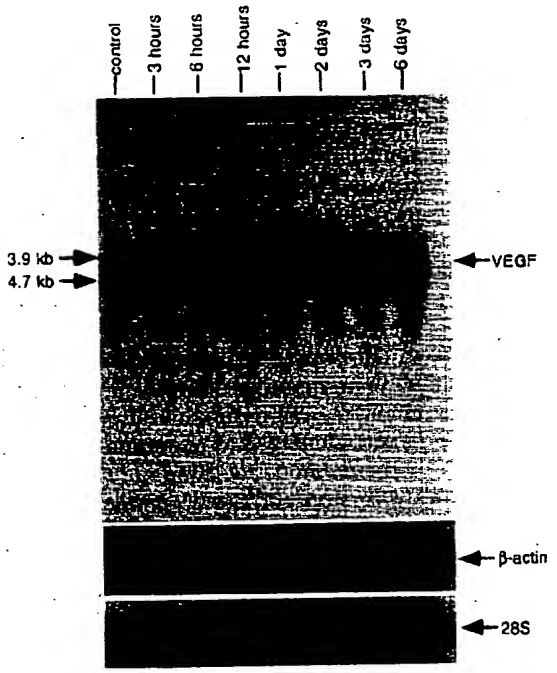

Fig. 1. Expression and response to hypoxia of vascular endothelial growth factor (VEGF) mRNA in rat brain. Total RNA was extracted from normal rats (control) or rats exposed to 9–6% O_2 for 3 h–6 days. Total RNA (10 μg) was loaded in each lane. Northern blots of total RNA sequentially hybridized with VEGF (*top*), β-actin (*middle*), and 28S (*bottom*) probes are shown.

mal effect occurred in 12–24 h. Enhanced VEGF mRNA persisted for at least 6 days.

Induction of VEGF protein production by hypoxia. We performed SDS-PAGE under reducing conditions and Western blot analysis on homogenized whole brain to detect VEGF protein as expected with VEGF mRNA expression. As shown in Fig. 3, one protein band at 23 kDa was detected with use of a polyclonal antibody to human VEGF. VEGF in rat brain was not increased until 12 h of hypoxia, although the VEGF mRNA increased as early as 3 h in hypoxia. A maximum induction of VEGF protein was reached after 2 and 3 days of hypoxia.

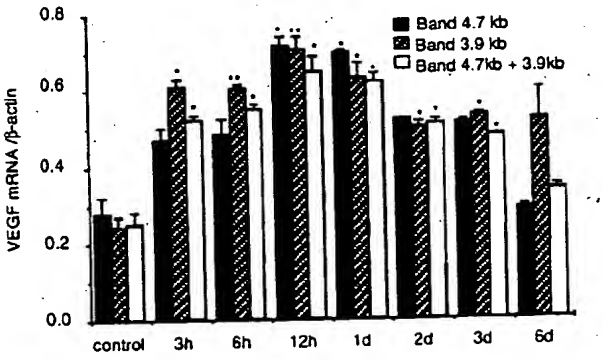

Fig. 2. Effects of hypoxia on VEGF mRNA expression in rat brain. Means ± SE are shown of VEGF mRNA optical density corrected for β-actin in rat brains removed during phases shown on horizontal axis. d, Day. Significantly different from control: $^{*}P < 0.05$, $^{**}P < 0.01$.

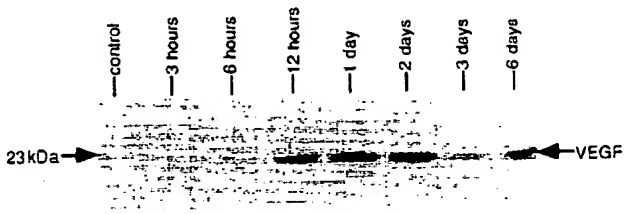

Fig. 3. Western blot analysis of brain tissue extract of normal rat (control) and rat exposed to hypoxia for 3 h–6 days. Total protein (40 μg) resolved under reducing condition (100 mM of 2-mercaptoethanol) was loaded in each lane and separated by 10% SDS-PAGE. Nitrocellulose blot was immunostained with polyclonal antibody against recombinant human VEGF. Band at 23 kDa is consistent in size to monomer of $VEGF_{165}$.

Upregulation of flt-1 mRNA during hypoxia. Northern blot analysis was performed for the mRNA expression of *flt-1*, one of the two VEGF receptors, in normal and hypoxic rat brain tissue. Figure 4 showed that *flt-1* mRNA was induced in rat brain after 3 days of hypoxia but then fell despite constant severe hypoxia.

DISCUSSION

Hypoxic exposure of awake rats induced a significant increase in brain VEGF mRNA expression as well as VEGF protein production. Interestingly, VEGF was upregulated primarily during the first few days of continued hypoxia, similar to the time course encountered in the development of symptoms and signs of HACE in humans ascending too rapidly to high altitude. The expression of VEGF mRNA was increased within 3 h of hypoxia, reached a peak at 12–24 h, and then declined. The production of VEGF protein peaked

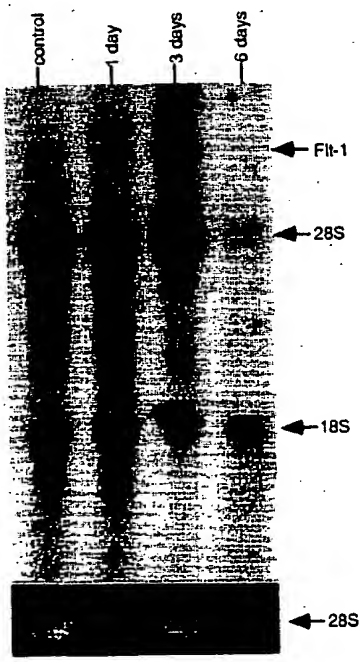

Fig. 4. Expression of *flt-1* mRNA in rat brain tissue after hypoxia. Total mRNA (10 μg) from normal rats or rats exposed to hypoxia for 1, 3, or 6 days was loaded in each lane. Blot was hybridized with *flt-1* cDNA probe. 28S ribosome in ethidium bromide-stained gel was used as reference for normalizing total RNA loading.

at 48 h. Similar results were reported by others. In rat heart muscle after coronary arterial ligation, Hashimoto et al. (10) found that VEGF mRNA was evident at 30 min, peaked at 1–2 h, and decreased at 6 h, suggesting that VEGF is an early and transient regulatory factor in response to hypoxia. Tuder et al. (24) reported that VEGF mRNA increased within 2 h of hypoxia in the isolated perfused anoxic lung. VEGF mRNA was also expressed during chronic hypoxia for up to 32 days (24). Previous evidence showed that VEGF was inducible by local (ischemic) hypoxia in brain (23). It was reported that, in brain tumors, VEGF mRNA was strongly expressed in the most ischemic and necrotic areas while not present in the white matter of normal brain where gliomas normally arise (23).

VEGF expression in rat brain tissue after hypoxia suggests a possible role for VEGF in regulating baseline microvascular permeability, perhaps facilitating tissue nutrition and waste removal. Our observations support the thesis that VEGF may act as a mediator in the process of hypoxic cerebral edema, assuming the role of a link between tissue hypoxia and an angiogenesis response. LaManna et al. (14) demonstrated capillary budding in superficial cerebral cortex of rats exposed to 1 wk of 0.5 atm in an hypobaric chamber. They also presented evidence that capillary density in rat brain increased after 3 wk of moderate hypoxia (380 Torr) (15). The increased vascularity of the brain in hypobaric hypoxia progresses from an early phase of the microvascular hypertrophy to later microvascular hyperplasia (9). Although our present results could not determine whether increased expression of VEGF led to neovascularization, other studies showed evidence that sustained production of VEGF in hypoxic brain is likely to elicit an angiogenic response (9). First, there is a significant elevation of VEGF gene expression in highly vascularized and edema-associated brain tumor, compared with brain tumors with less neovascularization and little or no edema (2). In extensively vascularized tumors such as gliomas and glioblastomas, the degree of vascularity appears to be related quantitatively to VEGF expression (23). Second, anti-VEGF antibody can block capillary ingrowth into tumors (13). Third, a cause-and-effect relationship between VEGF production and neovascularization was established through the observations of the angiogenic effect of VEGF. Banai et al. (1) showed that, after 4 wk of treatment, the numerical density of intramyocardial distribution vessels was increased by 89% by administration of VEGF into the coronary bed of ischemic myocardium, compared with saline-treated hearts. Their results suggested involvement of VEGF in coronary capillary regrowth in ischemic hearts (10). In regard to HACE, the permeability-enhancing effect of VEGF, which has been found to be 50,000 times more potent than histamine (20), on microvascular vessels may play an important role in the development of cerebral edema under high-altitude exposure. Its stimulation of von Willebrand factor from endothelial cells (4) and induction of thromboplastin activity (7) may be associated with the formation of cerebral thrombosis and petechial hemorrhage in HACE. In our animal model, brain surface vascularity appeared more congested in the hypoxic animals than in controls. Along with the thrombosis and petechial hemorrhage in HACE, brain edema increases interstitial pressure and may lead to compression closure of capillaries, adding local ischemia to tissue hypoxia, which, in return, is a potent inducer of VEGF production (23).

Two VEGF mRNA transcriptions of 3.9 and 4.7 kb were found by Northern blot analysis in rat brain tissue. The signal intensity of both VEGF mRNA transcriptions at 12–24 h after hypoxia was increased up to threefold in hypoxic brain compared with normal brain. The 3.9-kb pattern of hybridization on Northern blot analysis was identical to that observed by others in rats (10, 16). As previously described (11), VEGF may exist in four different homodimeric molecular species because of alternative splicing of mRNA, with each monomer having 121, 165, 189, or 206 amino acids ($VEGF_{121}$, $VEGF_{165}$, $VEGF_{189}$, and $VEGF_{206}$, respectively). $VEGF_{165}$ is the most abundant molecular species in all human tissues except placenta, in which $VEGF_{121}$ is predominant (11). The VEGF isoforms have different properties in vitro, which may determine their function in vivo. The two shorter forms, $VEGF_{121}$ and $VEGF_{165}$, are secreted and likely to be available in physiological conditions (11). In contrast, the longer ones, $VEGF_{189}$ and $VEGF_{206}$, are bound to heparin-containing proteoglycans in the cell surface or in the basement membrane. The sequence of $VEGF_{189}$ is the same as that reported for human vascular permeability factor, a protein identified from tumor cell lines on the basis of its ability to induce vascular leakage and protein extravasation (12). Later observations indicate that all four molecular species of VEGF can promote dye extravasation when applied in a guinea pig skin-permeability assay (11). A fifth splice variant, $VEGF_{145}$, has also been identified from human endometrium and myometrium (6). The bands at 3.9 and 4.7 kb seem to represent $VEGF_{165}$ and $VEGF_{139}$, respectively (16). Western blot analysis of rat brain lysates, resolved under reducing conditions with use of a polyclonal antibody, showed one VEGF band at 23 kDa, which is consistent in size to the monomer of $VEGF_{165}$.

VEGF is said to bind with high affinity to endothelial cells in arteries, veins, and microvessels through its two tyrosine kinase receptors: the fms-like tyrosine kinase receptor (*flt-1*) and the tyrosine kinase receptor (KDR) (8, 22). Both *flt-1* and KDR are expressed exclusively in endothelial cells. *Flt-1* was found to be upregulated in tumor endothelial cells, although it is not present in the endothelium of normal brain (18). Studies have disclosed that the expression of the *flt-1* and KDR transcripts can be upregulated by hypoxia both in vitro (5) and in vivo (24). In our animal model, the *flt-1* transcript is upregulated in rat brain after 3 days of hypoxia.

Blocking the action of a paracrine mediator that acts on the vasculature may have a significant inhibitory effect on tumor growth. Treatment with VEGF anti-

body has proved to be therapeutic for several highly vascularized and aggressive malignancies (13). Angiogenesis is inhibited by dexamethasone (21). Cultured bovine aortic and pulmonary artery endothelial cell monolayers subjected to hypoxia showed an increase in monolayer permeability that was prevented by addition of the dexamethasone before or during hypoxia (21). Dexamethasone is the most effective known pharmacological treatment of HACE (21). Its mechanism of action on cerebral edema is unknown. This association suggests that blockade of the first stages of angiogenesis may be involved. The relationship between dexamethasone and VEGF remains to be determined. Anti-VEGF therapy may provide a rational approach for dealing with this illness.

In conclusion, our results demonstrate that the transcription of VEGF and the production of VEGF protein in rat brain were upregulated during the first week of hypoxia. Because VEGF is thought to play an important role in angiogenesis, our findings support the hypothesis that the angiogenesis process may be involved in the development of HACE. However, we did not attempt to demonstrate cerebral edema. Direct evidence for a causative relationship between expression of VEGF and brain edema (or petechial hemorrhage) must await additional studies in which the consequences of altered expression of VEGF in brain tissue will be determined. Further study should also include the potential ways to prevent and treat HACE.

We thank Mary Stafford for excellent animal work. We are grateful to Larry Brown, Rubin M. Tuder, and Masabumi Shibuya for their gift of VEGF cDNA and *flt-1* cDNA. Many thanks to Dongwei Gou, Jiangfeng Xu, Mary R. Matili, Franklin Ives, and Shanhong Lin for expert technical assistance and to Michael Matthay, Grace Ma, Peter O'Haro, Timothy P. Quinn, and Hui Yuan for helpful suggestions and comments.

This work was supported by the Department of Anesthesia, University of California, San Francisco, CA.

Present address of F. Xu: 552 MRB II, Dept. of Medicine/Hematology, Vanderbilt Univ. School of Medicine, Nashville, TN 37232-6305.

Address for reprint requests: J. W. Severinghaus, Box 0542, UCSF, San Francisco, CA 94143-0542 (E-mail: jws@itsa.ucsf.edu).

Received 31 March 1997; accepted in final form 20 February 1998.

REFERENCES

1. **Banai, S., M. T. Jacklitsch, and M. Shou.** Angiogenic-induced enhancement of collateral blood flow to ischemic myocardium by vascular endothelial growth factor in dog. *Circulation* 89: 2183–2189, 1994.
2. **Berkman, R. A., M. J. Merill, W. C. Reinhold, W. T. Tonacci, A. Saxena, W. C. Clark, J. T. Robertson, I. U. Ali, and E. H. Oldfield.** Expression of the vascular permeability/vascular endothelial growth factor gene in central nervous system neoplasms. *J. Clin. Invest.* 91: 153–159, 1993.
3. **Breier, G., U. Albrecht, S. Sterrer, and W. Risau.** Expression of vascular endothelial growth factor during embryonic angiogenesis and endothelial cell differentiation. *Development* 114: 521–532, 1992.
4. **Brock, T. A., H. F. Dvorak, and D. R. Senger.** Tumor-secreted vascular permeability factor increases cytosolic Ca^{++} and von Willebrand factor release in human endothelial cells. *Am. J. Pathol.* 138: 213–221, 1991.
5. **Brogi, E., G. Schatteman, T. Wu, E. A. Kim, L. Varticovski, B. Keyt, and J. M. Isner.** Hypoxia-induced paracrine regulation of vascular endothelial growth factor receptor expression. *J. Clin. Invest.* 97: 469–476, 1996.
6. **Charnock-Jones, D. S. C., A. M. Sharkey, and J. Raiput-Williams.** Identification and localization of alternately spliced mRNA for vascular endothelial growth factor in human uterus and estrogen regulation in endometrial carcinoma cell lines. *Biol. Reprod.* 48: 1120–1128, 1993.
7. **Clauss, M., M. Gerlach, H. Gerlach, J. Brett, F. Wang, P. C. Familletti, Y.-C. E. Pan, J. V. Olander, D. T. Connolly, and D. Stern.** Vascular permeability factor: a tumor-derived polypeptide that induces endothelial cell and monocyte procoagulant activity, and promotes monocyte migration. *J. Exp. Med.* 172: 1535–1545, 1990.
8. **De Vries, C., J. A. Escobedo, H. Ueno, H. K. Houck, N. Ferrara, and L. T. Williams.** The fms-like tyrosine kinase, a receptor for vascular endothelial growth factor. *Science* 255: 989–991, 1991.
9. **Harik, S. I., M. A. Hritz, and J. C. LaManna.** Hypoxia-induced brain angiogenesis in the adult rat. *J. Physiol. (Lond.)* 485: 525–530, 1995.
10. **Hashimoto, E., T. Ogita, T. Nakaoka, R. Matsuoka, A. Takao, and Y. Kira.** Rapid induction of vascular endothelial growth factor expression by transient ischemia in rat heart. *Am. J. Physiol.* 267 (*Heart Circ. Physiol.* 36): H1948–H1954, 1994.
11. **Houck, K. A., N. Ferrara, J. Winer, G. Cachianes, B. Li, and D. W. Leung.** The vascular endothelial growth factor family: identification of a fourth molecular species and characterization of alternative splicing of RNA. *Mol. Endocrinol.* 5: 1806–1814, 1991.
12. **Keck, P. J., S. D. Hauser, G. Krivi, K. Sanzo, T. Warren, J. Feder, and D. T. Connolly.** Vascular permeability factor, an endothelial cell mitogen related to PDGF. *Science* 246: 1309–1312, 1989.
13. **Kim, K. J., B. Li, J. Winer, M. Armanini, N. Gillett, H. S. Phillips, and N. Ferrara.** Inhibition of vascular endothelial growth factor-induced angiogenesis suppresses tumor growth in vivo. *Nature* 362: 841–844, 1993.
14. **LaManna, J. C., K. D. Boehm, V. Mironov, A. G. Hudetz, M. A. Hritz, J. K. Yun, and S. I. Harik.** Increased basic fibroblastic growth factor mRNA in the brains of rats exposed to hypobaric hypoxia. *Adv. Exp. Med. Biol.* 361: 497–502, 1994.
15. **LaManna, J. C., B. R. Cordisco, D. E. Knuese, and A. G. Hudetz.** Increased capillary segment length in cerebral cortical microvessels of rats exposed to 3 weeks of hypobaric hypoxia. *Adv. Exp. Med. Biol.* 345: 627–631, 1994.
16. **Monacci, W. T., M. J. Merrill, and E. H. Oldfield.** Expression of vascular permeability factor/vascular endothelial growth factor in normal rat tissues. *Am J. Physiol.* 264 (*Cell Physiol.* 33): C995–C1002, 1993.
17. **Plate, K. H., G. Breier, B. Millauer, A. Ullrich, and W. Risau.** Up-regulation of vascular endothelial growth factor and its cognate receptors in a rat-glioma model of tumor angiogenesis. *Cancer Res.* 53: 5822–5827, 1993.
18. **Plate, K. H., G. Breier, H. A. Weich, and W. Risau.** Vascular endothelial growth factor is a potential tumor angiogenesis factor in human gliomas in vivo. *Nature* 359: 845–848, 1992.
19. **Robertson, P. L., M. Du Bois, P. D. Bowman, and G. W. Goldstein.** Angiogenesis in developing rat brain: an in vivo and in vitro study. *Dev. Brain Res.* 23: 219–223, 1985.
20. **Senger, D. R., D. T. Connolly, L. Van de Water, J. Feder, and H. F. Dvorak.** Purification and NH_2-terminal amino acid sequence of guinea pig tumor-secreted vascular permeability factor. *Cancer Res.* 50: 572–578, 1990.
21. **Severinghaus, J. W.** Hypothetical roles of angiogenesis, osmotic swelling, and ischemia in high-altitude cerebral edema. *J. Appl. Physiol.* 79: 375–379, 1995.
22. **Shibuya, M., S. Yamaguchi, A. Yamane, T. Ikeda, A. Toji, H. Matushime, and M. Sato.** Nucleotide sequence and expression of a novel human receptor-type tyrosine kinase gene (flt) closely related to the fms family. *Oncogene* 5: 519–524, 1990.
23. **Shweiki, D., A. Itin, D. Soffer, and E. Keshet.** Vascular endothelial growth factor induced by hypoxia may mediate hypoxia-initiated angiogenesis. *Nature* 359: 843–845, 1992.
24. **Tuder, R. M., B. E. Flook, and N. F. Voelkel.** Increased gene expression for VEGF and the VEGF receptors KDR/flk and flt in lungs exposed to acute or to chronic hypoxia. *J. Clin. Invest.* 95: 1798–1807, 1995.

Vol. 6, 957–965, March 2000

Treatment for Malignant Pleural Effusion of Human Lung Adenocarcinoma by Inhibition of Vascular Endothelial Growth Factor Receptor Tyrosine Kinase Phosphorylation[1]

Seiji Yano, Roy S. Herbst, Hisashi Shinohara, Barbara Knighton, Corazon D. Bucana, Jerald J. Killion, Jeanette Wood, and Isaiah J. Fidler[2]

Department of Cancer Biology, The University of Texas M. D. Anderson Cancer Center, Houston, Texas 77030 [S. Y., R. S. H., H. S., B. K., C. D. B., J. J. K., I. J. F.], and Oncology Research, Novartis, Ltd., CH-4002 Basel, Switzerland [J. W.]

ABSTRACT

Malignant pleural effusion (PE) is associated with advanced human lung cancer. We found recently, using a nude mouse model, that vascular endothelial growth factor/vascular permeability factor (VEGF/VPF) is responsible for PE induced by non-small cell human lung carcinoma cells. The purpose of this study was to determine the therapeutic potential of a VEGF/VPF receptor tyrosine kinase phosphorylation inhibitor, PTK 787, against PE formed by human lung adenocarcinoma (PC14PE6) cells. PTK 787 did not affect the *in vitro* proliferation of PC14PE6 cells, whereas it specifically inhibited proliferation of human dermal microvascular endothelial cells stimulated by VEGF/VPF. A specific platelet-derived growth factor receptor tyrosine kinase inhibitor, CGP57148 (used as a control because PTK 787 also inhibits platelet-derived growth factor receptor tyrosine kinases), had no effect on proliferation of PC14PE6 or human dermal microvascular endothelial cells. i.v. injection of PC14PE6 cells into nude mice produced lung lesions and a large volume of PE containing a high level of VEGF/VPF. Oral treatment with CGP57148 had no effect on PE or lung metastasis. In contrast, oral treatment with PTK 787 significantly reduced the formation of PE but not the number of lung lesions. Furthermore, treatment with PTK 787 significantly suppressed vascular hyperpermeability of PE-bearing mice but did not affect the VEGF/VPF level in PE or expression of VEGF/VPF protein and mRNA in the lung tumors of PC14PE6 cells *in vivo*. These findings indicate that PTK 787 reduced PE formation mainly by inhibiting vascular permeability, suggesting that this VEGF/VPF receptor tyrosine kinase inhibitor could be useful for the control of malignant PE.

INTRODUCTION

Malignant PE[3] is associated with highly symptomatic, advanced-stage lung cancer. Most patients with PE present with progressive dyspnea, cough, or chest pain that compromises their quality of life (1). Malignant PE is most often caused by lung adenocarcinoma, because this type often forms a primary tumor in the periphery of the lung and invades the pleural cavity (1). Malignant PE has consistently been shown to indicate a poor prognosis in advanced lung cancer patients, being associated with high morbidity and mortality (2, 3). Previous reports demonstrate that drainage followed by instillation of sclerosing agents is useful for controlling PE and improving the quality of life of patients. However, the efficacy of this treatment is variable and does not extend the survival of lung cancer patients (1, 4). Clearly, a more effective therapy for malignant PE is needed.

Among the possible targets for PE treatment is VEGF, also called VPF (5), an important multifunctional cytokine that promotes developmental, physiological, and pathological neovascularization (6–8). VEGF/VPF consists of at least four isoforms (VEGF121, VEGF165, VEGF189, and VEGF206), arising through alternate splicing of mRNA from a single gene (6). It can be produced by various cell types, including many tumor cells and activated macrophages (6). VEGF/VPF has been shown to stimulate the proliferation and migration of endothelial cells and to induce the expression of metalloproteinases and plasminogen activity by these cells (6, 9–12). The cytokine is also a powerful inducer of vascular hyperpermeability. Through this property, the molecule plays a central role in ascites fluid formation by murine tumors and human ovarian cancer cell lines in animal models (13–17).

Received 10/7/99; revised 12/9/99; accepted 12/13/99.

The costs of publication of this article were defrayed in part by the payment of page charges. This article must therefore be hereby marked *advertisement* in accordance with 18 U.S.C. Section 1734 solely to indicate this fact.

[1] Supported in part by Cancer Center Support Core Grant CA16672 and Grant R35-CA42107 (to I. J. F.) from the National Cancer Institute, NIH.

[2] To whom requests for reprints should be addressed, at the Department of Cancer Biology, Box 173, The University of Texas M. D. Anderson Cancer Center, 1515 Holcombe Boulevard, Houston, TX 77030. Phone: (713) 792-8577; Fax: (713) 792-8747; E-mail: ifidler@notes.mdacc.tmc.edu.

[3] The abbreviations used are: PE, pleural effusion; VEGF/VPF, vascular endothelial growth factor/vascular permeability factor; Flt-1, fms-like tyrosine kinase; Flk-1, fetal liver kinase; KDR, kinase insert domain-containing receptor; FBS, fetal bovine serum; bFGF, basic fibroblast growth factor; PDGF, platelet-derived growth factor; IL, interleukin; rh, recombinant human; ISH, *in situ* hybridization; IHC, immunohistochemistry; HDMEC, human dermal microvascular endothelial cell; PTK 787/ZK232394, 1-[4-chloroanilino]-4-[pyridylmethyl] phthalazine dihydrochloride.

syringe, and the volume of PE was measured using the syringe. The blood and PE harvested were centrifuged for 20 min (100 × *g*) at 4°C. The serum and supernatant of PE were stored at −70°C until the ELISA was performed. The lungs were fixed in Bouin's solution, and the number of lung lesions was determined with the aid of a dissecting microscope.

Although this model does not entirely mimic all steps for PE formation in humans, this is one model in which PE is reproducibly developed, as reported previously (18).

Assays of VEGF/VPF, bFGF, and IL-8 Protein Levels. Levels of VEGF/VPF, bFGF, and IL-8 protein in culture supernatants, mouse serum, and PE were determined using ELISA kits according to the manufacturer's instructions (R&D Systems, Minneapolis, MN).

Oligonucleotide Probes. We designed antisense oligonucleotide DNA probes complementary to the mRNA transcripts of the *VEGF/VPF* genes based on published reports of the cDNA sequence (15) TGGTGATGTTGGACTCCTCAGTGGGCU, 57.7% guanosine-cytosine (GC) content. The specificity of the oligonucleotide sequence was initially determined by a GenBank European Molecular Biology Library database search with the use of the Genetics Computer Group sequence analysis program (Madison, WI) based on the FastA algorithm. A poly$(dT)_{20}$ oligonucleotide was used to verify the integrity and lack of degradation of mRNA in each sample. All DNA probes were synthesized with six biotin molecules (hyperbiotinylated) at the 3′ end via direct coupling using standard phosphoramidite chemistry (Research Genetics, Huntsville, AL).

ISH. ISH was performed as described previously (30). Tissue sections (4 μm) of formalin-fixed, paraffin-embedded specimens were mounted on silane-treated ProbeOn slides (Fisher Scientific Co.). The slides were placed in the Microprobe slide holder (Fisher Scientific Co.), dewaxed, and rehydrated with Autodewaxer and Autoalcohol (Research Genetics), digested with pepsin, and then hybridized by use of the Microprobe manual staining system (Fisher Scientific Co.). The probes were hybridized for 45 min at 45°C, and the samples were then washed three times for 2 min each time with 2× SSC (1× SSC = 0.15 M NaCl, 0.15 M sodium citrate) at 45°C. RNase-free water was used to make up Tris buffer and 2× SSC solutions. The samples were then incubated with alkaline phosphate-labeled avidin for 30 min at 45°C, rinsed in 50 nM Tris buffer (pH 7.6), rinsed with alkaline phosphate enhancer for 1 min, and incubated with a chromogen substrate for 20 min at 45°C. Additional incubation with fresh chromogen was done if it was necessary to enhance a weak reaction. A positive enzymatic reaction in this assay stained red. Known positive controls were used in each hybridization reaction. Controls for endogenous alkaline phosphate included treatment of the sample in the absence of the biotinylated probe and use of chromogen alone.

Histology and IHC. The lungs of nude mice were harvested at autopsy, cut into 5-mm thickness, and placed in either buffered 10% formalin solution or OCT compound (Miles Laboratories, Elkhart, IN) to be snap-frozen in liquid nitrogen. For VEGF/VPF staining, tissue sections (4 μm thick) of formalin-fixed, paraffin-embedded specimens were deparaffinized in xylene, rehydrated in graded alcohol, transferred to PBS, and treated with pepsin for 20 min at room temperature. For CD31 staining, frozen tissue sections (8 μm thick) were fixed with cold acetone. The slides were rinsed twice with PBS, and endogenous peroxidase was blocked by use of 3% hydrogen peroxide in PBS for 12 min. The samples were washed three times with PBS and incubated for 10 min at room temperature with a protein-blocking solution consisting of PBS (pH 7.5) containing 5% normal horse serum and 1% normal goat serum. Excess blocking solution was drained, and the samples were incubated for 18 h at 4°C with a 1:400 dilution of rabbit polyclonal anti-VEGF/VPF antibody (Santa Cruz Biotechnology, Santa Cruz, CA) or a 1:100 dilution of monoclonal rat anti-CD31 antibody (PharMingen, San Diego, CA). The samples were then rinsed four times with PBS and incubated for 60 min at room temperature with the appropriate dilution of peroxidase-conjugated antirabbit IgG or antirat IgG. The slides were rinsed with PBS and incubated for 5 min with diaminobenzidine (Research Genetics, Huntsville, AL). The sections were then washed three times with distilled water, counterstained with Gill's hematoxylin, washed once with distilled water and once with PBS, and rinsed again with distilled water. The slides were mounted with a Universal mount (Research Genetics) and examined using a bright-field microscope. A positive reaction was indicated by a reddish-brown precipitate in the cytoplasm. Sections (4 μm thick) of formalin-fixed, paraffin-embedded tumors were also stained with H&E for routine histological examination.

Vascular Density. Blood vessels in solid tumors growing in the lungs of nude mice were counted under light microscope after immune staining of sections with anti-CD31 antibody. Areas containing the highest number of capillaries and small venules were identified by scanning the tumor sections at low power (×40). After the areas of high vascular density were identified, individual vessels were counted in ×100 fields [×10 objective and ×10 ocular (0.145 mm^2)/field)]. On the basis of criteria described by Weidner *et al.* (31), observation of a vessel lumen was not required for a structure to be classified as a vessel.

Permeability Assay (Miles Assay). The Miles assay uses intradermal injection of test substances and intravascular injection of Evans blue dye (which binds to endogenous serum albumin) as a tracer to assay permeability in peripheral vessels. The assay was performed essentially as described (32, 33) with minor modification. To reduce individual variation, nude mice without downy hair were carefully chosen, and each mouse was kept separately during the assay. Nude mice were injected i.v. with 200 μl of 0.5% Evans blue dye (Sigma Chemical Co., St. Louis, MO). Ten min later, 50-μl of samples were injected intradermally in rows on the dorsal skin. Thirty min after the injection with samples, the mice were killed, and the skin was removed. Wheals (5 mm in diameter) were resected and incubated in 500 μl of formamide at 37°C for 48 h to extract Evans blue dye. The absorbance of the extracts was read at 630 nm in a spectrophotometer.

Statistical Analysis. The significance of differences in data of *in vitro* experiments, the Miles assay, and vessel density were analyzed using Student's *t* test (two-tailed). The remaining *in vivo* data were analyzed using the Mann-Whitney *U* test or χ^2 test.

Recently, we developed a model for PE by human lung adenocarcinoma cells (PC14 and its highly metastatic variant, PC14PE6) in nude and severe combined immunodeficiency mice (18) and clarified the role of VEGF/VPF in PE formation. The i.v. injection of PC14 and PC14PE6 cells, expressing high levels of VEGF/VPF, produced lung lesions that in turn produced large-volume PE in mice. On the other hand, i.v. or intrathoracic injection of H226 cells (VEGF/VPF low-expressing human lung squamous cell carcinoma) produced lung lesions without detectable PE. Interestingly, *VEGF/VPF* gene transfection into H226 cells resulted in induction of PE when tumor cells were injected intrathoracicly.[4] This evidence suggests that VEGF/VPF plays a crucial role in PE formation by human non-small cell carcinoma cells.

Two VEGF/VPF receptors have been identified: Flt-1 and the Flk-1/kinase insert domain-containing receptor (KDR), are high-affinity VEGF/VPF receptors with an extracellular domain containing seven immunoglobulin-like domains and a split tyrosine kinase intracellular domain (6). Flk-1 has 85% homology with the human homologue, KDR. Both Flt-1 and Flk-1/KDR have been shown to be important regulatory systems for vasculogenesis and physiological angiogenesis (19–24). However, the interaction of VEGF/VPF with Flk-1/KDR is thought to be the more important interaction for tumor angiogenesis because it is essential for induction of the full spectrum of VEGF/VPF functions (6). In fact, many compounds and molecules developed to block VEGF/VPF activities mediated by Flk-1/KDR have been shown to have antiangiogenic activity in animal models (25–27).

One such molecule is an inhibitor of tyrosine kinase phosphorylation of Flk-1/KDR and Flt-1, called PTK 787 (28). PTK 787 directly inhibits phosphorylation of the VEGF/VPF receptor tyrosine kinases and suppresses angiogenesis induced by VEGF/VPF. At slightly higher doses, it also inhibits PDGF receptor tyrosine kinase phosphorylation (28). It can be given p.o., is well tolerated, and has been demonstrated to inhibit the growth of several carcinomas in nude mice (28).

In this study, we examined the therapeutic efficiency of PTK 787 against malignant PE caused by human lung adenocarcinoma cells (PC14PE6) established in nude mice. PTK 787 specifically inhibited VEGF/VPF-induced proliferation of human dermal endothelial cells and had no direct effect against PC14PE6 cells. We found that oral feeding with PTK 787 suppressed the formation of malignant PE by inhibiting vascular permeability. These findings suggest that therapy with the VEGF/VPF receptor tyrosine kinase phosphorylation inhibitor PTK 787 is worthy of study in clinical trials.

MATERIALS AND METHODS

Cell Lines. The human lung adenocarcinoma cell line PC14PE6 was maintained in Eagle's minimal essential medium supplemented with 10% FBS, sodium pyruvate, nonessential amino acids, L-glutamine, 2-fold vitamin solution, and penicillin-streptomycin (Flow Laboratories, Rockville, MD) in a 10-cm dish and incubated in 5% CO_2-95% air at 37°C. PC14PE6 cells were free of *Mycoplasma* and pathogenic murine viruses (assayed by Microbiological Associates, Bethesda, MD). Cultures were maintained for no longer than 6 weeks after recovery from frozen stocks. HDMECs (Cascade Biologicals, Portland, OR) were cultured in Medium 131 with Microvascular Growth Supplement (Cascade Biologicals). For proliferation assays, HDMECs were used at passages 2–5.

Reagents. rh VEGF165, rhbFGF, and antihuman VEGF polyclonal antibody were purchased from R&D Systems (Minneapolis, MN). PTK 787/ZK232394 was discovered and synthesized in the Department of Oncology Research, Novartis Pharmaceuticals (Basel, Switzerland) and was profiled in collaboration with the Institute of Molecular Medicine (Tumor Biology Center, Freiburg, Germany), as well as the Oncology Research Laboratories of Schering AG (Berlin, Germany). The studies described in this report were performed with either a dihydrochloride or succinate salt. For *in vitro* assays, a stock solution of 10 mM of PTK787/ZK 222584 was prepared in DMSO. This was diluted further in buffer or medium so that the concentration of DMSO in assay systems did not exceed 0.1%. For *in vivo* studies, the vehicle for the dihydrochloride salt was distilled water. The succinate salt was suspended in vehicle containing 5% DMSO and 0.5% Tween 80 in distilled water (28). The PDGF receptor tyrosine kinase phosphorylation inhibitor CGP57148 (28, 29) was from Novartis.

Cell Proliferation Assay. HDMECs (5×10^3/well) plated in triplicate in 96-well plates precoated with 1.5% gelatin were incubated overnight in supplemented M131 medium. PC14PE6 cells (2×10^3/well) plated in triplicate in 96-well plates were incubated in MEM containing 5% FBS. The cells were then washed and incubated for 72 h with test samples in fresh MEM containing 5% FBS. The proliferative activity was determined by the 3-(4,4-dimethylthiazol-2-yl)-2.5-diphenyltetrazolium bromide assay using an MR-5000 96-well microtiter plate reader set at 570 nm (12).

Animals. Male athymic BALB/c nude mice were purchased from the Animal Production Area of the National Cancer Institute, Frederick Cancer Research Facility (Frederick, MD). The mice were housed in laminar flow cabinets under specific pathogen-free conditions and used at 6–8 weeks of age. Animals were maintained in facilities approved by the American Association for Accreditation of Laboratory Animal Care and in accordance with current regulations and standards of the United States Department of Agriculture, Department of Health and Human Services, and NIH.

Model for Lung Metastasis and PE. Cultured PC14PE6 cells were harvested by pipetting. The cells were washed twice and resuspended in Ca^{2+}- and Mg^{2+}-free HBSS. Cell viability was determined by a trypan blue exclusion test, and only single-cell suspensions of >90% viability were used. Tumor cells (1×10^6/300 μl of HBSS) were injected into the lateral tail vein of unanesthetized nude mice (18). After the indicated periods, mice were euthanized by methoxyflurane, the subclavian artery was severed, and blood was harvested. The chest wall was then cut carefully with a pair of scissors, PE was harvested using a 1-ml

[4] S. Yano, H. Shinohara, R. S. Herbst, H. Kuniyasu, C. D. Bucana, L. M. Ellis, and I. J. Fidler. Production of malignant pleural effusions is dependent on invasion of the pleura and expression of vascular endothelial growth factor/vascular permeability factor by human lung cancer cells, submitted for publication.

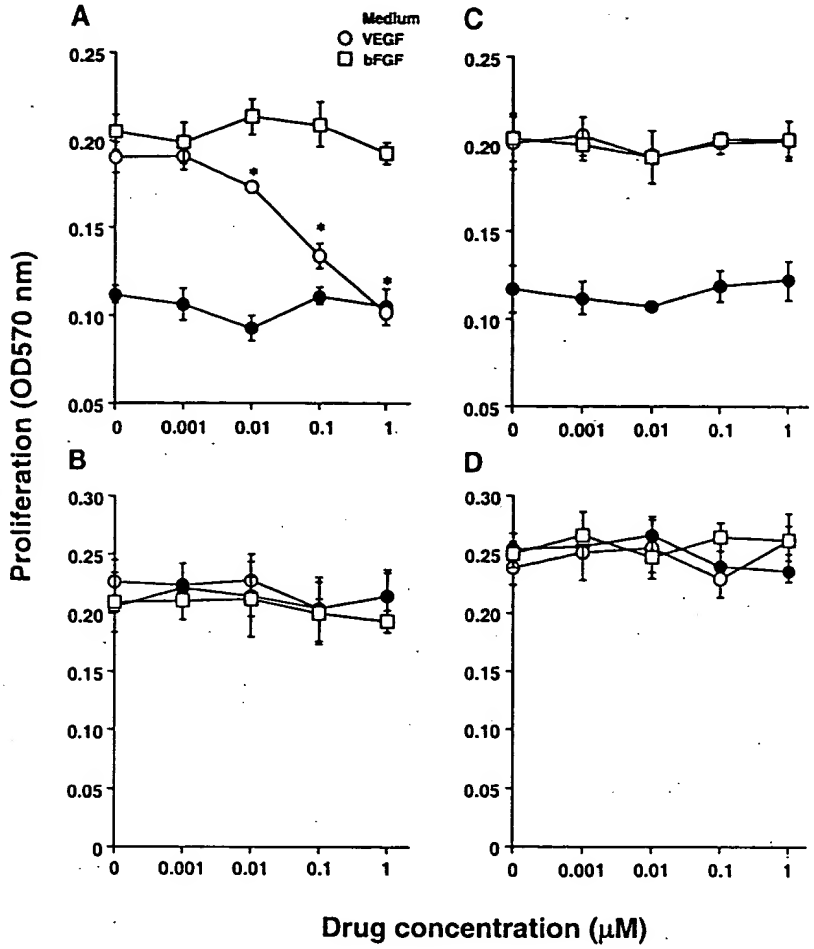

Fig. 1 Effects of PTK 787 and CGP 57148 on *in vitro* proliferation of HDMECs and PC14PE6 cells. HDMECs (5×10^3/well; *A* and *C*) plated in 96-well plates were incubated overnight in supplemented M131 medium. PC14PE6 cells (2×10^3/well; *B* and *D*) were plated in triplicate in 96-well plates and were incubated overnight in MEM containing 5% FBS. The cells were then washed and incubated with different doses of PTK 787 (*A* and *B*) or CGP57148 (*C* and *D*), in the presence or absence of rhVEGF165 (20 ng/ml) or rhbFGF (20 ng/ml) in fresh MEM containing 5% FBS. The 3-(4,4-dimethylthiazol-2-yl)-2.5-diphenyl-tetrazolium bromide assay was performed after 72 h, as described in "Materials and Methods." The values shown represent the means of triplicate cultures; *bars*, SD. The results shown are representative of four independent experiments with similar results. *, $P < 0.05$, compared with the respective control.

RESULTS

PKT 787 Inhibited Proliferation of Endothelial Cells but not Lung Cancer Cells. In the first set of experiments, we examined the effect of PTK 787 on the proliferation of HDMECs and PC14PE6 cells *in vitro*. PTK 787 did not affect proliferation of HDMECs incubated in medium alone (Fig. 1*A*). Addition of rhVEGF/VPF or rhbFGF to the medium significantly stimulated HDMEC proliferation, suggesting that HDMECs express receptors for VEGF/VPF and bFGF, as is the case with most endothelial cell lines. Under these experimental conditions, PTK 787 inhibited proliferation of HDMECs stimulated by rhVEGF165 but not rhbFGF, indicating the specificity of PTK 787 to VEGF/VPF receptors (Fig. 1*A*). In contrast, PTK 787 did not affect proliferation of PC14PE6 cells, irrespective of the presence of rhVEGF165 or rhbFGF (Fig. 1*B*). Moreover, a PDGF-receptor tyrosine kinase phosphorylation inhibitor, CGP57148, used as a control did not affect the proliferation of HDMECs or PC14PE6 cells, irrespective of the presence of rhVEGF165 or rhbFGF (Fig. 1, *C* and *D*).

Treatment with PTK 787 Inhibited PE Formation. We next examined the therapeutic effects of PTK 787 on PE formation by PC14PE6 cells. The effective dose of PTK 787 was chosen according to a previous report (28). PC14PE6 cells (1×10^6) were injected i.v. into nude mice. Oral feeding with PTK 787 commenced 14 days after tumor injection (because at this time, the PC14PE6 cells progress to micrometastases in the lung) and continued until mice were killed. In the first experiment, all mice in the control group developed lung metastases and PE, and treatment with 10 mg/kg PTK 787 had no effect on lung metastasis, lung weight (represents total tumor volume), or PE formation (Table 1). Treatment with 100 mg/kg PTK 787 inhibited lung weight, although the reduction in the number of lung metastases did not reach significance. In addition, PE formation (both incidence and volume) was remarkably inhibited in this group. In experiment 2, we examined the effect of a lower dose of PTK 787 (50 mg/kg) on formation of PE and lung metastasis. All mice of the control group developed lung metastasis and PE, and treatment with 10 mg/kg PTK 787 again had no effect, consistent with the results in experiment 1. The number of lung metastases or lung weight was not inhibited significantly by treatment with 50 mg/kg PTK 787; however, this treatment remarkably inhibited PE formation (both incidence and volume). In experiment 3, the effect of oral treatment with the PDGF receptor tyrosine kinase inhibitor CGP57148 was examined using the same model. Although therapy with

Table 1 Effect of VEGF/VPF receptor tyrosine kinase phosphorylation inhibitor on the formation of lung metastasis and PE by PC14PE6 cells in nude mice

PC14PE6 cells (1×10^6) were injected i.v. in nude mice on day 0. The mice were given oral feedings with distilled water (control), PTK 787 (started on day 14), or CGP57148 (started on day 7). Daily therapy continued until day 48. The mice were killed on day 49, and lung metastasis, lung weight, and PE were evaluated as described in "Materials and Methods."

		Lung metastasis			Lung weight (mg)		PE		
								Volume (μl)	
Experiment	Treatment	Incidence	Median	Range	Median	Range	Incidence	Median	Range
1	Control	10/10	64	26–115	600	302–680	10/10	630	20–900
	PTK 787 10 mg/kg	10/10	54	2–97	548	251–994	9/10	650	<20–1060
	PTK 787 100 mg/kg	9/9	44	4–76	286[a]	218–620	4/9[b]	<20[a]	<20–700
2	Control	10/10	53	6–>150	637	290–910	10/10	803	30–990
	PTK 787 10 mg/kg	9/9	44	1–>150	420	195–718	7/9	780	<20–1000
	PTK 787 50 mg/kg	7/9	26	0–103	405	212–600	5/9[b]	20[a]	<20–799
3	Control	10/10	59	38–139	573	241–944	10/10	690	150–1050
	CGP57148 10 mg/kg	7/8	58	4–>150	559	185–796	6/8	550	<20–1010
	CGP57148 50 mg/kg	10/10	48	3–>150	543	208–661	8/10	500	<20–1430

[a] Significantly different from control group ($P < 0.05$; Mann-Whitney U test).
[b] Significantly different from control group ($P < 0.01$; χ^2 test).

Table 2 Effect of treatment with PTK787 on the levels of angiogenic cytokines in the serum and PE of PC14PE6 cell-bearing nude mice

Data shown represent mean ± SD of three mice.

	VEGF/VPF (ng/ml)		bFGF (ng/ml)		IL-8 (ng/ml)	
Treatment	Serum	PE	Serum	PE	Serum	PE
Control	<0.09	60.99 ± 36.36	0.02 ± 0.03	0.23 ± 0.17	0.07 ± 0.15	3.33 ± 1.09
PTK 787 10 mg/kg	<0.09	63.85 ± 17.10	0.03 ± 0.06	0.07 ± 0.03	0.52 ± 0.01	2.99 ± 0.34
PTK 787 50 mg/kg	<0.09	73.70 ± 21.54	0.04 ± 0.07	0.39 ± 0.33	0.73 ± 0.32	4.10 ± 0.56

CGP57148 was started earlier (on day 7) than therapy with PTK 787, it had no significant therapeutic effects on the formation of PE or lung metastasis. These results suggest that PTK 787 specifically inhibits PE formation produced by PC14PE6 cells. It also inhibited lung weight (total tumor volume of lung metastases) at the highest dose (100 mg/kg) tested. On the basis of these results, we chose to use 50 mg/kg PTK 787 in the following experiments.

Treatment with PTK 787 Inhibited Tumor Vascularization but not VEGF/VPF Expression. To better determine the mechanism by which treatment with PTK 787 inhibited PE formation, we examined the effect of treatment with PTK 787 on VEGF/VPF production by PC14PE6 cells *in vivo*. We first measured the levels of VEGF/VPF, as well as bFGF and IL-8, in both the serum and the PE that developed in PTK 787-treated, PC14PE6-bearing mice treated and untreated controls. As shown in Table 2, treatment with PTK 787 did not suppress the levels of VEGF/VPF, bFGF, or IL-8 in the serum or PE. Next, we examined the effect of PTK 787 treatment on VEGF/VPF expression in lung tumors by ISH and IHC. Treatment with PTK 787 did not affect VEGF/VPF expression in lung metastasis produced by PC14PE6 cells (Fig. 2). We also found that production of bFGF or IL-8 in lung metastases was not affected by treatment with PTK 787 *in vivo* (data not shown). However, angiogenesis (one of the two major phenomena induced by VEGF/VPF) quantitated in lung lesions of PTK 787-treated mice was inhibited compared with that of control mice (number of CD31 positive cells ×100 field; 34 ± 7 *versus* 52 ± 5; $P < 0.05$). This effect, in the absence of decreased cytokine levels, suggests that treatment with PTK 787 might exert its effect on endothelial cells as opposed to tumor cells.

Treatment with PTK 787 Inhibited Vascular Permeability. The other major activity of VEGF/VPF is thought to be the induction of vascular hyperpermeability (13). Therefore, we examined the effect of treatment with PTK 787 on vascular permeability. Nude mice were treated with or without 50 mg/kg PTK 787 or CGP57148 for 3 days, and then a skin permeability assay (Miles assay) was performed. As shown in Fig. 3*A*, rhVEGF165 and PE (containing 30 ng/ml VEGF/VPF) caused by PC14PE6 cells induced vascular hyperpermeability in control and CGP57148-treated mice. However, neither rhVEGF165 nor PE produced *in vivo* by PC14PE6 cells significantly enhanced permeability in mice treated with PTK 787. These findings indicate that treatment with PTK 787 can inhibit induction of hyperpermeability caused by VEGF/VPF, presumably by blocking VEGF/VPF receptor function. We further explored how many treatments with PTK 787 were necessary for inhibition of vascular permeability. Results shown in Fig. 3*B* indicate that a 2–3-day treatment with PTK 787 was enough to inhibit the induction of vascular permeability in this assay.

Finally, we investigated the effect of treatment with PTK 787 on vascular permeability of PE-bearing mice. Nude mice were injected with PC14PE6 cells. Five weeks later, the mice were given oral feeding with or without PTK 787 (50 mg/kg)

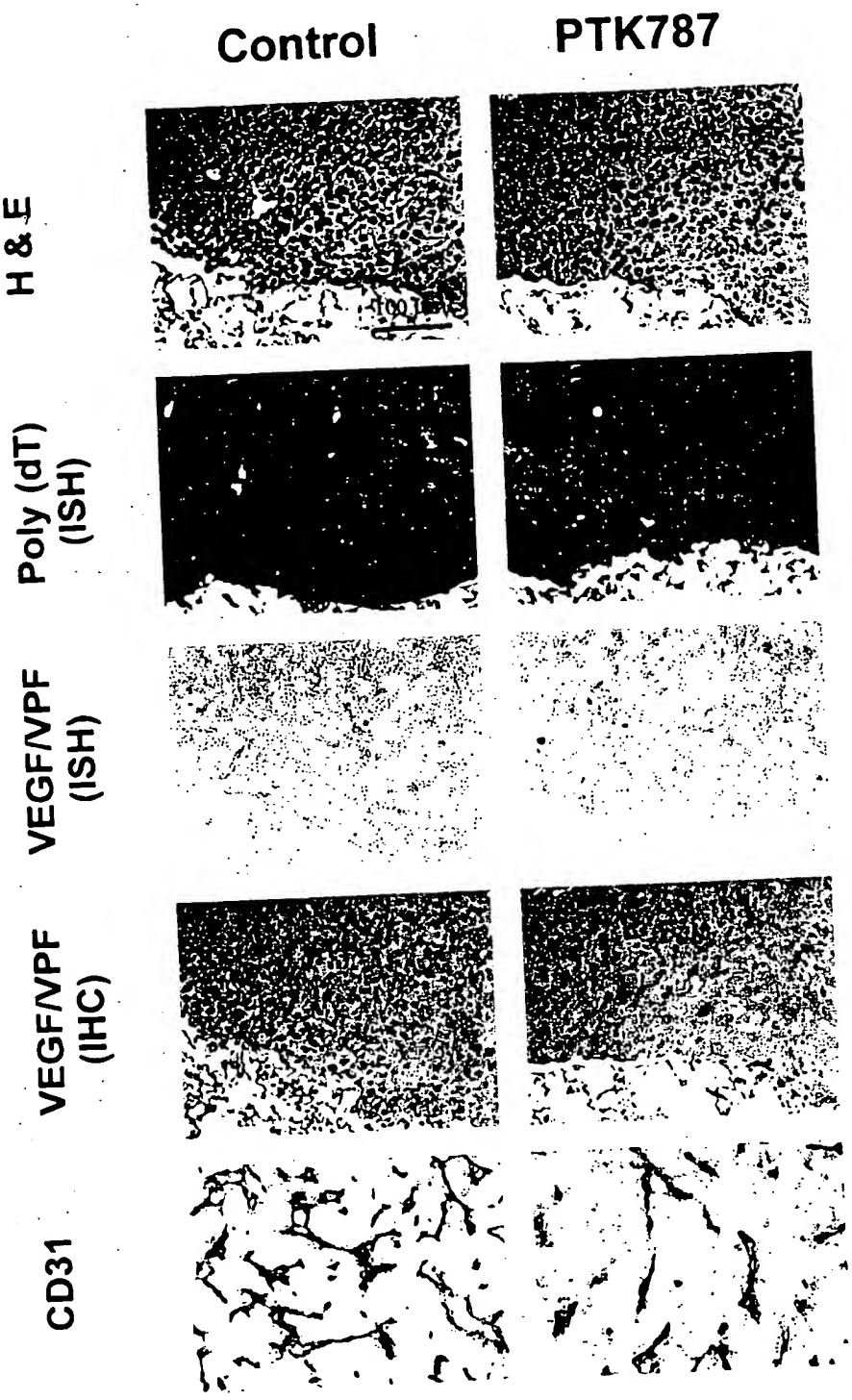

Fig. 2 Effect of oral treatment with PTK 787 on VEGF/VPF expression and vascularization in lung tumors produced by PC14PE6 cells. PC14PE6 cells (1×10^6) were injected i.v. into nude mice. Oral feeding with distilled water (control) or PTK 787 (50 mg/kg) was started 14 days after tumor injection and continued until the mice were killed. VEGF/VPF expression in lung tumors was examined by ISH and IHC. Vascularization was examined after the staining with anti-CD31 antibody, as described in "Materials and Methods."

for 6 days. Two h after the last oral feeding, the mice were injected with Evans blue dye. Fifteen min later, the mice were killed, and PE was carefully harvested. After the centrifugation of PE, the absorbance of the supernatant from the PE was measured at 630 nm. In the control group (without PTK787 treatment), $A_{630\ nm}$ (mean ± SE) of PE with or without Evans blue dye injection was 0.465 ± 0.081 and 0.094 ± 0.011, respectively. These results showed that Evans blue dye-bound endogenous albumin had leaked into PE, indicating increased vascular permeability of PE-bearing mice (33). Under these experimental conditions, treatment of PE-bearing mice with PTK 787 significantly inhibited leaking of

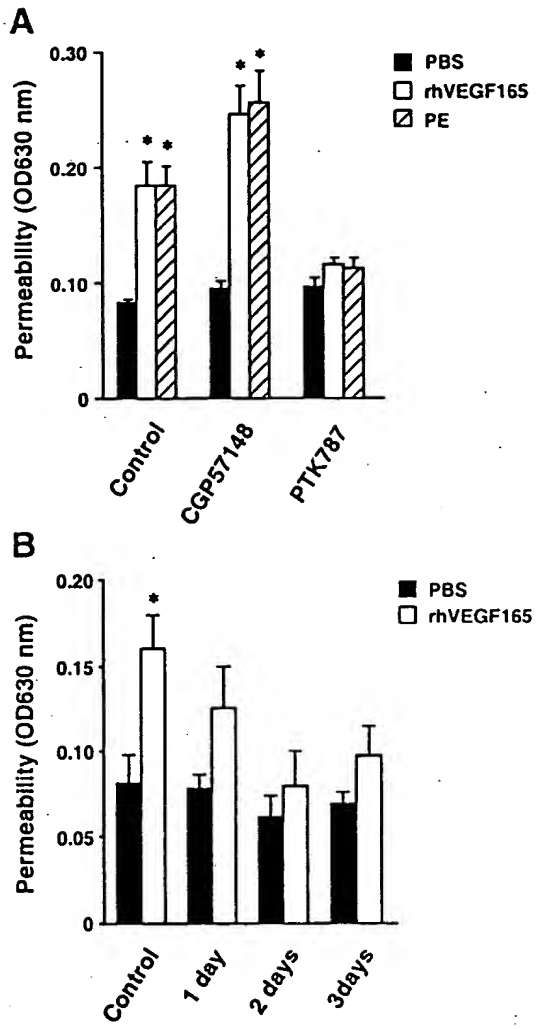

Fig. 3 Effect of treatment with PTK 787 and CGP 57148 on vascular permeability in the skin measured by the Miles assay. *A*, nude mice were given oral feeding with distilled water (*Control*), CGP 57148 (50 mg/kg), or PTK 787 (50 mg/kg) for 3 days. Two h after the last oral feeding, 50 μl of PBS, rhVEGF165 (30 ng/ml), or PE (containing 30 ng/ml VEGF) were injected intradermally into nude mice preinjected with 0.5% Evans blue dye (200 μl). Permeability was determined by the Miles assay as described in "Materials and Methods" and quantitated by measuring the absorbance at 630 nm. Data represent the means for groups of five mice; *bars*, SE. *, $P < 0.05$. *B*, nude mice were given oral feeding with distilled water (*Control*) or PTK 787 (50 mg/kg) for 1, 2, or 3 days. Two h after the last oral feeding, 50 μl of PBS or rhVEGF165 (30 ng/ml) were injected intradermally into nude mice preinjected with 0.5% Evans blue dye (200 μl). Permeability was determined by the Miles assay as described in "Materials and Methods" and quantitated by the absorbance at 630 nm. The data represent the means for groups of five mice; *bars*, SE. *, $P < 0.05$.

Evans blue dye into PE ($A_{630\ nm}$: 0.229 ± 0.038; Fig. 4). These findings further suggest that treatment with PTK 787 inhibited vascular permeability of PE-bearing mice.

DISCUSSION

Recently, we developed an animal model for PE (18) and found that VEGF/VPF is responsible for PE formation produced

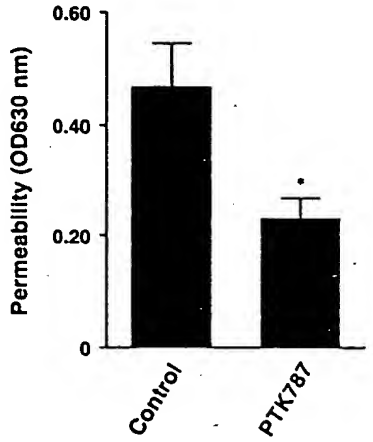

Fig. 4 Effect of treatment with PTK 787 on vascular permeability of PE-bearing mice. PC14PE6 cells (1×10^6) were injected i.v. into nude mice on day 0. The mice were given oral feedings with distilled water (*Control*) or PTK 787 (50 mg/kg) on days 35–40 daily. Two h after the last oral feeding, the mice were injected with 0.5% Evans blue dye (100 μl). Fifteen min later, the mice were killed, and PE was carefully harvested and then centrifuged. The $A_{630\ nm}$ of the supernatants of PE was measured. The data represent the means for groups of four mice; bars, SE. *, $P < 0.05$.

by non-small cell lung carcinoma cells in this model. Here, we demonstrate that treatment with a VEGF/VPF receptor tyrosine kinase phosphorylation inhibitor, PTK 787, can inhibit PE formation by human lung adenocarcinoma cells in this model through the inhibition of vascular permeability.

The interaction of VEGF/VPF and its receptors (Flt-1 and Flk-1/KDR) has been shown to play an important role in angiogenesis of malignant diseases (25–27). Therefore, VEGF/VPF and its receptors (especially Flk-1/KDR) represent ideal targets for antiangiogenesis therapy. PTK 787 is a selective inhibitor of VEGF/VPF receptor tyrosine kinase phosphorylation and has been shown to inhibit VEGF/VPF-mediated responses *in vitro* and *in vivo* (28).

In this study, we found that PTK 787 did not affect the *in vitro* proliferation of PC14PE6 cells, whereas it specifically inhibited the proliferation of HDMECs (presumably expressing VEGF/VPF receptors) stimulated with VEGF/VPF. In addition, treatment with PTK 787 inhibited vascularization in lung tumors produced by PC14PE6 cells, although it did not affect VEGF/VPF expression in tumors formed by PC14PE6 cells. These findings strongly suggest that treatment with PTK 787 directly inhibits endothelial cell function but not tumor cell function.

The two major functions of VEGF/VPF are induction of angiogenesis and vascular hyperpermeability, both of which are thought to be mediated mainly by Flk-1/KDR (6, 33). In this study, we found that treatment with PTK 787 inhibited the two major functions of VEGF/VPF. Treatment with the highest dose (100 mg/kg) of PTK 787 inhibited vascularization in the lung metastasis and it inhibited total tumor volume, represented by lung weight. However, this treatment did not significantly reduce the number of lung metastases, and there was no significant correlation between the number of lung metastases and the volume of PE (Fig. 5). This is not unexpected because angio-

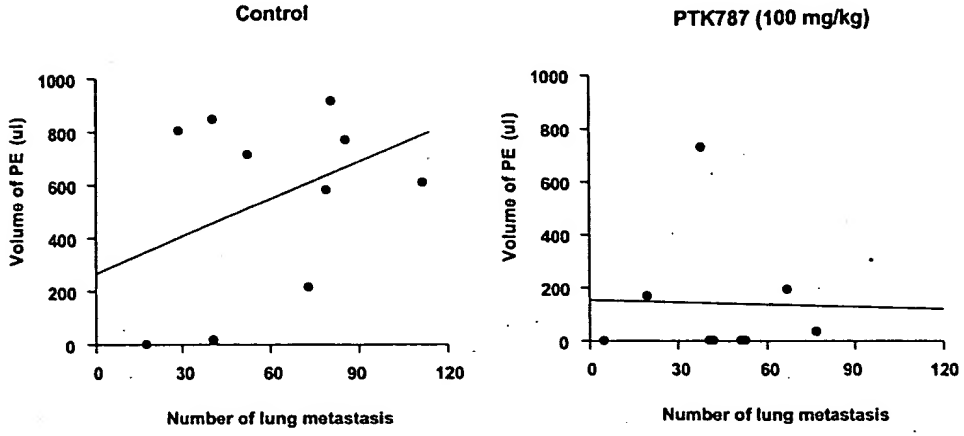

Fig. 5 Lack of correlation between the number of visible lung metastases and volume of malignant PE. PC14PE6 cells (1×10^6) were injected i.v. into nude mice on day 0. The mice ($n = 10$) were given oral feedings with distilled water (control) or PTK 787 ($n = 10$; starting on day 14). Daily oral treatments continued until day 48. The mice were killed on day 49, when lung metastasis and PE were evaluated as described in "Materials and Methods."

genesis is not necessary for small tumors (<1–2 mm in diameter; Ref. 34). On the other hand, skin vascular permeability induced by rhVEGF/VPF or PE (containing VEGF/VPF) was significantly inhibited by treatment of the mice with PTK 787 as shown in Fig. 3. Moreover, treatment with 50 mg/kg PTK 787 for 6 days significantly inhibited the vascular permeability of PE-bearing mice (Fig. 4). Collectively, these findings suggest that a primary mechanism by which treatment with PTK 787 inhibited PE was suppression of vascular permeability.

Lung cancer is the leading cause of malignant PE (1), and at least 25% of all of the patients with lung cancer will develop PE at some time during the course of the disease (35). The standard treatment for PE, drainage followed by instillation of sclerosing agents, produces variable results (1, 4, 36). We found recently that in a nude mouse model for non-small cell lung carcinoma cells, PE formation directly correlates with expression of VEGF/VPF by the tumor cells. Moreover, the levels of VEGF/VPF in malignant PE of lung cancer patients are much higher than that in PE caused by benign diseases, including heart failure and pulmonary tuberculosis (37). In this study, we showed the therapeutic potential of PTK 787 against malignant PE caused by human lung adenocarcinoma cells in an animal model.

Recently, various compounds that inhibit the function of VEGF/VPF and VEGF/VPF receptors, including humanized neutralization antibody for VEGF/VPF (38), dominant-negative VEGF/VPF (39), soluble VEGF/VPF receptors (26, 40), and low molecular weight compounds that inhibit VEGF/VPF receptor tyrosine kinases (27) have been developed, and their antiangiogenic activities have been demonstrated. The main advantages of PTK 787 over these compounds are as follows: (*a*) PTK 787 is a smaller compound with a low molecular weight and is easier to synthesize; (*b*) PTK 787 can be administered p.o. and hence may improve patient compliance. PTK 787 was very effective in this animal model. The drug administered daily for at least 35 days did not produce undesirable side effects. To confirm its efficacy, it will be necessary to evaluate the ability of PTK 787 to control malignant PE with a high level of VEGF/VPF in lung cancer patients receiving long-term treatment.

In summary, we demonstrate that the p.o.-administered VEGF/VPF receptor tyrosine kinase inhibitor PTK 787 inhibits the formation of malignant PE by human lung adenocarcinoma cells, through the inhibition of vascular permeability. Therefore, PTK 787 could be useful for the control of malignant PE in lung cancer patients, and clinical trials are warranted.

REFERENCES

1. Reed, C. E. Management of the malignant pleural effusion. *In:* H. I. Pass, J. B. Mitchell, D. H. Johnson, and A. T. Turrisi (eds.), Lung Cancer: Principles and Practice, pp. 643–654. Philadelphia: Lippincott-Raven, 1996.

2. Sugiura, S., Ando, Y., Minami, H., Ando, M., Sakai, S., and Shimokata, K. Prognostic value of pleural effusion in patients with non-small cell lung cancer. Clin. Cancer Res., *3:* 47–50, 1997.

3. Naito, T., Satoh, H., Ishikawa, H., Yamashita, Y. T., Kamma, H., Takahashi, H., Ohtsuka, M., and Hasegawa, S. Pleural effusion as a significant prognostic factor in non-small cell lung cancer. Anticancer Res., *17:* 4743–4746, 1997.

4. Light, R. W. Malignant pleural effusions. *In:* R. W. Light (ed.), Pleural Diseases, pp. 94–116. Baltimore, MD: Williams & Wilkins, 1995.

5. Senger, D. R., Galli, S. J., Dvorak, A. M., Perruzzi, C. A., Harvey, V. S., and Dvorak, H. F. Tumor cells secrete a vascular permeability factor that promotes accumulation of ascites fluid. Science (Washington DC), *219:* 983–985, 1983.

6. Ferrara, N. The role of vascular endothelial growth factor in the regulation of blood vessel growth. *In:* R. Bicknell, C. E. Lewis, and N. Ferrara (eds.), Tumor Angiogenesis, pp. 185–199. New York: Oxford University Press, Inc., 1997.

7. Carmeliet, P., Ferreira, V., Breier, G., Pollefeyt, S., Kieckens, L., Gertsenstein, M., Fahrig, M., Vandenhoeck, A., Harpal, K., Eberhardt, C., Declercq, C., Pawling, J., Moons, L., Collen, D., Risau, W., and Nagy, A. Abnormal blood vessel development and lethality in embryos lacking a single *VEGF* allele. Nature (Lond.), *380:* 435–439, 1996.

8. Ferrara, N., Carver-Moore, K., Chen, H., Dowd, M., Lu, L., O'Shea, K. S., Powell-Braxton, L., Hillan, K. J., and Moore, M. W. Heterozygous embryonic lethality induced by targeted inactivation of the *VEGF* gene. Nature (Lond.), *380:* 439–442, 1996.

9. Ferrara, N., and Henzel, W. J. Pituitary follicular cells secrete a novel heparin-binding growth factor specific for vascular endothelial cells. Biochem. Biophys. Res. Commun., *161:* 851–859, 1989.

10. Pepper, M. S., Ferrara, N., Orci, L., and Montesana, R. Vascular endothelial growth factor (VEGF) induces plasminogen activators and plasminogen activator inhibitor type 1 in microvascular endothelial cells. Biochem. Biophys. Res. Commun., *181:* 902–908, 1991.

11. Unemori, E., Ferrara, N., Bauer, E. A., and Amento, E. P. Vascular endothelial growth factor induces interstitial collagenase expression in human endothelial cells. J. Cell. Physiol., *153:* 557–562, 1992.

12. Kumar, R., Yoneda, J., Bucana, C. D., and Fidler, I. J. Regulation of distinct steps of angiogenesis by different angiogenic molecules. Int. J. Oncol., *12:* 749–757, 1998.

13. Dvorak, H. F., Brown, L. F., Detmar, M., and Dvorak, A. M. Vascular permeability factor/vascular endothelial growth factor, microvascular hyperpermeability, and angiogenesis. Am. J. Pathol., *146:* 1029–1039, 1995.

14. Nagy, J. A., Masse, E. M., Herzberg, K. T., Meyers, M. S., Yeo, K. T., Yeo, T. K., Sioussat, T. M., and Dvorak, H. F. Pathogenesis of ascites tumor growth: vascular permeability factor, vascular hyperpermeability, and ascites fluid accumulation. Cancer Res., *55:* 360–368, 1995.

15. Yoneda, J., Kuniyasu, H., Crispens, M. A., Price, J. E., Bucana, C. D., and Fidler, I. J. Expression of angiogenesis-related genes and progression of human ovarian carcinomas in nude mice. J. Natl. Cancer Inst., *90:* 447–454, 1998.

16. Luo, J. C., Yamaguchi, S., Shinkai, A., Shitara, K., and Shibuya, M. Significant expression of vascular endothelial growth factor/vascular permeability factor in mouse ascites tumors. Cancer Res., *58:* 2652–2660, 1998.

17. Luo, J. C., Toyoda, M., and Shibuya, M. Differential inhibition of fluid accumulation and tumor growth in two mouse ascites tumors by an antivascular endothelial growth factor/permeability factor neutralizing antibody. Cancer Res., *58:* 2594–2600, 1998.

18. Yano, S., Nokihara, H., Hanibuchi, M., Parajuli, P., Shinohara, T., Kawano, T., and Sone, S. Model of malignant pleural effusion of human lung adenocarcinoma in SCID mice. Oncol. Res., *9:* 573–579, 1997.

19. Risau, W. Mechanisms of angiogenesis. Nature (Lond.), *386:* 671–674, 1997.

20. Shalaby, F., Rossant, J., Yamaguchi, T. P., Gertsenstein, M., Wu, X. F., Breitman, M. L., and Schuh, A. C. Failure of blood-island formation and vasculogenesis in Flk-1-deficient mice. Nature (Lond.), *376:* 62–66, 1995.

21. Fong, G. H., Rossant, J., Gertsenstein, M., and Breitman, M. L. Role of the Flt-1 receptor tyrosine kinase in regulating the assembly of vascular endothelium. Nature (Lond.), *376:* 66–70, 1995.

22. Clauss, M., Weich, H., Breier, G., Knies, U., Rockl, W., Waltenberger, J., and Risau, W. The vascular endothelial growth factor receptor Flt-1 mediates biological activities. Implications for a functional role of placenta growth factor in monocyte activation and chemotaxis. J. Biol. Chem., *271:* 17629–17634, 1996.

23. Keyt, B. A., Nguyen, H. V., Berleau, L. T., Duarte, C. M., Park, J., Chen, H., and Ferrara, N. Identification of vascular endothelial growth factor determinants for binding KDR and FLT-1 receptors: generation of receptor-selective VEGF variants by site-directed mutagenesis. J. Biol. Chem., *271:* 5638–5646, 1996.

24. Keyt, B. A., Berleau, L. T., Nguyen, H. V., Chen, H., Heinsohn, H., Vandlen, R., and Ferrara, N. The carboxyl-terminal domain (111–165) of vascular endothelial growth factor is critical for its mitogenic potency. J. Biol. Chem., *271:* 7788–7795, 1996.

25. Millauer, B., Shawver, L. K., Plate, K. H., Risau, W., and Ullrich, A. Glioblastoma growth inhibited *in vivo* by a dominant-negative Flk-1 mutant. Nature (Lond.), *367:* 576–579, 1994.

26. Lin, P., Sankar, S., Shan, S., Dewhirst, M. W., Polverini, P. J., Quinn, T. Q., and Peters, K. G. Inhibition of tumor growth by targeting tumor endothelium using a soluble vascular endothelial growth factor receptor. Cell Growth Differ., *9:* 49–58, 1998.

27. Fong, T. A., Shawver, L. K., Sun, L., Tang, C., App, H., Powell, T. J., Kim, Y. H., Schreck, R., Wang, X., Risau, W., Ullrich, A., Hirth, K. P., and McMahon, G. SU5416 is a potent and selective inhibitor of the vascular endothelial growth factor receptor (Flk-1/KDR) that inhibits tyrosine kinase catalysis, tumor vascularization, and growth of multiple tumor types. Cancer Res., *59:* 99–106, 1999.

28. Wood, J. M., Bold, G., Frei, J., Stover, D., Hofmann, F., Buchdunger, E., Mestan, J., Towbin, H., Schnell, C., Mett, H., O'Reilly, T., Cozens, R., Rösel, J., Siemeister, G., Menrad, A., Schirner, M., Thierauch, K-H., Schneider, M. R., Totzke, F., Martiny-Baron, G., Drevs, J., and Marmé, D. PTK 787/ZK 222584, a novel and potent inhibitor of VEGF receptor tyrosine kinases, impairs VEGF-induced responses and tumor growth after oral administration. Cancer Res., in press, 2000.

29. Carroll, M., Ohno, J. S., Tamura, S., Buchdunger, E., Zimmermann, J., Lydon, N. B., Gilliland, D. G., and Druker, B. J. CGP57148, a tyrosine kinase inhibitor, inhibits the growth of cells expressing BCR-ABL, and TEL-PDGFR fusion proteins. Blood, *90:* 4947–4952, 1997.

30. Kuniyasu, H., Ellis, L. M., Evans, D. B., Abbruzzese, J. L., Fenoglio, C. J., Bucana, C. D., Cleary, K. R., Tahara, E., and Fidler, I. J. Relative expression of E-cadherin and type IV collagenase genes predicts disease outcome in patients with resectable pancreatic carcinoma. Clin. Cancer Res., *5:* 25–33, 1999.

31. Weidner, N., Semple, J. P., Welch, W. R., and Folkman, J. Tumor angiogenesis and metastasis–correlation in invasive breast carcinoma. N. Engl. J. Med., *324:* 1–8, 1991.

32. Heiss, J. D., Papavassiliou, E., Merrill, M. J., Nieman, L., Knightly, J. J., Walbridge, S., Edwards, N. A., and Oldfield, E. H. Mechanism of dexamethasone suppression of brain tumor-associated vascular permeability in rats: involvement of the glucocorticoid receptor and vascular permeability factor. J. Clin. Investig., *98:* 1400–1408, 1996.

33. Hiratsuka, S., Minowa, O., Kuno, J., Noda, T., and Shibuya, M. Flt-1 lacking the tyrosine kinase domain is sufficient for normal development and angiogenesis in mice. Proc. Natl. Acad. Sci. USA, *95:* 9349–9354, 1998.

34. Fidler, I. J., and Ellis, L. M. The implications of angiogenesis for the biology and therapy of cancer metastasis. Cell, *79:* 185–188, 1994.

35. Tattersall, M. Management of malignant pleural effusion. Aust. N. Z. J. Med., *28:* 394–396, 1998.

36. Ruckdeschel, J. C. Management of malignant pleural effusions. Semin. Oncol., *22:* 58–63, 1995.

37. Yanagawa, H., Takeuchi, E., Suzuki, Y., Ohmoto, Y., Bando, H., and Sone, S. Vascular endothelial growth factor in malignant pleural effusion associated with lung cancer. Cancer Immunol. Immunother., in press, 2000.

38. Presta, L. G., Chen, H., O'Connor, S. J., Chisholm, V., Meng, Y. G., Krummen, L., Winkler, M., and Ferrara, N. Humanization of an anti-vascular endothelial growth factor monoclonal antibody for the therapy of solid tumors and other disorders. Cancer Res., *57:* 4593–4599, 1997.

39. Siemeister, G., Schirner, M., Reusch, P., Barleon, B., Marme, D., and Martiny-Baron, G. An antagonistic vascular endothelial growth factor (VEGF) variant inhibits VEGF-stimulated receptor autophosphorylation and proliferation of human endothelial cells. Proc. Natl. Acad. Sci. USA, *95:* 4625–4629, 1998.

40. Goldman, C. K., Kendall, R. L., Cabrera, G., Soroceanu, L., Heike, Y., Gillespie, G. Y., Siegal, G. P., Mao, X., Bett, A. J., Huckle, W. R., Thomas, K. A., and Curiel, D. T. Paracrine expression of a native soluble vascular endothelial growth factor receptor inhibits tumor growth, metastasis, and mortality rate. Proc. Natl. Acad. Sci. USA, *95:* 8795–8800, 1998.

Exhibit 6

THE JOURNAL OF BIOLOGICAL CHEMISTRY Vol. 273, No. 2, Issue of January 9, pp. 1052–1057, 1998

Printed in U.S.A.

Down-regulation of Vascular Endothelial Growth Factor in a Human Colon Carcinoma Cell Line Transfected with an Antisense Expression Vector Specific for c-*src**

(Received for publication, June 23, 1997, and in revised form, October 28, 1997)

Lee M. Ellis‡§, Charles A. Staley¶, Wenbiao Liu§, R. Y. Declan Fleming‡, Nila U. Parikh‖, Corazon D. Bucana§, and Gary E. Gallick‖**

From the Departments of ‡Surgical Oncology, §Cell Biology, and ‖Tumor Biology, University of Texas M. D. Anderson Cancer Center, Houston, Texas 77030 and the ¶Department of Surgical Oncology, Emory University School of Medicine, Atlanta, Georgia 30322

Vascular endothelial growth factor (VEGF) is implicated in the angiogenesis of human colon cancer. Recent evidence suggests that factors that regulate VEGF expression may partially depend on c-*src*-mediated signal transduction pathways. The tyrosine kinase activity of Src is activated in most colon tumors and cell lines. We established stable subclones of the human colon adenocarcinoma cell line HT29 in which Src expression and activity are decreased specifically as a result of a transfected antisense expression vector. This study determined whether VEGF expression is decreased in these cell lines and whether the smaller size and reduced growth rate of antisense vector-transfected cell lines *in vivo* might result, in part, from reduced vascularization of tumors. Northern blot analysis of these cell lines revealed that VEGF mRNA expression was decreased in proportion to the decrease in Src kinase activity. Under hypoxic conditions, cells with decreased Src activity had a <2-fold increase in VEGF expression, whereas parental cells had a >50-fold increase. VEGF protein in the supernatants of cells was also reduced in antisense transfectants compared with that from parental cells. In nude mice, subcutaneous tumors from antisense transfectants showed a significant reduction in vascularity. These results suggest that Src activity regulates the expression of VEGF in colon tumor cells.

Neovascularization is a critical requirement for tumor growth and metastasis formation. Numerous angiogenic factors that regulate this process have been identified (1). Among them is vascular endothelial growth factor (VEGF),[1] which has been implicated in the neovascularization of a wide variety of tumors (2–8). VEGF, also known as vascular permeability factor, is a 36–45-kDa dimeric glycoprotein that has been identified in the conditioned media from numerous cell lines and that is expressed in many tumors (2–12). The gene for this angiogenic factor has ~20% homology to platelet-derived growth factor and ~50% homology to placenta growth factor (13, 14). Recently, several studies suggested that VEGF is the angiogenic factor most closely associated with induction and maintenance of the neovasculature in human colon cancer (2, 10, 15, 16). In primary tumors, the expression of VEGF mRNA is increased in tumors relative to histologically normal bowel mucosa (8, 17). Further studies have implicated VEGF expression in tumor progression and metastasis. We have demonstrated that VEGF expression is greater in colon tumors that have metastasized than in nonmetastatic tumors (2). Using a murine model system for colon cancer, Warren *et al.* (16) demonstrated that a monoclonal antibody to VEGF inhibits subcutaneous tumor formation in a dose- and time-dependent manner and reduces the number and size of liver metastases.

Although VEGF has undergone considerable study in recent years, the factors in the tumor environment and subsequent signal transduction pathways that regulate VEGF production have yet to be elucidated fully. One environmental condition known to enhance VEGF expression is hypoxia (18–20). Recently, hypoxia was demonstrated to be mediated, in part, by specific activation of the protein-tyrosine kinase activity of Src (18). In addition, cell lines transfected with v-*src* (a constitutively activated homolog of c-*src*) have been found to have increased VEGF expression (21). These observations may be of particular relevance to colon tumorigenesis and progression because >80% of primary colon tumors have significantly increased Src activity (22, 23), and further increases in Src activity are observed in the majority of colon tumor metastases (22, 24). Additionally, most colon tumor cell lines are known to express VEGF (10). However, in the HEP3b hepatoma cell line, recent studies have suggested no relationship between Src activation and VEGF production (25).

A potential relationship between Src activation and VEGF production in colon tumor cells has yet to be demonstrated. Recently, we established stable subclones of the well characterized human colon adenocarcinoma cell line HT29 in which Src expression and activity are decreased as a result of a transfected antisense expression vector specific for inhibition of Src (26). The cell lines demonstrated decreased growth in nude mice proportionately to the reduction in c-*src* levels (26). The purpose of this study was to determine whether VEGF expression and associated biologic activity were decreased by specific down-regulation of Src kinase activity and whether the smaller size and reduced growth rate of antisense vector-transfected cell lines *in vivo* might result, in part, from reduced vascularization of tumors.

EXPERIMENTAL PROCEDURES

Construction of c-src Expression Vectors—A construct spanning the translation start site of c-*src* was generated by annealing two primers,

* The work was supported in part by the Gillson Longenbaugh Foundation, American Cancer Society Career Development Award 94-21 (to L. M. E.), and National Institutes of Health Grant T-32 CA09599 (to R. Y. D. F.) and Grants CA65527 and CA53617 (to G. E. G). The costs of publication of this article were defrayed in part by the payment of page charges. This article must therefore be hereby marked "*advertisement*" in accordance with 18 U.S.C. Section 1734 solely to indicate this fact.

** To whom correspondence should be addressed: Dept. of Tumor Biology, University of Texas M. D. Anderson Cancer Center, 1515 Holcombe Blvd., P. O. Box 108, Houston, TX 77030. Tel.: 713-792-3657; Fax: 713-794-4784.

[1] The abbreviations used are: VEGF, vascular endothelial growth factor; PCR, polymerase chain reaction; HT29-P cells, HT29 parental cells; DMEM, Dulbecco's modified Eagle's medium; FBS, fetal bovine serum; PBS, phosphate-buffered saline; RT, reverse transcription.

5'-AGCTTGGACCATGGGTAGCAACAAGAGCAAGCCCAAGGAT-3' and 5'-CTAGATCCTTGGGCTTGCTCTTGTTGCTACCCATGGTCCA-3'. The sense construct was synthesized in a similar manner with primers 5'-AGCTATCCTTGGGCTTGCTCTTGTTGCTACCCATGGTC-CT-3' and 5'-CTAGAGGACCATGGGTAGCAACAAGAGCAAGCCCA-AGGAT-3'. The pcDNAI plasmid (Invitrogen, San Diego, CA) was then digested with *Hin*dIII and *Xba*I, and a ligation reaction was performed to insert the sense and antisense constructs. *Escherichia coli* was transformed by the plasmids; selected clones were harvested; the bacteria were lysed by alkali treatment; and the plasmids were purified. Confirmation of the correct insert was determined by the polymerase chain reaction (PCR) followed by DNA sequencing.

Transfection—HT29 parental (HT29-P) cells were grown to 70% confluency under the conditions described below. Cells were transfected in serum-free medium for 6 h with 100 μg of LipofectAMINE (Life Technologies, Inc.) and 16 μg of plasmid DNA. The medium was then replenished with medium supplemented with 250 μg/ml G418 (Life Technologies, Inc.). Colonies resistant to G418 were expanded, and the resulting clones were screened for expression and activity of Src, as described below.

Cell Culture—HT29 cells, derived from a colon adenocarcinoma (27), were maintained in Dulbecco's modified Eagle's medium (DMEM) with Earle's salts and 2 mM glutamine (Life Technologies, Inc.) supplemented with 10% fetal bovine serum (FBS; Hyclone Laboratories, Logan, UT). Stable HT29 subclones expressing c-*src* "sense" (HT29-S8 and HT29-S20) and "antisense" (HT29-AS15 and HT29-AS33) constructs were also maintained under these conditions, except that the medium was supplemented with 250 μg/ml G418. For experiments examining the effect of tumor cell-conditioned medium on endothelial cell proliferation, HT29-P cells and subclones were grown to 100% confluence in DMEM supplemented with 1% FBS for 24 h.

Immunoprecipitation and Immune Complex Kinase Assays—Prior to lysis, cells were rinsed twice with ice-cold phosphate-buffered saline (PBS). Detergent lysates were made in a standard radioimmune precipitation assay buffer. Cells were homogenized and clarified by centrifugation at 10,000 × *g*. Cell lysates (250 μg of protein) were reacted for 2 h with either monoclonal antibody 327 (Oncogene Science Inc., Cambridge, MA) for immunoprecipitation of Src or monoclonal antibody 1B7 (Wako Bioproducts, Richmond, VA) for immunoprecipitation of Yes. Immune complexes were formed by incubation with 6 μg of rabbit anti-mouse IgG (Organon Teknika, Durham, NC) for 1 h and then with 50 μl of 10% (v/v) Formalin-fixed Pansorbin (*Staphylococcus aureus*, Cowan strain; Calbiochem) for 30 min. Pellets were washed three times in a buffer consisting of 0.1% Triton X-100, 150 mM NaCl, and 10 mM sodium phosphate. Immune complex kinase assays were performed by standard procedures as described previously (22). Briefly, reactions were initiated by adding to each sample 10 μCi of [γ-^{32}P]ATP, 10 mM Mg^{2+}, and 100 μM sodium orthovanadate in 20 mM HEPES. After 10 min at 25 °C, reactions were terminated by adding SDS sample buffer. Proteins were separated by SDS-polyacrylamide gel electrophoresis on 8% polyacrylamide gels, and radioactive proteins were detected by autoradiography.

Immunoblotting—Clarified cell lysates (250 μg/lane) were separated by SDS-polyacrylamide gel electrophoresis on 10% polyacrylamide gels and electroblotted onto nitrocellulose membranes (Schleicher & Schuell) using standard procedures (22). Membranes were blocked with 15% skimmed milk in PBS and then incubated with anti-Src or anti-Yes antibodies at a 1:1000 dilution followed by horseradish peroxidase-conjugated rabbit anti-mouse IgG. Specific binding of antibody was determined using the ECL detection system (Amersham Corp.).

mRNA Extraction and Northern Blot Analysis—Polyadenylated mRNA was extracted from tumor cells grown under confluent conditions in culture using the TRI reagent kit (Molecular Research Center, Inc. Cincinnati, OH). Twenty μg of total RNA was fractionated on 1% denaturing formaldehyde-agarose gels, transferred to a Hybond nylon membrane (Amersham Corp.) by capillary elution, and UV-cross-linked at 120,000 μJ/cm^2 using a UV Stratalinker 1800 (Stratagene, La Jolla, CA). Following prehybridization, the membranes were probed for VEGF and glyceraldehyde-3-phosphate dehydrogenase. Each cDNA probe was purified by agarose gel electrophoresis, recovered using a QIAEX gel extraction kit (QIAGEN Inc., Chatsworth, CA), and radiolabeled by the random primer technique using a commercially available kit (Amersham Corp.) that utilizes [α-^{32}P]dCTP (Amersham Corp.). Nylon filters were washed at 65 °C with 30 mM NaCl, 3 mM sodium citrate (pH 7.2), and 0.1% (w/v) SDS. Autoradiography was then performed.

A 1.28-kilobase glyceraldehyde-3-phosphate dehydrogenase probe (American Type Culture Collection, Rockville, MD) was used as an internal control. The VEGF probe, a 204-base pair fragment of human VEGF cDNA, was a gift from Dr. Brygida Berse (Harvard Medical School, Boston, MA) (17).

Semiquantitative Reverse Transcription-Polymerase Chain Reaction—cDNA was synthesized from total RNA extracted from HT29-P cells and antisense cell lines (HT29-AS33 and HT29-AS15) by reverse transcription (RT) in a 20-μl reaction containing 0.5 μg of random primers (Life Technologies, Inc.), 200 units of SuperScript™ RNase H$^-$ reverse transcriptase (Life Technologies, Inc.), 0.1 μg of mRNA, 4 μl of 5 × RT buffer (375 mM KCl, 250 mM Tris-HCl (pH 8.3 at room temperature), and 15 mM $MgCl_2$), 5 mM dithiothreitol, 0.1 mM each dNTP, 20 units of RNasin (Life Technologies, Inc.), and diethyl pyrocarbonate-treated water. Each mixture was incubated at 37 °C for 1 h and then quick-chilled on ice.

Each PCR was performed using a 50-μl reaction mixture containing 5 μl of RT reaction mixture, 1 × PCR buffer (50 mM KCl, 10 mM Tris-HCl (pH 9.0 at room temperature), and 1% Triton X-100), 0.2 mM dNTP, 1.5 mM $MgCl_2$, 2.5 units of *Taq* polymerase (Promega, Madison, WI), 50 pmol/μl VEGF primers, and 50 pmol/μl β-actin primers. The mixture was overlaid with mineral oil and then amplified with a TemTronic DNA amplification system using the following amplification profile: an initial denaturation at 94 °C for 5 min, denaturation at 93 °C for 1 min, annealing at 59 °C for 1 min, extension at 72 °C for varying cycle numbers, and a final elongation step at 72 °C for 10 min. The PCR products were then electrophoresed on a 2% agarose gel, stained with 0.5 μg/ml ethidium bromide, visualized under UV light, and photographed with Polaroid Type 55 positive/negative film. Specific amplification was determined by the size of the product on the gel relative to that of known DNA molecular weight marker V (Boehringer Mannheim). The amount of PCR product was determined by measuring the density of the specific bands on the negative film with a densitometer.

RT products were amplified by PCR using specific primers for β-actin (design of primers based on published sequence (GenBank™/EMBL Data Bank accession number M10277)) (sense, 5'-ACACTGTGCCC-ATCTACGAGG-3'; and antisense, 5'-AGGGGCCGGACTCGTCATACT-3') and for VEGF (28) (sense, 5'-CACATAGGAGAGATGAGCTTC-3'; and antisense, 5'-CCGCCTCGGCTTGTCACAT-3') in separate reactions for 18–28 cycles under the above conditions, and the products were quantitated by densitometry. Curves depicting product quantity relative to the number of PCR cycles were generated, and the PCR cycle number that generated product quantities representing the up-slope of the curve was selected for quantitative PCR of each specific set of primers. Semiquantitative PCR was performed for β-actin (22 cycles) and VEGF (22 cycles).

Densitometric Quantitation—Protein kinase activity and VEGF mRNA expression were quantitated by densitometry of autoradiograms using the ImageQuant™ software program (Molecular Dynamics, Inc., Sunnyvale, CA) in the linear range of the film. Semiquantitative PCR products were separated by agarose gel electrophoresis, and after ethidium bromide staining, they were exposed to UV light and photographed with Polaroid Type 55 positive/negative film. The positive bands on the film were quantitated by densitometry using β-actin as an internal control.

Determination of VEGF Protein Levels in Cell Supernatants—For these determinations, equal densities as opposed to equal numbers of cells were chosen because of previous experiments in colon tumor cells demonstrating that density affects VEGF expression (29, 30). Thus, HT29-P cells were seeded at 20 × 10^6, HT29-AS33 cells at 25 × 10^6, and HT29-AS15 cells at 40 × 10^6 cells/100-mm tissue culture plate to compensate for size differences in these cells. Cells were grown for 24 h in DMEM/F-12 (1:1 mixture) supplemented with 10% FBS, washed three times with PBS, and changed to 7.5 ml of DMEM/F-12 (1:1 mixture) supplemented with 1% FBS. Cell supernatants were collected, filtered, and stored at −12 °C, and concomitantly, cell pellets were harvested by trypsinization, and cell number was determined. The amount of VEGF protein in the supernatant was determined with an enzyme-linked immunosorbent assay kit (R&D Systems, Minneapolis, MN) according to the manufacturer's instructions. VEGF was expressed as pg of VEGF protein/10^6 cells/24 h.

Effects of Hypoxia on VEGF Expression in HT29-P Cells and Transfectants—HT29-P and HT29-AS15 cells were grown to confluence in standard medium. The medium was changed, and cells were then transferred to a hypoxia chamber (Proox Model 110, Reming Bioinstruments Co., Redfield, NY). Control cultures were harvested just prior to hypoxic exposure (t = 0), and protein and RNA were harvested. Identical cultures were then incubated for 4, 6, and 24 h, and cells were harvested at these time points for protein and RNA analysis.

Quantitation of Murine Tumor Microvasculature—Cells from clones to be tested were grown in tissue culture to log phase (~70% confluent),

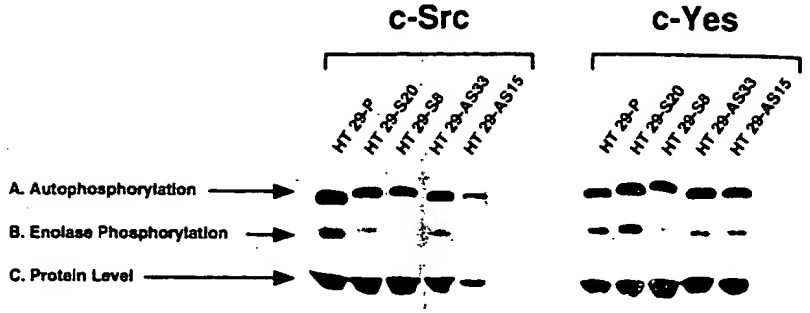

FIG. 1. **Expression and activity of Src and Yes in HT29-P cells, HT29-S8 and HT29-S20 sense transfected subclones, and HT29-AS33 and HT29-AS15 antisense transfected subclones.** Stable HT29 subclones were isolated, and cell lysates were subjected to immunoblotting and immune complex kinase assays for Src and Yes as described under "Experimental Procedures." *Row A*, autophosphorylation of Src and Yes; *row B*, phosphorylation of the exogenous substrate enolase; *row C*, relative levels of Src and Yes.

trypsinized, and counted with the aid of a hemocytometer. 1×10^6 cells of each clone were injected subcutaneously in the flank of eight nude mice/cell type. For quantitation of tumor microvasculature, tumors were harvested after 60 days and frozen in liquid nitrogen. Cryostat sections of tissues previously frozen in O.C.T. compound were fixed sequentially (5 min each) with acetone, acetone/chloroform (1:1), and acetone. The sections were washed three times, and endogenous peroxidase was blocked with 3% hydrogen peroxide in methanol for 12 min. The samples were washed three times with PBS and incubated with a protein-blocking solution consisting of PBS containing 1% normal goat serum and 1% horse serum for 20 min at room temperature. Excess blocking reagent was drained off, and the samples were incubated with the primary antibody (rat anti-mouse CD31 antibody, 1:100 dilution; Pharmingen, San Diego, CA) overnight at 4 °C. Sections were washed with PBS and incubated with the secondary antibody (peroxidase-labeled mouse anti-rat antibody, 1:200 dilution; Boehringer Mannheim) for 1 h. Sections were washed four times with PBS, rinsed briefly with distilled water, and then incubated with stable diaminobenzadine (Research Genetics, Huntsville, AL) for 20 min to develop the peroxidase signal. Sections were counterstained with Mayer's hematoxylin (Sigma), washed, mounted with Universal Mount (Research Genetics), and dried on a 60 °C hot plate. Because heterogeneity in vascularization was observed, the four most vascular areas of each tumor were identified, and vessels were quantitated. Vessel counts in HT29-P and HT29-AS15 tumors were compared by two-tailed, unpaired Student's *t* test.

RESULTS

Expression and Activity of Src and Yes in HT29 Transfectants—Expression vectors spanning the translation start site of c-*src* in the sense and antisense orientations were made and transfected into HT29-P cells, and G418-resistant clones were isolated as described under "Experimental Procedures." Each clone was then screened for expression and activity of Src. To examine specificity of effects on Src, each clone was also screened for expression and activity of the related tyrosine kinase, Yes. The results with two antisense and two sense transfectants are shown in Fig. 1. When HT29-P cells were compared with the two sense transfectants, HT29-S8 and HT29-S20, no differences were apparent in autophosphorylation (Fig. 1, *row A*), phosphorylation of the exogenous substrate enolase (*row B*), or expression of either Src or Yes (*row C*). In contrast, the antisense clone HT29-AS15 had a 4.0-fold reduction in Src (*row C*) and 4.5-fold reduction in autophosphorylation (*row A*) and enolase phosphorylation (*row B*). Clone HT29-AS33 was intermediate in level and activity of Src, with expression reduced 2.0-fold (*row C*) and autophosphorylation (*row A*) and enolase phosphorylation (*row B*) reduced 2.5-fold. As is also shown in Fig. 1, neither the levels nor protein-tyrosine kinase activities of Yes were altered in the antisense transfectants relative to the sense transfectants or HT29-P cells. Therefore, the effects of the antisense expression vector were specific for Src.

Effect of Src on VEGF mRNA Expression—Transfection of the parental cell line with the control expression vector (sense) caused a minor increase in VEGF mRNA expression (Fig. 2). However, the establishment of cell lines with decreased Src kinase activity demonstrated a decrease in mRNA expression at levels of 54% (HT29-AS33) and 23% (HT29-AS15) of the average of the sense transfected cell lines. This incremental

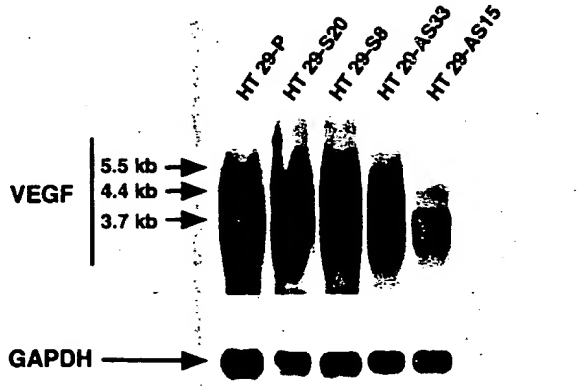

FIG. 2. **Expression of VEGF mRNA in experimental colon cancer cell lines.** VEGF mRNA expression as determined by Northern blot analysis (described under "Experimental Procedures") in cell lines with decreased Src kinase activity (HT29-AS15 and HT29-AS33) is compared with that in control cell lines (HT29-P, HT29-S8, and HT29-S20). *kb*, kilobase; *GAPDH*, glyceraldehyde-3-phosphate dehydrogenase.

decrease in VEGF mRNA expression correlated with the alteration in Src kinase activity: the transfected cell line that exhibited the greatest decrease in Src kinase activity (HT29-AS15) also exhibited the greatest decrease in VEGF mRNA expression.

Effect of Src on Expression of Various Isoforms of VEGF—Semiquantitative PCR of the various isoforms of VEGF demonstrated a decrease in overall VEGF expression in both HT29-AS33 and HT29-AS15 cells (Fig. 3). The most abundant isoform expressed was VEGF-165. There was a relatively equal decrease in the expression of all VEGF isoforms in the antisense clones. The overall decrease in VEGF expression in the antisense clones by semiquantitative RT-PCR confirmed our findings by Northern blotting.

Determination of VEGF Protein Levels in Cell Supernatants—To examine directly the amount of VEGF protein produced in the various clones, supernatants from cultures grown to identical confluencies were harvested, and VEGF expression was determined by enzyme-linked immunosorbent assay. A decrease in VEGF protein was observed in the supernatant of cells with decreased Src activity (Fig. 4). This decrease was proportional to the decrease in Src activity in the two antisense transfected cell lines. These results demonstrate that decreased expression of mRNA corresponds with decreased VEGF protein expression.

Effects of Hypoxia on VEGF Expression in HT29-P Cells and Transfectants—The above results demonstrate that the expression of Src in colon tumor cells leads to the constitutive expression of VEGF, a critical factor in tumor cell growth. However, neovascularization of tumors also results from local hypoxia as the tumor volume exceeds its blood supply. As hypoxic stimulation of VEGF in fibroblasts has been associated with activation of Src protein-tyrosine kinase, we examined the response to hypoxia in HT29-P and transfected subclones. Cells were grown to equal densities, transferred to hypoxic chambers,

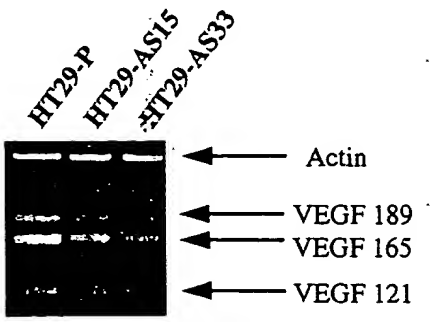

FIG. 3. **Expression of the various isoforms of VEGF in the experimental cell lines.** As described under "Experimental Procedures," RNA was isolated from the cell lines, and cDNA was synthesized by reverse transcription. The polymerase chain reaction with primers specific for VEGF was then used to amplify the cDNA; β-actin was used as an internal control.

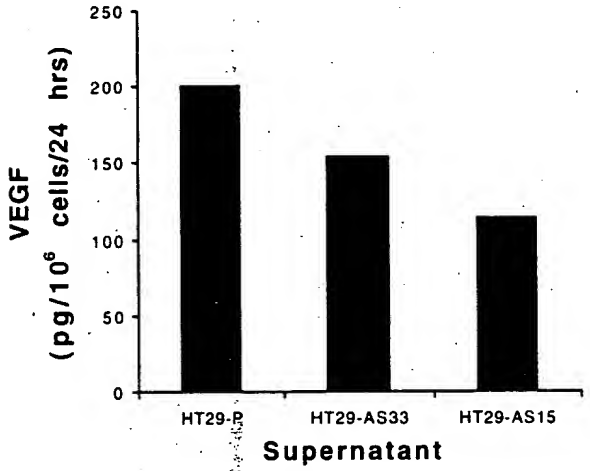

FIG. 4. **VEGF protein levels in the supernatant from cells with decreased Src activity.** HT29-P, HT29-AS33, and HT29-AS15 cells were plated at 100% confluence and grown in DMEM/nutrient mixture F-12 supplemented with 1% FBS for 24 h as described under "Experimental Procedures." Cells were counted, and VEGF protein levels were determined by enzyme-linked immunosorbent assay. VEGF protein levels are expressed as pg of VEGF protein/10^6 cells/24 h.

harvested at specific times, and processed for RNA and protein as described under "Experimental Procedures." For these studies, HT29 parental cells were compared with HT29-AS15, the antisense transfectant expressing the least Src. The ability of hypoxia to induce VEGF mRNA in these clones is compared in Fig. 5. VEGF mRNA was markedly induced in a time-dependent manner in HT29-P cells, with a >50-fold increase observed after 24 h. In contrast, a <2-fold increase in VEGF mRNA expression was observed in HT29-AS15 cells. These results demonstrate that not only is the constitutive production of VEGF reduced by lowering Src expression, the ability of hypoxia to induce further expression of VEGF is severely impaired. To confirm that induction of VEGF mRNA by hypoxia was Src-dependent, the expression and activity of Src were compared in these clones under identical conditions. In HT29-P cells, Src kinase activity was stimulated in a time-dependent manner, with a maximum stimulation of 4.5-fold occurring 4 h after the onset of hypoxic conditions, whereas only a 1.1-fold increase in activity was observed in HT29-AS15 cells under identical conditions (data not shown).

Effect of Src on in Vivo Tumor Vascularity—For this determination, HT29-P and HT29-AS15 cells were implanted in the subcutis of nude mice as described under "Experimental Procedures." Tumors were harvested when they were ~1 cm in diameter. Mean vessel counts were determined by counting the most vascularized areas of the respective tumors, after immunostaining with rat CD31 antibody, as described. In tumors grown from HT29-AS15 cells, vessel counts were significantly reduced relative to those tumors grown from HT29-P cells (31.8 ± 2.8 *versus* 53.0 ± 1.5 (mean ± S.E.), respectively; $p < 0.0001$) (Fig. 6). These results demonstrate that reduction in constitutive and inducible VEGF production in c-*src* antisense transfected clones corresponds with decreased vascularization of the tumor. However, we cannot rule out that other factors, such as different growth rates and metabolic requirements, contribute to changes in tumor vascularization.

DISCUSSION

Angiogenesis is an essential step in tumor growth and metastasis, and this process is driven by the balance of positive and negative effector molecules (31). In human colon cancers and established cell lines, VEGF appears to be the angiogenic factor most closely associated with neovascularization. Several lines of evidence implicate VEGF production as important to colon tumorigenicity and/or metastatic potential. Increases in VEGF are observed in primary tumors relative to normal tissue (7, 8) and in metastatic tumors relative to nonmetastatic tumors (2, 3). Using colon tumor cell lines in mouse models, Warren *et al.* (16) found that a VEGF antibody greatly inhibits the growth of subcutaneous xenografts and the number and size of experimental metastases. These results suggest that the production of VEGF is important to colon tumor cell growth and progression. However, other factors have also been implicated in the process of colon cancer angiogenesis. Subcutaneous injection into nude mice of several HT29 subclones with varying degrees of differentiation has demonstrated a positive correlation between vessel counts and the ability of the cells to express platelet-derived growth factor-B *in vitro* (32). Thus, in different subclones from even the same cell line, different angiogenic factors might be important to induction of neovascularization.

The signal transduction pathways by which VEGF is induced remain to be elucidated fully. However, recent experiments have implicated specific activation of the protein-tyrosine kinase activities of the *src* family of proto-oncogenes as important in the induction of VEGF. Mukhopadhyay *et al.* (18) examined the role of activated c-*src* in hypoxic induction of VEGF. Hypoxia was found to increase VEGF expression in U87 glioma cells and 293 kidney cells, and this induction was inhibited by genistein, an inhibitor of tyrosine kinases. When the effects of hypoxia on *src* family protein-tyrosine kinases were analyzed, Src activity, but not Yes or Fyn activity, was increased. Transfection of v-*src* into U87 glioma cells and 293 kidney cells also increased the hypoxic induction of VEGF, whereas transfection of cells with a dominant-negative form of c-*src* partially inhibited VEGF induction. To examine the potential role of Src in hypoxic induction of VEGF, fibroblasts derived from mice with a c-*src* disruption were employed. These cells exhibited a 50–70% decrease in hypoxic induction of VEGF mRNA, with a compensatory activation of Fyn. These results strongly suggest a specific role for Src in promoting angiogenesis. In addition, Rak *et al.* (33) demonstrated that transfection with v-*src* increased VEGF expression and induced tumorigenicity in an immortalized rat intestinal epithelial cell line. Conditioned media from cells transfected with v-*src* were able to increase endothelial cell proliferation, and this increase was blocked by the addition of antibodies to VEGF. These results suggest that activation of Src is important to VEGF induction in several cell systems. In contrast, in HEP3b hepatoma cells, hypoxic induction of VEGF did not appear to be Src-dependent (25).

Several laboratories have demonstrated that the specific activity of Src is greatly increased in the majority of colon tumors

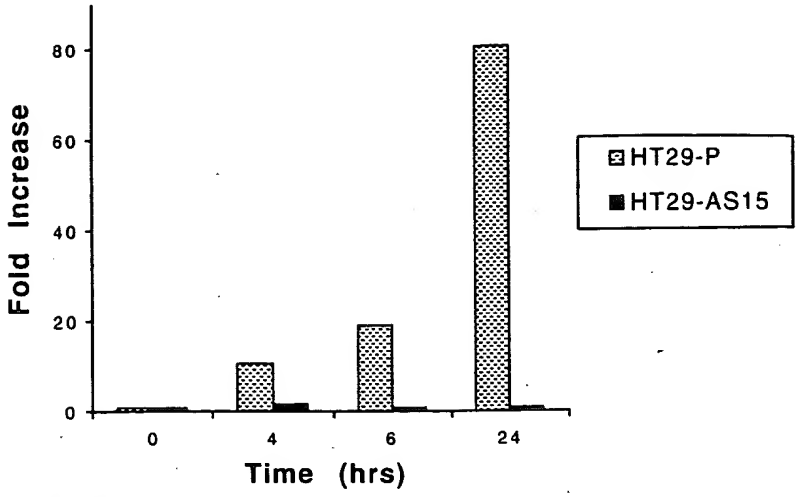

FIG. 5. **Expression of VEGF mRNA in HT29-P and HT29-AS15 cells after hypoxia.** Cells were grown to confluence and then incubated under hypoxic conditions as described under "Experimental Procedures." Cells were harvested at the time points indicated, and VEGF mRNA expression was determined by Northern blot analysis. Data are expressed as -fold increase over control cells for each cell line at $t = 0$ (prior to hypoxic exposure) using 28 S ribosomal RNA as an internal control.

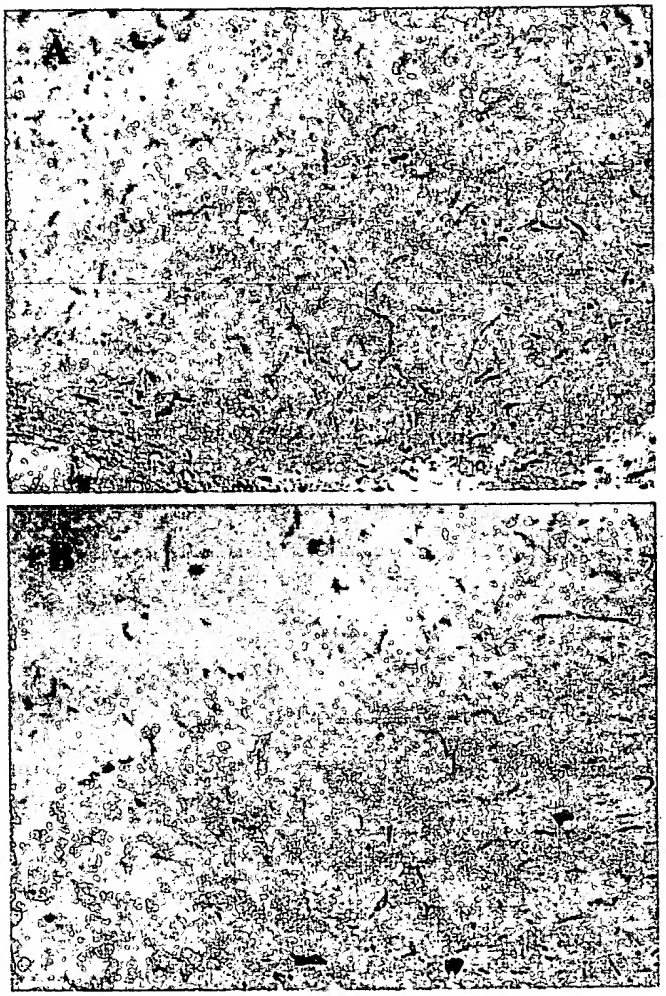

FIG. 6. **Immunohistochemical staining for vessels in tumor xenografts.** Subcutaneous tumors were grown in nude mice from the HT29-P and HT29-AS15 cell lines. The tumors were embedded in paraffin and stained for endothelial cells with CD31 antibodies as described under "Experimental Procedures."

and cell lines (22, 23, 34). The importance of this activation to colon cell tumorigenicity has been uncertain. Recently, we developed cell lines from HT29-P cells with reduced c-*src* expression and activity by transfection with an antisense expression vector specific for c-*src* (26). These cells proliferate more slowly than parental cells *in vitro*, and tumorigenicity in nude mice is reduced (26). Furthermore, tumors from antisense transfectants were limited in size, even after >1 year of growth in mice. Therefore, the present study was undertaken to determine whether limited growth, in part, resulted from reduced expression and/or induction of VEGF in the antisense transfected cell lines. The results in this paper demonstrate that reduction of Src expression and activity, but not those of the related Yes, directly corresponds to decreased levels of VEGF mRNA and decreased biologic activity of VEGF. Furthermore, fewer blood vessels are observed in tumors that form after injection of the cell lines transfected with the Src antisense constructs. These results suggest that in addition to the role of Src in regulating cell proliferation, activation of Src in colon tumorigenesis may promote tumor growth via induction of VEGF, which in turn induces neovascularization. Further evidence for this possibility was derived from studies on the effect of hypoxia on induction of VEGF mRNA expression in HT29 parental cells and the antisense transfected clone HT29-AS15. In the HT29 parental cells, a >50-fold induction of VEGF mRNA was observed. This induction far exceeded that observed by Mukhopadhyay *et al.* (18) in fibroblasts, where hypoxia resulted in a maximum 4.5-fold induction of VEGF mRNA. Our results therefore suggest that the higher expression and specific activity of Src kinase in colon tumor cells can augment the ability of hypoxia to induce VEGF. However, in HT29-AS15 cells, in which c-*src* expression has been reduced 4-fold, the ability of hypoxia to induce VEGF mRNA is severely impaired. These results suggest that in this colon tumor cell system, Src kinase regulates both inducible and constitutive pathways leading to VEGF production. Further confirmation of the ability of Src kinase to regulate inducible VEGF expression was derived from a study of Fleming *et al.* (30), in which the ability of cell density to up-regulate VEGF expression was diminished in the antisense transfected clones relative to HT29 parental cells.

While our results suggest that constitutive Src activation may be a primary pathway leading to production of angiogenic factors in colon cancer, other pathways resulting from genetic changes in colon cancer may also be responsible for the induction of angiogenic factors. For example, 40–50% of colon tumors are known to have activating *ras* mutations (35, 36), and previous studies have demonstrated that Ras activation is sufficient to induce VEGF (33, 37). Additionally, in 293 kidney cells, induction of the promoter of VEGF by transfection of v-*src* is inhibited by overexpression of wild-type p53 (21). Approximately 50–60% of colon cancers exhibit p53 mutations (38), whereas >80% contain activated Src kinase. The relationship between p53 status, Src activation, and VEGF production in colon tumor cells thus requires further study. Nevertheless, the data presented in this paper suggest an important role for Src

activation and VEGF expression in the tumorigenicity, progression, and vascularization of human colon tumors.

Acknowledgment—We thank Melissa Burkett for editorial assistance.

REFERENCES

1. Folkman, J. (1995) *N. Engl. J. Med.* **333**, 1757–1763
2. Takahashi, Y., Kitadai, Y., Bucana, C. D., Cleary, K. R., and Ellis, L. M. (1995) *Cancer Res.* **55**, 3964–3968
3. Takahashi, Y., Cleary, K. R., Mai, M., Kitadai, Y., Bucana, C. D., and Ellis, L. M. (1996) *Clin. Cancer Res.* **2**, 1679–1684
4. Toi, M., Inada, K., Hoshina, S., Suzuki, H., Kondo, S., and Tominaga, T. (1995) *Clin. Cancer Res.* **1**, 961–964
5. Mattern, J., Koomägi, R., and Volm, M. (1995) *Int. J. Oncol.* **6**, 1059–1062
6. Mattern, J., Koomägi, R., and Volm, M. (1996) *Br. J. Cancer* **73**, 931–934
7. Brown, L. F., Berse, B., Jackman, R. W., Tognazzi, K., Manseau, E. J., Dvorak, H. F., and Senger, D. R. (1993) *Am. J. Pathol.* **143**, 1255–1262
8. Brown, L. F., Berse, B., Jackman, R. W., Tognazzi, K., Manseau, E. J., Senger, D. R., and Dvorak, H. F. (1993) *Cancer Res.* **53**, 4727–4735
9. Ferrara, N., and Henzel, W. J. (1989) *Biochem. Biophys. Res. Commun.* **161**, 851–858
10. Ellis, L. M., Liu, W., and Wilson, M. (1996) *Surgery (St. Louis)* **120**, 871–878
11. Dvorak, H. F., Dvorak, A. M., Manseau, E. J., Wiberg, L., and Churchill, W. H. (1979) *J. Natl. Cancer. Inst.* **62**, 1459–1472
12. Plate, K. H., Breier, G., Weich, H. A., and Risau, W. (1992) *Nature* **359**, 845–848
13. Keck, P. J., Hauser, S. D., Krivi, G., Snazo, K., Warren, T., Feder, J., and Connolly, D. T. (1989) *Science* **2**, 1309–1312
14. Maglione, D., Guerriero, V., Viglietto, G., Delli-Bovi, P., and Persico, M. G. (1991) *Proc. Natl. Acad. Sci. U. S. A.* **88**, 9267–9271
15. Takahashi, Y., Tucker, S. L., Kitadai, Y., Koura, A. N., Bucana, C. D., Cleary, K. R., and Ellis, L. M. (1997) *Arch. Surg.* **132**, 541–546
16. Warren, R. S., Yuan, H., Matli, M. R., Gillett, N. A., and Ferrara, N. (1995) *J. Clin. Invest.* **95**, 1789–1797
17. Berse, B., Brown, L. F., Van de Water, L., Dvorak, H. A., and Senger, D. R. (1992) *Mol. Biol. Cell* **3**, 211–220
18. Mukhopadhyay, D., Tsiokas, L., Zhou, X. M., Foster, D., Brugge, J. S., and Sukhatme, V. P. (1995) *Nature* **375**, 577–581
19. Shima, D. T., Deutsch, U., and D'Amore, P. A. (1995) *FEBS Lett.* **370**, 203–208
20. Shweiki, D., Itin, A., Soffer, D., and Keshet, E. (1992) *Nature* **359**, 843–845
21. Mukhopadhyay, D., Tsiokas, L., and Sukhatme, V. P. (1995) *Cancer Res.* **55**, 6161–6165
22. Talamonti, M. S., Roh, M. S., Curley, S. A., and Gallick, G. E. (1993) *J. Clin. Invest.* **91**, 53–60
23. Cartwright, C. A., Meisler, A. I., and Eckhart, W. (1990) *Proc. Natl. Acad. Sci. U. S. A.* **87**, 558–562
24. Termuhlen, P. M., Curley, S. A., Talamonti, M. A., Saboorian, M. H., and Gallick, G. E. (1993) *J. Surg. Res.* **54**, 293–298
25. Gleade, J. G., and Ratcliffe, P. J. (1997) *Blood* **89**, 503–509
26. Staley, C. A., Parikh, N. U., and Gallick, G. E. (1997) *Cell Growth Differ.* **8**, 269–274
27. Fogh, J., and Trempe, G. (1975) in *Human Tumor Cells* (Fogh, J., ed.) pp. 115–141, Plenum Publishing Corp., New York
28. Anthony, F. W., Wheeler, T., Elcock, C. L., Pickett, M., and Thomas, E. J. (1994) *Placenta* **15**, 557–561
29. Koura, A. N., Radinsky, R., Kitadai, Y., Takahashi, Y., Liu, W., Singh, R., and Ellis, L. M. (1996) *Cancer Res.* **56**, 3891–3894
30. Fleming, R. Y. D., Ellis, L. M., Parikh, N. U., Liu, W., Staley, C. A., and Gallick, G. E. (1997) *Surgery* **122**, 501–507
31. Fidler, I. J., and Ellis, L. M. (1994) *Cell* **79**, 185–188
32. Hsu, S., Huang, F., and Friedman, E. (1995) *J. Cell. Physiol.* **165**, 239–245
33. Rak, J., Mitsuhashi, Y., Bayko, L., Filmus, J., Shirasawa, S., Sasazuki, T., and Kerbel, R. S. (1995) *Cancer Res.* **55**, 4575–4580
34. Bolen, J. B., Veillette, A., Schwartz, A. M., DeSeau, V., and Rosen, N. (1987) *Proc. Natl. Acad. Sci. U. S. A.* **84**, 2251–2255
35. Forrester, K., Almoguera, A., Han, K., Grizzle, W. E., and Perucho, M. (1987) *Nature* **327**, 298–303
36. Bos, J. L., Fearon, E. R., Hamilton, S. R., Verlaan-de Vries, M., van Boom, J. H., van der Eb, A. J., and Vogelstein, B. (1987) *Nature* **327**, 293–297
37. Grugel, S., Finkenzeller, G., Weindel, K., Barleon, B., and Marme, D. (1995) *J. Biol. Chem.* **270**, 25915–25919
38. Baker, S. J., Preisinger, A. C., Jessup, J. M., Paraskeva, C., Markowitz, S., Willson, J. K., Hamilton, S., and Vogelstein, B. (1990) *Cancer Res.* **50**, 7717–7722

Exhibit 7

American Journal of Pathology, Vol. 155, No. 4, October 1999

Hepatocellular Hypoxia-Induced Vascular Endothelial Growth Factor Expression and Angiogenesis in Experimental Biliary Cirrhosis

Olivier Rosmorduc,*† Dominique Wendum,‡ Christophe Corpechot,† Bruno Galy,§ Nicole Sebbagh,‡ James Raleigh,¶ Chantal Housset,*† and Raoul Poupon*†

From the Service d'Hépatogastroentérologie, INSERM U 402,† and Service d'Anatomopathologie,‡ CHU Saint-Antoine, Paris; INSERM U 397,§ CHU Rangueil, Toulouse, France; and the Department of Radiation Oncology,¶ University of North Carolina at Chapel Hill, Chapel Hill, North Carolina*

We tested the potential role of vascular endothelial growth factor (VEGF) and of fibroblast growth factor-2 (FGF-2) in the angiogenesis associated with experimental liver fibrogenesis induced by common bile duct ligation in Sprague-Dawley rats. In normal rats, VEGF and FGF-2 immunoreactivities were restricted to less than 3% of hepatocytes. One week after bile duct ligation, hypoxia was demonstrated by the immunodetection of pimonidazole adducts unevenly distributed throughout the lobule. After 2 weeks, hypoxia and VEGF expression were detected in >95% of hepatocytes and coexisted with an increase in periportal vascular endothelial cell proliferation, as ascertained by Ki67 immunolabeling. Subsequently, at 3 weeks the density of von Willebrand-labeled vascular section in fibrotic areas significantly increased. Semiquantitative reverse transcription polymerase chain reaction showed that $VEGF_{120}$ and $VEGF_{164}$ transcripts, that correspond to secreted isoforms, increased within 2 weeks, while $VEGF_{188}$ transcripts remained unchanged. FGF-2 mainly consisting of a 22-kd isoform, according to Western blot, was identified by immunohistochemistry in 49% and 100% of hepatocytes at 3 and 7 weeks, respectively. Our data provide evidence that in biliary-type liver fibrogenesis, angiogenesis is stimulated primarily by VEGF in response to hepatocellular hypoxia while FGF-2 likely contributes to the maintenance of angiogenesis at later stages. ***(Am J Pathol 1999, 155:1065–1073)***

In their pioneering studies, Rappaport and co-workers showed that the development of scars in the cirrhotic liver was invariably accompanied by an intense vascular proliferation. These authors suggested that tissue remodeling and fibrous repair might represent the "road builder" for collateral flow in cirrhosis[1] Their observations have been fully confirmed by others showing that in cirrhotic tissues, the regenerative nodules are surrounded by a dense vascular plexus.[2,3] Yet, the mechanisms triggering this intense vascular proliferative response remain to be determined.

Vascular endothelial growth factor (VEGF) and fibroblast growth factor-2 (FGF-2) are the most potent angiogenic factors identified thus far. Their role in vascular proliferation associated with tumor growth or wound healing has been widely documented in different organs.[4] In addition, it has been demonstrated that hypoxia was the main inducer of VEGF expression[5] which, in turn, stimulates local proliferation of capillaries to increase oxygen delivery. Besides beneficial effects, this vascular response may nevertheless also result in deleterious effects best illustrated by tumor growth and proliferative retinopathy.[6,7]

We and others[8,9] have recently observed an up-regulation of VEGF in the cirrhotic liver of patients with or without hepatocellular carcinoma, suggesting that this factor might be responsible for cirrhosis-associated angiogenesis. Intrahepatic shunts and capillarization of sinusoids are well established characteristics of cirrhosis that restrict the access of blood solutes to hepatocytes.[10–12] In addition, a decrease in the hepatic microvascular perfusion secondary to biliary obstruction in rat has been recently shown to occur long before the onset of cirrhosis, within 7 days following bile duct ligation (BDL).[13] Whether these vascular morphological and functional alterations may induce chronic hypoxia in the fibrotic liver and thereby elicit an angiogenic response is unknown.

The aim of the present study was to investigate the role of VEGF and FGF-2 in an experimental model of biliary fibrosis. We next studied the role of hypoxia in triggering VEGF expression and thereby in stimulating angiogenesis in this model.

Supported by grants from the Delegation à la Recherche Clinique of Assistance Publique-Hôpitaux de Paris (project CRC96131) and U.S. National Cancer Institute Grant R42 CA68826.

Accepted for publication June 3, 1999.

Address reprint requests to Olivier Rosmorduc, M.D., Ph.D., Service d'Hepatogastroenterologie, Hôpital Saint-Antoine, 184 rue du Faubourg Saint-Antoine, 75571 Paris Cedex 12, France. E-mail: olivier.rosmorduc@sat.ap-hop-paris.fr.

Materials and Methods

Animal Model of Cholestatic Liver Injury

Male Sprague-Dawley rats were used at a body weight of 200 to 250 g. The common bile duct was ligated as described previously[14] while normal and sham-operated rats were used as controls. At various times after surgery (3 days, 1, 2, 3, 4, 5, 6, and 7 weeks), rats were euthanized with an overdose of ketamine (Parke-Davis, Courbevoie, France). Cholestasis was monitored by serum bilirubin level. At the time of sacrifice, arterial and mixed venous blood samples were withdrawn for the measurement of oxygen tension (PO_2) and liver tissue was processed as described below.

Histology and Immunohistochemistry

Liver samples were fixed in 10% buffered formalin, paraffin-embedded and sectioned at 4 μm. Tissue sections were stained with hematoxylin-phloxin-safran before standard histology. Immunolabeling was performed using polyclonal antibodies against VEGF (a goat polyclonal IgG: sc-152-G and a rabbit polyclonal IgG: sc-507) (1:100) (Santa Cruz Biotechnology, Santa Cruz, CA) and FGF-2 (1:100) (Santa Cruz Biotechnology) and monoclonal antibodies against von Willebrand factor (vWF) (1:200) (Dako, Glostrup, Denmark). An avidin-biotin-peroxidase technique (Vectastain ABC Kit, Vector, Burlingame, CA) was used for VEGF, FGF-2, and vWF detection. For vWF, immunoperoxidase was performed after microwave antigen retrieval (750 W, 3 × 5 minutes in citrate buffer 0.01 mol/L, pH 6). Before immunostaining, endogenous biotin was blocked using a commercial kit (Eurobio, France) and endogenous peroxidase activity was inhibited in 3% alcoholic hydrogen peroxide for 30 minutes. Color development was achieved with 3-amino-9 ethyl carbazole. The controls were obtained by omitting the first antibody and were all negative. Two independent sections of each sample were evaluated. The cells exhibiting a moderate to intense signal for VEGF and FGF-2 were considered as positive and counted. At least 400 hepatocytes were analyzed in two independent fields. Cell proliferation was assessed by means of a three-step immunoperoxidase method with a monoclonal antibody raised against Ki67 (Novocastra, Newcastle, UK). The cell nuclei were identified as positive or negative and counted. At least 1200 hepatocytes and 600 bile duct epithelial cells were analyzed in three independent fields. Endothelial cell proliferation was assessed by counting the percentage of Ki67 positive endothelial cell nuclei in the periportal vessels of five independent high-magnification (×400) fields per animal. The vascular density in the periportal fibrosis was assessed by determining the count of vWF-labeled vessel sections in 10 successive high-magnification (×400) fields per animal using an eyepiece with a net micrometer (Carl Zeiss, Jena, Germany). The liver samples of at least two rats at each time point (normal rats, 1, 3, and 6 weeks after BDL) were examined. The same procedure was applied to determine the count of bile duct-sections. For endothelial cell proliferation and vascular density data, mean values for more than two groups (at each time point) were compared by analysis of variance (Kruskall-Wallis test) and in case of significance, Scheffé or Games-Howell tests were used to detect difference between single groups. All results were expressed as mean ± SEM.

Reverse Transcription Polymerase Chain Reaction Analysis of VEGF Transcripts

Total RNAs were extracted by a guanidinium thiocyanate based method using a commercial kit (Trizol, Gibco BRL). Five micrograms of RNAs were reverse transcribed using a commercial kit (Pharmacia Biotech). Samples of cDNA were subjected to VEGF amplification combined with GAPDH co-amplification by polymerase chain reaction (PCR). The VEGF and GAPDH oligonucleotide primers were designed based on published rat cDNA sequences in EMBL database. The VEGF sense primer was 5′-ACCTCCACCATGCCAAGT-3′ (position on cDNA: 54–71) and the antisense primer was 5′-TAGTTCCCGAAAC-CCTGA-3′ (position on cDNA: 602–619). The GAPDH sense primer was 5′-CCATGGAGAAGGCTGGGG-3′ (position on cDNA: 335–352) and the antisense primer, 5′-CAAAGTTGTCATGGATGACC-3′ (position on cDNA: 510–529). PCR was performed in a 50-μl reaction mixture containing: 10 mmol/L Tris-HCl, pH 9.0); 50 mmol/L KCl; 1.5 mmol/L $MgCl_2$; 0.2 mmol/L dNTPs; 25 pmol/L of each VEGF primer; and 2.5 pmol/L of each GAPDH primer. The PCR conditions were as follow: 94°C for 7 minutes, then 25, 28, 31, 34, and 37 cycles of 1 minute denaturation at 94°C, 1 minute annealing at 57°C, 1 minute 30 seconds extension at 72°C, and a 10-minute terminal extension at 72°C. To monitor the kinetics of PCR product formation, aliquots were withdrawn at different PCR cycles and analyzed by Southern blot after hybridization of the membrane with specific VEGF and GAPDH ^{32}P-labeled probes. PCR products were semiquantified by optical density scanning of the blot.

Western Blot Analysis of FGF-2 Expression

Tissue samples were homogenized using an all-glass homogenizer in ice-cold lysis buffer (Tris 20 mmol/L, pH 7.5; NaCl, 150 mmol/L; SDS, 2%; EDTA, 5 mmol/L; aprotinin, 5 mg/ml; leupeptin, 1 mg/ml; pepstatin, 0.7 mg/ml; *N*-tosyl-L-lysine chloromethylketone, 50 mg/ml; *N*-tosyl-L-phenylalanine chloromethylketone, 100 mg/ml; soybean trypsin inhibitor, 100 mg/ml; phenylmethylsulfonyl fluoride, 1 mmol/L) and then sonicated. The cellular debris were pelleted by two 20-minute centrifugations (15,000 × *g*) at 4°C. The protein concentration was determined by the BCA protein assay (Pierce, Rockford, IL) and aliquots were stored at −80°C. Equal amounts of proteins were heated at 95°C for 4 minutes in SDS, dithiothreitol, and β-mercaptoethanol containing sample buffer and fractionated by 12% SDS-PAGE. After transfer onto a nitrocellulose membrane, FGF-2 was detected by using a rabbit anti-FGF-2 polyclonal antibody (Santa Cruz Biotechnology) at a dilution of 1:500. Immune complexes

were revealed by means of a horseradish peroxidase-conjugated anti-rabbit IgG antibody and an enhanced chemiluminescence kit (Amersham).

Hypoxia Assay

Pimonidazole binding has been used to assess changes in hepatic tissue oxygenation.[15] Nitroimidazole compounds such as pimonidazole are reductively activated and covalently bound to macromolecules in cells at low oxygen concentration.[15] In brief, the rats were injected with pimonidazole (120 mg/ml intravenously) 1 hour before killing at 1 week, 2 weeks, and 4 weeks following bile duct ligation or sham operation. Liver tissue was formalin-fixed and embedded in paraffin. Pimonidazole adducts were detected in formalin-fixed paraffin-embedded tissues with a biotin-streptavidin-peroxidase indirect immunostaining method modified for rat liver as previously described, using a monoclonal antibody provided by J. A. Raleigh.[16]

Results

Vascular Proliferation Associated with Cholestatic Liver Injury

Bile duct ligation triggered major structural changes in the liver architecture, as previously described.[3,17] After 3 days, ductular reaction was readily detectable, and after 3 weeks, the ductular reaction was intense and associated with extensive fibrosis. After 7 weeks, biliary cirrhosis was present. Increased cell proliferation in response to cholestatic liver injury occurred in both parenchymal and nonparenchymal liver cells, as established before. The kinetics of cell proliferation as ascertained by Ki67 immunolabeling varied according to cell types: bile duct epithelial cells were the first to proliferate and reached a plateau at 3 days, whereas the proliferation of hepatocytes peaked at 1 week. The rate of positive nuclei in bile ducts raised from 1.5% in normal liver to 38% at 3 days, while that of hepatocytes raised from 1.5% in normal liver to 18% at 1 week. Proliferation of the vascular endothelial cells lining periportal vessels was determined on the same liver sections by the number of Ki67-positive nuclei in these cells. While no significant change was noted up to 1 week, inasmuch as 1.79 ± 1.79%, 6.25 ± 2.19% (ns) and 13.01 ± 2.98% (ns) of nuclei were positive in normal rats, 3 days and 1 week after bile duct ligation, respectively, an increase in the rate of Ki67-labeled nuclei occurred thereafter and reached 27.86 ± 3.59% at 2 weeks ($P < 0.05$ as compared with normal, 3 days and 1 week) (Figure 1, A and B).

After vascular endothelial cells has been identified by von Willebrand factor immunolabeling, vessel sections within the ductular reaction were counted to determine vascular density, as described under Materials and Methods. In normal rats, vWF was restricted to the endothelium of portal veins (Figure 2A) and central veins (not shown). One week after BDL, there was no significant change in vascular density (Figure 2B). In contrast, after

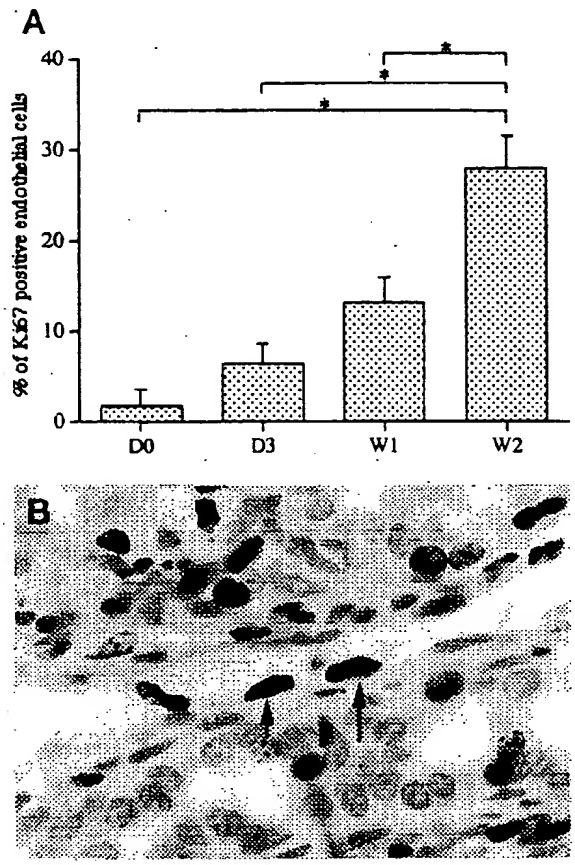

Figure 1. Time course of vascular endothelial cell proliferation after BDL. Vascular endothelial cell proliferation was assessed by Ki67 immunodetection on liver tissue sections. A represents the percentage of labeled endothelial cell nuclei in periportal area vessels from normal rats (D0), and 3 days (D3), 1 week (W1), and 2 weeks (W2) after BDL. While no significant change was observed up to 1 week, an increase in the rate of Ki67-labeled nuclei occurred at 2 weeks. All of the results are expressed as means ± SEM. *$P < 0.05$. B illustrates immunodetection of Ki67 in endothelial cells of periportal vessels at 2 weeks. Positive nuclei are indicated by arrows. Immunoperoxidase technique with hematoxylin counterstain. Magnification, ×1000.

3 weeks and 6 weeks, there was a marked increase in vWF-labeled vessels that were located within ductular reaction (Figure 2, C and D). The results are entirely consistent with the time course of vascular endothelial cell proliferation as shown in Figure 1. Similarly, the proliferation of bile duct epithelial cells was followed by a significant increase in bile duct sections at 1 week. The quantification of vascular density is shown in Figure 2E (left) in parallel with that of ductular proliferation (Figure 2E, right), that was assessed by the same method. However, both proliferation events occurred at different time points.

Hepatic Expression of Angiogenic Factors VEGF and FGF-2 in Cholestatic Liver Injury

On liver sections from normal rats, VEGF and FGF-2 immunolabeling was detected in the first row of perivenular hepatocytes (Figure 3, A and B). In addition, 3% of hepatocytes unevenly distributed within the lobule dis-

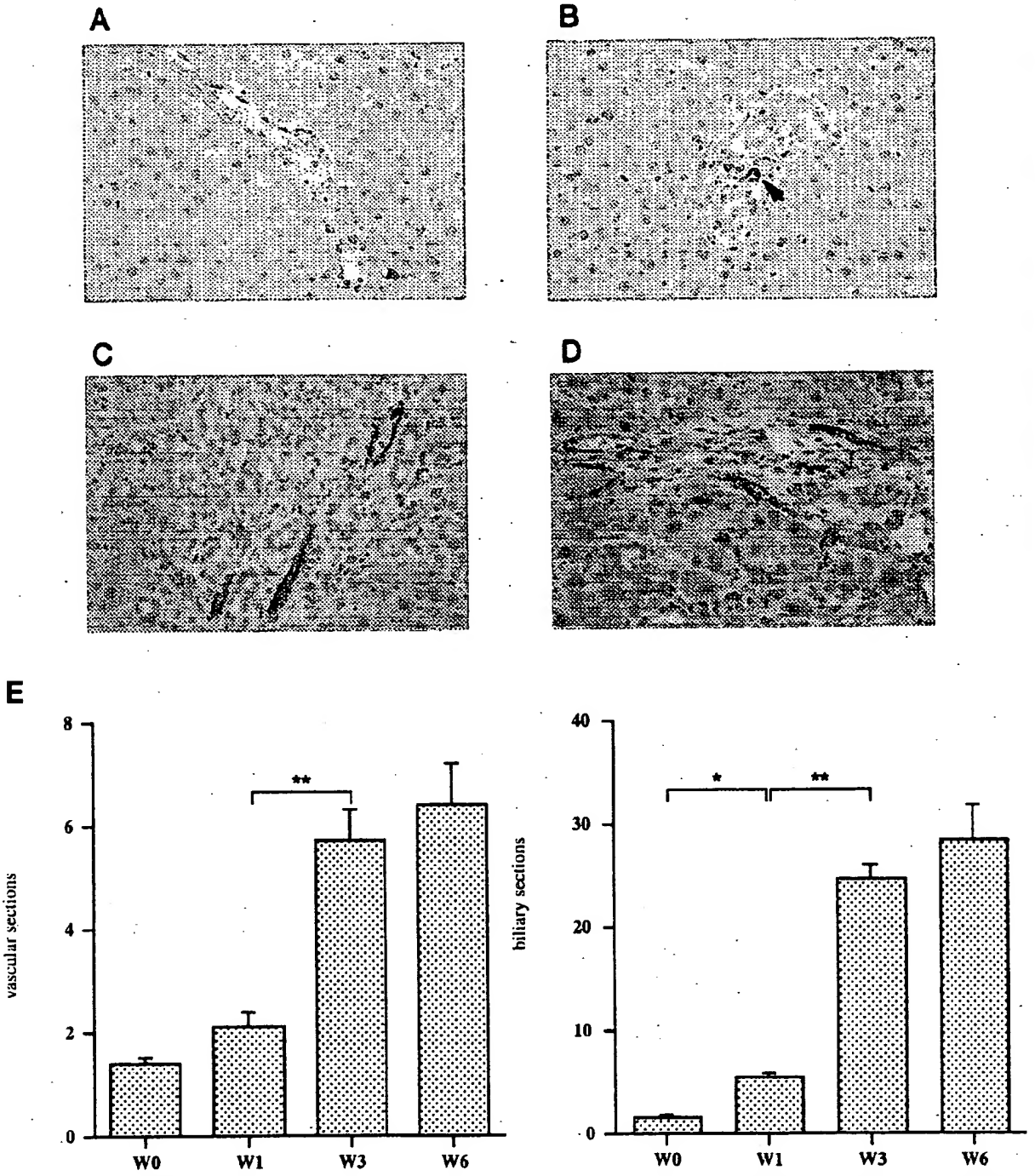

Figure 2. Angiogenesis associated with the development of biliary-type liver fibrosis. Vascular endothelial cells were labeled by an anti-vWF antibody in the liver of normal rats (A), 1 week (B), 3 weeks (C), and 6 weeks (D) after BDL. The number of vessel sections per field at each time point is presented (E; left panel): normal (W0); 1 week (W1); 3 weeks (W3), $P < 0.0001$ as compared with 1 week; and 6 weeks (W6). The number of bile duct sections per field was assessed by the same method (E; right panel): normal (W0); 1 week (W1), $P < 0.05$ as compared with normal; 3 weeks (W3), $P < 0.0001$ as compared with 1 week; and 6 weeks (W6). All of the results are expressed as means ± SEM ($n = 20$); $^{*}P < 0.05$; $^{**}P < 0.0001$. Immunoperoxidase technique with hematoxylin counterstain. Magnification, ×400 (A–D).

played FGF-2 reactivity. The labeling intensity was high in 1%, and moderate in 2% of hepatocytes (Figure 3B). No expression was found in the other cell types. Two weeks (data not shown) and 3 weeks (Figure 3C) after BDL, more than 95% of hepatocytes exhibited VEGF immunolabeling. Seven weeks after BDL, an intense and homogeneous signal for VEGF was observed in 100% of hepatocytes (Figure 3E). VEGF immunolabeling was restricted to hepatocytes and was undetectable in nonparenchymal cells, including bile duct epithelial cells and myofibro-

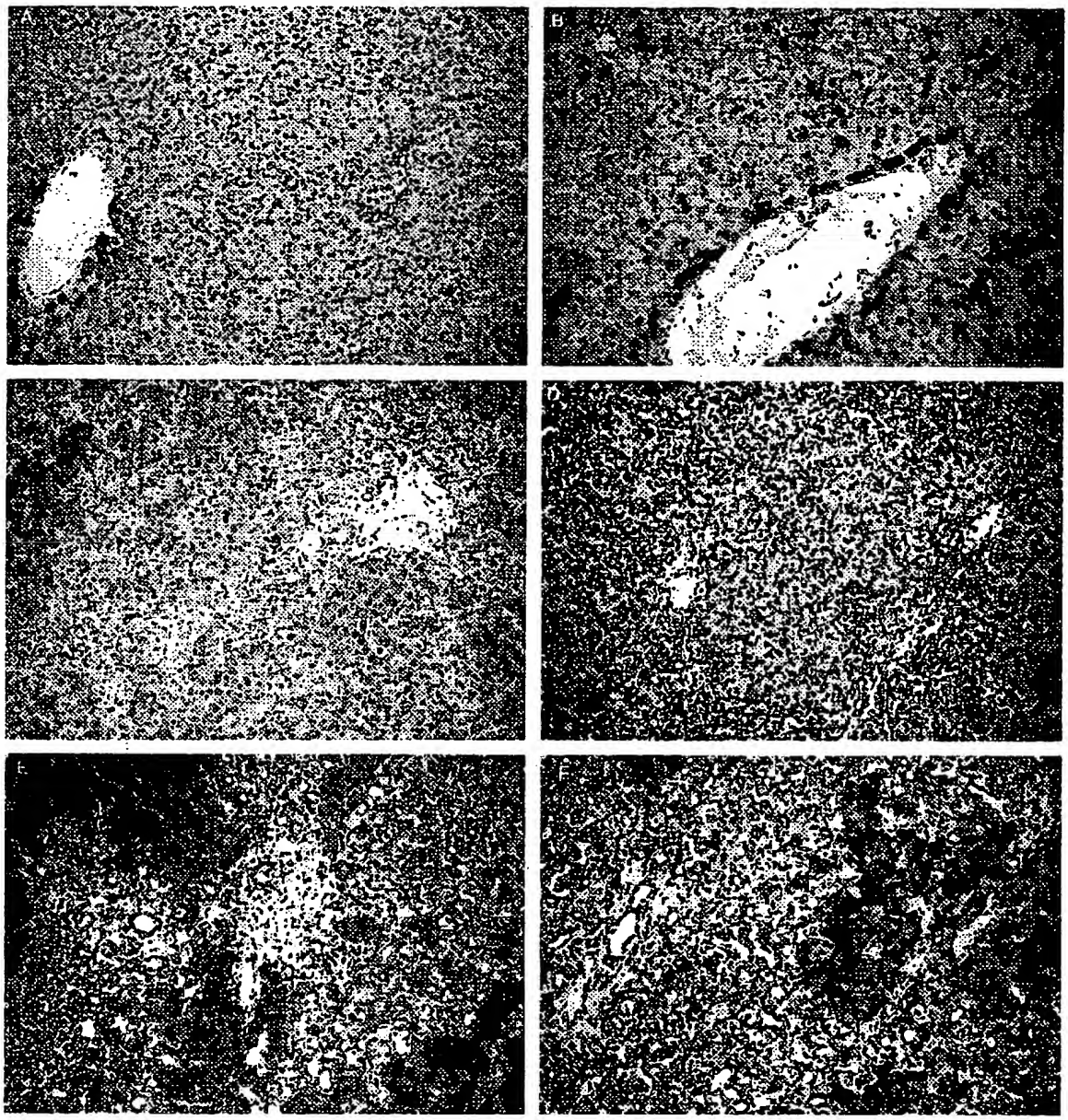

Figure 3. Increased expression of VEGF and FGF-2 after BDL. VEGF (A, C, E) and FGF-2 (B, D, F) were detected by immunohistochemistry. In normal rats (A, B), the liver architecture was normal and the expression of VEGF and FGF-2 was detected in perivenular hepatocytes. A few scattered hepatocytes (3%) within the lobule also displayed FGF-2 immunoreactivity (B). Three weeks after BDL (C, D), at the stage of intense ductular reaction and extensive fibrosis, more than 95% of hepatocytes exhibited a signal for VEGF (C), while a signal for FGF-2 was identified in 49% of hepatocytes (intense in 9%, moderate in 40%). At 7 weeks after BDL (E, F), at the stage of biliary cirrhosis, a signal for VEGF was detected in 100% of hepatocytes, while a signal for FGF-2 was detected in more than 95% of hepatocytes (intense in 35% of hepatocytes unevenly distributed within the lobule). Immunoperoxidase technique with hematoxylin counterstain. Magnification, ×100 (A–D) and ×200 (E, F).

blasts. A similar pattern of VEGF expression was obtained with the two different polyclonal anti-VEGF antibodies that we have used (data not shown). FGF-2 expression also increased after BDL but the time course and distribution pattern differed from those of VEGF (Figure 3, D and F). A significant signal for FGF-2 was detected in 49% (intense in 9%) of hepatocytes 3 weeks after BDL (Figure 3D) and in more than 95% (intense in 35%) of hepatocytes after 7 weeks (Figure 3F).

Since different molecular species of rat VEGF (120, 164, and 188 amino acids) and human VEGF (121, 165, 189, and 206 amino acids) have been identified and reported to be produced by alternative splicing of mRNA,[18,19] we investigated whether specific isoform transcripts were induced by cholestatic liver injury. We characterized the kinetics of expression of these different transcripts by RT-PCR 2, 4, and 6 weeks after BDL. Sham-operated rats were used as controls. Three bands

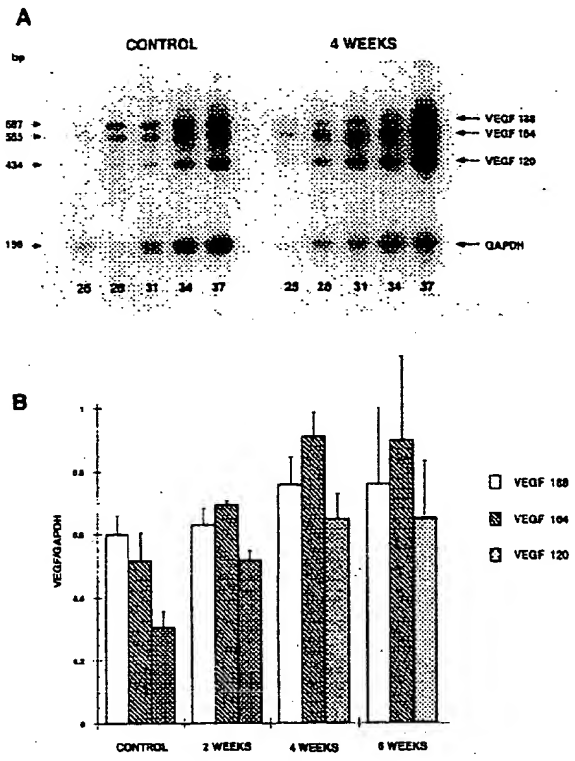

Figure 4. BDL-induced expression of VEGF transcripts. Whole liver RNA extracts were prepared from normal rats (control) rats and 2 weeks, 4 weeks, and 6 weeks after BDL. Total RNAs (5 μg) were subjected to RT-PCR for VEGF and GAPDH as described under Materials and Methods. Aliquots were withdrawn from the PCR mixture after the indicated numbers of cycles (25, 28, 31, 34, and 37) and analyzed by Southern blotting. The signal intensities of bands corresponding to the 120-, 164-, and 188-amino acid VEGF isoforms and to GAPDH were determined by scanning densitometry. A: representative autoradiograms obtained from a control animal and 4 weeks after BDL. B: Relative abundance of the three transcripts was determined after 31 PCR cycles in control and BDL rats at 2, 4, and 6 weeks (results are expressed as means ± SEM, $n = 3$).

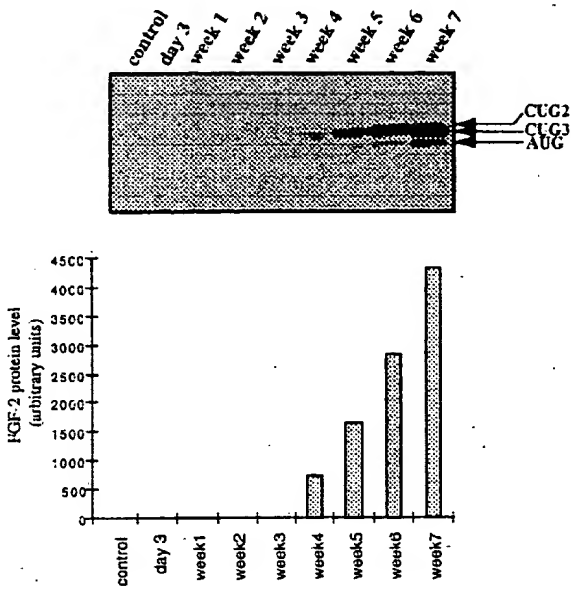

Figure 5. BDL-induced expression of FGF-2 isoforms. Total proteins from whole liver were subjected to Western blot analysis as described under Materials and Methods. The time after BDL is indicated at the top of the lanes. The control consists of total proteins extracted from a normal rat liver. The bands corresponding to the 18-kd (AUG), 21-kd (CUG3), and 22-kd (CUG2) isoforms are indicated. FGF-2 isoforms were quantified by scanning densitometry and the total amount of the different isoforms are represented on the histogram at the bottom of the figure.

at 434, 565, and 687 bp were amplified in the different liver samples. Sequence analysis of these bands showed that they corresponded to the 120-, 164- and 188-amino-acid isoforms of VEGF, respectively. The band at 687 bp corresponding to the 188-amino-acid isoform was the predominant form in the sham-operated animals and remained unchanged after BDL (Figure 4, A and B). In contrast, the bands at 434 and 565 bp, corresponding to the 120- and 164-amino-acid isoforms respectively, increased by 1.5 to 2-fold 4 weeks after BDL. Moreover, the transcript of 164-amino acid isoform became predominant within 2 weeks after BDL (Figure 4, A and B).

Unlike VEGF isoforms, the different molecular forms of FGF-2 represent alternative translation products derived from a single mRNA[20,21] and were therefore analyzed by immunoblot. Consistent with immunohistochemistry, Western blot analysis showed that up-regulation of FGF-2 expression was evident after the fourth week following BDL and increased progressively up to week 7 (Figure 5). Three isoforms of 18, 21, and 22 kd were detected (Figure 5). The former corresponds to an AUG codon initiated form while the 21- and 22-kd peptides are initiated at codons CUG3 and CUG2, respectively.[21] The 22-kd FGF-2 was the main isoform expressed in all samples and the 31-kd FGF-2 initiated at CUG1 codon[22] was undetectable even after long time exposures.

We concluded from these data that cholestatic liver injury induces within 2 weeks a shift in VEGF isoform transcripts associated with an increase in VEGF immunoreactivity in hepatocytes and a delayed increase in FGF-2 expression, also mainly in hepatocytes.

Induction of Liver Hypoxia

The demonstration of an intense hepatocellular overexpression of VEGF following BDL prompted us to investigate the role of liver hypoxia as a triggering event. In normal rats (Figure 6A, top) pimonidazole adducts were undetectable in the liver. One week after BDL, a patchy staining for pimonidazole adducts was observed (data not shown). Two weeks and 4 weeks after surgery (Figure 6, B and C, respectively; top), pimonidazole adducts were detected in more than 95% of hepatocytes. In normal rats (Figure 6A, bottom) and at 1 week (data not shown), VEGF was detected in perivenular hepatocytes. Pimonidazole adducts and VEGF expression displayed the same pattern on adjacent liver sections 2 weeks (Figure 6B, bottom) as well as 4 weeks after BDL (Figure 6C, bottom). Determination of PO_2 in the peripheral arterial blood from the same animals revealed no significant change in the oxygen tension of rats 3 weeks, 4 weeks as well as 6 weeks after BDL, as compared with normal rats.

We conclude from these data indicate that hypoxia selectively occurs in hepatocytes and immediately precedes the induction of VEGF in these cells after BDL.

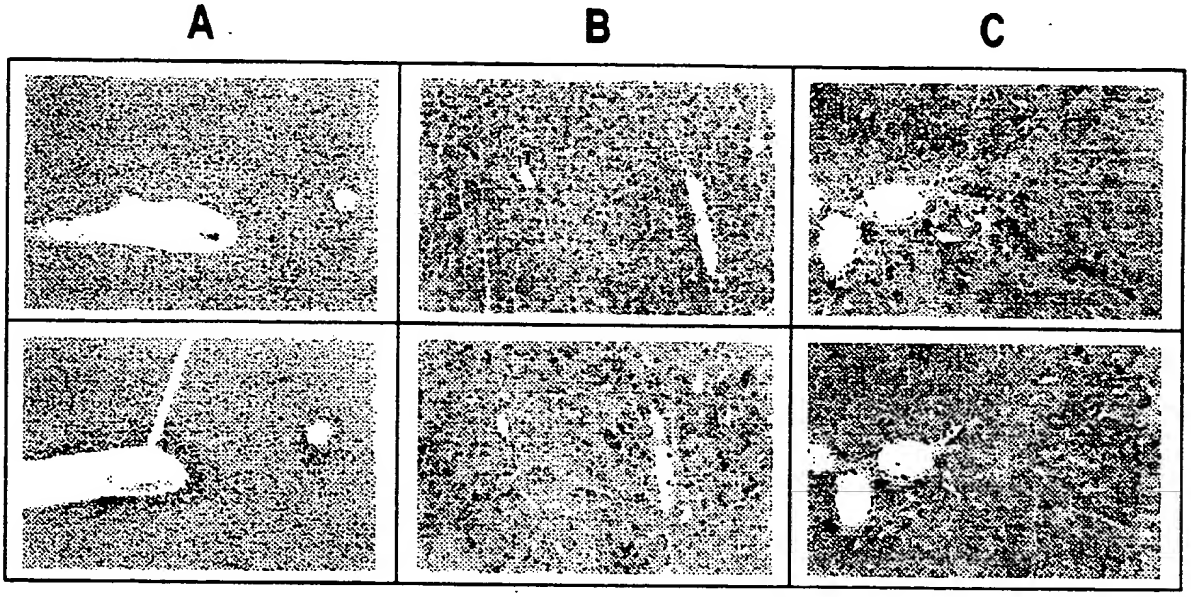

Figure 6. BDL-induced hypoxia of the liver. **Top:** In normal rats (A) pimonidazole adducts were not detected in the liver. Two weeks (B) and 4 weeks (C) after surgery, pimonidazole adducts were detected in more than 95% of hepatocytes. **Bottom:** In normal rats (A), VEGF was detected in perivenular hepatocytes. Two weeks (B) and 4 weeks (C) after BDL. VEGF expression displayed the same pattern as pimonidazole adducts on adjacent liver sections. Immunoperoxidase technique with hematoxylin counterstain. Magnification, ×100 (A) and ×200 (B, C).

Discussion

Our study provides first evidence for the induction of angiogenic factors VEGF and FGF-2 leading to vascular proliferation during experimental liver fibrogenesis. In addition, we demonstrate that hypoxia occurs in hepatocytes before the onset of cirrhosis and immediately precedes VEGF induction. Our results therefore suggest that hypoxia-induced expression of VEGF in hepatocytes might be the triggering event in the development of microvascular proliferation associated with liver fibrogenesis and might thereby contribute to the remodeling of liver architecture .

It has been established that sinusoidal perfusion is impaired in cirrhosis, whatever its cause[12,13] and regenerative nodules in human and experimental cirrhosis are constantly surrounded by a dense perinodular vascular plexus.[1–3] These numerous and tortuous microvessels originate from intrahepatic vascular branches, progress together with the fibrous repair process and bypass the obstructed normal route.[1] These observations suggest that an impaired oxygen delivery to the hepatocytes may occur in cirrhosis as a result of intrahepatic shunts or capillarization of the sinusoids, leading to hepatocyte hypoxia.[23] In agreement with this view, we identified angiogenesis and hypoxia in cirrhotic tissues. However, our data indicate that hypoxia, VEGF induction, and angiogenesis precede the onset of cirrhotic lesions. Early hypoxia is compatible with the occurrence of liver blood supply impairment long before cirrhosis[13].

The immunochemistry data showed an early induction of VEGF in hepatocytes. Furthermore, this VEGF expression paralleled an increase in the level of transcripts coding for the secreted isoforms $VEGF_{120}$ and $VEGF_{164}$ which act directly on the proliferation and migration of vascular endothelial cells. These isoforms also increase the permeability of microvessels to circulating macromolecules.[19] In contrast to $VEGF_{121}$ and $VEGF_{165}$, human $VEGF_{189}$ binds to the extracellular matrix and requires hydrolysis by proteases like plasmin to be activated.[24] Of note, plasma urokinase-type plasminogen activator increases in liver cirrhosis[25] and myofibroblastic hepatic stellate cells synthesize components of the plasminogen-activating system, generating plasmin that plays a key role in matrix remodeling.[26] In addition, VEGF has other biological activities (such as induction of the expression of different proteases by endothelial cells[27,28] and stimulation of endothelial cells and monocyte procoagulant activity[29]) that might also indirectly induce microvascular remodeling in the liver by promoting monocyte migration and adhesion of activated neutrophil.[13,29] The time course of vessel proliferation after BDL was entirely consistent with an angiogenic response to VEGF induction.

By immunochemistry, we also found an up-regulation of FGF-2 was delayed by comparison with VEGF expression after BDL. Western blot analysis indicated that the 22-kd FGF-2 was the main isoform expressed in this experimental model. FGF-2 acts as a potent mitogen and an inducer of cell migration in different cell types, including endothelial cells and fibroblasts.[30] Low and high molecular weight isoforms of human FGF-2 generated by alternative initiation of translation have been described.[21,31] It has been suggested that the low molecular weight form (18 kd) might modulate cell motility and proliferation through interaction with its cell surface receptor while the high molecular weight isoforms (22 to 24 kd) might only act as a mitogen through an intracellular mechanism.[20] FGF-2 expression has been shown to be associated with fibrous septa in both human and exper-

imental chronic liver diseases.[32] In addition, a synergism between FGF-2 and VEGF in the induction of angiogenesis and activated hepatic stellate cell proliferation has been demonstrated[33]. Finally, FGF-2 has been shown to inhibit endothelial cell apoptosis.[34] Altogether, these data suggest that FGF-2 might contribute to maintain a vascular proliferative reaction previously induced by VEGF.

Our results strongly argue for the role of hepatocyte hypoxia as an early triggering event in the induction of VEGF in this experimental model. It has been previously demonstrated that hypoxia induces VEGF at both mRNA and protein level.[35,36] Furthermore, hypoxia-induced upregulation of VEGF expression has been shown to involve both a transcriptional activation[37] and a stabilization of transcripts.[38] However, we cannot definitively exclude an additional role of factors produced by activated inflammatory cells,[39,40] since certain cytokines or growth factors (ie, EGF, HGF, PDGF, TGF-β) are able to stimulate VEGF expression in specific cell types.[41–44] Nevertheless, infiltration by inflammatory cells remained moderate in our experiments. In addition, the induction of VEGF in hepatocytes was associated with the concomitant occurrence of hypoxia in the same areas. In contrast, the expression of FGF-2, which has been shown to be insensitive to hypoxia,[43,45] was induced later and did not respond to the same distribution pattern suggesting that the inducing factors involved in the expression of the two angiogenic factors are different.

In conclusion, our results demonstrate for the first time the sequential induction of two major angiogenic factors, VEGF and FGF-2, during biliary-type liver fibrogenesis. They suggest that hypoxia might be a major factor implicated in the induction of VEGF and in the marked angiogenesis occurring at an early stage before the onset of cirrhotic lesions. Further studies are now required to determine the importance of these factors in liver diseases and whether their modulation might influence the progression of liver tissue repair.

Acknowledgments

We thank Colette Rey, Véronique Barbu, and Marielle Baudrimont for expert assistance.

References

1. Rappaport AM, MacPhee PJ, Fisher MM, Phillips MJ: The scarring of the liver acini (cirrhosis): tridimensional and microcirculatory consideration. Virchows Arch (Pathol Anat) 1983, 402:107–137
2. Yamamoto T, Kobayashi T, Phillips M: Perinodular arteriolar plexus in liver cirrhosis: scanning electron microscopy of microvascular casts. Liver 1984, 4:50–54
3. Haratake J, Hisaoka M, Yamamoto O, Horie A: Morphological changes of hepatic microcirculation in experimental rat cirrhosis: a scanning electron microscopic study. Hepatology 1991, 13:952–956
4. Folkman J: Clinical applications of research on angiogenesis. N Engl J Med 1995, 333:1757–1763
5. Shweiki D, Itin A, Soffer D, Keshet E: Vascular endothelial growth factor induced by hypoxia may mediate hypoxia-initiated angiogenesis. Nature 1992, 359:843–845
6. Maxwell PH, Dachs GU, Gleadle JM, Nicholls LG, Harris AL, Stratford IJ, Hankinson O, Pugh CW, Ratcliffe PJ: Hypoxia-inducible factor-1 modulates gene expression in solid tumors and influences both angiogenesis and tumor growth. Proc Natl Acad Sci USA 1997, 94:8104–8109
7. Folkman J: Tumor angiogenesis. The Molecular Basis of Cancer. Edited by J Mendelsohn, PM Howley, MA Israel, LA Liotta. Philadelphia, WB Saunders, 1995, pp 206–232
8. Rosmorduc O, Wendum D, Galy B, Huez I, Prat H, de Saint-Maur PP, Poupon R: Expression of the angiogenic factors basic FGF and VEGF in human cirrhosis and hepatocellular carcinoma (Abstract). Hepatology 1996, 24:341A
9. El-Assal ON, Yamanoi A, Soda Y, Yamaguchi M, Igarashi M, Yamamoto A, Nabika T, Nagasue N: Clinical significance of microvessel density and vascular endothelial growth factor expression in hepatocellular carcinoma and surrounding liver: possible involvement of vascular endothelial growth factor in the angiogenesis of cirrhotic liver. Hepatology 1998, 27:1554–1562
10. Huet P-M, Goresky C, Villeneuve J-P, Marleau D: Assessment of liver microcirculation in human cirrhosis. J Clin Invest 1982, 70:1234–1244
11. Varin F, Huet P-M: Hepatic microcirculation in the perfused cirrhotic rat liver. J Clin Invest 1985, 76:1904–1912
12. Villeneuve J-P, Dagenais M, Huet P-M, Roy A, Lapointe R, Marleau D: The hepatic microcirculation in the isolated perfused human liver. Hepatology 1996, 23:24–31
13. Koeppel TA, Trauner M, Baas JC, Thies JC, Schlosser SF, Post S, Gebhard M-M, Herfarth C, Boyer JL, Otto G: Extrahepatic biliary obstruction impairs microvascular perfusion and increases leukocyte adhesion in rat liver. Hepatology 1997, 26:1085–1091
14. Alpini G, Lenzi R, Sarkozi L, Tavoloni N: Biliary physiology in rats with bile ductular cell hyperplasia: evidence for a secretory function of proliferated bile ductules. J Clin Invest 1988, 81:569–578
15. Arteel GE, Thurman RG, Yates JM, Raleigh JA: Evidence that hypoxia markers detect oxygen gradients in liver: pimonidazole and retrograde perfusion of rat liver. Br J Cancer 1995, 72:889–895
16. Arteel GE, Iimuro Y, Yin M, Raleigh JA, Thurman RG: Chronic enteral ethanol treatment causes hypoxia in rat liver tissue in vivo. Hepatology 1997, 25:920–926
17. Nakano S, Haratake J, Hashimoto H: Alterations in bile ducts and peribiliary microcirculation in rats after common bile duct ligation. Hepatology 1995, 21:1380–1386
18. Cullinan-Bove K, Koos R: Vascular endothelial growth factor/vascular permeability factor expression in the rat uterus: rapid stimulation by estrogen correlates with estrogen-induced increases in uterine capillary permeability and growth. Endocrinology 1993, 133:829–837
19. Dvorak HF, Brown LF, Detmar M, Dvorak AM: Vascular permeability factor/vascular endothelial growth factor, microvascular hyperpermeability and angiogenesis. Am J Pathol 1995, 146:1029–1039
20. Biktalvi A, Klein S, Pintucci G, Quarto N, Mignatti P: Differential modulation of cell phenotype by different molecular weight forms of basic fibroblast growth factor: possible intracellular signaling by the high molecular weight forms. J Cell Biol 1995, 129:233–243
21. Prats H, Kaghad M, Prats AC, Klagsbrun M, Lélias JM, Liauzun P, Chalon P, Tauber JP, Amalric F, Smith JA: High molecular mass forms of basic fibroblast growth factor are initiated by alternative CUG codons. Proc Natl Acad Sci USA 1989, 86:1836–1840
22. Kevil C, Carter P, Hu B, DeBenedetti A: Transiational enhancement of FGF-2 by eIF-4 factors, and alternate utilization of CUG and AUG codons for translation initiation. Oncogene 1995, 11:2339–2348
23. Morgan D, McLean A: Therapeutic implications of impaired hepatic oxygen diffusion in chronic liver disease. Hepatology 199*, 14:1280–1282
24. Plouet J, Moro F, Bertagnolli S, Coldeboeuf N, Mazarguil H, Clamens S, Bayard F: Extracellular cleavage of the vascular endothelial growth factor 189-amino acid form by urokinase is required for its mitogenic effect. J Biol Chem 1997, 272:13390–13396
25. Sato S, Higashi T, Ougushi S, Hino N, Tsuji T: Elevated urokinase-type plasminogen activator plasma levels are associated with deterioration of liver function but not with hepatocellular carcinoma. J Gastroenterol 1994, 29:745–750
26. Leyland H, Gentry J, Arthur M, Benyon R: The plasminogen-activating system in hepatic stellate cells. Hepatology 1996, 24:1172–1176
27. Unemori E, Ferrara N, Bauer E, Amento E: Vascular endothelial

growth factor induces interstitial collagenase expression in human endothelial cells. J Cell Physiol 1992, 153:557–562
28. Pepper M, Ferrara N, Orci L, Montesano R: Vascular endothelial growth factor (VEGF) induces plasminogen activators and plasminogen activator inhibitor-1 in microvascular endothelial cells. Biochem Biophys Res Commun 1991, 181:902–906
29. Clauss M, Gerlach M, Gerlach H, Brett J, Wang F, Familletti P, Pan Y-C, Olander J, Connolly D, Stern D: Vascular permeability factor: a tumor-derived polypeptide that induces endothelial cell and monocyte procoagulant activity, and promotes monocyte migration. J Exp Med 1990, 172:1535–1545
30. Basilico C, Moscatelli D: The FGF family of growth factors, and oncogenes. Adv Cancer Res 1992, 59:115–165
31. Bugler B, Amalric F, Prats H: Alternative initiation of translation determines cytoplasmic or nuclear localization of basic fibroblast growth factor. Mol Cell Biol 1991, 11:573–577
32. Charlotte F, Win K, Préaux A, Dhumeaux D, Zafrani E, Mavier P: Immunolocalization of heparin-binding growth factors (HBGF) types 1 and 2 in rat liver: selective hyperexpression of HBGF-2 in carbon tetrachloride-induced fibrosis. J Pathol 1993, 169:471–476
33. Ankoma-Sey V, Matli M, Chang K, Laiazar A, Donner D, Wong L, Warren R, Friedman S: Coordinated induction of VEGF receptors in mesenchymal cell types during rat hepatic wound healing. Oncogene 1998, 17:115–121
34. Karsan A, Yee E, Poirier G, Zhou P, Craig R, Harlan J: Fibroblast growth factor-2 inhibits endothelial cell apoptosis by Bcl-2-dependent and independent mechanisms. Am J Pathol 1997, 151:1775–1784
35. Hayashi T, Abe K, Suzuki H, Itoyama Y: Rapid induction of vascular endothelial growth factor gene expression after transient middle cerebral artery occlusion in rats. Stroke 1997, 28:2039–2044
36. Vasir B, Aiello L, Yoon K, Quickel R, Bonner-Weir S, Weir G: Hypoxia induces vascular endothelial growth factor gene and protein expression in cultured rat islet cells. Diabetes 1998, 47:1894–1903
37. Forsythe J, Jiang B-H, Iyer N, Agani F, Leung S, Koos R, Semenza G: Activation of vascular endothelial growth factor gene transcription by hypoxia-inducible factor 1. Mol Cell Biol 1996, 16:4604–4613
38. Stein I, Neeman M, Shweiki A, Itin A, Keshet E: Stabilization of vascular endothelial factor mRNA by hypoxia and hypoglycemia and coregulation with other ischemia-induced genes. Mol Cell Biol 1995, 15:5363–5368
39. Saperstein LA, Jirtle RL, Farouk M, Thompson HJ, Chung KS, Meyers W: Transforming growth factor-β1 and mannose 6-phosphate/insulin-like growth factor-II receptor expression during intrahepatic bile duct hyperplasia and biliary fibrosis in the rat. Hepatology 1994, 19:412–417
40. Napoli J, Prentice D, Niirami C, Bishop A, Desmond P, McCaughan GW: Sequential increases in the intrahepatic expression of epidermal growth factor, basic fibroblast growth factor and transforming growth factor-β in a bile duct ligated rat model of cirrhosis. Hepatology 1997, 26:624–633
41. Dolecki GJ, Connolly DT: Effects of a variety of cytokines and inducing agents on vascular permeability factor mRNA level in U937 cells. Biochem Biophys Res Commun 1991, 180:572–578
42. Finkenzeller G, Technau A, Marme D: Hypoxia-induced transcription of the vascular endothelial growth factor gene is independent of functional AP-1 transcription factor. Biochem Biophys Res Commun 1995, 208:432–439
43. Brogi E, Wu T, Namiki A, Isner JM: Indirect angiogenic cytokines upregulate VEGF and bFGF gene expression in vascular smooth muscle cells, whereas hypoxia upregulates VEGF expression only. Circulation 1994, 90:649–652
44. Pertovaara L, Kaipainen A, Mustonen T, Orpana A, Ferrara N, Saksela O, Alitalo K: Vascular endothelial growth factor is induced in response to transforming growth factor-β in fibroblastic and epithelial cells. J Biol Chem 1994, 269:6271–6274
45. Levy AP, Levy NS, Wegner S, Goldberg MA: Transcriptional regulation of vascular endothelial growth factor by hypoxia. J Biol Chem 1995, 270:13333–13340

Exhibit 8

Angiogenesis and Remodeling of Airway Vasculature in Chronic Inflammation

DONALD M. McDONALD

Cardiovascular Research Institute and Department of Anatomy, University of California, San Francisco, California

Angiogenesis and microvascular remodeling are known features of chronic inflammatory diseases such as asthma and chronic bronchitis, but the mechanisms and consequences of the changes are just beginning to be elucidated. In a model of chronic airway inflammation produced by *Mycoplasma pulmonis* infection of the airways of mice or rats, angiogenesis and microvascular remodeling create vessels that mediate leukocyte influx and leak plasma proteins into the airway mucosa. These vascular changes are driven by the immune response to the organisms. Plasma leakage results from gaps between endothelial cells, as well as from increased vascular surface area and probably other changes in the newly formed and remodeled blood vessels. Treatment with long-acting β_2 agonists can reduce but not eliminate the plasma occurring after infection. In addition to the elevated baseline leakage, the remodeled vessels in the airway mucosa are abnormally sensitive to substance P, but not to platelet-activating factor or serotonin, suggesting that the infection leads to a selective upregulation of NK1 receptors on the vasculature. The formation of new vessels and the remodeling of existing vessels are likely to be induced by multiple growth factors, including vascular endothelial growth factor (VEGF) and angiopoietin 1 (Ang1). VEGF increases vascular permeability, but Ang1 has the opposite effect. This feature is consistent with evidence that VEGF and Ang1 play complementary and coordinated roles in vascular growth and remodeling and have powerful effects on vascular function. Regulation of vascular permeability by VEGF and Ang1 may be their most rapid and potent actions in the adult, as these effects can occur independent of their effects on angiogenesis and vascular remodeling. The ability of Ang1 to block plasma leakage without producing angiogenesis may be therapeutically advantageous. Furthermore, because VEGF and Ang1 have additive effects in promoting angiogenesis but opposite effects on vascular permeability, they could be used together to avoid the formation of leaky vessels in therapeutic angiogenesis. Finally, the elucidation of the protective effect of Ang1 on blood vessel leakiness to plasma proteins raises the possibility of a new strategy for reducing airway edema in inflammatory airway diseases such as asthma and chronic bronchitis.

Keywords: angiogenesis; endothelial cells; microvasculature; *Mycoplasma pulmonis*; plasma leakage; vascular permeability; vascular remodeling

Angiogenesis and microvascular remodeling are elements of the tissue remodeling in chronic inflammatory diseases and tumors. Both types of change in the microvasculature result from endothelial cell proliferation and often occur together, but they represent different phenomena and responses to different stimuli. Angiogenesis is the growth of new blood vessels from existing ones, whereas microvascular remodeling involves structural alterations—usually enlargement—of arterioles, capillaries or venules, without the formation of new vessels. As inflammatory or neoplastic diseases evolve, the microvasculature undergoes progressive changes in structure and function. Blood vessels enlarge or proliferate to supply nutrients to accumulations of inflammatory cells in chronically inflamed tissues or dividing cancer cells in enlarging tumors.

Changes in the microvasculature in chronic disease may be out of proportion to the increased metabolic needs of tissues because of the overproduction of growth factors that stimulate vessel growth and remodeling. Also, blood vessels in diseased tissues usually have multiple abnormalities, ranging from the expression of molecules not found on normal vessels to alterations in endothelial barrier function and leakiness. The strategy of using the abnormal vasculature of a diseased organ as a therapeutic target is now being used in promising efforts toward inhibiting angiogenesis in cancer, arthritis, and diabetic retinopathy. In addition, vessel leakiness is being exploited to enable tissue access of liposome delivery systems, viral vectors, or other therapeutic agents that do not readily cross the normal endothelium. Despite this progress, research on the pathophysiologic and therapeutic implications of angiogenesis and microvascular remodeling in airway disease is still at an early stage.

BACKGROUND OF ANGIOGENESIS AND MICROVASCULAR REMODELING IN AIRWAY DISEASE

The literature on angiogenesis and microvascular remodeling in human airway disease is relatively sparse, but there are clues that changes in the airway microvasculature have long been recognized as a feature of asthma. For example, it was recognized many years ago that the airway mucosa in fatal asthma is edematous and contains dilated, congested blood vessels (1–3). Early studies also showed that the airway wall of subjects with asthma is abnormally thick (4, 5), a feature that has been confirmed more recently by morphometric studies (6–8) and computed tomography (9–11). The increased wall thickness would necessitate an expansion of the microvasculature to accommodate the extra tissue mass, and the abundant, enlarged, and congested mucosal blood vessels contribute to the wall thickness. This vascular contribution is functionally important, because even modest increases in wall thickness can amplify decreases in airway conductance produced by bronchoconstriction (6, 12–14).

Some early studies of the pathology of asthma probably missed changes in the airway vasculature because the tiny mucosal blood vessels are inconspicuous in conventional histological sections. However, immunohistochemical methods using antibodies to vascular markers have made it much easier to visualize these vessels in bronchial biopsies and autopsy

(Received in original form June 15, 2001; accepted in final form August 9, 2001)

Supported in part by National Institutes of Health grants HL-24136 and HL-59157 from the National Heart, Lung, and Blood Institute.

Correspondence and requests for reprints should be addressed to Donald M. McDonald, M.D., Ph.D., Cardiovascular Research Institute, Room S1363, University of California, 513 Parnassus Avenue, San Francisco, CA 94143-0130. E-mail: dmcd@itsa.ucsf.edu

Am J Respir Crit Care Med Vol 164. pp S39–S45, 2001
DOI: 10.1164/rccm2106065
Internet address: www.atsjournals.org

specimens, and changes in the airway microvasculature in human inflammatory respiratory disease are now better documented. The presence of angiogenesis in asthma and other airway diseases is being documented by an increasing number of studies (15–26). Furthermore, blood vessels previously described as enlarged, congested capillaries are now known to be a manifestation of microvascular remodeling instead of simple vasodilatation (22, 27). Nonetheless, the mechanism and therapeutic implications of alterations in airway blood vessels are just beginning to be elucidated, and changes in the microvasculature still represent an important gap in the understanding of the pathophysiology of asthma and other chronic inflammatory airway diseases.

We have sought to develop a better understanding of angiogenesis and vascular remodeling in chronic airway inflammation through the use of animal models. One objective has been to characterize changes in vascular architecture and endothelial cell phenotype in chronic airway inflammation. Another objective has been to learn the mechanism of leakiness of the new or remodeled blood vessels. A third objective has been to contrast the roles in angiogenesis and microvascular remodeling of two endothelial cell-specific growth factors, vascular endothelial growth factor (VEGF) and angiopoietin 1 (Ang1).

MYCOPLASMA INFECTION MODEL OF CHRONIC AIRWAY INFLAMMATION

Mycoplasma pulmonis infection in mice and rats (28, 29) has proven to be a useful model for studying angiogenesis and microvascular remodeling in chronic inflammatory airway disease (30). This infection in rodents has certain features in common with both asthma and chronic bronchitis in humans. Pathogen-free mice or rats are inoculated intranasally with *M. pulmonis* and then are maintained in a barrier facility to avoid other infections for days, weeks, or months as a chronic respiratory disease develops (28, 29). The microvasculature of the airway mucosa begins to change soon after infection, and angiogenesis and microvascular remodeling become long-lasting features of the disease (27, 31). In this model, growth factors and other cytokines produced by resident airway cells and inflammatory cells drive extensive remodeling of the airway wall, providing an opportunity to examine, step by step, the changes occurring during the development of chronic inflammation. Remodeling of the airway wall reflects changes in the microvasculature, inflammatory cell influx, epithelial thickening, mucous gland hypertrophy, and fibrosis of the airway wall (27, 28, 32, 33). However, the roles of specific types of cells, growth factors, and inflammatory mediators are still being elucidated.

The peak in endothelial cell proliferation in the airway mucosa occurs only 5 d after the onset of *M. pulmonis* infection (31), even though changes in the microvasculature continue to evolve and persist throughout the life of the animal. Angiogenesis is the dominant change in the microvasculature of the airway mucosa of rats (Figure 1A and 1B) (33, 34). Both microvascular remodeling and angiogenesis occur in mice, with the relative proportions of each being genetically controlled, in part because of strain-related differences in the immune response to *M. pulmonis* infection. Both remodeling and angiogenesis occur in the airways of C57BL/6 mice (Figure 1C and 1D), but microvascular remodeling is the main change in C3H mice (Figure 1D and 1E) (27).

Functional changes in the microvasculature accompany the conspicuous morphological changes in blood vessel number, size, and architecture. Endothelial cells of the remodeled vessels upregulate P-selectin and support leukocyte adherence and migration (31, 35). The remodeled endothelial cells also avidly take up cationic liposomes and upregulate neurokinin 1 (NK1) receptors, leading to an unusual sensitivity to substance P not found in pathogen-free mice (36–38).

LEAKINESS OF REMODELED MICROVASCULATURE IN CHRONIC AIRWAY INFLAMMATION

Blood vessels in the airway mucosa after *M. pulmonis* infection might be expected to leak, because newly formed and remodeled blood vessels typically have abnormalities in endothelial barrier function (39–41). When we initially examined this issue in infected rats, no significant increase in baseline leakage was detected (30). By using a more sensitive approach, we found that the microvasculature of the infected tracheal mucosa is indeed leakier than normal under baseline conditions in the absence of other stimuli (42). Compared with the airways of pathogen-free rats, where the small amount of baseline leakage and the baseline clearance are in equilibrium, the airways of rats infected for 4 wk accumulate two to five times as much Evans blue tracer over a period of 30 min. The increased baseline leakage comes from newly formed and remodeled blood vessels, as shown by binding of extravasated *Ricinus communis* agglutinin I (RCA-I) lectin (Figure 1F and 1G), focal extravasation of the tracer Monastral blue, staining of endothelial cell borders with silver nitrate, and direct observation by scanning electron microscopy (42).

Several factors are likely to participate in the leakiness of remodeled blood vessels. An increase in endothelial permeability resulting from focal separations $\sim$ 400 nm in diameter between endothelial cells is likely to be involved (42–44). The increase in the lumenal surface area created by angiogenesis and microvascular enlargement would add to the leakage. In addition, the enlargement of arterioles may lower upstream resistance and increase the transmural driving force for leakage. Impaired clearance of extravasated proteins via lymphatics could be another factor, although this has not been documented experimentally.

In normal vessels, histamine, bradykinin, substance P, and 5-hydroxytryptamine (5-HT) cause plasma leakage through the formation of focal gaps between endothelial cells (43–46). However, endothelial gaps may not be the only route for extravasation in remodeled vessels. Endothelial fenestrae, transcytotic vesicles, vesiculo-vacuolar organelles (VVOs), and monolayer defects all may contribute to increased plasma extravasation in pathological conditions accompanied by angiogenesis and microvascular remodeling (47–49). The size and other biophysical properties of each route across the endothelium would determine the size of molecules or particles affected, but the relative contributions of these factors have been difficult to quantify. The largest route for leakage, a pathway that can accommodate particles < 2 μm in diameter, results from defects in the endothelial monolayer of tumor vessels (41, 49), but similar defects have not been described in airway inflammation.

Angiogenic and remodeled vessels that form after *M. pulmonis* infection are abnormally sensitive to certain stimuli that evoke plasma leakage. In particular, substance P and the sensory nerve irritant capsaicin trigger an abnormally large amount of plasma leakage in the airways of infected rats (Figure 1H and 1I) (32, 42, 50). This vascular hyperreactivity is due to an increase in the expression of NK1 receptors on endothelial cells of the remodeled vessels (37). The hyperreactivity appears to be specific to substance P and other NK1 receptor agonists, as leakage produced by platelet-activating factor (PAF) and 5-HT is not exaggerated in the infected rats (42). Therefore, the remodeled microvasculature overresponds to substance P but apparently does

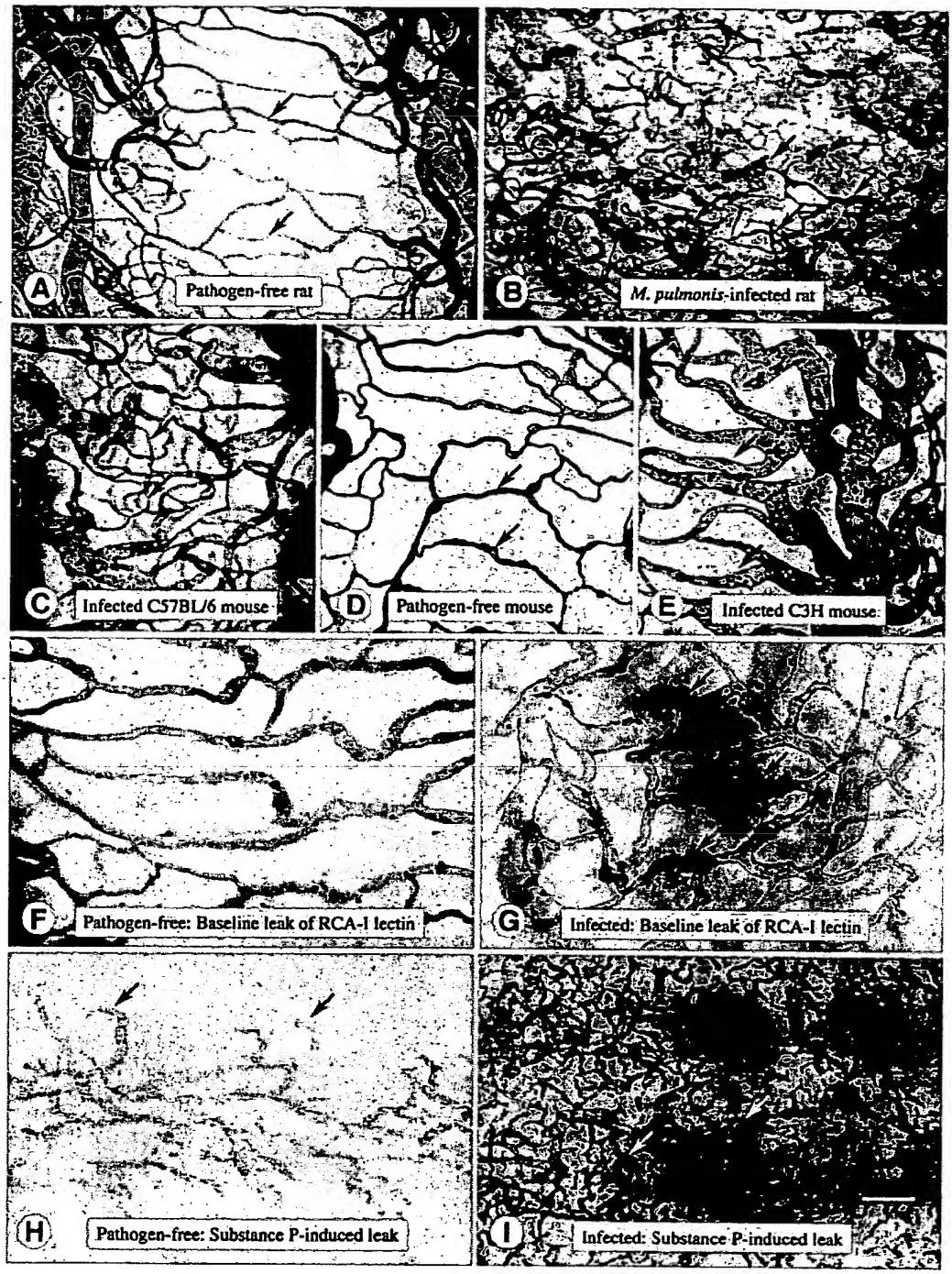

Figure 1. Comparison of the microvasculature in the tracheal mucosa of pathogen-free and *M. pulmonis*-infected rats (*A–B, F–I*) and mice (*C–E*). Tracheal whole mounts showing microvasculature stained with *Lycopersicon esculentum* lectin (*A–G*). (*A*) Pathogen-free rat: simple pattern of normal vasculature, with relatively straight capillaries (*arrows*) spanning cartilaginous ring (33). (*B*) *M. pulmonis*-infected rat at 4 wk: abundant, tortuous, capillary-size angiogenic vessels (*arrows*), some of which are located in focal regions of lymphoid tissue (33). (*C*) *M. pulmonis*-infected C57BL/6 mouse (8 wk) showing vascular remodeling consisting of new capillary-like vessels (angiogenesis, *arrow*) in addition to enlargement of existing vessels (27). (*D*) Pathogen-free mouse showing normal tracheal capillaries (*arrow*) (27). (*E*) *M. pulmonis*-infected C3H mouse (8 wk) showing prominent microvascular enlargement (*arrow*) without new capillary-like vessels (27). (*F, G*) Differences in the microvasculature of tracheas in pathogen-free (*F*) and *M. pulmonis*-infected (*G*) Wistar rats (42): *Ricinus communis* agglutinin I lectin stains the tracheal microvasculature uniformly in the pathogen-free rat (*F*), but sites of lectin leakage, appearing as diffuse extravascular staining (*arrows*), are prominent in the infected rat (*G*). (*H–I*) Distribution of leaky, Monastral blue-labeled blood vessels in rat tracheal mucosa after substance P (33). (*H*) Pathogen-free rat: Monastral blue labeling of normal postcapillary venules that became leaky after substance P (*arrows*). (*I*) *M. pulmonis*-infected rat at 4 wk: Monastral blue labeling of numerous, tortuous angiogenic blood vessels (*arrows*) that are smaller and more heavily labeled than most normal postcapillary venules. Tissue stained by esterase histochemistry to demonstrate regions of abundant mucosal lymphoid tissue (brown, *I*). Scale bar in *I* applies to all figures, *A–B* and *H–I*, 100 μm; *C–E*, 90 μm; *F–G*, 70 μm.

not have a generalized hypersensitivity to inflammatory mediators.

THERAPEUTIC APPROACHES TO DECREASING MICROVASCULAR REMODELING AND PLASMA LEAKAGE

Many substances are known to cause plasma leakage by increasing vascular permeability but only a few have the opposite effect. β_2-Adrenergic receptor agonists constitute one class of agents that decrease plasma leakage. These agents are commonly used in the treatment of chronic airway disease and are known to inhibit plasma leakage evoked by a variety of stimuli including antigen, substance P, bradykinin, and PAF (51–54).

In the airways of rats with *M. pulmonis* infection, baseline leak is reduced by inhalation of a single nebulized dose of the β_2-agonist salmeterol over 10 min (42, 54). Dose–response studies have shown that this treatment significantly reduces baseline leakage in infected rats. The reduction occurs at the same dosage of salmeterol that abolishes ovalbumin-induced late-phase leakage and

leukocyte adhesion in pathogen-free rats (54). A 5-h delay after treatment is necessary to achieve maximal inhibition because of the relatively slow onset but prolonged action of salmeterol (54). The highest dose used (5 mg/ml in the nebulizer), which completely eliminates the late-phase leakage after allergen, reduces baseline leakage in airways of infected rats by 60%. The inhibitory effect of salmeterol on plasma leakage is thought to be mediated by β_2-receptors because it is blocked by prior administration of the β_2-receptor antagonist ICI-118,551 (54).

The antileak action of β_2 agonists is probably related to the inhibition of endothelial gap formation (53). However, effects on airway smooth muscle cells, mast cells, epithelial cells, and nerves may contribute, considering the multiplicity of actions of these agents (55). For example, β_2 agonists can reduce the release of leak-producing inflammatory mediators from sensory nerves (56) and mast cells (57). The β_2-agonist salmeterol also may reduce angiogenesis and vascular remodeling in the airways of individuals with asthma (23).

Glucocorticoids can reverse the remodeling and the leakiness of the airway vasculature produced by *M. pulmonis* infection. Rats that develop chronic disease during the 6 wk after *M. pulmonis* infection and then are treated with dexamethasone for 4 wk have a normal airway microvasculature and a normal response to substance P (34). Treatment with oxytetracycline to reduce the number of infecting organisms has the same effect. In the absence of treatment, infected rats have extensive microvascular remodeling and as much as a 3-fold increase in substance P-induced plasma leakage (34). Similar results have been obtained in C3H mice infected with *M. pulmonis* for 4 d and then treated with dexamethasone for 10 d (35). These findings indicate that even severe structural remodeling and leakiness of the airway microvasculature are reversible in these animal models (34, 35). Related findings in subjects with asthma suggest that some reversal is also possible in human airway disease (23).

CONTRASTING EFFECTS OF VEGF AND Ang1 AS ENDOTHELIAL CELL-SPECIFIC GROWTH FACTORS

The endothelial cell-specific growth factors, VEGF and angiopoietin 1 (Ang1), have potent and clinically relevant actions on the microvasculature (58). Both of these growth factors play essential but separate roles in vascular development in the embryo. VEGF is key to the formation of the initial vascular plexus in early development. Indeed, in the absence of VEGF, the primitive vasculature does not develop normally and the embryo dies (59). VEGF expression increases in the airways of subjects with asthma and correlates with mucosal vascularity (24, 25). Ang1 is also essential for development of the vasculature but in a different way than VEGF. Mice lacking Ang1, or its tyrosine kinase receptor Tie2, die because primitive endothelial cell tubes do not evolve into mature vessels (60, 61). Ang1 appears to be essential for maturation of the vasculature from primitive tubes into a hierarchical network of vessels composed of endothelial cells and pericytes or smooth muscle cells. A second angiopoietin, angiopoietin 2 (Ang2), antagonizes the effects of Ang1 on Tie2 receptors and in some contexts acts as a natural inhibitor of Ang1 (62). Whereas Ang1 is widely expressed in normal adult tissues, Ang2 is expressed mainly at sites of vascular remodeling such as the ovary, placenta, uterus, and tumors (62–64). Ang2 expression in the presence of VEGF is accompanied by angiogenesis, but Ang2 expression in the absence of VEGF is associated with vascular regression (63).

In collaboration with G. Yancopoulos (Regeneron Pharmaceuticals, Tarrytown, NY), who discovered the angiopoietins, we examined some of the distinctive differences in the actions of VEGF and Ang1 on the adult microvasculature by using transgenic mice and adenovirus-transfected mice that overexpress these growth factors. The model of transgenic overexpression in the skin, using the keratin 14 (K14) promoter, made it possible to deliver VEGF, Ang1, or both in a sustained, tissue-specific manner. In the skin of transgenic mice that overexpress VEGF in basal keratinocytes (K14-VEGF mice), capillary-like blood vessels are unusually abundant and tortuous (Figure 2A and 2B) (65). There also is exaggerated leukocyte rolling and adhesion (66). By contrast, the skin of transgenic mice that overexpress Ang1 in the epidermis (K14-Ang1 mice) appears reddened because of enlarged dermal blood vessels, yet the number of vessels is about normal (Figure 2A and 2C) (65, 67). Although the enlarged vessels in K14-Ang1 mouse skin have the location of capillaries, the vessels resemble venules in size and expression of P-selectin and von Willebrand factor (vWF), which are not normally expressed by dermal capillaries in mice (27, 65). The skin of double transgenic mice, produced by breeding K14-Ang1 mice with K14-VEGF mice, overexpresses both Ang1 and VEGF (K14-Ang1/VEGF mice) and have enlarged venule-like vessels, similar to those in K14-Ang1 mice, as well as abundant capillary-like vessels, similar to those in K14-VEGF mice (Figure 2D) (65).

Despite their relatively normal appearance, the unusually abundant dermal blood vessels in K14-VEGF mice are leaky under baseline conditions (65, 66), as might be expected because of the leak-producing action of VEGF (40). The leaky vessels are also abnormally sensitive to inflammatory stimuli as exemplified by their exaggerated leakage response to mustard oil (Figure 2E). Because of their venule-like features, the enlarged dermal vessels in K14-Ang1 mice seemed likely to be leaky and especially sensitive to inflammatory mediators. However, these vessels turned out to have normal baseline leakage and unusual resistance to leakage induced by mustard oil (Figure 2E) as well as by 5-HT, platelet-activating factor, and VEGF (65). Because of the contrasting actions of VEGF and Ang1 in these models, we determined whether the proleakage effect of VEGF or the antileakage effect of Ang1 dominates in the skin of K14-Ang1/VEGF double transgenic mice (65). We found that the antileakage phenotype of Ang1 dominates in these mice. Baseline plasma leakage in K14-Ang1/VEGF mice is in the normal range, and mustard oil-induced leakage is significantly less than that in K14-VEGF mice (Figure 2E) (65).

Studies of the mechanism of the antileakage effect of Ang1 are just beginning. One of the first questions to be answered is whether the decrease in leakage results from a reduction in the number or size of leaky sites in the endothelium or from a decrease in the hydrostatic driving force across the endothelium due to hemodynamic changes. We addressed this question by taking advantage of the observation that leaky sites expose focal regions of the endothelial basement membrane to the vessel lumen (45). We visualized these focal sites by perfusing through the vasculature a biotinylated lectin (RCA-I) that avidly binds to regions of exposed basement membrane (68). In untreated vessels, RCA-I faintly stains the lumenal surface of the endothelium but does not extravasate and does not stain the basement membrane (Figure 2G). However, after treatment of wild-type mice with mustard oil, RCA-I strongly stains focal regions of exposed basement membrane in venules in addition to the faint staining of the lumenal surface (Figure 2H). This intense focal staining is restricted to venules, as is the leakage in other models of acute inflammation (45). In contrast, in K14-Ang1 mice treated with mustard

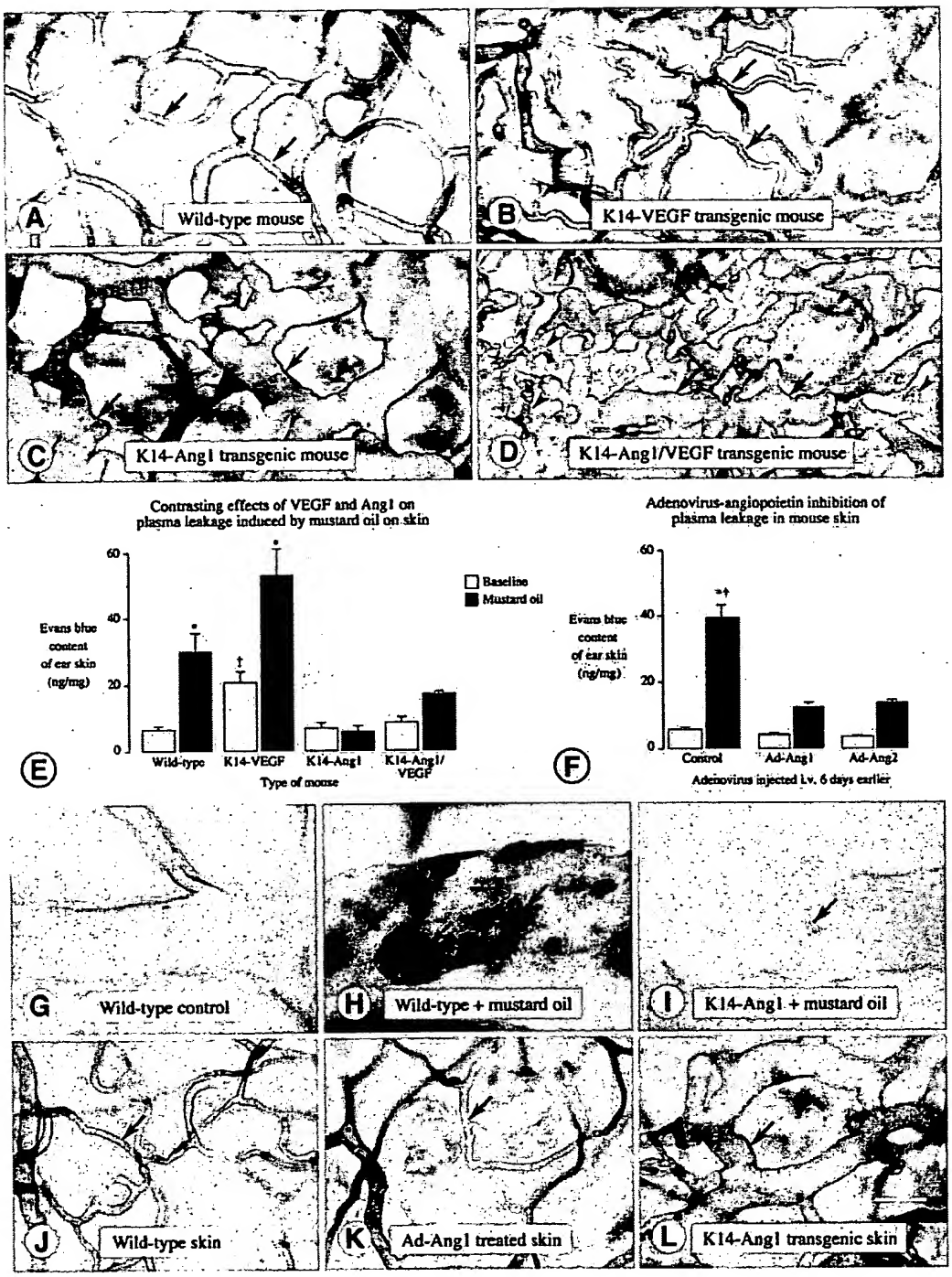

Figure 2. (*A–D*) Comparison of ear skin vasculature, stained by perfusion of biotinylated *Lycopersicon esculentum* lectin, in wild-type mouse (*A*), K14-VEGF transgenic mouse (*B*), K14-Ang1 transgenic mouse (*C*), and K14-Ang1/VEGF double transgenic mouse (*D*) (65). (*E*). Comparison of Evans blue leakage, with or without mustard oil, in ear skin of same four types of mice as shown in (*A–D*) (65) (*$p < 0.05$ compared with baseline; †$p < 0.05$ compared with wild type). (*F*) Comparison of Evans blue leakage, with or without mustard oil, in controls and 6 d after systemic injection of Ad-Ang1 or Ad-Ang2 (70). (*G–I*) *Ricinus communis* agglutinin I lectin-stained control venule in wild-type mouse (*G*, no mustard oil and no leaky sites) compared with leaky venule after mustard oil in wild-type mouse (*H*, abundant leaky sites, *arrows*) and with nonleaky venule after mustard oil in K14-Ang1 mouse (*I*, one leaky site, *arrow*) (65). (*J–L*) Blood vessels (*arrows*) in ear skin are the same size in untreated wild-type mouse (*J*) and in wild-type mouse 5 d after Ad-Ang1 (*K*). By comparison, skin blood vessels are markedly enlarged (*arrow*) in K14-Ang1 transgenic mouse (*L*) (65, 70). Scale bar in (*L*) applies to all figures: (*A–D*) and (*J–L*), 40 μm; (*G–I*), 15 μm.

oil, RCA-I faintly stains the lumenal surface of vessels but rarely the basement membrane because of the lack of leaky sites (Figure 2I) (65). The presence of occasional focal staining of exposed endothelial basement membrane of venules in K14-Ang1 mice (Figure 2I) indicates that Ang1 reduces leakage and does not abolish the RCA-I-binding properties of the basement membrane. Arterioles and capillaries do not have indications of leakage in K14-Ang1 mice, as in wild-type mice (65). These results suggesting that the anti-leakage action of Ang1 is not due to hemodynamic changes are consistent with the leak-inhibiting effect of Ang1 on monolayer cultures of endothelial cells *in vitro* (69).

Collectively, these findings led to two unexpected conclusions: (*1*) Ang1 can block vessel leakiness produced by VEGF as well as by inflammatory mediators; and (*2*) new capillary-like vessels formed by VEGF overexpression need not be leaky, as they do not leak in a setting where Ang1 is coexpressed transgenically.

Because of these intriguing findings in transgenic mice, we asked whether Ang1 can reduce leakage in the adult without prolonged expression inherent in K14-Ang1 transgenic mice. For this purpose we used a model in which VEGF or Ang1 is produced systemically after intravenous injection of an adenoviral vector–growth factor gene construct that turns the liver

into a bioreactor (70). This approach made it possible to deliver sustained high concentrations of Angl or VEGF throughout the body and to examine their effects on blood vessel leakiness. We used adenoviral vectors that expressed Angl (Ad-Angl), VEGF (Ad-VEGF), or a control gene (Ad-green fluorescent protein).

Published data indicate that localized administration of Ad-VEGF is followed by the formation of bizarre blood vessels at the injection site (71). By comparison, our experiments revealed that systemic delivery of a large dose ($> 2.5 \times 10^8$ PFU) of Ad-VEGF causes lethal plasma leakage (70). Mice die with severe multiorgan vessel leakiness and edema within 2 d after injection of Ad-VEGF in the dose we used. The injection of the same dose of Ad-Angl has the opposite effect. Ad-Angl-treated mice are healthy and the amount of plasma leakage in ear skin is in the normal range, but the leakage after mustard oil is significantly reduced (Figure 2F) (70). Administration of Ad-Angl also diminishes the leakage produced by local injection of VEGF. This protection against leakage is evident within 1 d after injection of Ad-Angl and lasts more than 10 d. The antileak effect of Ad-Angl is not accompanied by discernible enlargement of the skin microvasculature (Figure 2J and 2K), unlike the vascular enlargement found in the skin of K14-Angl transgenic mice (Figure 2L).

These adenoviral transfection experiments suggest that the antileakage effect of Angl occurs rapidly in mice with a wild-type genetic background and is independent of the vessel enlargement found in K14-Angl transgenic mice. Studies using Ad-Angl showed that the antileakage effect in the skin is not accompanied by enlargement of the skin microvasculature, thus separating the antileakage action from the remodeling action (70). However, enlarged dermal blood vessels are evident in the skin of K14-Angl transgenic mice (65), and our preliminary studies have shown signs of venular enlargement in the airway mucosa of mice treated with Ad-Angl. As for the mechanism of Angl-induced microvascular enlargement, endothelial cell proliferation presumably contributes, but the cell survival action of Angl may also be a factor (72, 73). The presence of prominent enlargement of venules in airway inflammation, as described above (Figure 1E) (27), adds to the interest in understanding the mechanism of Angl-induced microvascular remodeling.

In conclusion, alterations in the microvasculature participate in the pathophysiology of chronic inflammatory airway disease. Vascular changes that are well documented in animal models have also been found in human asthma. Angiogenesis and microvascular remodeling not only result in more or larger blood vessels in the airway mucosa but also result in functionally abnormal blood vessels. Sustained leakage, leukocyte adhesion, and selective upregulation of NK1 receptors are examples of the abnormalities. However, these abnormalities and the vascular remodeling are potentially reversible by therapeutic intervention. VEGF and Angl may play complementary and coordinated roles in vascular remodeling, but they have opposite effects on blood vessel leakiness. The discovery of the antileakage action of Angl offers a possible new strategy for reducing airway edema in chronic inflammatory airway diseases such as bronchitis and asthma.

Acknowledgment: The author thanks Drs. Peter Baluk, Taichi Ezaki, Gavin Thurston, and George Yancopoulos, and Ms. Marilyn Kwan and Mr. Antonio Gómez, for their important contributions to the research described.

References

1. Unger L. Pathology of bronchial asthma with five autopsy reports. *South Med J* 1945;38:513–523.
2. Walzer I, Frost TT. Death occurring in bronchial asthma: a report of five cases. *J Allergy* 1952;23:204–214.
3. Dunnill MS. The pathology of asthma, with special references to changes in the bronchial mucosa. *J Clin Pathol* 1960;13:27–33.
4. Huber HL, Koessler KK. The pathology of bronchial asthma. *Arch Intern Med* 1922;30:689–760.
5. Macdonald IG. The local and constitutional pathology of bronchial asthma. *Ann Intern Med* 1932;6:253–277.
6. James AL, Pare PD, Hogg JC. The mechanics of airway narrowing in asthma. *Am Rev Respir Dis* 1989;139:242–246.
7. Carroll N, Elliot J, Morton A, James A. The structure of large and small airways in nonfatal and fatal asthma. *Am Rev Respir Dis* 1993;147: 405–410.
8. Bai TR, Cooper J, Koelmeyer T, Pare PD, Weir TD. The effect of age and duration of disease on airway structure in fatal asthma. *Am J Respir Crit Care Med* 2000;162:663–669.
9. Okazawa M, Muller N, McNamara AE, Child S, Verburgt L, Pare PD. Human airway narrowing measured using high resolution computed tomography. *Am J Respir Crit Care Med* 1996;154:1557–1562.
10. Awadh N, Muller NL, Park CS, Abboud RT, FitzGerald JM. Airway wall thickness in patients with near fatal asthma and control groups: assessment with high resolution computed tomographic scanning. *Thorax* 1998;53:248–253.
11. Niimi A, Matsumoto H, Amitani R, Nakano Y, Mishima M, Minakuchi M, Nishimura K, Itoh H, Izumi T. Airway wall thickness in asthma assessed by computed tomography. Relation to clinical indices. *Am J Respir Crit Care Med* 2000;162:1518–1523.
12. Metzger WJ, Zavala DC, Richerson HB, Moseley PL, Iwamoto P, Monick M, Sjoerdsma K, Hunninghake GW. Local allergen challenge and bronchoalveolar lavage of allergic asthmatic lungs. Description of a model and local airway inflammation. *Am Rev Respir Dis* 1987;135: 433–440.
13. Hogg JC. Pathology of asthma. *J Allergy Clin Immunol* 1993;92:1–5.
14. Bowden JJ, McDonald DM. The microvasculature as a participant in inflammation. In: Holgate ST, editor. Immunopharmacology of the respiratory system: the handbook of immunopharmacology. London: Academic Press; 1995, p. 147–168.
15. Kuwano K, Bosken CH, Pare PD, Bai TR, Wiggs BR, Hogg JC. Small airways dimensions in asthma and in chronic obstructive pulmonary disease. *Am Rev Respir Dis* 1993;148:1220–1225.
16. Fisseler-Eckhoff A, Rothstein D, Muller KM. Neovascularization in hyperplastic, metaplastic and potentially preneoplastic lesions of the bronchial mucosa. *Virchows Arch* 1996;429:95–100.
17. Carroll NG, Cooke C, James AL. Bronchial blood vessel dimensions in asthma. *Am J Respir Crit Care Med* 1997;155:689–695.
18. Charan NB, Baile EM, Pare PD. Bronchial vascular congestion and angiogenesis. *Eur Respir J* 1997;10:1173–1180.
19. Li X, Wilson JW. Increased vascularity of the bronchial mucosa in mild asthma. *Am J Respir Crit Care Med* 1997;156:229–233.
20. Orsida BE, Li X, Hickey B, Thien F, Wilson JW, Walters EH. Vascularity in asthmatic airways: relation to inhaled steroid dose. *Thorax* 1999; 54:289–295.
21. Wilson J. The bronchial microcirculation in asthma. *Clin Exp Allergy* 2000;30:51–53.
22. Tanaka H, Yamada G, Itoh T, Hashimoto M, Suzuki K, Tanaka S, Oashi K, Saikai T, Teramoto S, Takahashi H, Abe S. Airway hypervascularity in asthmatic patients assessed by side-viewing high-magnified bronchoscopy: a new point of view. *Am J Respir Crit Care Med* 2001;163:A787.
23. Orsida BE, Ward C, Li X, Bish R, Wilson JW, Thien F, Walters EH. Effect of a long-acting β_2-agonist over three months on airway wall vascular remodeling in asthma. *Am J Respir Crit Care Med* 2001;164: 117–121.
24. Hoshino M, Takahashi M, Aoike N. Expression of vascular endothelial growth factor, basic fibroblast growth factor, and angiogenin immunoreactivity in asthmatic airways and its relationship to angiogenesis. *J Allergy Clin Immunol* 2001;107:295–301.
25. Hoshino M, Nakamura Y, Hamid QA. Gene expression of vascular endothelial growth factor and its receptors and angiogenesis in bronchial asthma. *J Allergy Clin Immunol* 2001;107:1034–1038.
26. Walsh DA, Pearson CI. Angiogenesis in the pathogenesis of inflammatory joint and lung diseases. *Arthritis Res* 2001;3:147–153.
27. Thurston G, Murphy TJ, Baluk P, Lindsey JR, McDonald DM. Angiogenesis in mice with chronic airway inflammation: strain-dependent differences. *Am J Pathol* 1998;153:1099–1112.
28. Lindsey JR, Baker HJ, Overcash RG, Cassell GH, Hunt CE. Murine chronic respiratory disease. Significance as a research complication and experimental production with *Mycoplasma pulmonis*. *Am J Pathol* 1971;64:675–708.

29. Lindsey JR, Cassell H. Experimental *Mycoplasma pulmonis* infection in pathogen-free mice. Models for studying mycoplasmosis of the respiratory tract. *Am J Pathol* 1973;72:63–90.
30. McDonald DM. Experimental models of bronchial reactivity: effect of airway infections. In: Ogra PL, Mestecky J, Lamm ME, Strober W, Bienenstock J, McGhee JR, editors. San Diego, California: Academic Press; 1999. p. 1177–1185.
31. Ezaki T, Baluk P, Thurston G, La Barbara A, McDonald DM. Time course of endothelial cell proliferation and microvascular remodeling in chronic inflammation. *Am J Pathol* 2001;158:2043–2055.
32. McDonald DM, Schoeb TR, Lindsey JR. *Mycoplasma pulmonis* infections cause long-lasting potentiation of neurogenic inflammation in the respiratory tract of the rat. *J Clin Invest* 1991;87:787–799.
33. Dahlqvist Å, Umemoto EY, Brokaw JJ, Dupuis M, McDonald DM. Tissue macrophages associated with angiogenesis in chronic airway inflammation in rats. *Am J Respir Cell Mol Biol* 1999;20:237–247.
34. Bowden JJ, Schoeb TR, Lindsey JR, McDonald DM. Dexamethasone and oxytetracycline reverse the potentiation of neurogenic inflammation in airways of rats with *Mycoplasma pulmonis* infection. *Am J Respir Crit Care Med* 1994;150:1391–1401.
35. Thurston G, Maas K, La Barbara A, McLean JW, McDonald DM. Microvascular remodeling in chronic airway inflammation in mice. *Clin Exp Pharmacol Physiol* 2000;27:836–841.
36. McDonald DM. Upregulation of tachykinin receptors in chronic airway inflammation. *Pulm Pharmacol* 1995;8:203–205.
37. Baluk P, Bowden JJ, Lefevre PM, McDonald DM. Upregulation of substance P receptors in angiogenesis associated with chronic airway inflammation in rats. *Am J Physiol* 1997;273:L565–L571.
38. Thurston G, McLean JW, Rizen M, Baluk P, Haskell A, Murphy TJ, Hanahan D, McDonald DM. Cationic liposomes target angiogenic endothelial cells in tumors and chronic inflammation in mice. *J Clin Invest* 1998;101:1401–1413.
39. Schoefl GI. Studies on inflammation. III. Growing capillaries. Their structure and permeability. *Virchows Arch Pathol Anat* 1963;337:97–141.
40. Dvorak HF, Brown LF, Detmar M, Dvorak AM. Vascular permeability factor/vascular endothelial growth factor, microvascular hyperpermeability, and angiogenesis. *Am J Pathol* 1995;146:1029–1039.
41. Hobbs SK, Monsky WL, Yuan F, Roberts WG, Griffith L, Torchilin VP, Jain RK. Regulation of transport pathways in tumor vessels: role of tumor type and microenvironment. *Proc Natl Acad Sci USA* 1998;95:4607–4612.
42. Kwan ML, Gómez AD, Baluk P, Hashizume H, McDonald DM. Airway vasculature after mycoplasma infection: chronic leakiness and selective hypersensitivity to substance P. *Am J Physiol* 2001;280:L286–L297.
43. Baluk P, Hirata A, Thurston G, Fujiwara T, Neal CR, Michel CC, McDonald DM. Endothelial gaps: time course of formation and closure in inflamed venules of rats. *Am J Physiol* 1997;272:L155–L170.
44. McDonald DM, Thurston G, Baluk P. Endothelial gaps as sites for plasma leakage in inflammation. *Microcirculation* 1999;6:7–22.
45. Majno G, Palade GE. Studies on inflammation. I. The effect of histamine and serotonin on vascular permeability: an electron microscopic study. *J Biophys Biochem Cytol* 1961;11:571–605.
46. McDonald DM. Endothelial gaps and permeability of venules in rat tracheas exposed to inflammatory stimuli. *Am J Physiol* 1994;266:L61–L83.
47. Dvorak AM, Kohn S, Morgan ES, Fox P, Nagy JA, Dvorak HF. The vesiculo-vacuolar organelle (VVO): a distinct endothelial cell structure that provides a transcellular pathway for macromolecular extravasation. *J Leukoc Biol* 1996;59:100–115.
48. Roberts WG, Palade GE. Neovasculature induced by vascular endothelial growth factor is fenestrated. *Cancer Res* 1997;57:765–772.
49. Hashizume H, Baluk P, Morikawa S, McLean JW, Thurston G, Roberge S, Jain RK, McDonald DM. Openings between defective endothelial cells explain tumor vessel leakiness. *Am J Pathol* 2000;156:1363–1380.
50. McDonald DM. Infections intensify neurogenic plasma extravasation in the airway mucosa. *Am Rev Respir Dis* 1992;146:S40–S44.
51. Whelan CJ, Johnson M. Inhibition by salmeterol of increased vascular permeability and granulocyte accumulation in guinea-pig lung and skin. *Br J Pharmacol* 1992;105:831–838.
52. Sulakvelidze I, McDonald DM. Anti-edema action of formoterol in rat trachea does not depend on capsaicin-sensitive sensory nerves. *Am J Respir Crit Care Med* 1994;149:232–238.
53. Baluk P, McDonald DM. The β_2-adrenergic receptor agonist formoterol reduces microvascular leakage by inhibiting endothelial gap formation. *Am J Physiol* 1994;266:L461–L468.
54. Bolton PB, McDonald DM. Salmeterol reduces early and late phase plasma leakage and leukocyte adhesion in rat airways. *Am J Respir Crit Care Med* 1997;155:1428–1435.
55. Johnson M. The pharmacology of salmeterol. *Lung* 1990:168(Suppl):115–119.
56. Advenier C, Qian Y, Koune JDL, Molimard M, Candenas ML, Naline E. Formoterol and salbutamol inhibit bradykinin- and histamine-induced airway microvascular leakage in guinea-pig. *Br J Pharmacol* 1992;105:792–798.
57. Ishizaka T, Ishizaka K, Orange RP, Austen KF. Pharmacologic inhibition of the antigen-induced release of histamine and slow reacting substance of anaphylaxis (SRS-A) from monkey lung tissues mediated by human IgE. *J Immunol* 1971;106:1267–1273.
58. Yancopoulos GD, Davis S, Gale NW, Rudge JS, Wiegand SJ, Holash J. Vascular-specific growth factors and blood vessel formation. *Nature* 2000;407:242–248.
59. Ferrara N, Carver-Moore K, Chen H, Dowd M, Lu L, O'Shea KS, Powell-Braxton L, Hillan KJ, Moore MW. Heterozygous embryonic lethality induced by targeted inactivation of the VEGF gene. *Nature* 1996;380:439–442.
60. Sato TN, Tozawa Y, Deutsch U, Wolburg-Buchholz K, Fujiwara Y, Gendron-Maguire M, Gridley T, Wolburg H, Risau W, Qin Y. Distinct roles of the receptor tyrosine kinases Tie-1 and Tie-2 in blood vessel formation. *Nature* 1995;376:70–74.
61. Suri C, Jones PF, Patan S, Bartunkova S, Maisonpierre PC, Davis S, Sato TN, Yancopoulos GD. Requisite role of angiopoietin-1, a ligand for the TIE2 receptor, during embryonic angiogenesis. *Cell* 1996;87:1171–1180.
62. Maisonpierre PC, Suri C, Jones PF, Bartunkova S, Wiegand SJ, Radziejewski C, Compton D, McClain J, Aldrich TH, Papadopoulos N, Daly TJ, Davis S, Sato TN, Yancopoulos GD. Angiopoietin-2, a natural antagonist for Tie2 that disrupts in vivo angiogenesis. *Science* 1997;277:55–60.
63. Holash J, Maisonpierre PC, Compton D, Boland P, Alexander CR, Zagzag D, Yancopoulos GD, Wiegand SJ. Vessel cooption, regression, and growth in tumors mediated by angiopoietins and VEGF. *Science* 1999;284:1994–1998.
64. Zagzag D, Amirnovin R, Greco MA, Yee H, Holash J, Wiegand SJ, Zabski S, Yancopoulos GD, Grumet M. Vascular apoptosis and involution in gliomas precede neovascularization: a novel concept for glioma growth and angiogenesis. *Lab Invest* 2000;80:837–849.
65. Thurston G, Suri C, Smith K, McClain J, Sato TN, Yancopoulos GD, McDonald DM. Leakage-resistant blood vessels in mice transgenically overexpressing angiopoietin-1. *Science* 1999;286:2511–2514.
66. Detmar M, Brown LF, Schon MP, Elicker BM, Velasco P, Richard L, Fukumura D, Monsky W, Claffey KP, Jain RK. Increased microvascular density and enhanced leukocyte rolling and adhesion in the skin of VEGF transgenic mice. *J Invest Dermatol* 1998;111:1–6.
67. Suri C, McClain J, Thurston G, McDonald DM, Zhou H, Oldmixon EH, Sato TN, Yancopoulos GD. Increased vascularization in mice overexpressing angiopoietin-1. *Science* 1998;282:468–471.
68. Thurston G, Baluk P, Hirata A, McDonald DM. Permeability-related changes revealed at endothelial cell borders in inflamed venules by lectin binding. *Am J Physiol* 1996;271:H2547–H2562.
69. Gamble JR, Drew J, Trezise L, Underwood A, Parsons M, Lisa Kasminkas L, Rudge J, Yancopoulos G, Vadas MA. Angiopoietin-1 is an antipermeability and anti-inflammatory agent in vitro and targets cell junctions. *Circ Res* 2000;87:603–607.
70. Thurston G, Rudge JS, Ioffe E, Zhou H, Ross L, Croll SD, Glazer N, Holash J, McDonald DM, Yancopoulos GD. Angiopoietin-1 protects the adult vasculature against plasma leakage. *Nat Med* 2000;6:460–463.
71. Pettersson A, Nagy JA, Brown LF, Sundberg C, Morgan E, Jungles S, Carter R, Krieger JE, Manseau EJ, Harvey VS, Eckelhoefer IA, Feng D, Dvorak AM, Mulligan RC, Dvorak HF. Heterogeneity of the angiogenic response induced in different normal adult tissues by vascular permeability factor/vascular endothelial growth factor. *Lab Invest* 2000;80:99–115.
72. Kim I, Kim HG, So JN, Kim JH, Kwak HJ, Koh GY. Angiopoietin-1 regulates endothelial cell survival through the phosphatidylinositol 3'-kinase/Akt signal transduction pathway. *Circ Res* 2000;86:24–29.
73. Papapetropoulos A, Fulton D, Mahboubi K, Kalb RG, O'Connor DS, Li F, Altieri DC, Sessa WC. Angiopoietin-1 inhibits endothelial cell apoptosis via the Akt/survivin pathway. *J Biol Chem* 2000;275:9102–9105.

The Vascular Endothelial Growth Factor Receptor KDR/Flk-1 Is a Major Regulator of Malignant Ascites Formation in the Mouse Hepatocellular Carcinoma Model

HITOSHI YOSHIJI,[1] SHIGEKI KURIYAMA,[1] DANIEL J. HICKLIN,[2] JAMES HUBER,[2] JUNICHI YOSHII,[1] YASUHIDE IKENAKA,[1] RYUICHI NOGUCHI,[1] TOSHIYA NAKATANI,[1] HIROHISA TSUJINOUE,[1] AND HIROSHI FUKUI[1]

The vascular endothelial growth factor-A (VEGF-A), also known as the vascular permeability factor (VPF), has been shown to play an important role in malignant ascites formation. The effects of VEGF-A are mediated through flt-1 and kinase insert domain–containing receptor/fetal liver kinase (KDR/Flk-1) receptors. It has been shown that KDR/Flk-1 is a predominant receptor in solid hepatocellular carcinoma (HCC) development, but the role of this receptor in hepatic ascites formation has not yet been elucidated. In this study, we examined the role of KDR/Flk-1 in the murine MH134 hepatic malignant ascites formation by means of VEGF-A– and KDR/Flk-1–specific neutralizing antibodies (VEGF-A nAb and KDR/Flk-1 nAb, respectively). The mean volume of ascites, number of tumor cells in ascites, and the peritoneal capillary permeability were significantly suppressed by VEGF-A nAb and KDR/Flk-1 nAb treatment. These inhibitory effects of KDR/Flk-1 nAb were more potent than those of VEGF-A nAb. The autophosphorylation of KDR/Flk-1 in the peritoneal wall was almost completely abolished by KDR/Flk-1 nAb, whereas a certain level of activation was still shown by VEGF-A nAb treatment. Another VEGF-family, VEGF-C, which also binds KDR/Flk-1, was detected in the ascites. Furthermore, in the therapeutic experiment, although both VEGF-A nAb and KDR/Flk-1 nAb prolonged the survival rate of ascites-bearing mice, the latter showed a more significant impact on the survival of animals. These results suggest that KDR/Flk-1 is a major regulator of malignant hepatic ascites formation, and that in addition to VEGF-A, VEGF-C may also be involved in the malignant ascites formation via KDR/Flk-1 activation. (HEPATOLOGY 2001;33:841-847.)

Hepatocellular carcinoma (HCC) is one of the most common malignancies in the world, especially in Asia and Africa. Its annual incidence is estimated to be 250,000 to 1,000,000. The prognosis of HCC is still very poor, because it develops multicentrically and is associated in most cases with chronic liver diseases.[1-3] Furthermore, invasion of HCC to the peritoneum causes malignant ascites, which is experienced frequently in patients with advanced HCC. The patient's quality of life with this condition is seriously decreased as a result of the abdominal distension and pressure on the chest cavity. Although various alternative therapies, such as diuretic medicine and ascites drainage have been employed, there is still no satisfactory therapeutic modalities for malignant hepatic ascites.

It has been reported that hyperpermeability of capillaries lining the peritoneal cavity would be one of the essential factors for the accumulation of malignant ascites.[4-8] The hyperpermeability of capillaries has been shown to be mediated by various factors. Among them, it has been suggested that the vascular endothelial growth factor-A (VEGF-A) is one of the factors responsible.[5-9] VEGF-A is originally identified as a vascular permeability factor (VPF), which possesses a potent ability to permeate capillaries to a 50,000-fold higher level than histamine.[10-12] It induces extravasation of plasma proteins, such as fibrinogen, which, when deposited in the extracellular matrix, may serve as a foundation for the formation of tumor stroma and new capillaries. A high VEGF-A level has been found in human and mouse malignant ascites, and a high concentration of VEGF-A in the leaky capillaries lining the peritoneal cavity was found in the ascites of tumor-bearing animals.[5-8] VEGF-A specific neutralizing antibody (nAb) showed a significant inhibitory effect on experimental malignant ascites accumulation.[5,9]

The biological activities of VEGF-A are mediated mainly via 2 type III tyrosine kinase receptors: flt-1 and kinase insert domain–containing receptor/fetal liver kinase (KDR/Flk-1). It has been suggested that flt-1 and KDR/Flk-1 serve different roles in the angiogenesis and signal transduction pathways.[13-17] In solid tumor development, the use of dominant-negative KDR/Flk-1 and several other methods that also inhibit the VEGF-KDR/Flk-1 interaction substantially reduced tumor growth and angiogenesis.[18-25] Recently, it has been shown that the nonspecific VEGF tyrosine kinase receptor inhibitor and KDR/Flk-1 nAb inhibited the experimental ovarian malignant ascites.[26,27] In the solid HCC development, VEGF-A and KDR/Flk-1 have been shown to play an impor-

Abbreviations: HCC, hepatocellular carcinoma; KDR/Flk-1, kinase insert domain-containing receptor/fetal liver kinase-1; VEGF, vascular endothelial growth factor; VPF, vascular permeability factor; nAb, neutralizing antibody; PBS, phosphate-buffered saline; ELISA, enzyme-linked immunosorbent assay; MTT, 3-(-4,5-diethylthiazol-2-yl)-2,5-diphenyltetrazolium bromide.

From the [1]Third Department of Internal Medicine, Nara Medical University, Nara 634-8522, Japan; and the [2] Department of Immunology, ImClone Systems Incorporated, New York, NY.

Received October 11, 2000; accepted January 22, 2001.

Address reprint requests to: Hitoshi Yoshiji, M.D., Ph.D., Third Department of Internal Medicine, Nara Medical University, Shijo-cho 840, Kashihara Nara 634-8522, Japan. E-mail: yoshijih@naramed-u.ac.jp; fax: (81) 744-24-7122.

0270-9139/01/3304-0012$35.00/0
doi:10.1053/jhep.2001.23312

tant role,[28-33] but the role of these factors in malignant hepatic ascites formation has not yet been elucidated.

In this study, we examined the role of KDR/Flk-1 in malignant hepatic ascites formation and the survival of ascites-bearing mice by means of KDR/Flk-1 nAb in comparison with VEGF-A nAb.

MATERIALS AND METHODS

Cell Lines and Cell Culture. The murine HCC cell line, MH134, which was originally induced by carbon tetrachloride in C3H/He mice, was generously provided by Chugai (Tokyo, Japan). MH134 cells, which are highly tumorigenic and moderately differentiated, are grown in syngeneic recipients in an ascites form.[34] These MH134 cells have been shown to produce the endogenous VEGF in the ascites.[8] These cells were grown in RPMI 1640 medium (Nissui, Tokyo, Japan) supplemented with 10% (vol/vol) heat-inactivated fetal calf serum, 0.3 mg/ml. glutamine, 100 units/mL ampicillin, and 100 μg/mL streptomycin at 37°C in air with 5% CO_2.

Anti-KDR/Flk-1 and Anti-VEGF-A nAbs. The anti–KDR/Flk-1–specific neutralizing antibody (KDR/ Flk-1 nAb; DC101) was generated as described previously.[25,35] Briefly, KDR/Flk-1 nAb was produced under large-scale culture conditions in serum-free media. KDR/Flk-1 nAb was purified from conditioned media by affinity chromatography on a Gammabind-G-Sepharose column (Pharmacia biotech, Piscataway, NJ). The purity of KDR/Flk-1 nAb was >99% as determined by sodium dodecyl sulfate–polyacrylamide gel electrophoresis, and was verified to be free of endotoxin (1 <EU/mL) using a limulus amebocyte lysate endotoxin detection kit (Pyrogen Tplus, Bio-Whittaker, Walkersville, MD). The anti–VEGF-A nAb, AF-493-NA, was purchased from R & D Systems (Minneapolis, MN). AF-493-NA has been shown to significantly neutralize VEGF-A bioactivity, and it possesses the ability to neutralize the bioactivity of 10 ng/mL rm-VEGF at the lowest dosage of 0.35 μg/mL.[9]

Animal Treatment and Collection of Ascites. Eight-week-old female C3H/He mice were purchased from Japan SLC (Hamamatsu, Japan). All animal experiments were performed in accordance with the approved protocols and recommendations for the proper care and use of laboratory animals. To establish the malignant ascites, 1×10^5 of MH134 cells were inoculated into C3H/He mice intraperitoneally on day 0. On day 2, the mice were divided randomly into 4 groups (n = 7 each). The first group did not receive treatment and was used as a control group. The animals in the second group received an intravenous injection via the tail vein of VEGF-A nAb in 50 μL phosphate-buffered saline (PBS) every 2 days. The mechanism of VEGF-A neutralization in the ascites was described previously.[9] To estimate the total amount of VEGF-A protein at the respective VEGF-A nAb injection dates, preliminary chronological studies were performed to measure the VEGF-A level in the ascites. The dose of VEGF-A nAb was over 20-fold higher than the amounts of VEGF-A accumulated in the ascites. The third group received KDR/Flk-1 nAb (400 μg/50 μL PBS per mouse) every 2 days. The dose of KDR/Flk-1 nAb in this experiment was the same as in the previous study that showed a significant suppression of activation of KDR/Flk-1 in the murine HCC model.[25] The animals in the fourth group received the same isotype (IgG) raised against mouse IgA (400 μg/50 μL PBS per mouse) every 2 days (Pharmingen, San, Diego, CA). On day 9, all animals were anesthetized with ether, a small incision was made on the central abdominal skin, and the abdominal skin was peeled to avoid breaking the peritoneum. The malignant ascites was completely aspirated using a syringe with a 22-gauge needle through the peritoneum under direct visualization; then the volume of ascites was determined. All procedures were performed aseptically under a laminar flow hood. The collected ascites was centrifuged at 15,000 rpm for 15 minutes at 4°C. To count the total number of tumor cells, the pellet was recovered and resuspended in PBS. To examine the discontinuous effect of KDR/Flk-1 nAb, we designed the following experiment. After treatment of KDR/Flk-1 nAb until day 9, we divided the mice into 2 groups (n = 5 each). KDR/Flk-1 nAb treatment was continued in 1 group, and was halted in the other. On day 18, all mice were killed, and the volume of ascites was examined.

For the therapeutic experiment, C3H/He mice were inoculated intraperitoneally with MH134 on day 0. On day 8, when all animals developed an apparent malignant ascites, they were divided randomly into 4 groups in the same manner as in the ascites-formation experiment (n = 10 for each group). Treatment from day 8 also was identical to that described above for each group. The animals were observed daily for the signs of morbidity. In the preliminary study, we found that the mice died of chest compression and dyspnea within a few days when the girth of the abdomen reached a certain size (critical girth). We therefore killed the mice when the animals showed the critical girth of abdomen.

VEGF-A and VEGF-C Measurement. The supernatants of the aspirated ascites were used for the VEGF-A and VEGF-C measurements. VEGF-A level was measured by an enzyme-linked immunosorbent assay (ELISA) kit in accordance with the supplier's instructions (R & D systems). Because the ELISA system for VEGF-C was not available, the expression level of VEGF-C was determined by the Western Blot analysis as previously described,[28,36] using an amplified alkaline phosphatase immunoblot assay kit (Bio-Rad, Hercules, CA) and antibody against VEGF-C (sc-7132) (Santa Cruz, Santa Cruz, CA).

Peritoneal-Cavity Permeability Assay. To evaluate the peritoneal-cavity capillary permeability, 1 mL of 0.5 % Evans Blue dye (Nakalai, Kyoto, Japan) was injected intravenously into the tail vein 8 days after the MH134 tumor cell inoculation. Two hours later, the mice were killed, and the ascites was aspirated as described before. The relative concentration of dye leaking into the ascites was determined from the optical density at 540 nm using a spectrophotometer.

In Vitro *Proliferation Assay.* The effects of VEGF-A nAb and KDR/Flk-1 nAb (20 μg/mL) on *in vitro* proliferation of MH134 were evaluated. This amount of KDR/Flk-1 nAb significantly suppressed the endothelial cell proliferation *in vitro*.[35] *In vitro* proliferation was determined by the MTT assay as described previously.[28] Briefly, cell proliferation was quantified via conversion of tetrazolium, 3-(-4,5-diethylthiazol-2-yl)-2,5-diphenyltetrazolium bromide (MTT) by cells cultured in 96-well plates. The absorbance with a 540-nm filter represents conversion to formazan, which is directly proportional to the number of living cells. The absorbance was read with an ELISA plate recorder (n = 6 per group).

Immunoprecipitation. Immunoprecipitation was performed as previously described.[25,36] Fifteen minutes after either VEGF-A nAb, KDR/ Flk-1 nAb, or control IgG was injected intravenously into the ascites-bearing mice, the peritoneal wall was resected from 3 mice in each group and snap-frozen immediately. The pooled peritoneal wall lysate solution was immunoprecipitated with KDR/Flk-1 before conducting sodium dodecyl sulfate–polyacrylamide gel electrophoresis. After the transfer, the membrane was stained with Ponceau solution (Sigma, St. Louis, MO) to confirm that the same amount of protein was immunoprecipitated. The blots were developed by the same method as described above with antiphosphotyrosine. Antityrosine (4G10) was obtained from Up-State Biotechnology (Lake Placid, NY).

Statistical Analysis. The Mann-Whitney *U* test was used for the statistical analysis. For the survival of animals, Kaplan-Meier curves were established for each group, and the survivals were compared by means of the log rank test.

RESULTS

VEGF-A and VEGF-C Expression in Tumor Ascites. First, we examined the total amount of VEGF-A in the accumulated malignant ascites to determine the required VEGF-A nAb at the respective period. As shown in Fig. 1, the total amount of VEGF-A in the ascites increased over time. In the preliminary study, we found that there was no difference in the neutralizing activity of VEGF-A nAb between 20-fold and 40-fold amount of VEGF-A expression in MH134 *in vitro* (data not shown). We therefore used at least over 20-fold for the in-

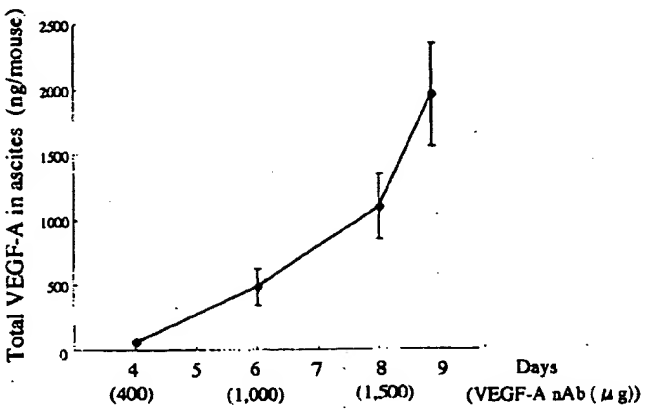

FIG. 1. Kinetics of VEGF-A accumulation in the ascites of mice inoculated intraperitoneally with MH134 cells. The tumor-bearing mice were killed at successive intervals after intraperitoneal injection of 1×10^5 MH134 cells per mouse. After the ascites was taken, the amount of VEGF-A was determined by ELISA. The data represent the mean ± SD (n = 7). The *lower column* represents the injected amount of VEGF-A nAb at the respective period.

jected VEGF-A nAb, which was similarly used in the previous studies.[9] The amount of VEGF-A nAb used was always over 20 times than the accumulated VEGF-A level (Fig. 1, lower column), and these doses were higher than the amount of KDR/Flk-1 nAb (400 μg) except on day 2. As shown in Fig. 2, 9 days after the MH134 tumor cell inoculation, a high level of VEGF-A was observed in the untreated control mice (370 ± 35 ng/mL; n = 7). Treatment with VEGF-A nAb almost abolished the accumulation of VEGF-A in the ascites (10 ± 6 ng/mL; n= 7) ($P < .01$). In contrast, neither KDR/Flk-1 nAb nor control IgG treatment affected the VEGF-A protein level in the ascites.

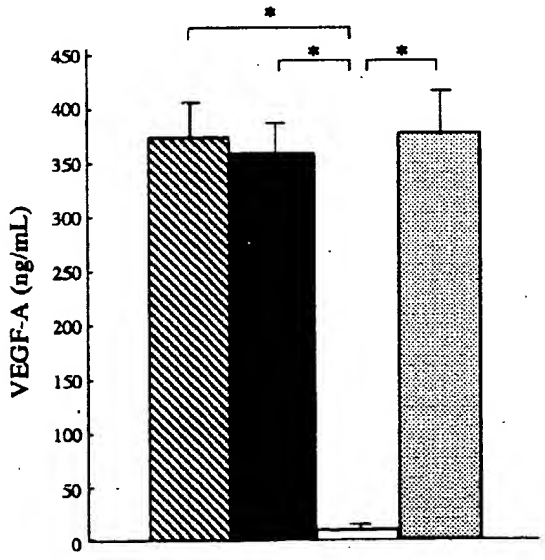

FIG. 2. Effects of VEGF-A nAb and KDR/FIK-1 nAb on VEGF-A protein level in the malignant ascites. Nine days after intraperitoneal inoculation of 1×10^5 MH134 cells, VEGF-A level in the ascites was measured by ELISA. The data represent the mean ± SD (n = 7). *Statistically significant difference compared with the control group ($P < .01$). (▨), Control; (■), IgG; (□), VEGF-A nAb; (▩), KDR/Flk-1 nAb.

Because other VEGF ligands can bind KDR/Flk-1, namely VEGF-C, we next examined this ligand protein expression level in the ascites. VEGF-C expression in the ascites was found to be at a comparable level in all control IgG-, VEGF-A nAb–, and KDR/Flk-1 nAb–treated groups (Fig. 3A).

Effects of VEGF-A nAb and KDR/Flk-1 nAb on Ascites Formation and Peritoneal Capillary Permeability. To examine the role of VEGF-A and KDR/Flk-1 in malignant ascites formation, we first investigated the effects of VEGF-A nAb and KDR/ Flk-1 nAb in the mouse ascites tumor model. As shown in Fig. 4A and 4B, the mean volume of ascites fluid and the number of tumor cells in the animals that received VEGF-A nAb or KDR/Flk-1 nAb were significantly lower than those in the untreated mice or mice treated with the same dose of control IgG ($P < .01$). Interestingly, the inhibitory effects of KDR/Flk-1 nAb were more potent than those of VEGF-A nAb in terms of ascites volume and tumor cell numbers ($P < .05$).

Consistent with the above-mentioned results, the permeability of the capillaries in the peritoneal cavity was suppressed significantly in the VEGF-A nAb and KDR/Flk-1 nAb groups compared with the untreated or control IgG-treated groups ($P < .01$), and the treatment with KDR/Flk-1 nAb was more effective in reducing the capillary permeability in the peritoneum of mice than that of VEGF-A nAb ($P < .05$) (Fig. 5). All mice in these experiments did not reach the critical girth size of the abdomen (data not shown). Next, we examined whether or not the ascites again began to accumulate by halting treatment of KDR/ Flk-1 nAb. From day 9, one group

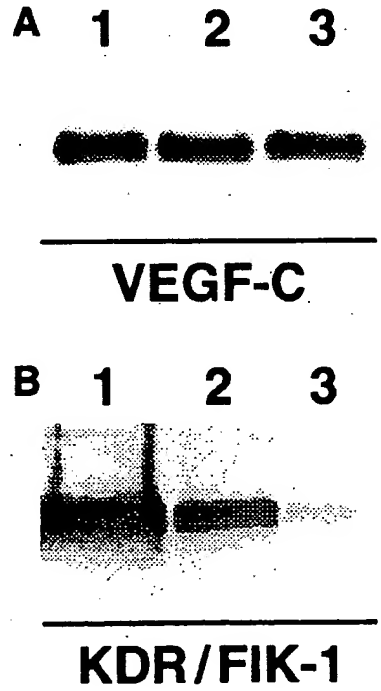

FIG. 3. VEGF-C expression in the malignant ascites (A) and KDR/Flk-1 receptor activation in situ (B). (A) Nine days after intraperitoneal inoculation of 1×10^5 MH134 cells into C3H/He mice, the VEGF-C level in the malignant ascites was examined by the Western blotting. (B) Immunoprecipitation for KDR/Flk-1 and phosphotyrosine in the peritoneal wall. Fifteen minutes after the injection of VEGF-A nAb and KDR/Flk-1 nAb or control IgG, the peritoneal wall was resected from 3 mice and pooled. The peritoneal wall lysate solution was concentrated and used for immunoprecipitation. *Lane 1*, control IgG; *lane 2*, VEGF-A nAb; *lane 3*, KDR/Flk-1 nAb–treated group.

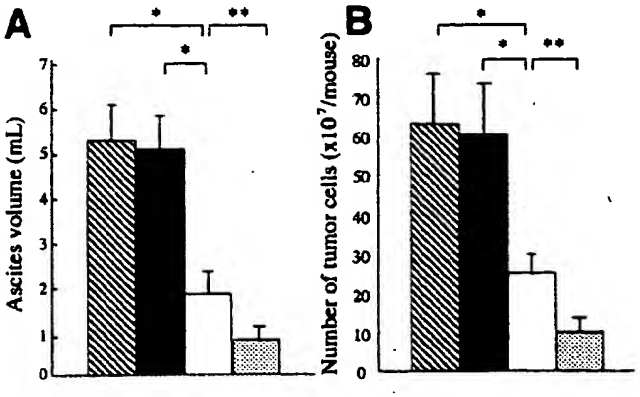

FIG. 4. Effect of VEGF-A nAb and KDR/Flk-1 nAb on malignant tumor ascites formation. One × 10^5 of MH134 cells were syngenetically inoculated into C3H/He mice intraperitoneally on day 0. From day 2, VEGF-A nAb, KDR/Flk-1 nAb, and control IgG were administered intravenously twice a week at the doses described in Materials and Methods. On day 9, malignant ascites was aspirated and the ascites volume (A), and tumor cell numbers in the ascites fluid were calculated (B). The data represent the mean ± SD (n = 7). * and **Statistically significant differences between the indicated 2 groups ($P < .01$ and $P < .05$, respectively). (▨), Control; (■), IgG; (□), VEGF-A nAb; (▩), KDR/Flk-1 nAb.

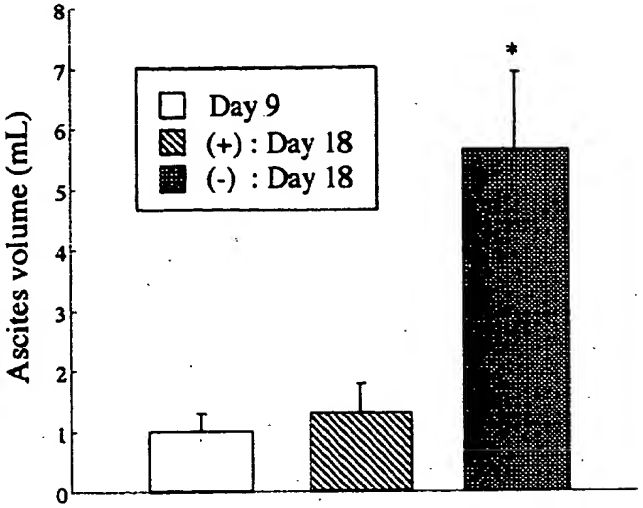

FIG. 6. Discontinuous effect of KDR/Flk-1 nAb treatment on the ascites accumulation. After the treatment with KDR/Flk-1 nAb every 2 days until day 9, we divided the mice into 2 groups (n = 5 each). KDR/Flk-1 nAb treatment was continued in 1 group, and was halted in the other from day 9. On day 18, all mice were killed and the volume of ascites was examined. The data represent the mean ± SD. *Statistically significant difference compared with the other group ($P < .01$). (+), KDR/Flk-1 nAb treatment was continued; (−), KDR/Flk-1 nAb treatment was discontinued from day 9.

continued the treatment of KDR/Flk-1 nAb, whereas the other group was discontinued. On day 18, all mice were killed and examined for the ascites volume. As shown in Fig. 6, ascites did not increase until day 18 with the continued treatment of KDR/Flk-1 nAb. On the contrary, ascites again accumulated after discontinuation of KDR/Flk-1 nAb treatment. These results strongly suggested that ascites formation was predominantly mediated by KDR/Flk-1 signaling cascade.

Effect of VEGF-A nAb and KDR/Flk-1 nAb on In Vitro *Proliferation of Ascites Tumor.* To examine whether VEGF-A nAb and KDR/Flk-1 nAb could directly inhibit the MH134 tumor growth, we examined the effect of these Abs on *in vitro* proliferation. The *in vitro* proliferation rate was examined by the MTT assay at 24, 48, and 72 hours after harvest. As shown in Fig. 7, there was no significant difference between all groups. These results suggested that VEGF-A nAb and KDR/Flk-1 nAb did not inhibit ascites formation mediated by the direct inhibition of the tumor growth.

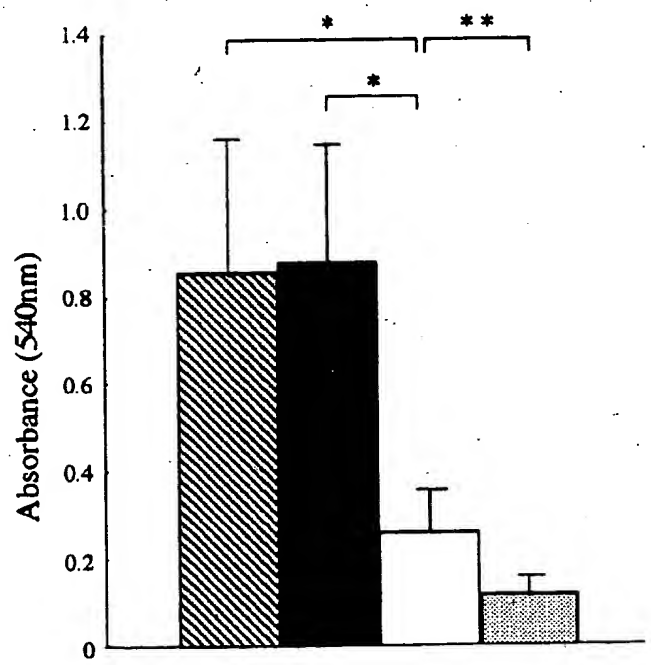

FIG. 5. Effects of VEGF-A nAb and KDR/FIK-1 nAb on the peritoneal capillary permeability. Two hours after the injection of 1 mL of 0.5% Evans blue into the tail vein, the relative concentration of the dye leaking into the peritoneal cavity was measured with a spectrophotometer at 540 nm. The data represent the mean ± SD (n = 7). * and **Statistically significant differences between the indicated 2 groups ($P < .01$ and $P < .05$, respectively). (▨), Control; (■), IgG; (□), VEGF-A nAb; (▩), KDR/Flk-1 nAb.

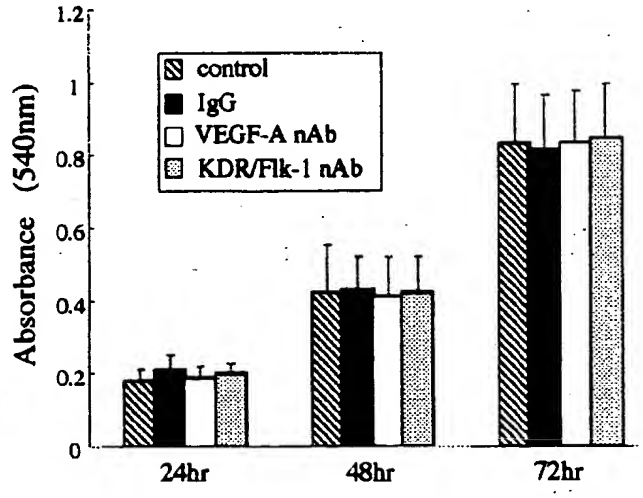

FIG. 7. Effects of VEGF-A nAb and KDR/Flk-1 nAb (20 μg/mL) on *in vitro* proliferation of MH134 tumor cells. The cell proliferation rate was measured by the MTT assay after harvest at 24, 48, and 72 hours as described. The data represent the mean ± SD (n = 6 per group).

KDR/Flk-1 Receptor Activation In Situ. To determine the effect of VEGF-A nAb and KDR/Flk-1 nAb on the activation of KDR/Flk-1, we investigated tyrosine-phosphorylated KDR/Flk-1 in the peritoneal wall. As shown in Fig. 3B, the control IgG-treated group showed a phosphorylated 230 kd, corresponding to the activated KDR/Flk-1. VEGF-A nAb and KDR/Flk-1 nAb significantly inhibited KDR/Flk-1 phosphorylation compared with the control IgG-treated group. Consistent with the above-mentioned results, KDR/Flk-1 nAb treatment was more effective in inhibiting KDR/Flk-1 phosphorylation than that of VEGF-A nAb, *i.e.*, KDR/Flk-1 nAb almost completely abolished the KDR/Flk-1 activation, whereas in the VEGF-A nAb treatment group, a certain level of phosphorylation of KDR/Flk-1 was still found.

Therapeutic Effects of VEGF-A nAb and KDR/Flk-1 nAb on Carcinomatous Peritonitis. To evaluate the feasibility of VEGF-A nAb and KDR/Flk-1 nAb treatment of hepatic malignant ascites, the effectiveness of this therapy on the survival of ascites-bearing mice was investigated. As shown in Fig. 8, all the untreated and control IgG-treated animals died within 16 days after intraperitoneal inoculation of MH134 cells (the mean survival period of the untreated and control IgG-treated animals was 10.8 and 11.2 days, respectively). The treatment with VEGF-A nAb (the mean survival period was 19.0 days) and KDR/Flk-1 nAb (23.5 days) significantly prolonged survival of the ascites-bearing mice compared with the untreated or control IgG-treated group ($P < .01$). A significant prolongation of the survival was found in animals treated with KDR/Flk-1 nAb compared with those treated with VEGF-A nAb ($P < .05$). The abdominal girth of all mice increased in parallel over time. Neither invasion nor metastasis to the other organs, such as the liver, could be found macroscopically in the mice during the study period (data not shown).

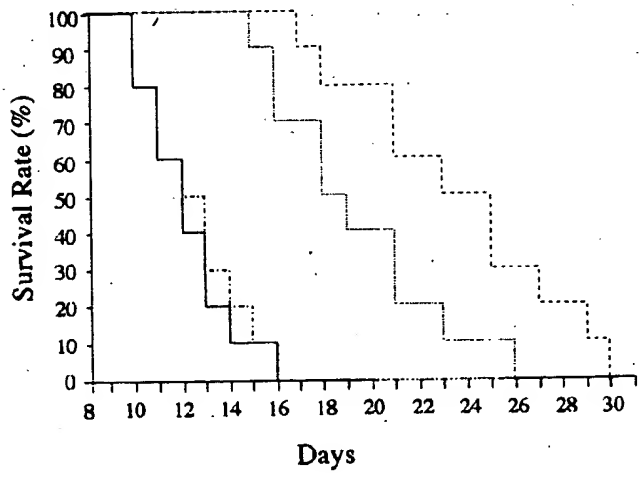

FIG. 8. Therapeutic effects of VEGF-A nAb and KDR/Flk-1 nAb on carcinomatous peritonitis. 1×10^5 MH134 cells were syngenetically intraperitoneally inoculated into C3H/He mice. On day 8, when all animals developed apparent malignant ascites, the mice were divided into 4 groups. The control IgG, VEGF-A nAb, and KDR/Flk-1 nAb groups were treated with the respective administered doses described in Materials and Methods ($n = 10$ each). An untreated group was used as the control ($n = 10$). Survival of the animals was observed every day. The survival rates of mice injected with either VEGF-A nAb or KDR/Flk-1 nAb were significantly higher than those of the untreated and control IgG-treated mice ($P < .01$), using the log rank test. The survival rate of KDR/Flk-1 nAb–treated mice was significantly higher than that of VEGF-A nAb ($P < .05$), using the log rank test. *Solid line*, control; *dotted/dashed line*, IgG; *dotted line*, VEGF-A nAb; *dashed line*, KDR/Flk-1 nAb.

DISCUSSION

VEGF-A and its receptor interaction have been shown to play a central role in many physiologic and pathologic processes.[10-12,37-40] It has been shown that the accumulation of the tumor ascites fluid results greatly from increased permeability of the capillaries in the peritoneal lining. Abundant VEGF-A activity has been found in the mouse, guinea pig, and human tumor ascites fluid, and the increased capillary permeability correlated with the appearance of VEGF-A in the ascites fluid.[4-8] The role of VEGF-A, however, in HCC ascites has not been examined.

The effects of VEGF-A are mediated mainly through two high-affinity receptors: flt-1 and KDR/Flk-1. It has been suggested that flt-1 and KDR/Flk-1 serve different roles in the angiogenesis and signal transduction pathway.[12-17] In solid-tumor angiogenesis, KDR/Flk-1 has been shown to be a predominant receptor. Suppression of KDR/Flk-1 by mechanisms such as dominant-negative KDR/Flk-1 and KDR/Flk-1 nAb showed adequate inhibition of solid-tumor development, including HCC.[18-25] It also has been reported that KDR/ Flk-1 was a predominant receptor in VEGF-A–mediated vascular permeability.[41] The nonspecific VEGF-A receptor kinase inhibitor and KDR/Flk-1 nAb inhibited the ovarian tumor ascites.[26,27] In solid-HCC development, we previously reported that KDR/Flk-1 was a predominant receptor of VEGF-A–mediated bioactivity in the murine HCC model.[28,29] The role of KDR/Flk-1, however, in the HCC ascites formation has not yet been elucidated either.

In this study, we showed that KDR/Flk-1 nAb significantly inhibited the ascites accumulation and the increase in tumor cell numbers in the ascites fluid, and these inhibitory effects seemed to be more potent than those of VEGF-A nAb treatment. Furthermore, in the therapeutic experiment, KDR/Flk-1 nAb treatment significantly prolonged survival of the ascites-bearing mice compared with VEGF-A nAb treatment. It is difficult to simply compare the inhibitory effect of the ligand (VEGF-A) and its receptor (KDR/Flk-1) neutralization. However, we at least found that the treatment with VEGF-A nAb abolished the VEGF-A protein level in the ascites, and KDR/Flk-1 nAb almost completely suppressed activation of this receptor at the dose that we used in this study. We therefore could assess the suppressive effect of each factor in this HCC ascites model.

Apart from VEGF-A, other VEGF ligands can also bind KDR/Flk-1. VEGF-C is capable of binding to and activating KDR/Flk-1 and flt-4, but not flt-1.[10-12] It has been reported that KDR/Flk-1 played a critical role in the signal transduction pathway for the vascular permeability activity of VEGF-C.[42] In this study, we found VEGF-C in the malignant ascites, and activation of KDR/Flk-1 was still observed as a result of VEGF-A inhibition. Because VEGF-C nAb is not currently available, it is difficult at this time to elucidate the exact involvement of each VEGF-family member. A recent study, however, has shown that VEGF-A and VEGF-C showed synergistic effect, and that the redundant biological effects of VEGF-A and VEGF-C depended on binding and activation of KDR/ Flk-1.[43] It may be possible that VEGF-A and VEGF-C acted cooperatively in hepatic malignant ascites formation via activation of the KDR/Flk-1 receptor. Further studies are required to examine the individual role of these VEGF family members.

A previous report showed that the peritoneal neovascularization correlated with ascites formation 5 weeks after the tumor inoculation.[5] In this study, however, we did not find a significant difference in the capillary density of the peritoneal wall (data not shown). The exact reason for this discrepancy is not clear, but it has been shown recently that the VEGF concentrations in ascites did not consistently correlate with the capillary density in the peritoneal wall in the mouse tumor ascites, including MH 134.[8] Another report suggested that tumor-derived VEGF-A is obligatory for ascites formation, but not for intraperitoneal tumor growth and angiogenesis.[5] This report also suggested that inhibition of angiogenesis would only suppress the development and growth of the larger intraperitoneal tumors. Although MH134 cells can grow in syngeneic hosts in both solid and ascites forms, intraperitoneal injection of MH134 cells into C3H/He mice resulted in development of malignant ascites without development of intraperitoneally disseminated solid tumors. Because MH134 did not form intraperitoneal tumors, it is possible that dependency of this tumor ascites on angiogenesis would be much less compared with that of solid tumors or other types of tumor ascites. Alternatively, new vessels that developed in response to VEGF-A and VEGF-C expressed by MH134 may have not developed sufficiently during the survival period of the mice in this experiment, because angiogenesis of the peritoneal wall seemed to require at least more than 10 days.[9]

In summary, we show here that KDR/Flk-1 is a major regulator of malignant hepatic ascites formation, and in addition to VEGF-A, VEGF-C may also be involved in the development of malignant hepatic ascites formation. Furthermore, because KDR/Flk-1 nAb significantly prolonged the survival of the malignant ascites-bearing mice, inhibition of KDR/Flk-1 may be a potential future target for the treatment of malignant hepatic ascites.

REFERENCES

1. Okuda K, Musha H, Nakajima Y, Kubo Y, Shimokawa Y, Nagasaki Y, Sawa Y et al. Clinicopathologic features of encapsulated hepatocellular carcinoma: a study of 26 cases. Cancer 1977;40:1240-1245.
2. Simonetti RG, Camma C, Fiorello F, Politi F, D'Amico G, Pagliaro L. Hepatocellular carcinoma. A worldwide problem and the major risk factors. Dig Dis Sci 1991;36:962-972.
3. Yamanaka N, Okamoto E, Toyosaka A, Mitunobu M, Fujihara S, Kato T, Fujimoto J, et al. Prognostic factors after hepatectomy for hepatocellular carcinomas. A univariate and multivariate analysis. Cancer 1990;65: 1104-1110.
4. Senger DR., Galli SJ, Dvorak AM, Perruzzi CA, Harvey VS, Dvorak HF. Tumor cells secrete a vascular permeability factor that promotes accumulation of ascites fluid. Science 1983;219:983-985.
5. Mesiano S, Ferrara N, Jaffe RB. Role of vascular endothelial growth factor in ovarian cancer: inhibition of ascites formation by immunoneutralization. Am J Pathol 1998;153:1249-1256.
6. Nagy JA, Masse EM, Herzberg KT, Meyers MS, Yeo KT, Yeo TK, Sioussat TM, et al. Pathogenesis of ascites tumor growth: vascular permeability factor, vascular hyperpermeability, and ascites fluid accumulation. Cancer Res 1995;55:360-368.
7. Yeo KT, Wang HH, Nagy JA, Sioussat TM, Ledbetter SR, Hoogewerf AJ, Zhou Y, et al. Vascular permeability factor (vascular endothelial growth factor) in guinea pig and human tumor and inflammatory effusions. Cancer Res 1993;53:2912-2918.
8. Luo JC, Yamaguchi S, Shinkai A, Shitara K, Shibuya M. Significant expression of vascular endothelial growth factor/vascular permeability factor in mouse ascites tumors. Cancer Res 1998;58:2652-2660.
9. Luo JC, Toyoda M, Shibuya M. Differential inhibition of fluid accumulation and tumor growth in two mouse ascites tumors by an antivascular endothelial growth factor/permeability factor neutralizing antibody. Cancer Res 1998;58:2594-2600.
10. Shibuya, M. Role of VEGF-flt receptor system in normal and tumor angiogenesis. Adv Cancer Res 1995;67:281-316.
11. Ferrara, N, Davis-Smyth, T. The biology of vascular endothelial growth factor Endocr Rev 1997;18:4-25.
12. Neufeld G, Cohen T, Gengrinovitch, S, Poltorak, Z. Vascular endothelial growth factor (VEGF) and its receptors. FASEB J 1999;13:9-22.
13. Kroll J, Waltenberger J. The vascular endothelial growth factor receptor KDR activates multiple signal transduction pathways in porcine aortic endothelial cells. J Biol Chem 1997;272:32521-32527.
14. Waltenberger J, Claesson-Welsh L, Siegbahn A, Shibuya M, Heldin CH. Different signal transduction properties of KDR and Flt1, two receptors for vascular endothelial growth factor. J Biol Chem 1994;269:26988-26995.
15. Shalaby F, Rossant J, Yamaguchi TP, Gertsenstein M, Wu XF, Breitman ML, Schuh AC. Failure of blood-island formation and vasculogenesis in Flk-1–deficient mice. Nature 1995;376:62-66.
16. Fong GH, Rossant J, Gertsenstein M, Breitman ML. Role of the Flt-1 receptor tyrosine kinase in regulating the assembly of vascular endothelium. Nature 1995;376:66-70.
17. Millauer B, Wizigmann-Voos S, Schnurch H, Martinez R, Moller NP, Risau W, Ullrich A. High affinity VEGF binding and developmental expression suggest Flk-1 as a major regulator of vasculogenesis and angiogenesis. Cell 1993;72:835-846.
18. Kim KJ, Li B, Winer J, Armanini M, Gillett N, Phillips HS, Ferrara N. Inhibition of vascular endothelial growth factor–induced angiogenesis suppresses tumour growth in vivo. Nature 1993;362:841-844.
19. Millauer B, Longhi MP, Plate KH, Shawver LK, Risau W, Ullrich A, Strawn LM. Dominant-negative inhibition of Flk-1 suppresses the growth of many tumor types in vivo. Cancer Res 1996;56:1615-1620.
20. Skobe M, Rockwell P, Goldstein N, Vosseler S, Fusenig NE. Halting angiogenesis suppresses carcinoma cell invasion. Nat Med 1997;3:1222-1227.
21. Strawn LM, McMahon G, App H, Schreck R, Kuchler WR, Longhi MP, Hui TH, et al. Flk-1 as a target for tumor growth inhibition. Cancer Res 1996;56:3540-3545.
22. Fong TA, Shawver LK, Sun L, Tang C, App H, Powell TJ, Kim YH, et al. SU5416 is a potent and selective inhibitor of the vascular endothelial growth factor receptor (Flk-1/KDR) that inhibits tyrosine kinase catalysis, tumor vascularization, and growth of multiple tumor types. Cancer Res 1999;59:99-106.
23. Prewett M, Huber J, Li Y, Santiago A, O'Connor W, King K, Overholser J, Hooper A, et al. Antivascular endothelial growth factor receptor (fetal liver kinase 1) monoclonal antibody inhibits tumor angiogenesis and growth of several mouse and human tumors. Cancer Res 1999;59:5209-5218.
24. Angelov L, Salhin AB, Roncari L, McMahon G, Guha A. Inhibition of angiogenesis by blocking activation of the vascular endothelial growth factor receptor 2 leads to decreased growth of neurogenic sarcomas. Cancer Res 1999;59:5536-5541.
25. Yoshiji H, Kuriyama S, Hicklin DJ, Huber J, Yoshii J, Miyamoto Y, Kawata M, et al. KDR/Flk-1 is a major regulator of vascular endothelial growth factor–induced tumor development and angiogenesis in murine hepatocellular carcinoma cells. HEPATOLOGY 1999;30:1179-1186.
26. Xu L, Yoneda J, Herrera C, Wood J, Killion JJ, Fidler IJ. Inhibition of malignant ascites and growth of human ovarian carcinoma by oral administration of a potent inhibitor of the vascular endothelial growth factor receptor tyrosine kinases. Int J Oncol 2000;16:445-454.
27. Stoelcker B, Echtenacher B, Weich HA, Sztajer H, Hicklin DJ, Mannel DN. VEGF/Flk-1 interaction, a requirement for malignant ascites recurrence. J Interferon Cytokine Res 2000;20:511-517.
28. Yoshiji H, Kuriyama S, Yoshii J, Yamazaki M, Kikukawa M, Tsujinoue H, Nakatani T, Fukui H. Vascular endothelial growth factor tightly regulates *in vivo* development of murine hepatocellular carcinoma cells. HEPATOLOGY 1998;28:1489-1496.
29. Chow NH, Hsu PI, Lin XZ, Yang HB, Chan SH, Cheng KS, Huang SM, et al. Expression of vascular endothelial growth factor in normal liver and hepatocellular carcinoma: an immunohistochemical study. Hum Pathol 1997;28:698-703.
30. Mise M, Arii S, Higashituji H, Furutani M, Niwano M, Harada T, Ishigami S, et al. Clinical significance of vascular endothelial growth factor and basic fibroblast growth factor gene expression in liver tumor. HEPATOLOGY 1996;23:455-464.
31. Miura H, Miyazaki T, Kuroda M, Oka T, Machinami R, Kodama T, Shibuya M, et al. Increased expression of vascular endothelial growth factor in human hepatocellular carcinoma. J Hepatol 1997;27:854-861.
32. Suzuki K, Hayashi N, Miyamoto Y, Yamamoto M, Ohkawa K, Ito Y, Sasaki Y, et al. Expression of vascular permeability factor/vascular endothelial

growth factor in human hepatocellular carcinoma. Cancer Res 1996;56: 3004-3009.
33. Yamaguchi R, Yano H, Iemura A, Ogasawara S, Haramaki M, Kojiro M. Expression of vascular endothelial growth factor in human hepatocellular carcinoma. HEPATOLOGY 1998;28:68-77.
34. Sato H, Belkin M, Essner E. Experiments on an ascites hepatoma.III. The conversion of mouse hepatoma into the ascitic form. J Natl Cancer Inst 1956;17:1-21.
35. Rockwell P, Neufeld G, Glassman A, Caron D, Goldstein N. I. *In vitro* neutralization of vascular endothelial growth factor activation of flk-1 by a monoclonal antibody. Mol Cell Differ 1995;3:91-109.
36. Yoshiji H, Kuriyama S, Ways DK, Yoshii J, Miyamoto Y, Kawata M, Ikenaka Y, et al. Protein kinase C lies on the signaling pathway for vascular endothelial growth factor–mediated tumor development and angiogenesis. Cancer Res 1999;59:4413-4418.
37. Folkman J. Angiogenesis in cancer, vascular, rheumatoid and other disease. Nat Med 1995;1:27-31.
38. Fidler IJ, Ellis LM. The implications of angiogenesis for the biology and therapy of cancer metastasis. Cell 1994;79:185-188.
39. Ferrara, N, Alitalo K. Clinical applications of angiogenic growth factors and their inhibitors. Nat Med 1999;5:1359-1364.
40. Battegay EJ. Angiogenesis: mechanistic insights, neovascular diseases, and therapeutic prospects. J Mol Med 1995;73:333-346.
41. Ogawa S, Oku A, Sawano A, Yamaguchi S, Yazaki Y, Shibuya M. A novel type of vascular endothelial growth factor, VEGF-E (NZ-7 VEGF), preferentially utilizes KDR/Flk-1 receptor and carries a potent mitotic activity without heparin-binding domain. J Biol Chem 1998;273:31273-31282.
42. Joukov V, Kumar V, Sorsa T, Arighi E, Weich H, Saksela O, Alitalo K. A recombinant mutant vascular endothelial growth factor-C that has lost vascular endothelial growth factor receptor-2 binding, activation, and vascular permeability activities. J Biol Chem 1998;273:6599-6602.
43. Pepper MS, Mandriota SJ, Jeltsch M, Kumar V, Alitalo K. Vascular endothelial growth factor (VEGF)-C synergizes with basic fibroblast growth factor and VEGF in the induction of angiogenesis in vitro and alters endothelial cell extracellular proteolytic activity. J Cell Physiol 1998;177: 439-452.

Exhibit 10

American Journal of Pathology, Vol. 153, No. 4, October 1998

Role of Vascular Endothelial Growth Factor in Ovarian Cancer

Inhibition of Ascites Formation by Immunoneutralization

Sam Mesiano,* Napoleone Ferrara,† and Robert B. Jaffe*

From the Reproductive Endocrinology Center, Department of Obstetrics, Gynecology and Reproductive Sciences, University of California, San Francisco, San Francisco, and Department of Cardiovascular Research,† Genentech, Inc., South San Francisco, California*

Ovarian cancer is characterized by the rapid growth of solid intraperitoneal tumors and large volumes of ascitic fluid. Vascular endothelial growth factor (VEGF) augments tumor growth by inducing neovascularization and may stimulate ascites formation by increasing vascular permeability. We examined the role of VEGF in ovarian carcinoma using *in vivo* models in which intraperitoneal or subcutaneous tumors were induced in immunodeficient mice using the human ovarian carcinoma cell line SKOV-3. After tumor engraftment (7 to 10 days), some mice were treated with a function-blocking VEGF antibody (A4.6.1) specific for human VEGF. A4.6.1 significantly ($P < 0.05$) inhibited subcutaneous SKOV-3 tumor growth compared with controls. However, tumor growth resumed when A4.6.1 treatment was discontinued. In mice bearing intraperitoneal tumors (IP mice), ascites production and intraperitoneal carcinomatosis were detected 3 to 7 weeks after SKOV-3 inoculation. Importantly, A4.6.1 completely inhibited ascites production in IP mice, although it only partially inhibited intraperitoneal tumor growth. Tumor burden was variable in A4.6.1-treated IP mice; some had minimal tumor, whereas in others tumor burden was similar to that of controls. When A4.6.1 treatment was stopped, IP mice rapidly (within 2 weeks) developed ascites and became cachectic. These data suggest that in ovarian cancer, tumor-derived VEGF is obligatory for ascites formation but not for intraperitoneal tumor growth. Neutralization of VEGF activity may have clinical application in inhibiting malignant ascites formation in ovarian cancer. ***(Am J Pathol 1998, 153:1249–1256)***

Angiogenesis, the development of new blood vessels from existing vasculature, is an essential component of solid tumor growth and metastasis.[1–5] It is now generally accepted that solid tumor growth must be accompanied by angiogenesis to provide the vascular support essential for the expanding tumor mass. Several angiogenic factors are expressed by many tumors, suggesting that tumors promote their own vascularization by activating the host endothelium. The importance of angiogenesis in tumor progression is indicated by studies showing that the angiogenic potential of tumors, assessed by tumor microvessel density, directly correlates with poor prognosis.[6–11] However, the mechanism of solid tumor angiogenesis at the molecular level is not well understood, and the relative importance of specific angiogenic factors in mediating vasculogenesis in specific malignancies is not well defined.

One angiogenic factor that is thought to play a key role in the vascularization of normal and neoplastic tissue is vascular endothelial growth factor (VEGF), also known as vascular permeability factor. VEGF is a potent and specific mitogen for endothelial cells,[12–17] stimulates the full cascade of events required for angiogenesis *in vitro* and *in vivo*,[17,18] and markedly augments the permeability of existing microvasculatature.[19–21] VEGF is expressed in many animal and human malignancies and by most transformed cells lines.[21–41] The effect of VEGF on vascular permeability is believed to be crucial for malignant ascites formation.[19,42,43] The actions of VEGF are mediated by at least two cell surface receptors, flt-1 and KDR.[44,45] The central role of VEGF in tumor growth has been demonstrated in studies using animal models in which tumor growth and vascularization *in vivo* were inhibited if VEGF activity was neutralized by function-blocking antibodies[46] or expression of antisense VEGF mRNA,[47] or if signaling was disrupted by dominant-negative mutation of the KDR receptor.[48]

Presented in part at the 43rd Annual Meeting of the Society for Gynecological Investigation, San Diego, CA, 1997.

Supported in part by National Institutes of Health grant PO1 CA64602.

SM's present address is Maternal Health Research Centre, Endocrine Unit, John Hunter Hospital, Newcastle, New South Wales, Australia.

Accepted for publication June 26, 1998.

Address reprint requests to Dr. Robert B. Jaffe, Reproductive Endocrinology Center, University of California, San Francisco, Box 0556, 505 Parnassus Ave., San Francisco, CA 94143-0556. E-mail: robert_jaffe@quickmail.ucsf.edu.

Ovarian cancer is characterized by widespread intraperitoneal carcinomatosis and the formation of large volumes of ascitic fluid.[49] VEGF may play a major role in the progression of ovarian cancer by influencing tumor growth through its promotion of tumor angiogenesis and ascites production through its stimulation of vascular permeability. Although VEGF has been detected in ovarian cancer,[26,37,50,51] so, too, have most other known angiogenic factors[37,52–59]; therefore, the role of VEGF as a regulator of angiogenesis in ovarian cancer growth is unclear. However, several studies have indicated that VEGF-regulated angiogenesis is an important component of ovarian cancer growth. Microvessel density and the level of VEGF expression in ovarian cancer directly correlate with poor prognosis, suggesting that angiogenesis, possibly mediated at least in part by VEGF, influences disease progression.[26,50,51] In a murine model of ovarian cancer, the drug FR118487, which inhibits angiogenesis by inhibiting basic fibroblast growth factor and VEGF activities,[60] suppressed the *in vivo* growth and metastasis of a murine ovarian cancer cell line.[61] In the present study, we directly assessed the role of VEGF in the growth and progression of ovarian cancer. To that end, we used the human ovarian carcinoma cell line SKOV-3 to develop an *in vivo* model of ovarian cancer in immunodeficient mice that recapitulated the intraperitoneal carcinomatosis and ascites production seen in women with this disease. We then used a function-blocking monoclonal antibody, which blocks access of VEGF to both the flt-1 and KDR receptors, to specifically inhibit tumor-derived VEGF activity and assessed the consequences on tumor growth, ascites formation, and disease progression.

Materials and Methods

Materials

A mouse monoclonal antibody (A4.6.1) directed against human VEGF was used to neutralize VEGF activity *in vivo*. Characterization of this antibody, including its high specificity toward human VEGF and its ability to inhibit VEGF activity *in vitro* and *in vivo*, as well as to block binding of VEGF to its receptors *in vivo*, has been described previously.[48,62] The antibody does not inhibit the activity of mouse VEGF (unpublished data). The human ovarian cystadenocarcinoma cell line, SKOV-3, was obtained from the American Type Culture Collection (Manassas, VA). One-month-old female immunodeficient mice (BALB/c nu/nu) were obtained from Simonsen Laboratories (Gilroy, CA), housed in isolated conditions, and fed autoclaved standard pellets and water. All protocols involving immunodeficient mice were approved by the Committee on Animal Care, University of California, San Francisco.

Cell Culture

The SKOV-3 cells were cultured in Dulbecco's modified Eagle's medium H-21 containing 10% fetal calf serum, glucose (4.5 g/L), penicillin G (100 U/ml), streptomycin (2.5 μg/ml), glutamine (2 mmol/L), and fungizone (2.5 μg/ml). All cell culture reagents were obtained from the Cell Culture Facility, University of California, San Francisco. Before *in vivo* inoculation, SKOV-3 cells were grown to confluence, harvested by trypsinization, and resuspended in Ca^{2+}/Mg^{2+}-free phosphate buffered saline (PBS). In preliminary studies, we determined that SKOV-3 cells express VEGF *in vivo* and *in vitro* using reverse transcription-polymerase chain reaction and immunocytochemistry, respectively, and that A4.6.1 does not affect their proliferation *in vitro* (data not shown).

In Vivo *Inoculation of SKOV3 Cells*

The SKOV-3 cells were prepared for inoculation as described above and injected as a bolus either into the peritoneum (IP group; $n = 31$; 10×10^6 cells per mouse in 200 μl of PBS) or into the dorsal subcutaneous tissue (SC group; $n = 8$; 5 to 10×10^6 cells in 50 μl of PBS) of athymic mice. Some SC mice received two boluses of SKOV-3 cells, one in each flank. Seven to 10 days after SKOV-3 inoculation, some of the mice (IP group, $n = 16$; SC group, $n = 5$) were treated with A4.6.1 (100 μg in 0.1 ml of PBS, intraperitoneally, twice per week), and the rest were treated with the same volume of vehicle. A4.6.1 treatment was delayed to ensure that tumor engraftment was not inhibited. The size of subcutaneous tumors was measured twice weekly using calipers fitted with a Vernier scale. For each tumor, two perpendicular measurements were obtained from which an estimate of tumor radius was derived. Tumor volume was then calculated based on the assumption that tumors were spherical. At the end of the experimental period, mice were killed by anesthetic overdose. At autopsy, SKOV-3 tumors were excised, fixed in 4% paraformaldehyde/100 mmol/L PBS, pH 7.4, at 4°C for 24 hours, and embedded in paraffin. Paraffin sections (10 μm) were used for histochemical analysis.

Statistics

Data were analyzed using the unpaired Student's t-test for statistical comparison between groups. Differences between groups were considered statistically significant at $P < 0.05$. Experiments were performed in triplicate.

Results

Experimental Model of Human Ovarian Cancer

All IP mice receiving PBS treatment (ie, control mice) developed a swollen abdomen, indicative of ascites formation and intraperitoneal carcinomatosis, within 3 to 6 weeks of SKOV-3 administration. Soon after (within 5 to 7 days) the appearance of abdominal swelling, PBS-treated IP mice became cachectic and as a consequence were euthanized in accordance with the animal care protocol. The intraperitoneal carcinomatosis in the IP mice closely resembled peritoneal metastases from

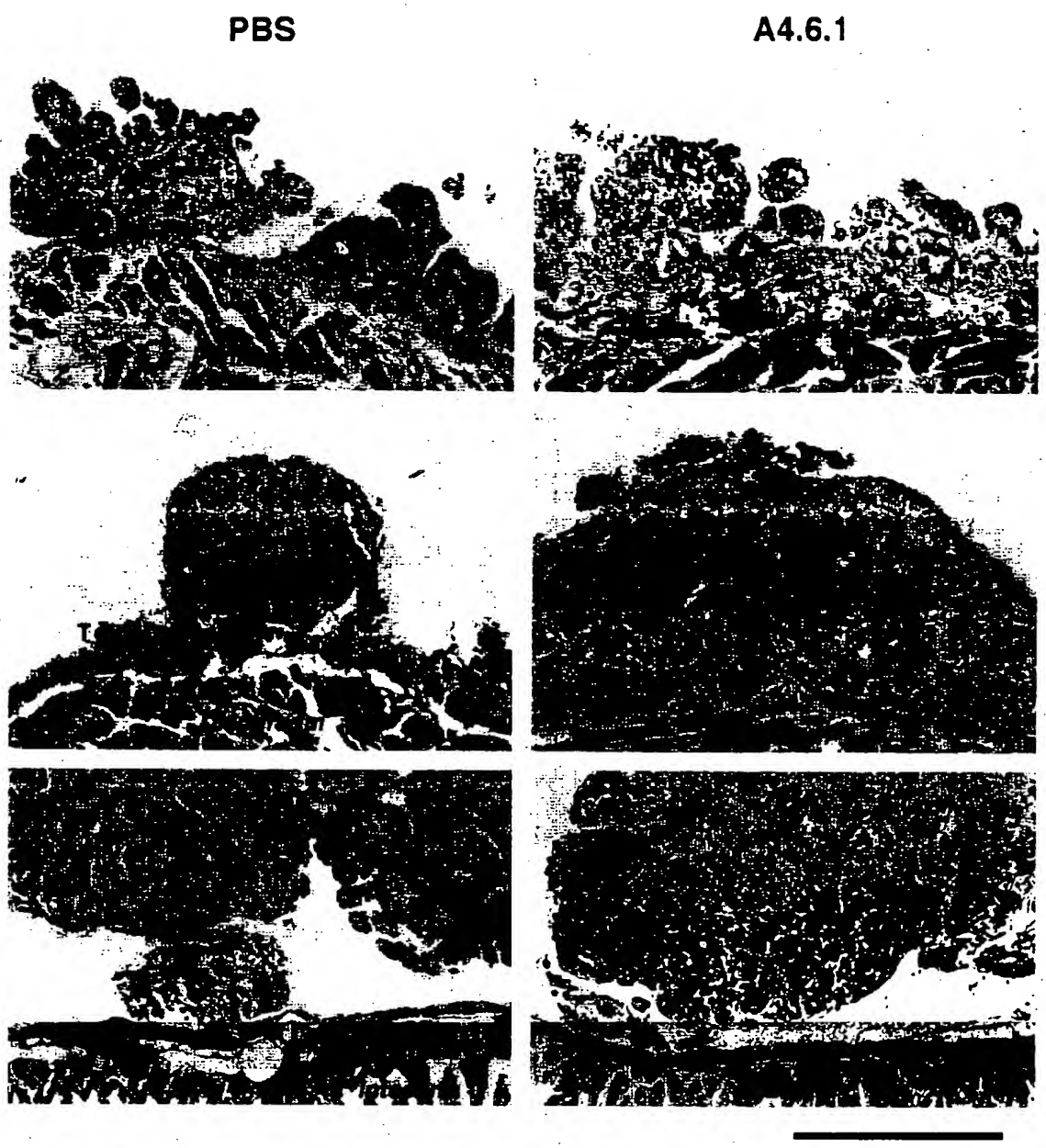

Figure 1. Histological appearance of intraperitoneal SKOV-3 tumors (T) derived from PBS-treated and antibody-treated (A4.6.1) mice approximately 5 weeks after intraperitoneal cell inoculation. H&E staining of 10-μm paraffin sections. Bar = 500 μm.

poorly differentiated stage III papillary serous ovarian cancer.[63] The neoplasms were characterized by trabecular and solid patterns of growth with variable degrees of cytological atypia. Numerous mitotic figures were identified, and papillary growth was common on the luminal side. In most tumors, desmoplastic stroma typical of ovarian cancer metastases was seen. Tumors were found on the surfaces of the peritoneum, diaphragm, intestines (Figure 1), uterus and associated fat, and stomach. Tumors were rarely found on the liver or spleen, and there was no evidence of visible metastasis to organs outside of the peritoneum. In general, the tumors did not invade the host tissue to which they were adherent; however, some focal invasion into muscle was seen. Extensive tumor growth was detected in the uterine fat, and foci of tumor were observed in the uterine lymphatics. The sites and extent of the peritoneal carcinomatosis and the production of ascitic fluid induced by intraperitoneal administration of SKOV-3 cells in immunodeficient mice were similar to those seen in women with ovarian epithelial cancer.

Role of VEGF in SKOV-3 Tumor Growth

To examine directly the role of tumor-derived VEGF in SKOV-3 tumor growth, we established an *in vivo* model in which SKOV-3 tumors were grown subcutaneously

in immunodeficient mice. Well defined subcutaneous tumors developed within 7 days of SKOV-3 inoculation and were of sufficient size to permit accurate measurement. Tumor growth was rapid, and within 3 weeks the subcutaneous foci were 5 to 10 mm in diameter and began to exhibit vascular islands that eventually formed blood-filled cysts. By 6 weeks, the largest tumors were approximately 20 mm in diameter and contained numerous cysts that eventually ruptured. At this stage of tumor progression, the mice were killed.

To assess the role of VEGF in tumor growth, some SC mice (n = 5 mice; 11 tumors) were treated with A4.6.1. Control mice (n = 3 mice; 6 tumors) were treated with PBS. In preliminary studies, we found that treatment with a nonspecific antibody of the same IgG type had no effect on tumor growth and was essentially equivalent to vehicle alone (data not shown). A4.6.1 significantly inhibited the growth of subcutaneous SKOV-3 tumors within 2 weeks of treatment (Figure 2); tumor size did not progress beyond the size attained at the initiation of A4.6.1 treatment and the tumors did not form cysts. After cessation of A4.6.1 treatment (Figure 2B), tumor growth resumed, and within 2 weeks the tumors developed blood-filled cysts and the mice had to be killed. In preliminary studies in which fewer cells were used for subcutaneous inoculation, after discontinuance of A4.6.1 treatment, tumor growth resumed and within 3 weeks the rate of growth paralleled that of controls. Tumor growth also was inhibited when A4.6.1 was administered late in tumor progression (30 days) (Figure 2B). Interestingly, in these tumors A4.6.1 appeared to deplete the contents of the cysts; their volume was markedly reduced, and some cysts involuted without rupture. In addition, tumors lost their red coloration and became more skin toned in appearance.

There was no evidence that A4.6.1 induced an antibody-dependent cellular cytotoxicity or a macrophage-mediated response that could have inhibited tumor growth. Histological examination of growth-inhibited subcutaneous tumors failed to demonstrate any significant inflammatory response (data not shown).

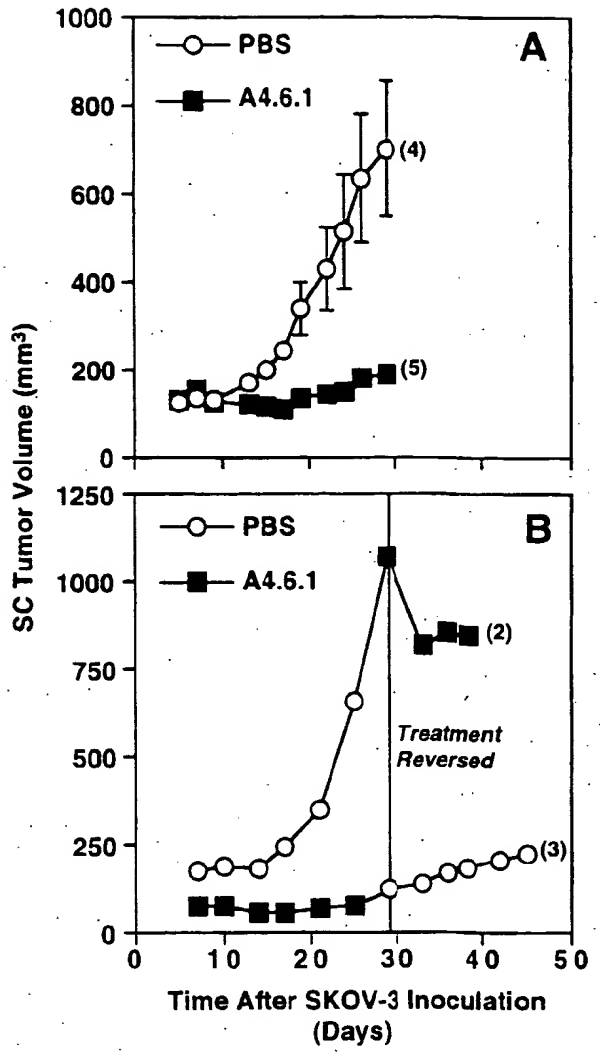

Figure 2. Effect of neutralization of tumor-derived VEGF activity on the growth of subcutaneous SKOV-3 tumors. Mice were treated with either PBS or antibody (A4.6.1, 100 μg) intraperitionally twice weekly for approximately 4 weeks. In A, all mice were killed at 30 days. In B, treatments were reversed at day 29. Numbers in parentheses represent the number of tumors analyzed in each group.

Role of VEGF in Intraperitoneal Tumor Growth

Studies of subcutaneous SKOV-3 tumor growth established the pivotal role of VEGF in tumor progression. However, as ovarian cancer is not a subcutaneous malignancy, we studied the effects of A4.6.1 treatment on the growth and progression of intraperitoneal SKOV-3 tumors. IP mice were treated with A4.6.1 (n = 16) or PBS (n = 15) in an identical fashion to those bearing subcutaneous tumors. However, intraperitoneal tumor growth could not be monitored directly and, because of its spread within the abdomen, could not be quantified accurately. Therefore, intraperitoneal tumor burden was assessed qualitatively at postmortem examination. In all animals, treatment was initiated 8 days after SKOV-3 inoculation and continued for various times.

In experiment 1 (Figure 3A), all animals were killed 21 days after SKOV-3 inoculation. At postmortem examination, two of the three PBS-treated animals exhibited abdominal swelling with a moderate level of ascites and had moderate and easily detectable intraperitoneal tumor burden. The remaining PBS-treated animal had no detectable abdominal swelling or ascites and only a mild tumor burden. None of the A4.6.1-treated IP animals showed signs of ascites formation or cachexia at the time of postmortem examination, and intraperitoneal SKOV-3 tumor burden was barely detectable. Interestingly, A4.6.1 inhibited the growth of small subcutaneous tumors at the site of SKOV-3 injection that developed in some IP animals.

In experiment 2 (Figure 3B), the effects of prolonged A4.6.1 treatment (n = 6) were examined. All of the PBS-treated animals (n = 6) displayed signs of ascites formation and cachexia at various times after SKOV-3 inoculation; the first PBS-treated animal was killed at 4.5 weeks

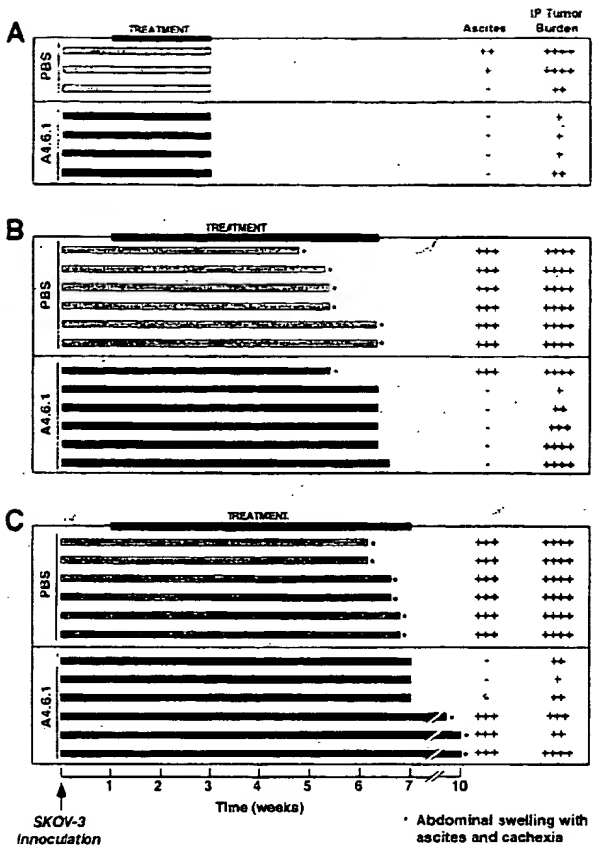

Figure 3. Effect of neutralization of tumor-derived VEGF on intraperitoneal SKOV-3 tumor development and ascites production in mice inoculated intraperitoneally with SKOV-3 cells. Shown are outcomes for individual animals in three separate experiments. Tumor burden was assessed qualitatively as follows: ++++, High, many clusters of large (5 to 10 mm in diameter) solid tumors easily visible in the peritoneal cavity; +++, Moderate, clusters of tumors (3 to 5 mm in diameter) readily visible but spread not as extensive as High; ++, Low, large tumors not apparent but small foci visible on peritoneum, omentum, uterine fat pads, and diaphragm; +, Scare, only small foci seen on peritoneum, omentum, and diaphragm. Extent of ascites production also was determined qualitatively as follows: +++, High, marked abdominal swelling with 5 to 10 ml of bloody ascites; ++, Moderate, distinct abdominal swelling with 3 to 5 ml of clear ascites; +, Low, no abdominal swelling, small volume of clear ascitic fluid detected at postmortem examination; −, No ascites detected.

and the last at 6.5 weeks because of severe cachexia associated with the developing ascites. One A4.6.1-treated animal exhibited ascites and cachexia and therefore was killed at 5.5 weeks. This mouse had a high tumor burden. Four of the A4.6.1-treated animals were killed at 6.5 weeks. The remaining A4.6.1-treated IP mouse was killed the following day. Five of the six A4.6.1-treated IP animals appeared normal at the time of postmortem examination, and no ascites formation could be detected. In A4.6.1-treated mice, intraperitoneal tumor burden was variable: in three of the six animals it was high and comparable with tumor burden in those mice receiving PBS alone, whereas in the other IP animals tumor burden ranged from moderate to scarce. The reason for the apparent lack of response in the one A4.6.1-treated mouse is uncertain.

In experiment 3 (Figure 3C), A4.6.1 treatment was stopped after the last PBS-treated animal was killed (approximately 7 weeks after SKOV-3 inoculation). At that time, three of the six A4.6.1-treated animals were killed. As with experiment 2, all of the PBS-treated animals exhibited abdominal swelling and became cachectic approximately 6 weeks after receiving SKOV-3 cells. All of these animals had severe ascites and a high intraperitoneal tumor burden. In contrast, the three A4.6.1-treated animals killed at 6.5 weeks had no detectable ascites and a variable, but clearly detectable, tumor burden. Importantly, within 2 to 3 weeks of cessation of A4.6.1 treatment, the remaining mice developed severe ascites, became cachectic, and had to be killed. The tumor burden in these animals varied from moderate to high.

Discussion

Ovarian cancer is a disease that begins in, and usually is limited to, the peritoneal cavity. The majority of women with ovarian cancer present with peritoneal carcinomatosis, the principal cause of morbidity and mortality. Ovarian cancer also is associated with malignant ascites formation; in most cases the first indication of ovarian cancer is swelling of the abdomen due to the accumulation of ascitic fluid.[63] VEGF is thought to play a major role in the progression of ovarian cancer by promoting the neovascularization and subsequent growth of solid intraperitoneal tumors and by inducing ascites formation by increasing the permeability of the tumor vasculature. Several studies have shown that VEGF is expressed by human ovarian carcinoma cells and that the level of expression directly correlates with poor prognosis. However, as ovarian carcinoma cells also express other angiogenic factors, the specific role of VEGF in the growth and progression of ovarian cancer is unclear. Therefore, the present study was conducted to determine the role of VEGF in the regulation of ovarian cancer growth and ascites formation.

We used the human cell line SKOV-3, derived from a human ovarian serous cystadenocarcinoma, which accounts for 40 to 50% of all ovarian epithelial cancers, to induce peritoneal carcinomatosis and ascites production in immunodeficient mice. This model closely mimicked human ovarian cancer in that: 1) carcinomatosis was confined to the peritoneum; 2) the progression of the disease involved ascites formation and cachexia (IP mice were asymptomatic until they began to develop ascites, which always was associated with a heavy intraperitoneal tumor burden); 3) the morphology of intraperitoneal SKOV-3 tumors closely resembled peritoneal metastases from poorly differentiated stage III ovarian cancer in women; and 4) in preliminary studies, we confirmed that SKOV-3 tumors, like human ovarian carcinomas, express VEGF.

To examine the role of VEGF in ovarian cancer, we specifically ablated tumor-derived VEGF activity in IP mice using the function-blocking antibody, A4.6.1. This neutralizing antibody, which blocks access of VEGF to both VEGF receptors, inhibits the activity of human, but not mouse, VEGF and therefore specifically blocks the activity of tumor-derived VEGF. The effects of A4.6.1 on

SKOV-3 tumor development were first examined using the subcutaneous model in which tumor growth could be monitored directly. We found that A4.6.1 was tumoristatic for SKOV-3 tumors grown subcutaneously: tumors failed to grow beyond the size attained at the beginning of the A4.6.1 treatment. However, when A4.6.1 treatment was stopped, the growth of subcutaneous tumors resumed. This observation is consistent with the concept that VEGF regulates, and is essential for, tumor neovascularization. Tumors could not grow further, because they could not stimulate the necessary vascularization to support a greater tumor mass. However, the existing vasculature likely was not affected by A4.6.1 treatment and therefore remained sufficient to maintain tumor size. Interestingly, when A4.6.1 was administered to SC mice bearing advanced tumors (10 to 15 mm in diameter with blood-filled cysts), tumor growth was inhibited and cysts regressed and involuted without rupturing. The regression of blood-filled cysts in response to VEGF inhibition suggests that tumor cyst formation is influenced by VEGF. This observation is consistent with the increase of vascular permeability caused by VEGF and suggests that VEGF may induce cyst formation by augmenting microvessel permeability. These data clearly demonstrated that tumor-derived VEGF is a necessary component of subcutaneous SKOV-3 tumor growth. However, ovarian cancer is not a subcutaneous disease but instead usually is limited to the peritoneal cavity. Therefore, we performed similar experiments using the intraperitoneal model.

In IP mice, inhibition of tumor-derived VEGF activity by A4.6.1 prolonged life and completely inhibited ascites formation. However, unlike its consistent tumoristatic action in SC mice, A4.6.1 only partially inhibited SKOV-3 tumor growth in IP mice. In some A4.6.1-treated IP mice, the extent of intraperitoneal tumor burden was similar to that of PBS-treated animals, whereas in others it was minimal. The reason that tumor-derived VEGF was obligatory for subcutaneous, but not intraperitoneal, SKOV-3 tumor growth is unclear. The peritoneal cavity offers a markedly different environment for tumor growth and spread than does the subcutaneous space. Within the peritoneum, SKOV-3 cells are not confined, as they are when administered as a subcutaneous bolus. Consequently, subcutaneous tumors grew only as a spherical mass under the skin, whereas in the peritoneum, tumors grew as thin sheets over a relatively large surface area with the occasional formation of solid tumor foci extending into the peritoneal cavity. With this mode of tumor growth and spread, it is likely that dependency on angiogenesis would be minimal, as the thin layers of tumor and some of the tumor buds would be small enough to survive by passive diffusion of nutrients from the underlying host vasculature and the surrounding peritoneal fluid. However, neovascularization clearly occurred in some intraperitoneal tumors, particularly the large solid tumors that formed on the pelvic organs. Thus, intraperitoneal carcinomatosis appears to have angiogenesis-independent and -dependent components; ie, formation and growth of the thin layers of tumor and some of the smaller solid buds would be independent of angiogenesis and be maintained by the pre-existing vasculature, whereas the larger solid intraperitoneal tumors would require neovascularization for continued growth. If this concept is correct, then inhibition of angiogenesis would only inhibit the development and growth of the larger intraperitoneal tumors. Consistent with this notion, we found that A4.6.1 did not inhibit the formation of tumor sheets on peritoneal surfaces or the formation of small solid tumor foci. However, large and presumably angiogenesis-dependent SKOV-3 tumors were detected in some A4.6.1-treated mice. It is unlikely that the dose of A4.6.1 was insufficient to inhibit SKOV-3 activity by intraperitoneal tumors, as the same dose was sufficient to act systemically and completely inhibit subcutaneous SKOV-3 tumor growth in SC mice. Furthermore, in some IP mice it was sufficient to inhibit the growth of a subcutaneous tumor that developed at the site of SKOV-3 inoculation. This indicates that VEGF-regulated angiogenesis may not be an essential factor in the growth of intraperitoneal carcinomatosis. Indeed, it is possible that other angiogenic factors, many of which have been detected in ovarian carcinoma cells, may have compensated for the lack of VEGF or may play a more prominent role in the control of intraperitoneal tumor angiogenesis. However, it is difficult to reconcile this possibility with an explanation of why such factors would not have supported angiogenesis in the subcutaneous model. It appears that the role of VEGF in tumor growth may be influenced by the site of tumor engraftment.

A4.6.1 completely inhibited ascites formation in IP mice, even though some animals had a tumor burden that was similar to that of controls that developed ascites and cachexia. When A4.6.1 treatment was stopped, IP mice rapidly developed ascites and became cachectic. VEGF is a potent stimulator of vascular permeability and is thought to play a major role in the development of malignant ascites.[43] Our data support the hypothesis that ascites formation in ovarian cancer is regulated by tumor-derived VEGF via the augmentation of tumor microvessel permeability. Ascites formation, as indicated by abdominal swelling, only became apparent relatively late in disease progression when tumor burden was high. It is possible that ascites was produced earlier; however, its rate of production was likely less than its rate of clearance from the peritoneal cavity. As tumor burden increased, the rate of ascites production likely became greater than the capacity for clearance and resulted in ascites accumulation and abdominal swelling with associated cachexia. Interestingly, in the SC mice, A4.6.1 reduced the volume of existing tumor cysts, suggesting that A4.6.1 could possibly reverse ascites accumulation if administered to IP mice exhibiting abdominal swelling. This possibility has important clinical implications, as it suggests that inhibition of VEGF activity may reverse the accumulation of ascitic fluid in women with ovarian cancer, which could significantly contribute to treatment of the disease. In summary, these data suggest that tumor-derived VEGF is not an essential regulator of peritoneal ovarian cancer growth but plays a pivotal role in malignant ascites formation likely by increasing vascular permeability.

Acknowledgments

We thank Janet Lee, Paul Goldsmith, Evelyn Garrett, Sharon Lojun, and Charles Zaloudek for their invaluable assistance.

References

1. Folkman J, Watson K, Ingber D, Hanahan D: Induction of angiogenesis during the transition from hyperplasia to neoplasia. Nature 1989, 339:58–61
2. Liotta LA, Kleinerman J, Saidel GM: Quantitative relationships of intravascular tumor cells, tumor vessels, and pulmonary metastases following tumor implantation. Cancer Res 1974, 4:997–1004
3. Weidner N, Semple JP, Welch WR, Folkman J: Tumor angiogenesis and metastasis: correlation in invasive breast carcinoma. N Engl J Med 1991, 324:1–8
4. Folkman J, Klagsbrun M: Vascular physiology: a family of angiogenic peptides. Nature 1987, 329:671–672
5. Folkman J: What is the evidence that tumors are angiogenesis dependent? J Natl Cancer Inst 1990, 82:4–6
6. Weidner N, Carroll PR, Flax J, Blumenfeld W, Folkman J: Tumor angiogenesis correlates with metastasis in invasive prostate carcinoma. Am J Pathol 1993, 143:401–409
7. Olivarez D, Ulbright T, DeRiese W, Foster R, Reister T, Einhorn L, Sledge G: Neovascularization in clinical stage A testicular germ cell tumor: prediction of metastatic disease. Cancer Res 1994, 54:2800–2082
8. Maeda K, Chung YS, Takatsuka S, Ogawa Y, Sawada T, Yamashita Y, Onoda N, Kato Y, Nitta A, Arimoto Y, Kondo Y, Sawa M: Tumor angiogenesis as a predictor of recurrence in gastric carcinoma. J Clin Oncol 1995, 13:477–481
9. Macchiarini P, Fontaini G, Hardin MJ, Squartini F, Angeletti CA: Relation of neovascularization to metastasis in non-small cell lung cancer. Lancet 1992, 340:145–146
10. Hollingsworth HC, Kohn EC, Steinberg SM, Rothenberg ML, Merino MJ: Tumor angiogenesis in advanced stage ovarian carcinoma. Am J Pathol 1995, 147:33–41
11. van Diest PJ, Zevering JP, Zevering LC, Baak JP: Prognostic value of microvessel quantitation in cisplatin treated FIGO 3 and 4 ovarian cancer patients. Pathol Res Pract 1995, 191:25–30
12. Conn G, Bayne ML, Soderman DD, Kwok PW, Sullivan KA, Palisi TM, Hope DA, Thomas KA: Amino acid and cDNA sequence of a vascular endothelial cell mitogen that is homologous to platelet-derived growth factor. Proc Natl Acad Sci USA 1990, 87:2628–2632
13. Connolly DT, Heuvelman DM, Nelson R, Olander JV, Eppley BL, Delfino JJ, Siegel NR, Leimgruber RM, Feder J: Tumor vascular permeability factor stimulates endothelial cell growth and angiogenesis. J Clin Invest 1989, 84:1470–1478
14. Ferrara N, Henzel WJ: Pituitary follicular cells secrete a novel heparin-binding growth factor specific for vascular endothelial cells. Biochem Biophys Res Commun 1989, 161:851–858
15. Gospodarowicz D, Abraham JA, Schilling J: Isolation and characterization of a vascular endothelial cell mitogen produced by pituitary-derived folliculostellate cells. Proc Natl Acad Sci USA 1989, 86:7311–7315
16. Keck PJ, Hauser SD, Krivi G, Sanzo K, Warren T, Feder J, Connolly DT: Vascular permeability factor, an endothelial cell mitogen related to PDGF. Science 1989, 246:1309–1312
17. Leung DW, Cachiane G, Kuang WJ, Goeddel DV, Ferrara N: Vascular endothelial growth factor s a secreted angiogenic mitogen. Science 1989, 246:1306–1309
18. Ferrara N, Jakeman L, Houck K, Leung DW: Molecular and biological properties of the vascular endothelial growth factor family of proteins Endocr Rev 1992, 13:18–32
19. Senger DR, Van de Water L, Brown LF, Nagy JA, Yeo KT, Yeo TK, Berse B, Jackman RW, Dvorak AM, Dvorak HF: Vascular permeability factor (VPF, VEGF) in tumor biology. Cancer Metastasis Rev 1993, 12:303–324
20. Dvorak HF, Sioussat TM, Brown LF, Berse B, Nagy JA, Sotrel A, Manseau EJ, Van de Water L, Senger DR: Distribution of vascular permeability factor (vascular endothelial growth factor) in tumors: concentration in tumor blood vessels. J Exp Med 1991, 174:1275–1278
21. Dvorak HF, Brown LF, Detmar M, Dvorak AM: Vascular permeability factor/vascular endothelial growth factor, microvascular hyperpermeability, and angiogenesis. Am J Pathol 1995, 146:1029–1039
22. Conn G, Soderman DD, Schaeffer MT, Wile M, Hatcher VB, Thomas KA: Purification of a glycoprotein vascular endothelial cell mitogen from rat glioma-derived cell line. Proc Natl Acad Sci USA 1990, 87:1323–1327
23. Weindel K, Marme D, Weich H: AIDS-associated Kaposi's sarcoma cells in culture express vascular endothelial growth factor. Biochem Biophys Res Commun 1992, 183:1167–1174
24. Weindel K, Moringlane J, Marme D, Weich H: Detection and quantification of vascular endothelial growth factor/vascular permeability factor in brain tumor tissue and cyst fluid: the key to angiogenesis? Neurosurgery 1994, 35:439–448
25. Berse B, Brown LF, Van de Water L, Dvorak HF, Senger DR: Vascular permeability factor (vascular endothelial growth factor) gene is expressed differentially in normal tissues, macrophages, and tumors. Mol Biol Cell 1992, 3:211–220
26. Boocock CA, Charnock-Jones S, Sharkey AM, McLaren J, Baker PJ, Wright KA, Twentyman PR, Smith SK: Expression of vascular endothelial growth factor and its receptors flt and KDR in ovarian carcinoma. J Natl Cancer Inst 1995, 87:506–516
27. Brown LF, Berse B, Jackman RW, Tognazzi K, Guidi AJ, Dvorak HF, Senger DR, Connolly JL, Schnitt SJ: Expression of vascular permeability factor (vascular endothelial growth factor) and its receptors in breast cancer. Hum Pathol 1995, 26:86–9
28. Brown LF, Berse B, Jackman RW, Tognazzi K, Manseau EJ, Senger DR, Dvorak HF: Expression of vascular permeability factor (vascular endothelial growth factor) and its receptors in adenocarcinomas of the gastrointestinal tract. Cancer Res 1995, 53:4727–4735
29. Brown LF, Berse B, Jackman RW, Tognazzi K, Manseau EJ, Dvorak HF, Senger DR: Increased expression of vascular permeability factor (vascular endothelial growth factor) and its receptors in kidney and bladder carcinomas. Am J Pathol 1993, 143:1255–1262
30. Detmar M, Brown LF, Claffey KP, Yeo KT, Kocher O, Jackman RW, Berse B, Dvorak HF: Overexpression of vascular permeability factor/vascular endothelial growth factor and its receptors in psoriasis. J Exp Med 1994, 180:1141–1146
31. Guidi AJ, Abu-Jawdeh G, Berse B, Jackman RW, Tognazzi K, Dvorak HF, Brown LF: Angiogenesis and vascular permeability factor (vascular endothelial growth factor) expression in cervical neoplasia. J Natl Cancer Inst 1995, 87:1237–1245
32. Guidi AJ, Abu-Jawdeh G, Tognazzi K, Dvorak HF, Brown LF: Expression of vascular permeability factor (vascular endothelial growth factor) and its receptors in endometrial carcinoma. Cancer 1996, 78:454–460
33. Plate KH, Breier G, Weich HA, Risau W: Vascular endothelial growth factor is a potential tumour angiogenesis factor in human gliomas in vivo. Nature 1992, 359:845–848
34. Senger DR, Galli SJ, Dvorak AM, Perruzzi CA, Harvey VS, Dvorak HF: Tumor cells secrete a vascular permeability factor that promotes accumulation of ascites fluid. Science 1983, 279:983–985
35. Senger DR, Perruzzi CA, Feder J, Dvorak HF: A highly conserved vascular permeability factor secreted by a variety of human and rodent tumor cell lines. Cancer Res 1986, 46:5629–5632
36. Yeo K-T, Wang HH, Nagy JA, Sioussat TM, Ledbetter SR, Hoogewerf AJ, Zhou Y, Masse EM, Senger DR, Dvorak HF, Yeo T-K: Vascular permeability factor (vascular endothelial growth factor) in guinea pig and human tumor and inflammatory effusions. Cancer Res 1993, 53:2912–2918
37. Olson TA, Mohanraj D, Carson LF, Ramakrishnan S: Vascular permeability factor gene expression in normal and neoplastic human ovaries. Cancer Res 1994, 54:276–280
38. Takeshita S, Zheng LP, Brogi E, Kearney M, Pu LQ, Bunting S, Ferrara N, Symes JF, Isner JM: Therapeutic angiogenesis: a single intraarterial bolus of vascular endothelial growth factor augments revascularization in a rabbit ischemic hind limb model. J Clin Invest 1994, 93:662–670
39. Alvarez JA, Baird A, Tatum A, Daucher J, Chorsky R, Gonzalez AM, Stopa EG: Localization of basic fibroblast growth factor and vascular

endothelial growth factor in human glial neoplasms. Mod Pathol 1992, 5:303–307
40. Doldi N, Origoni M, Bassan M, Ferrari D, Rossi M, Ferrari A: Vascular endothelial growth factor: expression in human vulvar neoplastic and nonneoplastic tissues. J Reprod Med 1996, 41:844–848
41. Doldi N, Bassan M, Guisano M, Broccoli V, Boncinelli E, Ferrari A: Vascular endothelial growth factor messenger ribonucleic acid expression in human ovarian and endometrial cancer. Gynecol Endocrinol 1996, 10:375–382
42. Sioussat TM, Dvorak HF, Brock TA, Senger DR: Inhibition of vascular permeability factor (vascular endothelial growth factor) with antipeptide antibodies. Arch Biochem Biophys 1993, 301:15–20
43. Nagy JA, Masse EM, Herzberg KT, Meyers MS, Yeo KT, Yeo TK, Sioussat TM, Dvorak HF: Pathogenesis of ascites tumor growth: vascular permeability factor, vascular hyperpermeability, and ascites fluid accumulation. Cancer Res 1995, 55:360–368
44. Terman BI, Carrion ME, Kovacs E, Rasmussen BA, Eddy RL, Shows TB: Identification of a new endothelial cell growth factor receptor tyrosine kinase. Oncogene 1991, 6:1677–1683
45. de Vries C, Escobedo JA, Ueno H, Houck K, Ferrara N, Williams LT: The fms-like tyrosine kinase, a receptor for vascular endothelial growth factor. Science 1992, 255:989–991
46. Kim KJ, Li B, Winer J, Armanini M, Gillet N, Phillips HS, Ferrara N: Inhibition of vascular endothelial growth factor-induced angiogenesis suppresses tumour growth in vivo. Nature 1993, 362:841–844
47. Claffey KP, Brown LF, del Aguila LF, Tognazzi K, Yeo KT, Manseau EJ, Dvorak HF: Expression of vascular permeability factor/vascular endothelial growth factor by melanoma cells increases tumor growth, angiogenesis, and experimental metastasis. Cancer Res 1996, 56: 172–181
48. Millauer B, Shawver LK, Plate KH, Risau W, Ullrich A: Glioblastoma growth inhibited in vivo by a dominant-negative Flk-1 mutant. Nature 1994, 367:576–579
49. Perez RP, Godwin AK, Hamilton TC, Ozols RF: Ovarian cancer biology. Semin Oncol 1991 18:186–204
50. Abu-Jawdeh GM, Faix JD, Niloff J, Tognazzi K, Manseau E, Dvorak HF, Brown LF: Strong expression of vascular permeability factor (vascular endothelial growth factor) and its receptors in ovarian borderline and malignant neoplasms. Lab Invest 1996, 74:1105–1115
51. Paley PJ, Staskus KA, Gebhard K, Mohanraj D, Twiggs LB, Carson LF, Ramakrishnan S: Vascular endothelial growth factor expression in early stage ovarian carcinoma. Cancer 1997, 80:98–106
52. Kutteh WH, Kutteh CC: Quantitation of tumor necrosis factor-alpha, interleukin-1 beta, and interleukin-6 in the effusions of ovarian epithelial neoplasms. Am J Obstet Gynecol 1992, 167:1864–1869
53. Stromberg K, Johnson GR, O'Connor DM, Sorensen CM, Gullick WJ, Kannan B: Frequent immunohistochemical detection of EGF supergene family members in ovarian carcinogenesis. Int J Gynecol Pathol 1994, 13:342–347
54. Kurachi H, Morishige K, Amemiya K, Adachi H, Hirota K, Miyake A, Tanizawa O: Importance of transforming growth factor α/epidermal growth factor receptor autocrine growth mechanism in an ovarian cancer cell line *in vivo*. Cancer Res 1991, 51:5956–5959
55. Reynolds K, Farzaneh F, Collins WP, Campbell S, Bourne TH, Lawton F, Moghaddam A, Harris AL, Bicknell R: Association of ovarian malignancy with expression of platelet-derived endothelial cell growth factor. J Natl Cancer Inst 1994, 86:1234–1238
56. Henriksen R, Funa K, Wilander E, Backstrom T, Ridderheim M, Oberg K: Expression and prognostic significance of platelet-derived growth factor and its receptors in epithelial ovarian neoplasms. Cancer Res 1993, 53:4550–4554
57. Henriksen R, Gobl A, Wilander E, Oberg K, Miyazono K, Funa K: Expression and prognostic significance of TGF-beta isotypes, latent TGF-beta 1 binding protein, TGF-beta type I and type II receptors, and endoglin in normal ovary and ovarian neoplasms. Lab Invest 1995, 73:213–220
58. Di Blasio AM, Cremonesi L, Vigano P, Ferrare M, Gospodarowicz D, Vignali M, Jaffe RB: Basic fibroblast growth factor and its receptor messenger ribonucleic acids are expressed in human ovarian epithelial neoplasms. Am J Obstet Gynecol 1993, 169: 1517–1523
59. Crickard K, Gross JL, Crickard U, Yoonessi M, Lele S, Herblin WF, Eidsvoog K: Basic fibroblast growth factor and receptor expression in human ovarian cancer. Gynecol Oncol 1994, 55:277–284
60. Otsuka T, Ohkawa T, Shibata T, Oku T, Okuhara M, Terano H, Kohsaka M, Imanaka H: A new potent angiogenesis inhibitor, FR-118487 J Microbiol Biotech 1991, 1:163–168
61. Mu J, Abe Y, Tsutsui T, Yamamoto N, Tai XG, Niwa O, Tsujimura T, Sato B, Terano H, Fujiwara H, Hamaoka T: Inhibition of growth and metastasis of ovarian carcinoma by administering a drug capable of interfering with vascular endothelial growth factor activity. Jpn J Cancer Res 1996, 87:963–971
62. Kim KJ, Li B, Houck K, Winer J, Ferrara N: The vascular endothelial growth factor proteins: identification of biologically relevant regions by neutralizing monoclonal antibodies. Growth Factors 1992, 7:53–64
63. Czernobilsky B: Common epithelial tumors of the ovary. Blaustein's Pathology of the Female Genital Tract. Edited by RJ Kurman. New York, Springer-Verlag, 1987